EGBE, P.I. 2022. *Stuck pipe prediction in deviated wellbores: a numerical and statistical analysis*. Robert Gordon University, PhD thesis. Hosted on OpenAIR [online]. Available from: https://doi.org/10.48526/rgu-wt-2071873

# Stuck pipe prediction in deviated wellbores: a numerical and statistical analysis.

EGBE, P.I.

2022

# STUCK PIPE PREDICTION IN DEVIATED WELLBORES: A NUMERICAL AND STATISTICAL ANALYSIS

PETER IDO EGBE

A thesis submitted in partial fulfilment of the requirements of the Robert Gordon University for the degree of Doctor of Philosophy

May 2022

**ACKNOWLEDGEMENTS**

My profound gratitude goes to Dr Ibiye Iyalla and Prof. Babs Oyeneyin, my principal supervisors who patiently supported me through this research in difficult and challenging times, constructively critiquing the work, encouraging, and pointing me in the right direction. Your invaluable contribution is deeply appreciated.

I also deeply thank my family (Dr Shama – my beloved wife), and my dear children (Veronica and Peter) for their sacrifice and keeping up with me as I pushed to complete this research. This would not have been possible without your understanding. It must not have been easy missing out on "family time". To my dear wife, keeping me "fed" and "watered" with strength to burn the midnight oil is deeply appreciated.

My thanks also go to my colleagues and friends at Saudi Aramco and beyond. Thank you for the very insightful technical discussions. Even when we disagreed, there was something new to learn. Thank you for encouraging me at those difficult times when all seemed hopeless.

Thanks to Saudi Aramco for allowing me the time and resources to build, test and implement the concept of the stuck pipe prediction tool which was only but a dream in 2015.

Above all, I thank God Almighty for His Grace and Favour throughout this research work.

## DEDICATION

This research work and thesis is dedicated to the memory of my late parents **Dr Fidelis A. Egbe and Mrs Veronica I. Egbe**. And to my late stepmother, **Mrs Mercy Mbang Elemi**. All of whom ill health took from me way too early and did not live long enough to see the fruits of their labour. Rest in perfect peace.

## ABSTRACT

Due to the significant non-productive times and recovery costs associated with stuck pipe events in oil and gas drilling operations, there is value in being able to predict an impending stuck pipe event. To achieve this, the use of numerical cuttings transport (hole cleaning) models and statistical analysis of real-time drilling data is proposed by this research.

Current cuttings transport models are based on unhindered, free settling in the wellbore, and do not adequately account for the effect of vortices created as the drill string rotates about its axis. This thesis addresses both shortcomings and presents improved cutting transport models that consider hindered centrifugal settling of drilled cuttings, effect of Taylor vortices, and Van der Waals forces. The implication is that the resulting cuttings settling velocity used to estimate critical transport velocities and flow rates are more representative. The transport ratio, a measure of the hole cleaning efficiency is consequently more realistically predicted.

Although several proprietary automated stuck pipe prediction tools exist in the industry, this research found that they broadly fall into five main groups. It is also apparent that current capabilities do not simultaneously and continuously combine real-time data, offset wells data, and well design analytical models in a single approach. On that basis, this thesis presents an integrated stuck pipe prediction concept that utilizes all three data streams called the "ROW" approach. The concept presented in this thesis was then coded into a tool called the stuck pipe index (SPI). The SPI tool risk assessment is determined in real-time; and is referenced by a

traffic light alert system (green – amber – red) to warn the user of an impending potential stuck pipe situation.

The numerical models developed in this research estimate critical velocities to within 10 – 15% and show strong agreement with published empirical data. Combined with the cuttings transport numerical models developed in this research, and other publicly available well design models (such as hydraulics and torque & drag), the SPI tool has been tested with several case histories and proven to detect stuck pipe events with warning alerts significantly ahead of the event. The tool has equally been deployed in real-time with >90% success rate, and without spurious alerts recorded. The results thus confirm that the developed numerical models, and the "ROW" approach are robust and offer an improvement to current industry capabilities in terms of accuracy and sensitivity to changing downhole wellbore conditions.

**Key words:** Wellbore, stuck pipe prediction, free settling, hindered centrifugal settling, Taylor vortices, critical transport velocities, settling velocities, hole cleaning efficiency, "ROW" approach.

# TABLE OF CONTENTS

**LIST OF FIGURES**

**LIST OF TABLES**

**NOMENCLATURE**

A area ($m^2$)

$A_p$ Cutting / particle cross-sectional area ($m^2$)

$C_D$ Drag coefficient

$C_{Do}$ Effective drag coefficient in quiescent fluid

$C_c$ Annular volumetric cuttings concentration (%)

D Diameter (m)

$E_{van}$ Van der Waal energy (N)

$F_b$ Buoyant force (N)

$F_D$ Drag force (N)

$F_e$ External force (N)

$F_L$ Lift force (N)

$F_{van}$ Van der Waal force (N)

$F_{vanR}$ Resultant Van der Waal force (N)

$F_T$ Cuttings transport ratio

$F_\theta$ Vortex cuttings transport ratio

g Gravity ($m^2/s$)

h Cuttings bed height (m)

M Mass (kg)

P Pressure ($N/m^2$)

r Radius (m)

$R_e$ Reynolds number

$R_{ep}$ Particle Reynolds number

$R_{eg}$ Generalized Reynolds number

t Time (s)

T Torque (Nm)

$T_a$ Taylor number

$T_{acr}$ Critical Taylor number

U Velocity (m/s)

$U_t$ Terminal velocity (m/s)

$V_{vortex}$ Vortex velocity (m/s)

$V_\theta$ Azimuthal velocity (m/s)

$V_{\theta max}$ Maximum azimuthal velocity (m/s)

$V_s$ Cuttings settling velocity (m/s)

$V_{so}$ Settling velocity of a single cutting / particle in a quiescent fluid (m/s)

$V_r$ Local particle velocity (m/s)

Greek

$\rho$ Density ($kg/m^3$)

$\omega$ Angular velocity (rad/s)

$\varepsilon$ Eccentricity

$\emptyset$ Drilled cuttings bed voidage or porosity (%)

$\mu$ Fluid viscosity (kg/m.s)

$\gamma$ Kinematic viscosity ($m^2/s$)

$\theta$ Wellbore inclination (degrees)

$\tau$ Yield stress (m)

Abbreviations

AAV Azimuthal annular velocity

ANN Artificial Neural Network

BHA Bottom hole assembly

CAFV Critical annular fluid velocity

CBR Case-based reasoning

CDV Cuttings deposition velocity

CFD Computational fluid design

| | |
|---|---|
| CFR | Critical flow rate |
| CHC | Circulate hole clean |
| CRV | Cuttings re-suspension velocity |
| CSV | Cuttings settling velocity |
| CTFV | Critical transport fluid velocity |
| ECD | Equivalent circulating density |
| HKLD | Hook load |
| HPHT | High pressure high temperature |
| LCZ | Lost circulation zone |
| LWD | Logging while drilling |
| MD | Measured depth |
| MDA | Multi-variate discriminant analysis |
| MTV | Minimum transport velocity |
| MWD | Measurement while drilling |
| NPT | Non-productive time |
| POOH | Pull out of hole |
| RoC | Rate of change |
| ROP | Rate of penetration |

| | |
|---|---|
| ROW | Real-time, Offset Wells, Well Design |
| RPM | Revolutions per minute |
| SPI | Stuck pipe index |
| SPP | Standpipe pressure |
| SVR | Support vector regression |
| T&D | Torque and drag |
| TD | Total depth |
| TRQ | Torque |

## 1. INTRODUCTION

The quest to extract hydrocarbons located in sub-surface reservoirs has required the drilling of oil and gas wells to provide a means of access to such reserves. The success of the well construction process is critically important in ensuring the hydrocarbons can be produced to surface. At the start of the oil and gas exploration and production efforts, simple vertical wells were usually sufficient to achieve that objective. As the search for hydrocarbons got into more difficult terrains, and challenging sub-surface basins, the structural complexity of the oil and gas wells being drilled increased (Ferreira et al., 2015). The industry transitioned from vertical wells to highly deviated wells including horizontal wells, and extended reach wells (with significant step-out ratios). With these came a new set of challenges, for example:

- Drilling in narrow pore pressure / fracture pressure margins
- Drilling with high differential pressure
- Drilling across mobile or unstable formations such as salt
- Poor or inefficient hole cleaning in highly deviated wells

The well construction process typically involves the drilling of sub-surface bore holes of various diameters which telescopically reduce in size until the reservoir section. Consequently, significant quantities of drilled solids are produced. These drilled solids require to be transported out of the wellbore efficiently to prevent the accumulation of a cuttings bed. A failure to properly ensure efficient hole cleaning can result in non-productive time (Alawami et al., 2019), and often severe operational issues including but not limited to:

1. Erratic or high rotary torque; and high drag during trips in and out of the wellbore
2. High shocks and vibrations which are detrimental to the drilling bottom hole assemblies (BHA) including logging while drilling (LWD) tools
3. High equivalent circulating densities (ECD) potentially leading to
    a) Formation breakdown and loss circulation
    b) Increased over-balance pressures (the difference between pore pressure and wellbore pressure)
4. Low rate of penetration (ROP)
5. Challenges with deploying or retrieving drill strings, casing strings, completion strings, and logging tools
6. Stuck pipe which could be:
    a) Mechanical (due to pack-off / bridging of drilled cuttings)
    b) Wellbore geometry (due to the well trajectory, BHA components, or an interaction of both)
    c) Differential (due to significant over-balance pressures across highly permeable zones)

All the above listed potential drilling challenges do contribute to non-productive time (NPT) during the drilling operation. However, stuck pipe events constitute the most expensive NPT component (Egbe et al., 2020).

A drill string is considered stuck if it cannot be conventionally retrieved from a wellbore by pulling out of or tripping into the wellbore. Typically, once a stuck pipe occurs, normal operations such as rotary drilling are impossible. For Saudi Aramco, Figures 1.1 and 1.2 respectively illustrate a statistical breakdown of stuck pipe mechanisms, and the activities prior to the stuck pipe events over a five-year period. By a significant margin, mechanical (pack-off / bridging) and wellbore (hole) geometry contribute the highest instances of stuck pipe events.

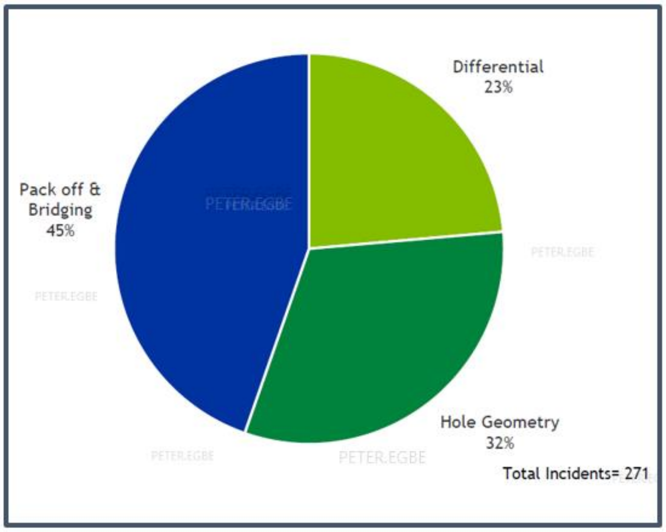


Figure 1.1: Statistical Distribution of Stuck Pipe Events Mechanism (Egbe et al., 2020)

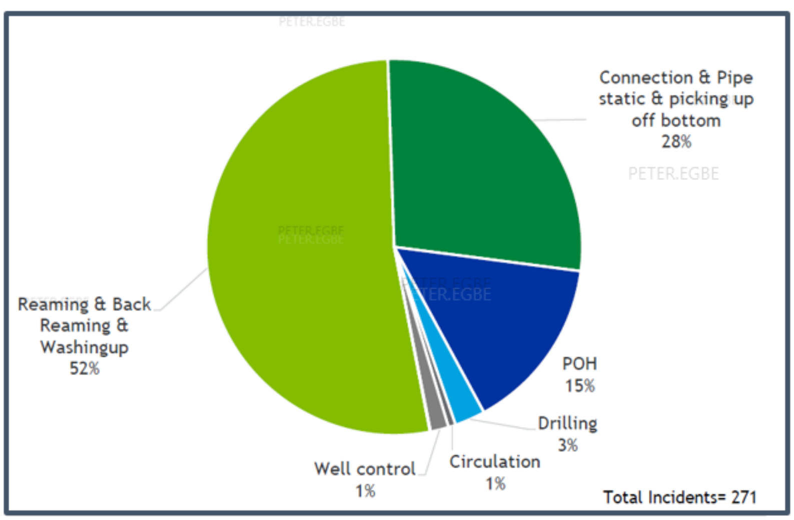


Figure 1.2: Statistics of Activities Being Performed Prior to Stuck Pipe Events (Egbe et al., 2020)

Historical statistics show that globally, stuck pipe events account for approximately 20 – 30% of the total NPT during drilling operations (Berdugo Arias et al., 2020, Muqeem et al., 2012). Thus, stuck pipe events cost the industry significant amounts ranging into several hundreds of millions of US Dollars per annum (Elmousalami et al., 2020). For a Middle East operator, this equated to approximately USD 40 – 50 MM per year. Hence there is a compelling case to investigate a means to predict the onset of stuck pipe events in real-time before it occurs.

## 1.1 Research Rationale

Efforts to proactively predict or identify the probability of stuck pipe events is not new in the industry. In many cases and usually with hindsight, a significant proportion of stuck pipe events can be prevented if the early warning signs are detected on time, and proactive actions taken to avoid it. If a stuck pipe event can be predicted or detected in "real-time" as drilling operations are in progress, the higher the probability that it can be averted. Therefore, time, is a critical factor.

One of the earliest studies was by Hempkins et al. (1987), who used 28 raw drilling parameters as arguments in a Multi-variate Discriminant Analysis (MDA) to classify mechanically, differentially, and non-stuck wells. Biegler and Kuhn (1994), Howard and Glover (1994), Wisnie and Zhu (1994), and Shoraka et al. (2011) improved on the work by Hempkins et al. (1987) as follows

- Biegler and Kuhn (1994) utilized physically meaningful combinations of the same raw drilling parameters. The combinations were in effect physical models related to wellbore stability, hole cleaning, differential sticking, and drag. They used discriminant analysis to create canonical functions for mechanically stuck, differentially stuck, and non-stuck events. Using Bayesian statistics, they defined curves over the two canonical function planes

- Howard and Glover (1994) used the same approach as Hempkins et al. (1987) but developed separate models for wells drilled using water-based mud and oil-based mud. They also considered physical well design models like those used by Biegler and Kuhn (1994)
- Wisnie and Zhu (1994) used logistic regression techniques to develop a method to quantify the probability of getting stuck and getting free, in both water-based and oil-based drilling mud. Their model was incorporated into a Monte Carlo simulation to predict the distribution of costs for a hole section
- Shoraka et al. (2011) combined a multi-variate discriminant analysis approach with multi-variate regression techniques on 26 raw drilling variables to develop static stuck pipe prediction models

The improvements noted above have all relied in one way or the other on some form of discriminant analysis, which is more of a tool for classification than for predicting probabilities. Multi-variate discriminant analysis is sensitive to the assumption of normality and will tend to overestimate the magnitude of association of the differences between independent variables, of which there are several in the analysis of a stuck pipe analysis. The work by some of these early researchers (Biegler and Kuhn, 1994; and Howard and Glover, 1994) did however trigger considerations to apply physics based well design models in the analysis of stuck pipe events.

As advances in artificial intelligence and machine learning progressed, the following researchers extended the statistical analysis method and capability:

- Miri et al. (2007) and Siruvuri et al. (2006) presented the use of Artificial Neural Networks (ANNs) as a technique to detect stuck pipe events by modernizing the statistical approach.
- Murillo et al. (2009) and Naraghi et al. (2013) used Adaptive Fuzzy Logic and Neural Network based on the constraints of different drilling variables.
- Support Vector Regression (SVR) techniques was used by Chamkalani et al. (2013) and Jahanbakhshi et al. (2012) to improve on the constraints posed by Artificial Neural Networks.
- Sadlier et al. (2013) and Ferreira et al. (2015) used Pattern Recognition or Case-Based Reasoning (CBR) approach incorporated with a decision support tool to match the real-time data patterns with historical stuck pipe cases.

A third approach uses analytical models such as torque and drag, or hydraulic models to identify the onset of potential drilling issues by comparing the real-time data (at specific intervals) with the pre-drill models.

- The work by Belaskie et al. (1994) where the surface drilling parameters data was combined with Measurements-While-Drilling (MWD) data to predict stuck pipe events is regarded as one of the pioneer studies utilizing this approach.
- Guzman et al. (2012) compared the pre-drill torque and drag with the real-time data to identify potential stuck pipe events.

- Salminen et al. (2017) used both torque and drag, and hydraulic analytical models, and showed improved accuracy and reliability in assessing stuck pipe risks.
- Zhang et al. (2019 used a hybrid approach which combines a transient solid transport model, torque and drag model, and drilling data driven model to evaluate the risk of stuck pipe in real-time based on the variation of rotary drilling torque
- Saini et al. (2020) applied a digital twinning approach using well design models (cuttings transport, hydraulics, torque & drag) to predict hole cleaning issues and prevent stuck pipe events. Their work focussed mainly on hole cleaning as a causal factor to stuck pipe events, but do not present a look-ahead method for predicting its occurrence
- Meor Hashim et al. (2021) implement a technique that splits into three separate modules (differential sticking module, wellbore geometry module, and hole cleaning module), where each module is used to predict stuck pipe for a specific defined applicable rig operation.

Based on these previous studies, the current techniques and capability for predicting and detecting the onset of a stuck pipe event may be broadly grouped as shown in Table 1.1.

Table 1.1 Current techniques and capability for predicting and detecting the onset of a stuck pipe event

| Group | Approach | Remarks | Researcher(s) |
|---|---|---|---|
| A | Statistical Approach | This approach focused mainly on statistical analysis of ***offset wells raw drilling data*** to classify stuck pipe mechanisms in already drilled wells as a means of predicting the potential for similar events in future wells.<br>Whilst the approach may be suited for a post-event assessment, or a pre-drill assessment, the "predictability" claimed by the various researchers in this group does not allow for a "continuous real-time" evaluation of the probability of a stuck pipe event occurring as drilling is in progress.<br>It may best be described as a daily surveillance tool with input coming from daily drilling reports on a 24-hourly basis. The challenge with this is that the string may already become stuck before the team has had a chance to input the next deciding batch of data points.<br>The work by Biegler and Kuhn (1994) and Howard and Glover (1994) where they combined raw drilling variables to create physical design models (related to wellbore stability, hole cleaning hydraulics, etc.), lay the foundations for the consideration of such models in assessing the potential for a stuck pipe event to occur. | Hempkins et al. (1987), Biegler and Kuhn (1994), Howard and Glover (1994), Wisnie and Zhu (1994), Shoraka et al. (2011) |
| B | Statistical approach enhanced with machine learning (such as ANNs, SVRs, SVM, Fuzzy Logic, ANFIS, etc.) | This combines statistical analysis of ***offset wells data*** with ***real-time drilling data*** using machine learning as a means of automation to predict stuck pipe events.<br>Predictive models developed using ANN, SVRs, Fuzzy Logic, etc. are trained using offset well data usually in the same field, or of the same well design. Once | Miri et al. (2007), Murillo et al. (2009), Siruvuri et al. (2006), Naraghi et al. (2013), Jahanbakhshi and Keshavarzi (2012), Chamkalani et al. (2013), Sadlier et al. |

| | | | |
|---|---|---|---|
| | | trained, the predictive models were utilized in real-time to monitor drilling operations.<br>Majority of the researchers found that ANN had advantages over conventional statistical methods (such as no reliance on physical models to make predictions, tolerance to data errors in statistical distribution, etc.). They however also noted, for example, limitations such as sensitivity to chaotic behaviour, tendency to over-fit, a long period to train the process. To resolve these limitations, other methods such as SVMs, Fuzzy Logic, and Adaptive Neuro Fuzzy Logic (ANFIS) were adopted by some researchers (Murillo et al., 2009) to achieve improved prediction accuracy and ability (Jahanbakhshi and Keshavarzi, 2012).<br>These efforts represented the first attempts at using machine learning to predict stuck pipe in real-time as drilling operations progressed. However, the shortcoming is the non-application of analytical well design models to serve as a road map. The absence of a road map presents a significant challenge as there is no benchmark against which the real-time drilling data could be compared to. | (2013), Meor Hashim, Yusoff, Arriffin, Mohamad, Gomes, Jose, Bidin (2021) |
| C | Analytical approach | This method focused on simply comparing ***real-time drilling data*** to a pre-drill ***well design analytical model*** such as Wellbore stability, Torque & drag, and hole cleaning hydraulics to identify conditions that could result in stuck pipe events. The pre-drill well design analytical model serves as the road map against which the drilling engineer compares actual well data to determine the magnitude of deviation. This may be at every stand or joint drilled. It may also be for a specific amount of footage. | Belaskie et al. (1994), Guzman et al. (2012) |

| | | | |
|---|---|---|---|
| | | Consequently, the approach is heavily reliant on the human interface and a level of subjectivity cannot be dismissed. There is no use of machine learning methods to introduce a real-time predictive capability; neither is there a use of statistical techniques to classify the data sets being analysed. Historic offset well data are also not referenced.<br>This is a disadvantage because changes in downhole conditions that can result in stuck pipe events occur very quickly, and leading indicators are easy to miss if the analysis and trending are not being done on a truly real-time scale, or within a reasonable cluster of data points. In terms of predicting stuck pipe events, this method is a semi real-time surveillance approach which is difficult to apply simultaneously on many wells. | |
| D | Analytical approach enhanced with machine learning (such as ANNs, SVRs, Fuzzy Logic, etc.) | Focused on comparing **real-time drilling data** to pre-drill **well design analytical models** such as Torque & drag, and hole cleaning hydraulic to predict / detect stuck pipe events; and automated with machine learning techniques (such as ANNs, SVRs, SVM, Fuzzy Logic, ANFIS, etc.). The method combines two types of analysis for the prediction of a stuck pipe event. The deviation of real-time data from real-time model predictions using hydraulics, and torque and drag (T&D) software; and trend analysis (i.e., rate of change) of real-time data (Salminen et al., 2017).<br>Based on a transient approach, this method can use real-time drilling data as input, and the well design models serve as road maps for evaluating and predicting stuck pipe risks. Thus, providing early warnings when a high-risk scenario for stuck pipe is detected (Zhang et al., 2019). | Salminen et al. (2017), Zhang et al. (2019), Meor Hashim et al. (2021), Saini et al. (2020) |

| | | | |
|---|---|---|---|
| E | Pattern recognition (e.g., CBR) | Compares ***real-time drilling data*** to historic ***offset wells*** stuck pipe events patterns and relies on machine learning or human interface to interpret and concur with the prediction (semi-automated). The significant disadvantage of this approach lies in the fact that sufficient and meaningful data sets must be collected to generate a recognizable pattern. Additionally, the approach is self-limiting, in that for it to work there must have been an exact, or similar previous case loaded in the database for comparison. | Sadlier et al. (2013), Ferreira et al. (2015) |

With reference to Table 1.1, it is apparent the current techniques do not simultaneously and continuously combine offset wells data, well design analytical models, and real-time drilling data in a single integrated approach.

Although current techniques have achieved varying levels of prediction success, the integrated approach is recommended because it combines all the strengths of the current techniques. For example, by utilizing historical offset well data in addition to well design models, the road maps created are more detailed, and consider actual events that have previously occurred simultaneously, in addition to theoretical assumptions. This in turn improves the accuracy of the physical well models which would previously have been hampered by inherent numerical or empirical model limitations. The combined approach also provides more than one option to validate the road map. Consequently, a more complete description of the subject well being drilled can be built, and the inherent downhole conditions can be better monitored in real-time.

The proposed integrated approach is also analogous to the “digital twin” concept which is being rapidly adopted in the oil and gas industry. It has demonstrated significant value in the airlines, and chemical process industries where condition-based maintenance of many critical pieces of equipment have been improved. The “digital twin” solution consists of three main parts; the physical system (in this case, the well being drilled), the virtual model that describes the physical system (i.e., the physics based well design model), and the exchange of data and information between the two (Tao et al., 2019). Accordingly, a digital twin is a virtual physics and data-based model that encompasses all the various subsystems, their properties, interactions among them, and interactions of the system with the environment. The well construction digital twin solution uses data-derived models from historical data and real-time data collected while drilling to make predictions. Hence, when applied to the stuck pipe prediction problem, the adoption of such a concept appears logical. When this is coupled with a machine learning capability, it is the position of this research that such an approach offers an improved accuracy and sensitivity in the prediction of probable stuck pipe risk compared to the current industry capability.

Based on the above, this research proposes a real-time stuck pipe predictive tool that utilizes the integrated approach called the **"ROW"** model to predict an impending stuck pipe event. In summary the approach is as follows:

- **R**eal-time surface drilling data will be assessed for rates of change from point-to-point, and in terms of anomaly detection analysis over a given time interval
- **O**ffset wells with stuck pipe case histories will be used for automatic pattern recognition, and identification of known problematic zones with drilling challenges
- **W**ell design analytical models will serve as benchmarks against which real-time drilling data will be compared (actual vs. model predicted) for deviation trend analysis based on a field specific, or well design specific acceptable deviation margin

The Venn diagram in Figure 1.3 illustrates these relationships. Figure 1.4 illustrates where current industry capabilities lie relative to the proposed combined approach.

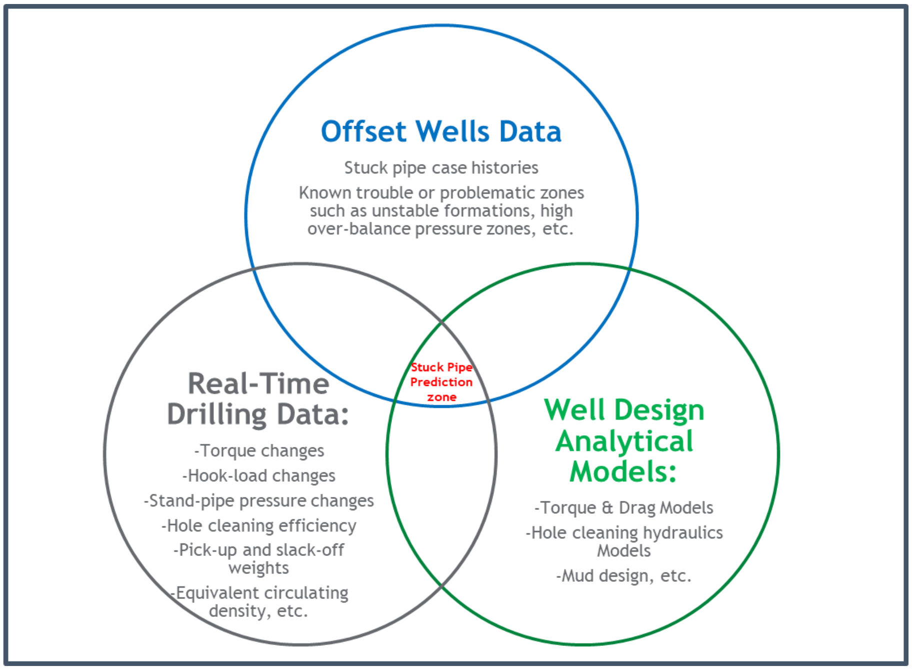


Figure 1.3: Real-Time / Offset Wells / Well Design (ROW) Analysis Model

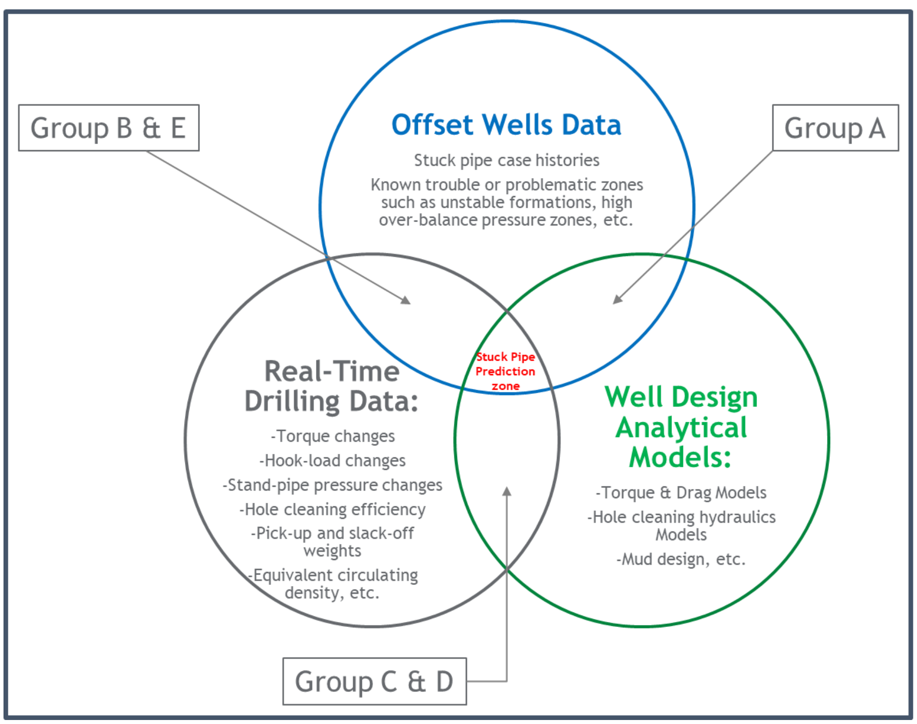


Figure 1.4: Current industry capability relative to proposed research approach

## 1.2 Research Aim and Objectives

The main aim of the research is to develop a new approach / technique to predict stuck pipe events before it occurs using a combination of real-time drilling data analysis, offset wells data & case histories, and wellbore analytical models (e.g., hole cleaning numerical models, hydraulic models, and torque & drag models). The objectives of the research will be to:

1. Determine the hole cleaning efficiency: This will be achieved by developing improved numerical models for:
    a. Annular cuttings concentration
    b. Azimuthal velocity based on Herschel-Bulkley rheology, and considering Taylor vortices
    c. Cuttings settling velocity taking the effect of hindered centrifugal settling into account
    d. Critical transport fluid velocity
    e. Critical cuttings re-suspension velocity taking the effect of Van Der Waals forces into account
2. Develop and test a technique / concept that can be used to predict the risk of a stuck pipe event occurring: This will be achieved by
    a. Using statistical and regression analyses to assess
        i. How real-time data changes from point to point (anomaly detection)
        ii. How deviation trends change over a defined period, and footage drilled

iii. Utilize physical well design models (hole cleaning hydraulics, and torque & drag) as road maps against which deviation changes (actual vs simulated) are compared in real-time as drilling is in progress. Hole cleaning hydraulic models will be developed as per objective #1 of this research. Torque & drag simulations will be as per existing industry models

iv. Identify intervals in historical offset wells where known stuck pipe events have occurred in such wells; and incorporate as part of the road map for monitoring wells across similar depths / formation in real-time while drilling

b. Evaluate the probability of a stuck pipe event occurring by using a risk estimation method to quantify the deterioration of downhole conditions as highlighted by real-time data changes from an observed trend, deviation from well design model road maps, and historical offset well data

c. Classify the assessed probability in a suitable risk ranking method that can be used to provide sufficient early warning to drilling crews in real-time as drilling progresses, and allow them take evasive actions to avoid the predicted stuck pipe event

## 1.3 Thesis Outline

The thesis is structured as follows:

**Chapter 1 (Introduction)**: Provides a brief introduction to oil and gas wells construction, and the impact of non-productive time contributed by stuck pipe events. The rationale for the research is discussed, including the aim and objectives of the thesis are outlined.

**Chapter 2 (Literature Review)**: Provides a literature review and description of the factors that influence hole cleaning during drilling operations. Specific concepts pertinent to this research are introduced. Discusses various cuttings transport numerical and empirical models developed and adopted by previous researchers.

**Chapter 3 (Methodology)**: Presents and discusses the numerical models developed in this research for the estimation of annular cuttings concentration, critical settling velocity, annular azimuthal velocity, critical transport fluid velocity, and critical cuttings re-suspension velocity.

**Chapter 4 (Application and Validation of Models)**: Presents the application and validation results for each of the models developed including a discussion of any limitations and deviations from existing models. Results from codifying the real-time stuck pipe prediction concept are also presented to validate the concept.

**Chapter 5**: Summarizes the findings of this research, and recommendations for areas of future research work and improvement.

## 2. LITERATURE REVIEW

In detecting and preventing an impending stuck pipe event, time is of the essence. Usually, and with sufficient hindsight, the indicators leading up to most stuck pipe events are clear, but are either not recognized, or in some instances ignored by the drilling teams. The earlier these indicators that could lead up to a potential stuck pipe event are detected and predicted, the higher the probability that it can be avoided. However, there does not exist one specific indicator that may be considered the leading indicator. Usually, it is a combination of several factors. Efforts have been made by previous researchers to develop automation methods and techniques for the early detection of stuck pipe events. These have ranged from statistical analysis to machine learning, and artificial intelligence techniques. However, no meaningful stuck pipe prediction effort may be deemed complete without the inclusion of physics-based models that attempt to describe the cuttings transport process during well construction operations. Such physics-based models may be static or transient. Over the past decades, several cuttings transport models have been proposed by previous researchers and are available in the literature. Although the detection rates from a "data analytics" only approach is equally commendable, it has been established that the combined or hybrid approach offers improved capabilities. The quality of the physics-based model is an important factor that drives the prediction accuracy that may be achieved in the hybrid approach.

Zhang et al. (2019) present physics-based model and data analytics combined approach to predict stuck pipe during drilling. They used an Ensemble Kalman Filter (EnKF) based data-driven model to provide parameters and coefficients for application in the physics-based models such as solids transport and torque & drag models. They found that the combination improved the reliability of the results predicted by the model. The same conclusions were reached by Guzman et al. (2012), who reported a 37% reduction in stuck pipe incidents achieved by utilizing equivalent circulating density (ECD), and torque & drag (T&D) data to modify and adjust well design models to avoid downhole challenges associated with hole cleaning, and wellbore stability.

This chapter will present the following:

- A summary of previous cuttings transport models by previous researchers; and the observed limitations
- A discussion of the factors that influence cuttings transport, and hole cleaning efficiency
- An introduction to specific fluid dynamics concepts considered pertinent to this research work
- An overview of previous efforts in developing various stuck pipe predictive methods and techniques; and the observed limitations

## 2.1 Review of Existing Solids Transport Studies and Applications in Drilling Operations

The challenges involving the transportation of solids are not unique to well construction drilling operations. Other applications exist such as in mining, slurry transportation (iron ore, minerals in pipelines, etc.), and quarries. However, it has to be stated that the transport of drilled cuttings to surface involves a uniquely different flow regime when compared to solids transport in, for example, pipelines or concentric annular profiles. Although some theories are common to transport of solids in channel, concentric, and eccentric flows; it is believed that the correlations used in solids transport in pipelines or open channel sedimentation flows should not be directly used for predicting solids transport efficiency in drilling operations where eccentric annular flow is usually the norm. The following bases are used to support this assertion:

1. Due to challenges of pipe eccentricity, flow velocities at the bottom of annular eccentric pipe flows are lower compared to single pipe flows or open channel flows (Li and Luft, 2014). This flow behaviour will no doubt influence the transportation efficiency of solids to the surface
2. Solids concentration or injection rates into the annulus / channels vary widely typically between less than 0.1% for sand production in a pipeline (Najmi et al., 2014) and more than 30% for slurry transport (Wilson et al., 2006)
3. The state of the transported solids (finely crushed / slurry-like, or if in the form of pebbles etc) influence the transportation efficiency (Li and Luft, 2014). In drilling there is normally a mix of finely drilled cuttings and medium to larger cuttings structure depending on the type of formation being drilled at the time
4. Solids transportation in a typical drilling operation may be sub-divided into 3 main phases: the drilling phase with or without string rotation, the stationary hole-cleaning phase, and the wiper trip hole cleaning phase (Li and Luft, 2014). For example, the speed of rotation of the drill string will positively influence solids transportation. Flow in channels, quarries, and flow lines do not take these into account (Li and Luft, 2014).

5. Complexity of the fluid mechanics due to the many variables which affect solids transportation in eccentric annuli (Elgaddafi et al., 2021).

### 2.1.1 Historical Approach to Solids Transport Studies

Between the early 1940's and the late 1970's, majority of the investigations conducted on solids transportation focused on vertical wells. This is unsurprising because in the early days of the industry, horizontal or highly deviated wells were not the norm.

From the 1980's onwards, after the first researchers tackled the topic, highly deviated, horizontal, and extended-reach wells (with significant step-out ratios) have become more widespread. This has hugely been driven by the need to explore for oil and gas in more difficult terrains, including the need to maximize production from wells by achieving greater reservoir contact in the identified pay zones. As a result, the focus for solids transport research has since shifted to deviated wellbores. Since then, several numerical, mechanistic, and empirical / semi-empirical works has been conducted by researchers. Some have used flow loop test data to develop their models. Some researchers have used curve-fitting methods on solids distribution tests to develop empirical correlations to predict the concentration of solids in the annulus (Li and Walker 1999, Li et al., 2002, Ozbayoglu et al., 2010, Duan et al., 2008, Bassal 1995, Becker 1987).

Several researchers developed empirical correlations including mechanistic models to predict the minimum transport velocity (MTV) (Ford et al., 1990, Oyeneyin et al., 2011, Mohammadsalehi and Malekzadeh, 2011, Mirhaj et al., 2007, Larsen 1990).

The MTV is also referred to as the critical deposition velocity (CDV) or critical transport fluid velocity (CTFV).

Other researchers went a step further by using data collected from stationary hole cleaning tests to predict concentrations of solids in the annulus including the height of the cuttings bed (Li et al., 2002, Khan 2008, Nguyen 2007, Sapru 2001). They even predicted how long it will take to clean the hole. In some other work, empirical correlations were developed to predict hole cleaning efficiency and wiper trip speeds based on data collected from wiper trip hole cleaning tests (Li et al., 2005, Walker and Li 2001).

Table 2.1 summarizes the work done by previous researchers over the years.

Table 2.1 Summary of Some Historic Cuttings Transport Studies

| **Researcher (s)** | **Summary of work done** |
|---|---|
| Tomren (1979) and Iyoho (1980) | Conducted experiments to assess cuttings concentration and bed height data at different hole deviation angles |
| Becker (1982) | Investigated the effect of mud weight and hole size on the cuttings concentration and bed height |
| Okpobiri (1982) | Proposed a semi-empirical correlation to determine frictional pressure losses and the minimum volumetric flow requirement when solids are conveyed with foam |
| Parker (1987) | Investigated the effect of hole wash-out and particle size on the cuttings concentration |

| | |
|---|---|
| Ford et al. (1990) | Conducted investigations on the effects of pipe rotation and eccentricity on cuttings transport efficiency in inclined well bores |
| Sifferman et al. (1992) | Studied the effect of various drilling parameters on hole cleaning in deviated wellbores between 45 – 90 degrees inclination |
| Hareland et al. (1993) | Investigated the effect of oil-based mud on cuttings concentration |
| Bassal (1995) and Eddy (1996) | Investigated the effect of drill string rotation |
| Sanchez et al. (1997) | Estimated the hole cleaning time using cuttings erosion tests |
| Adari et al. (2000) | Estimated the hole cleaning time using cuttings erosion tests |
| Sapru (2001) | Investigated the effect of pipe rotation on cuttings bed erosion |
| Martins et al. (2001), Ozbayoglu (2002) | Collected cuttings concentration and bed height data with foam fluids |
| Martins et al. (2002) | Studied solids return times with aerated fluids using a full-scale test facility |
| Vieira et al. (2002) | Conducted experimental tests to collect cuttings concentration and bed height data for a gasified fluid |
| Mendez (2002) | Investigated cuttings concentration and fluid critical velocities in gas-liquid flow conditions in horizontal wellbores. He also investigated the effect of pipe rotation |

| | |
|---|---|
| Naganawa et al. (2002) | Collected solids concentration data involving over 300 different flow conditions with aerated mud |
| Pereira (2003) | Investigated cuttings concentration and fluid critical velocities under gas-liquid flow conditions in wellbores between 30 – 60 degrees inclination |
| Zhou (2004) | Collected cuttings concentration data with aerated mud in a horizontal annulus by using a full-scale high pressure high temperature (HPHT) flow loop |
| Capo et al. (2006) | Collected cuttings concentration and bed height data with foam fluids |
| Valluri et al. (2006) | Estimated the hole cleaning time using cuttings erosion tests |
| Lourenco et al. (2006) | Studied solids return times with aerated fluids using a full-scale test facility |
| Nguyen (2007) | Investigated hole cleaning efficiency using a special surfactant fluid |
| Yu et al. (2007) | Studied cuttings concentration under simulated downhole conditions |
| Chen et al. (2007) | Collected cuttings concentration and bed height data with foamy fluids under simulated downhole conditions |
| Duan et al. (2008) | Collected cuttings concentration and bed height data with foamy fluids under simulated downhole conditions |
| Khan (2008) | Estimated the hole cleaning time using cuttings erosion tests |

| | |
|---|---|
| Avila et al. (2008) | Investigated the effect of pipe rotation on cuttings concentration and fluid critical velocities under gas-liquid flow conditions in wellbores of 30 – 60 degrees inclination |
| Ahmed et al. (2010) | Investigated the effect of a mechanical device on cuttings concentration |
| Osgouel (2010) | Investigated how to predict cuttings concentration with aerated fluid in horizontal wellbores |
| Xu (2010) | Collected cuttings concentration and bed height data with foamy fluids under simulated downhole conditions |
| Effiong (2013) | Studied cuttings bed height in a horizontal wellbore using a flow loop |
| Jacob (2013) | Investigated ways to predict the bed height in a wellbore washout section |
| Sayindla et al. (2017)<br>Werner et al. (2017) | Studied the effect of different oil-based and water-based drilling fluids with the same viscometric properties on cuttings transport ability |
| Bizhani and Kuru (2018) | Studied the effect of viscoelasticity on particle removal from a stationary sand bed deposited in a horizontal pipe |
| Hirpa and Kuru (2020) | Studied the influence of fluid elastic properties on the critical velocity, frictional pressure drops, and the turbulent-flow characteristics of polymer-fluid flow over a sand bed deposited in a horizontal pipe |
| Elgaddafi et al. (2021) | Investigated the critical transport velocity in conventional and fibrous based fluids |

#### 2.1.1.1 Limitations of Historic Solids Transport Studies

Most of the historic studies listed in Table 2.1 can be categorized as either theoretical or experimental / empirical works. The experimental approach is typically limited to a study of one or more variables, while others are held constant. Although experimental (or empirical) methods have yielded reasonable and accurate predictions, their application is limited to the range of data that were used to create the correlations because the wellbore cleanout process is a physically complex one (Elgaddafi et al., 2021; Bizhani and Kuru, 2017). The theoretical approach (i.e., mechanistic, and semi-mechanistic modeling), if developed properly, describes the physics of the problem into the model. As a result, models developed from a theoretical approach can be applied over a broader range of conditions.

Mechanistic hole-cleaning models consider the balance of moments around the pivoting point of a cutting particle as the necessary condition for the particle to move (Clark and Bickham 1994; Ramadan et al. 2003; Duan et al. 2007). The main forces to consider will typically be the fluid-hydrodynamic force (drag and lift force), buoyancy, and adhesion forces (i.e., Van der Waals). The accurate estimation of these hydrodynamic forces acting on the particle is not a trivial endeavor.

Semi-mechanistic models on the other hand consider the Shields stress (i.e., the dimensionless form of the fluid shear stress at the cuttings-bed interface) to determine the onset of particle movement (Peysson et al., 2009). Previous bed erosion studies assume the existence of a critical shear stress value. Bizhani and Kuru (2017) demonstrated that the bed shear stress calculated by use of the frictional pressure loss measurement was the most accurate and falls within 13% of the actual measured bed shear stress. Duan et al. (2007) correlations predict bed shear stress to within 20% of the actual values.

For both model types, it can be concluded that an accurate determination of the local effective fluid velocity at the bed surface, and the bed shear stress are critical. The main limitations of current models are summarized below

- The hydrodynamic forces are directly related to the fluid velocity; hence, the question of what “effective velocity” should be used for calculating these forces arises. For a single cutting lying on top of a cuttings pile, only the local fluid velocity measured around its centre of gravity should be considered (Bizhani and Kuru, 2017). Current literature summarized in Table 2.1 consider the maximum or average fluid velocity in the annulus; but do not consider, for example, the presence of azimuthal velocity due to string rotation, and its effect on the “local” effective velocity profile which should be the velocity used in the force calculations. Many of the studies also estimate a minimum velocity required to transport cuttings to surface. They all considered the Stokes law and slip velocity based on free settling
- The role of the flow turbulence in the dislodgment of the particles is important (Diplas et al., 2008). The Reynolds number is typically used to determine turbulent flow regime in current models. However, even when the flow may be laminar in the axial direction, it could be turbulent in the rotational direction (Taylor, 1923; Potter et al., 2002). In turbulent flow regimes, the effective fluid velocity is the instantaneous velocity which varies over time. Comparisons of local instantaneous and time averaged velocities near the cuttings bed interface show that there is a significant level of

velocity fluctuations near the bed interface that is caused by the turbulent nature of the flow and the uneven / rough surface of the cuttings bed. Bizhani and Kuru (2017) showed that the instantaneous velocity can be up to two times higher the average velocity value

- The role of granular materials in the creation of bed erosion is missing in current literature. Granular materials introduce Van der Waals forces which should not be ignored when resolving the hydrodynamic forces acting on a particle. Most mechanistic models incorporate drag, lift, and buoyancy forces. However, very few models account for the impact of adhesion between particles due to Van der Waals forces.
- The local arrangements (e.g., cubical, hexagonal, etc.) of particles in the bed can also influence the significance of each force. Bizhani and Kuru (2017) revealed that the local arrangement of particles in the bed affects local roughness height. Change in the roughness height will cause the local velocity to change accordingly. Although different definitions have been used for the bed roughness (Ramadan et al., 2003; Duan et al. 2007), Bizhani and Kuru (2017) have shown that it is approximately equal to twice the cuttings size.
- Houssais et al. (2015) dispute the existence of a critical shear stress value. They found that there is movement of the bed material even at small shear stresses. Thus, implying that particle movement does not stop at a well-defined shear stress; and that any number reported in literature as the "critical shear stress (or Shields number)" is subjective (Bizhani and Kuru,

2017). The effective local velocity profile also plays an important role in the estimation of the shear stress

Overall, the emerging body of research on sediment transport shows the inadequacies in the current hole-cleaning models. Treating the process of cuttings removal from a pure hydrodynamic-force framework (i.e., mechanistic modeling) is inadequate in capturing the true physics of the cutting removal. Similarly, the semi-mechanistic approach in modeling cuttings removal also omits some key features of the process and oversimplifies the interaction of cuttings with the fluid (Bizhani and Kuru, 2017).

Based on these conclusions, and as can be inferred from the summary in Table 2.1, none of the previous research works investigated the:

- Azimuthal velocity profile based on a Herschel-Bulkley fluid model due to string rotation, and its effects on the local velocity profile
- Inclusion of the effect of Taylor vortices in their numerical hole cleaning models, and its effect on the determination of turbulence and local instantaneous velocity
- Effect of hindered centrifugal settling in the estimation of cutting settling velocity
- Effect of combining the Van Dar Waal and drag forces in the equilibrium of moments equation for estimating the critical re-suspension velocity of a cutting just about to experience motion

Considering the above, the aim and objectives of this research has been summarized in section 1.2 of this thesis.

### 2.1.2 Summary of Effect of Drilling Parameters on the Efficiency of the Cuttings Transport Process during the drilling or running-in-hole phase

Zhang et al. (2014) investigated the cuttings bed forming patterns in an eccentric annulus at different hole inclinations. They considered the solids or cuttings injection rate to simulate the cuttings bed forming process, the fluid velocity, fluid, and particle properties. They studied the behavior of the solids between 30 to 90 degrees inclination. They found that at well inclination of between 60 to 90 degrees, a "stationary bed" of solids is formed. Above this stationary bed, and near the interface between the solids bed and fluid, a "moving layer" exists. Also, above the moving layer, is the free stream containing few solids. The thickness of the moving layer was found to be dependent on the magnitude of fluid velocity in the annulus, the extent of drill string eccentricity, solids concentration in the annulus, properties of the solids/cuttings and the drilling fluid properties. Depending on the magnitude of fluid velocity changes, the bed pattern is known to vary between that of a stationary bed to that of a "moving bed" at inclinations of 80 – 90 degrees.

At lower inclinations of between 30 – 60 degrees, Zhang et al. (2014) also found that a "waved bed" pattern occurs. The ease at which the waved beds form and its size, was found to depend on the well bore inclination, fluid velocity, cuttings or solids injection rate, solids properties (i.e., the shape, size, and density), and the drilling fluid properties.

If well bore inclination were to be reduced further, that is the well is tending towards vertical, and the fluid annular velocities are increased, the "waved bed" pattern increases. It was also discovered that by reducing the well bore inclinations, the continuous solids bed is minimized, resulting in what is termed a "packed dune". In this type of bed pattern, it has been demonstrated that solids slide downward from the backside of the dunes and become entrained in the flowing fluid stream. Once in the fluid stream, the solids are then carried forward and deposited at the front of the dunes. With further increases in fluid velocities and decrease in well bore inclination, the size of the packed dunes decreases until they completely disappear, and the sand bed pattern is called a "dispersed dune" (Zhang et al., 2014).

At a critical annular flow velocity, referred to as the "Critical Deposition Velocity – CDV (Larsen 1990) or the Minimum Transport Velocity – MTV (Ford et al., 1990; Oyeneyin et al., 2011), the dispersed dunes cease to exist, and a continuous moving bed of solids or cuttings forms. The sand bed pattern in this instance is referred to as the "moving bed" pattern. It is sometimes also referred to as the "suspension flow". Some detailed tests have been conducted under various conditions to determine the CDV or MTV (Jalukar 1993, Zarrough 1991). Similar bed patterns observations were noted in solids-gas-liquid flows (Vieira et al., 2002). All these findings support the popular two- or three-layer models used to develop mechanistic models for assessing hole cleaning efficiency.

Ford et al. (1990) and Oyeneyin et al. (2011) defined the MTV as "a *critical velocity below which a stationary bed will result*"

Larsen (1990) defined the CDV for deviated wells with inclinations between 40 – 90 degrees as *"the minimum superficial fluid velocity needed to maintain a continuously upward movement of all cuttings in the annulus during drilling"*. For a deviated well between 0 – 35 degrees inclination, Larsen (1990) further defined the CDV as *"the minimum fluid velocity required to maintain 5% drilled cuttings concentration by volume in the annulus during drilling"*.

As previously stated, essentially both the MTV and CDV refer to the same parameter – which is a critical velocity in a well bore annulus to ensure an efficient hole cleaning process. Several researchers have delved into the topic of determining the CDV or MTV at which solids will be transported efficiently to surface. Many have conducted various extents of research under different test conditions such as well bore inclination, well bore sizes, pipe RPM, pipe eccentricities, mud types, ROP, and string diameters. A summary of the effects of these drilling parameters on the solid / cutting concentration is discussed.

#### 2.1.2.1 Annulus fluid velocity and wellbore inclination

From separate studies first conducted by Tomren (1979) and Iyoho (1980), the following can be established:

1. As well bore inclination increased, the solids / cuttings concentration in the annulus increased starting from approximately ±20 degrees inclination. At between 45 – 65 degrees well bore inclination, and at less than optimum fluid flow rates, the solids/cuttings concentration approached a maximum. Depending on the magnitude of flow in the annulus, the well bore inclination at which the maximum solids concentration occurred differed slightly.
2. The so called "avalanche effect", a scenario where beds of solids can slide down the hole at certain flow rates, was found to occur at between 45 – 65 degrees inclination. At sufficiently higher flow rates the avalanche effect disappears.

3. At horizontal or near horizontal well bore inclinations, it was found that for annulus velocities higher than 1.91 ft/s the solids concentration did not significantly increase and was stable at the maximum value. However, below velocities of 1.91 ft/s, the solids concentration behaviour appeared to be less conclusive. Tomren (1979) and Iyoho (1980) observed that for a low flow rate, the thickness of the cuttings bed increased, and reached maximum at between 40 – 60 degrees wellbore inclination. They also observed that the cuttings bed in this range of wellbore inclinations was usually sliding downward against the flow and resulting in very high solids concentration (known as the "avalanche" effect). In general, it was concluded by Tomren et al. (1986) that cuttings bed formed at <2.5 ft/s and <3 ft/s at wellbore inclinations of 40 degrees and 50 degrees respectively.

#### 2.1.2.2 Rate of penetration and wellbore size

At constant flow rate and drilling fluid rheology, the solids / cuttings concentration increases with an increased ROP. The same correlation holds for well bore size – the bigger the well bore, the higher the concentration as more volume of drilled rock cutting is produced by the drilling bit action. Iyoho (1980) confirmed this in his study. Mud volume is also higher in a bigger wellbore; hence it is also dependent on downhole conditions.

#### 2.1.2.3 Drilling fluid rheology (density, plastic viscosity, yield point)

For a given fluid flow rate (or annular velocity), the higher the fluid density or viscosity, the higher the carrying capacity of the fluid. This results in lower solids concentration.

It has been demonstrated by Tomren (1979) that:

1. At lower fluid velocities, the viscosity (the fluid’s resistance to flow) is increased and does have a more pronounced effect on solids concentration. Generally, the fluid with a higher viscosity and density resulted in lower solids concentration because it has a better cutting suspension ability. However, once the solids deposit in a bed of a highly deviated wellbore, the higher viscous fluid is not able to entrain the particles by virtue of lower turbulence intensity (Li et al., 2005; Adari et al., 2000)
2. At higher fluid velocities, there was just a slight reduction in solids concentration if using a more viscous fluid. Further confirming that fluid velocities is the principal parameter in optimizing hole cleaning efficiency.

Becker (1982) demonstrated that a fluid with higher density resulted in lower solids concentration in the annulus because the higher viscosity improves the fluid’s cutting carrying capacity. Crucially, it was important that the absolute difference in mud densities of two fluids need to be significant to get the benefits of improved fluid carrying capacity.

#### 2.1.2.4 Pipe rotation and wellbore size

Due to the vortex effect created by string rotation, the higher the RPM the lower the solids concentration. The vortex effect moves the solids / cuttings into the fluid stream, and if the fluid velocity is optimized, solids concentration can be significantly reduced. Bassal (1995), using a flow loop of 8 inches I.D and inner string of 4 inches O.D found that for 65 degrees well bore inclinations and above, an RPM of between 80 – 150 RPM could result in a reduction of up to 50% in solids concentration.

The above conclusion has been verified from field experience. In addition, the optimum RPM differs with well bore size. Also from field experience, it has been found that for 12 ¼" well bore size, an RPM of between 120 – 150 RPM was optimum for hole cleaning (all other variables remaining constant). However, it has been demonstrated that above a certain pipe rotation speed, there was no further appreciable benefit of pipe rotation on reducing the required critical velocity to aid efficient well bore cleaning (Ozbayoglu et al., 2010, Ozbayoglu and Sorgun 2010).

#### 2.1.2.5 Pipe eccentricity, wellbore inclination, and wellbore size

Well bore size also influences the degree to which eccentricity may impact the solids concentration in the annulus. In a small hole size, and at low flow rates, the solids concentration will be maximum at inclinations of between 40 – 50 degrees (Tomren 1979).

1. High pipe eccentricity results in higher solids concentration. The reason being that there is very little flow (or in an extreme scenario, no flow in the case of highly viscous fluids) in the low side (or space) between the eccentric drill string and the well bore.
2. Highly deviated wells suffer more eccentricity due to gravity. For highly deviated well bores, relatively low viscous fluids are recommended for better hole cleaning efficiency.

#### 2.1.2.6 Bottom Hole Assembly (BHA) Configuration / Drive System, Wellbore Trajectory, and Wellbore Quality

The configuration and drive system of the drilling BHA can play a significant role in hole cleaning. In high angle or horizontal drilling where the risk of cuttings build up is high, the ability to drill with continuous string rotation can influence how efficient the hole cleaning process might be. A mud motor BHA that requires slide drilling at various intervals to achieve the directional objectives of the well may not provide the required RPM downhole to aid the cleaning process in the same way that a rotary steerable BHA can (Jerez et al., 2013). Although limited in dogleg deliverability, the rotary steerable system (RSS) BHAs have demonstrated value in ensuring smooth wellbore trajectories and higher quality of wellbore conditions relative to the mud motor BHAs. Even in cases where the perceived dogleg limitations exist, drilling teams have found innovative ways to extend the capabilities of such RSS BHAs (Yadav et al., 2014).

The quality of the wellbore is a critical factor in the stuck pipe risk potential. It affects the wellbore friction, torque and drag between the BHA and the wellbore wall. Two main approaches (the soft and stiff string) have been used within the industry to describe this interaction between the BHA and the wellbore. The main difference in both approach lies in how the bending stiffness and shearing forces are accounted for (Mirhaj et al., 2016). The most commonly used model for torque and drag in the industry is the soft string model. This is due to its simplicity and relative ease of use (Ohia et al., 2021). The stiff string model is recommended for use in highly tortuous trajectories, high dogleg severity, and stiff BHA tubulars (Zhang and Samuel, 2019). Tripping in or out a stiff BHA in a wellbore with high doglegs, cuttings accumulation, or severely enlarged wellbore with risk of key-seating only increases the risk of getting the BHA stuck. Prior planning and modeling ahead of the drilling operation in terms of the type of conditions that may be encountered while drilling, or during trips can help identify these risks and put in place a recovery or action plan to mitigate such risk of mechanical or differential stuck pipe events (Egbe and Iturrios, 2020).

#### 2.1.2.7 Solid / cutting properties (size, shape, and density)

For the same fluid properties of viscosity, the smaller the solids / cuttings, the higher the solids concentration in the annulus. The smaller solids are more difficult to clean out of the well bore at inclinations of between 65 – 90 degrees. If using low viscous fluids (e.g., water) the smaller solids are harder to transport out of the hole versus if using relatively higher viscous fluid (Duan et al., 2008).

Some of the main conclusions which can be drawn from these effects of drilling parameters are as follows:

1. The CDV or MTV varies with the wellbore size.
2. Irrespective of achieving a velocity greater than the defined CDV or MTV in a well bore annulus, a stationary bed can still form due to eccentricity. Higher pipe eccentricity results in a higher CDV or MTV required to efficiently transport the cuttings to surface
3. CDV or MTV increases as the well bore inclination increases; and the maximum CDV or MTV is usually within the 65 – 75 degrees well bore inclination range (Li and Luft 2014)

4. The drilling fluid type (water based versus oil based versus synthetic fluid) affects the CDV or MTV. Likewise, and as should be expected, the fluid properties affect the CDV or MTV. Fluids having higher mud densities, plastic viscosities (PV) and yield points (YP) usually require higher CDV or MTV and vice-versa (e.g., for the same test conditions, water will have a lower CDV compared to oil-based mud). Basically, the lower density and lower viscous fluids have a comparatively lower resistance to flow, creates a turbulent flow regime easily, and thus the CDV or MTV for such fluids are lower compared to denser more viscous fluids
5. The drilled cuttings size and density affect the CDV or MTV. The smaller sized cuttings are relatively more difficult to get out of the hole and require higher CDVs or MTVs compared to the larger sized cuttings. If the smaller cuttings are further allowed to settle, it is even harder to fluidize or re-suspend a second time around.
6. A high rate of penetration (ROP) results in a higher CDV or MTV. This is due to the increase in annulus solids concentration in the well

From these conclusions the annular fluid velocities and the well bore inclination are two very critical factors which impact the efficiency of hole cleaning in a well bore. Both these factors in turn greatly influence the CDV or MTV, which is an important factor to consider in solids transport modelling. The CDV or MTV is also intrinsically linked to the solids or cuttings concentration profile in a well bore annulus. Hence an accurate modelling of the solids or cuttings concentration profile in a well bore is important to accurately predict the hole cleaning efficiency.

Bourgoyne et al. (1986) introduced the concept of the “transport ratio”. The transport ratio is defined as the transport velocity divided by the mean annular velocity; and it may be used to give an indication of the ease at which solids / cuttings will be transported to surface. For a “positive” value of transport ratio, the solids / cuttings will be lifted to surface, and vice versa. As the solids / cuttings slip velocity increases the transport ratio decreases; and critically, the solids concentration in the annulus increases. This may be regarded as the onset, and perhaps inferred to as the tipping point at which the annulus starts to become loaded with drilled solids / cuttings.

### 2.1.3 Summary of Effect of Drilling Parameters on the Efficiency of the Cuttings Transport Process during the "stationary or wiper trip" hole cleaning phase

After the drilling phase has been completed and the well bore has been deepened to the planned section or total depth, any drilled cuttings still remaining in the hole must be removed. This is done to ensure the smooth deployment of casing tubulars or in some cases, down-hole production or injection tubulars (i.e., completion strings). Some of these tubulars are quite expensive so it is important that they can be deployed without issues such as a stuck pipe event. Historically, a significant proportion of stuck pipe events with either the drill string or with casing / down-hole completion systems have occurred post drilling operations (Egbe et al. 2020). This has always led to expensive remedial operations to rescue the well resulting in avoidable costs and non-productive time.

Post drilling operations, hole cleaning can be achieved either via a "wiper trip" or "circulating the hole clean (CHC) whilst the string is stationary". A wiper trip hole cleaning operation involves "pulling out of hole (POOH)" with the string whilst maintaining an optimum RPM and flow rate. The axial motion of the string together with the string rotation and flow rate agitates and moves the drilled cuttings into the flow stream. The bit nozzles also assist in fluidizing the solids / cuttings bed and enhance efficient transportation.

A stationary hole cleaning operation involves keeping the string relatively stationary, with limited axial movement (usually over a 30 – 90 feet interval), while pumping drilling fluid and rotating the string at an optimum flow rate and RPM.

Regardless of which hole cleaning practice is deployed, further optimization of well parameters may be required to enhance the cleaning efficiency. For example, "sweeping" pills may often be required; or improving the fluid properties such as density and/or viscosity to improve the fluid carrying capacity. Even staggering the fluid flow rate is a proven technique to use in ensuring efficient hole cleaning.

Many parameters affect how long we should circulate the well bore or how many wiper trips are required to ensure the well bore is clean. This section will provide an overview on how these parameters (either individually or combined) affect the hole cleaning efficiency. Bear in mind that even with the most efficient and optimized hole cleaning practice, we can never 100% fully recover all drilled cuttings to surface. This is mainly due to equipment limitations (e.g., pump output, RPM limitations, down-hole tool limitations). However, although that is the reality of the situation, we can strive to erode the bed height to an acceptable level that poses no challenge to the integrity of the well whilst running in hole with other tubulars.

Hole cleaning efficiency at the post-drilling phase, whether this is in the stationary or in the wiper trip mode is heavily influenced by the ability of solids or cuttings to be re-suspended from a state of rest after settling. The minimum critical velocity at which such solids / cuttings can be re-suspended again such that the bed height is eroded is referred to as the "critical re-suspension velocity" (Larsen 1990; Duan et al., 2009). It is also sometimes referred to as the "pick-up velocity" (Rabinovich and Kalman 2007) or the "particle rolling velocity" (Ramadan et al., 2003). For the sake of this research the "critical re-suspension velocity (CRV)" will be used. Rabinovich and Kalman (2007) developed a curve to predict the critical re-suspension velocity (CRV). The curve defined the relationship between the modified

Reynolds number and the Archimedes number; and the curve was divided into three zones.

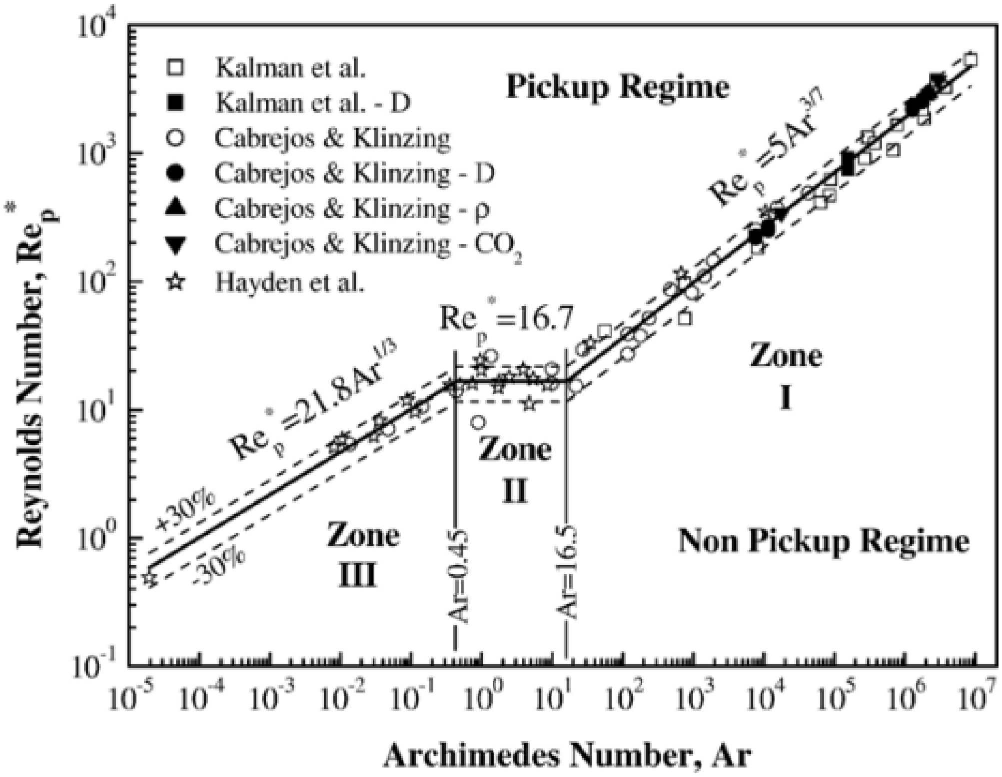


Figure 2.1: Modified Reynolds Number as a Function of Archimedes number (Rabinovich and Kalman 2007)

For each zone, the modified Reynolds number is defined by a power function of the Archimedes number.

- Zone I: was for large particles. The Archimedes number is high and the forces of cohesion in any fluid is negligible
- Zone II: was for smaller particles; and in dry systems the CRV was observed to increase as the particle diameter decreased

- Zone III: was for fine powders; and the forces of cohesion were found to be so high that the particles experienced motion in agglomerated groups

In summary, and with reference to the concept of Van der Waal's forces, it is apparent that the magnitude of cohesive forces experienced by the particles affects the CRV (Rabinovich and Kalman 2007). However, it should be noted that the study by Rabinovich and Kalman (2007) was for dry powders. This is not necessarily the condition that exists in the well bore. Never-the-less, the findings are aligned with field proven experiences that smaller solids / cuttings are more difficult to transport out of the well bore. Other researchers who have done similar work include Bizhani (2013), Corredor (2013), and Ramadan et al. (2003). Bizhani (2013) and Corredor (2013) determined the CRV in a horizontal but concentric annulus. In reality, the drill string is more eccentric than concentric in the well bore. In a fully eccentric scenario, the CRV would be higher compared to that observed in a concentric annulus, flow in a pipe, or in an open channel. Two important conclusions from the study conducted by Ramadan et al. (2003) are as follows:

- At the same test conditions, the CRV in a pipe flow will be the same as in a fully concentric annular flow. This then follows that if it can be robustly demonstrated that a drill string is fully concentric, correlations for pipe flow may be used to predict hole cleaning in deviated well bores. The questions however are thus
    a) How realistic is it that the drill string will be concentric to the well bore?
    b) When could a fully concentric drill string be envisaged; and under what condition (or set of conditions) would that be expected?

- The CRV increases as the well bore inclination increases; and with a maximum value obtained at approximately 60 degrees inclination

The above findings make logical sense because as the well bore inclination increases, so does the magnitude of eccentricity. And as the eccentricity increases, so would the CRV increase due to the low fluid velocity in the narrowing space between the sagging drill string and the wall of the well bore. In that instance, when the fluid velocity is lower than the CRV, the fluid erosion rate of the cuttings bed can be assumed to be negligible or tend towards zero. Li and Luft (2014) reached the same conclusions.

The effects of various drilling parameters on cuttings bed erosion time are discussed in sections 2.1.3.1 – 2.1.3.4.

#### 2.1.3.1 Annulus fluid velocity and drill pipe rotation

Investigations conducted by Adari et al. (2000) concluded the following:

1. At a specific given pump rate, the decrease in bed height is an exponential function and there is a minimum flow rate below which cuttings bed erosion would not occur. This further validates the fact that fluid velocity in the annulus is one of the critical factors that impact how long it takes to clean a well bore.
2. Applying pipe rotation (RPM) in the right range can save as much as 50% of hole cleaning time. This was also validated by Sapru (2001), who observed that even pipe rotation as low as 20 RPM made a difference
3. It should be noted that maintaining a fixed optimized flow rate does not necessarily always result in efficient hole cleaning. As the bed height is eroded, there may come a time where the flow rate may no longer be effective (the

exponential trend plateaus out). In such a situation the flow rate may need to be optimized (i.e., stepwise increase) to be able to effectively erode the new and reduced bed height. The benefit of a stepwise increase in flow rate to enhance hole cleaning has been observed in the field.

#### 2.1.3.2 Drilling fluid properties

For well bores with inclinations from 60 – 65 degrees to horizontal, less viscous fluids have been found to deliver greater bed erosion compared to relatively more viscous fluids. The less viscous fluids have been observed to create more agitation & turbulence, hence increasing the likelihood of being transported to surface. Relatively more viscous fluids are more likely to exhibit a laminar flow which will not be effective in eroding a bed height (Li et al., 2002, Adari et al., 2000).

However, it should be noted that although the less viscous fluids are more effective to erode an accumulated bed height, such fluids do not possess very good cuttings carrying capacity. As such a compromise must be made. More viscous fluids exhibit greater carrying capacity; and the higher a fluid's carrying capacity, the more efficient it is for solids transportation and the well bore cleaning process. Hence the challenge is to re-suspend solids which have settled and maintain such re-suspended solids in the fluid stream to be transported. From field experience this may be achieved either via mechanical means; or as is the common practice, via a combination of sweeping pills (low-viscous pills immediately followed by weighted high-viscous pills). In addition, pipe rotation at a suitable RPM would contribute to the hole cleaning efficiency.

#### 2.1.3.3 Drill pipe eccentricity and wellbore inclination

Yateem et al. (2013) demonstrated that:

1. The more inclined a well bore, the harder it is to efficiently clean that well bore.
2. The bed erosion rate is directly proportional to the well bore inclination; and it takes longer to clean such well bores

Eccentricity severely impacts bed erosion time by slowing the entrainment of solids into the fluid stream, and their subsequent transportation to surface. When the string was concentric, the conditions were more favorable for solids removal at lower fluid velocities.

#### 2.1.3.4 Wiper trip out of hole

The wiper trip hole cleaning method has been confirmed to be more efficient when compared to stationary hole cleaning method (Walker and Li 2001, Sample and Bourgoyne 1977). Yateem et al. (2013) demonstrated an exponential relationship between the solid's removal speed and the fluid velocity required to erode a bed using different post-drilling hole cleaning methods. It was concluded that the stationary cleaning methods required higher fluid velocities and longer times to erode a solids / cuttings bed.

Factors such as the fluid velocity in the annulus, well bore inclination, drilling fluid properties, solids properties, jetting, and string eccentricity affect the wiper trip speed. The optimum wiper trip speed is the speed at which the string can be POOH to achieve maximum removal of solids from the well bore. If the POOH speed is higher than this optimum, a certain volume of solids will not be recovered. Li and Walker (1999) and Walker and Li (2000) conducted investigations related to the optimum wiper trip speed. They developed a wiper trip hole cleaning efficiency curve relating hole cleaning efficiency to a dimensionless wiper trip speed.

## 2.2 Research Concepts Considered for Developing Cuttings Transport Models

In addition to the typical concepts used in the development of the various cuttings transport models, emphasize will be placed on the following concepts to help provide further insights in this research. Some of these have been referenced by previous researchers; and it is believed that the inclusion of the physics of these concepts do help in extending the current body of knowledge in the field.

### 2.2.1 Effect of Centrifugal Forces on Drilled Cuttings Settling Velocity

Recall that once the flow of drilling mud is stopped for a connection (i.e., make-up additional drill pipe), the drilled cuttings will experience a period of gravitational or centrifugal settling. However short that period may be, it is important to understand what happens in the annulus. To help this understanding, this section explores motion of solids through fluids.

Imagine a single drilled cutting falling by gravity (i.e., "free settling") through the drilling mud in the annulus of a vertical well. Three forces are known to act on that drilled cutting. These are as follows (Maude and Whitmore 1958):

1. External forces ($F_e$): could be gravitational or centrifugal
2. Buoyant forces ($F_b$): Acting along the same line of action of the external forces, but in opposite direction
3. Drag forces ($F_D$): Acting in the opposite direction to the drilled cutting motion and along the same line of motion

For simplicity (and because it is more often the case), it is assumed that the lines of action of all the forces acting on the drilled cutting are collinear (McCabe et al., 1993). This assumption will apply to vertical wells. For deviated or high angle wells (> 10 degrees wellbore inclination) which this research focuses on, the wellbore inclination from the vertical plane will be accounted for in the force balance equations to be developed.

As per work done by McCabe et al. (1993), and for a vertical well, the following force equations apply:

$$F_b = \frac{m\rho_f a_e}{\rho_s g_c} \qquad \text{Eqn. 2.1}$$

$$F_D = \frac{C_D U_0^2 \rho_f A_p}{2g_c} \qquad \text{Eqn. 2.2}$$

$$F_e = \frac{m a_e}{g_c} \qquad \text{Eqn. 2.3}$$

For the drilled cutting of density ($\rho_s$) falling through the mud of density ($\rho_f$), and under gravity (g) or centrifugal forces at a velocity, $U$, the resultant force acting on the cutting is (McCabe et al., 1993):

$$F_e - F_b - F_D$$

The acceleration of that drilled cutting is the rate of change of the velocity over time (t), $\frac{du}{dt}$. If the mass (m) of the cutting is assumed constant, and substituting for the above forces, McCabe et al. (1993) showed that:

$$\frac{du}{dt} = \frac{a_e(\rho_s - \rho_f)}{\rho_s} - \frac{C_D U^2 \rho_f A_p}{2m} \qquad \text{Eqn. 2.4}$$

If the cutting is falling due to gravity (g), $a_e$ is the acceleration due to gravity. Equation (2.4) then becomes

$$\frac{du}{dt} = \frac{g(\rho_s - \rho_f)}{\rho_s} - \frac{C_D U^2 \rho_f A_p}{2m} \qquad \text{Eqn. 2.5}$$

However, in a rotary drilling scenario where the string has been rotating at a particular revolutions per minute (RPM), the drilled cutting may still be under the influence of centrifugal forces while settling. Making a drill pipe connection typically last between 5 – 10 mins if done efficiently. The question thus arises: does the centrifugal forces decay completely in that time after the string rotation has been stopped? Or can we imagine that the drilling fluid may still be "swirling" for a period afterwards such that settling of the drilled cutting is influenced? McCabe et al. (1993) found that for a particle in a centrifugal field with an angular velocity, $\omega$, and radius of path, $r$, the acceleration due to that centrifugal field is:

$$a_e = r\omega^2 \qquad \text{Eqn. 2.6}$$

And equation (2.5) becomes

$$\frac{du}{dt} = \frac{r\omega^2(\rho_s - \rho_f)}{\rho_s} - \frac{C_D U^2 \rho_f A_p}{2m} \qquad \text{Eqn. 2.7}$$

For a drilled cutting experiencing "free fall", the cutting would reach a "terminal velocity ($u_t$)" at some point. At terminal velocity, the acceleration (i.e., the rate of change of velocity with time, $\frac{du}{dt}$) equals zero. And equations 2.5 and 2.7 can be resolved to obtain the expressions for terminal velocity in a gravitational or a centrifugal settling regime.

$$u_t = \sqrt{\frac{2g(\rho_s - \rho_f)m}{A_p \rho_s C_D \rho_f}}, \text{ for gravitational settling} \qquad \text{Eqn. 2.8}$$

$$u_t = \omega\sqrt{\frac{2r(\rho_s - \rho_f)m}{A_p \rho_s C_D \rho_f}}, \text{ for centrifugal settling} \qquad \text{Eqn. 2.9}$$

However, a drilled cutting is unlikely to exhibit free fall settling as a single individual cutting. It is more likely the case that the cuttings would exhibit cohesion amongst itself (due to Van der Waal's forces) and will settle in clusters. Even if it does not settle in clusters, because of the concentration of cuttings present in the annulus, the influence of other cuttings cannot be ignored. On this basis, the concept of "hindered settling" appears to be appropriate to consider. This does not imply that the constructs presented earlier are not applicable. It just means that it would be applied differently.

### 2.2.2 Hindered Settling in Stirred Tanks

"Hindered settling" in Chemical Engineering discipline is the process by which the settling of drilled cuttings particle is impeded due to the proximity of other cuttings. Consequently, if hindered settling is the more dominant settling mechanism taking place in an annulus, we can expect that it would influence several fluid factors notably the drag force experienced by the cutting. The drag coefficient, $C_D$, experienced by a cutting under free fall would be less than that experienced under hindered setting. The terminal velocity estimations (including the length of time taken to achieve it) would also be influenced as a result.

Maude & Whitmore (1958) present an empirical relationship for estimating the hindered settling velocity,$U_s$, from the terminal velocity ($U_t$) of a single isolated particle experiencing free settling as follows:

$$U_s = U_t(\varepsilon)^n \qquad \text{Eqn. 2.10}$$

Limitations on the above expression such as particle shape and size distribution exist. Nevertheless, it still provides a good estimation. "$\varepsilon$" and "$n$" are influenced by the fluid regime (Stoke's law and Newton's law region) at any given time. "$n$" is a function of the particle shape, size distribution, and Reynolds number. "$\varepsilon$" is the volume of solid per unit volume of suspension.

### 2.2.3 Taylor-Couette Flow

The Taylor-Couette flow is the result of the shear flow between a rotating inner cylinder, and a concentric or eccentric but stationary outer cylinder. The shear flow is driven by the motion of the inner cylinder in contact with a viscous fluid in the annular space between both cylinders. This is analogous to what obtains with a rotating drill string in a wellbore. The wellbore is the stationary outer cylinder.

Taylor (1923) demonstrated that in a case of viscous non-Newtonian fluid, the shear flow between both cylinders become unstable when the rotational speed of the inner cylinder exceeds a critical speed; thus, creating toroidal vortices which exist in pairs. As the nature of the flow regime varies along the axial, tangential, and radial (or rotational) directions, it is proposed that the Taylor number is more representative of the flow regime, than the traditionally used Reynolds number.

This view is supported by Potter et al. (2002) who state that as fluid is flowing through an annulus, if there is pipe rotation, the flow regime may be turbulent in the rotational direction even though it is laminar in the axial direction. Potter et al. (2002) also concluded from experiments that as the rotational Reynolds number exceeds 1,700, the laminar flow regime ceases to exist even though the axial Reynolds number was less than 2,300. The rotational number "1,700" is the critical

Taylor number ($Ta_{cr}$). Diprima (1960) and Stuart (1958) investigated Taylor's conclusions regarding fluid stability between rotating cylinders by applying non-linear theory; and they arrived at the same conclusions. Nakabayashi et al. (1974), Nouri et al. (1993), Nouri and Whitelaw (1994) agreed with Taylor (1923) and established that the magnitude of the critical Reynolds number decreased as the radial or rotating Reynolds number and ratio of eccentricity increased (Kim et al., 2006).

Ford et al. (1990) demonstrated in their experimental work that the cutting transport efficiency was greatly improved with string rotation. Lockett et al. (1993) qualitatively agreed with Ford et al. (1990) and demonstrated that should Taylor vortices be present in a drilling annulus, the cuttings bed formed on the low side of a high angle annulus will experience an oscillatory force due to the vortices. They also concluded that for a given strength of vortices, the peak of the oscillation is sufficient to lift cuttings with a mass less than some critical value, away from the wall of the wellbore.

Escudier et al. (2002) proposed that a velocity ratio relationship may be used to distinguish when flow between a concentric or eccentric annulus with inner cylinder (or free body) rotation is predominantly axial or rotation dominated, or mixed. Based on these research efforts, it is safe to conclude that the use of a Reynolds number criteria for defining turbulence in drilling operations has limitations because at Reynolds number greater than 1,700, inertial instabilities occur which lead to the well-known Taylor vortices. The theories of Taylor-Couette flow will be used to develop a relationship for the azimuthal velocity profile using a Herschel-Bulkley fluid model.

### 2.2.4 Van Der Waals Forces

Particles near each other experience inter-particle forces. As the solids or particles diminish in size, so does the magnitude of the inter-particle force increase due to the increase in surface area per unit volume. It has been established that for fine particles or solids in close contact, the Van Der Waals forces are the dominant forces (Hiemenz 1986). Van De Ven (1989) further found that the forces are attractive if the solids or particles are made of the same material. However, these attractions are not as a result of chemical electronic bonds. They are comparatively weak, and hence are susceptible to disturbance. At increased distances between interacting atoms or molecules, the Van Der Waals force quickly disappears. The concept however will be applied in this research to estimate the critical re-suspension velocity (CRV). As previously defined, the CRV is the velocity required to re-suspend a cuttings bed into the flow stream to be transported to surface.

### 2.2.5 Fluidized Beds

Consider a scenario during drilling, while the drilling mud is pumped through the drill string and past the cuttings bed generated by the action of the drill bit, a pressure drop will exist. This pressure drop will be directly proportional to the mud annular velocity. As the flow rate of the drilling mud in the annulus is further increased, the mud annular velocity would also increase, and may go over and above a critical annular velocity. As the mud annular velocity is increased towards and beyond the critical annular velocity, there would come a point in time where there will be less of an effect on the pressure drop. At this point, the pressure drop across the drilled cuttings bed will be relatively constant for a constant fully formed flow.

At the bottom of the well, the pressure-drop across the drilled cuttings bed for a constant flow rate of drilling mud with homogeneous rheological properties, and at a given depth will not change. By the concepts of fluidized bed theory, the pressure-drop, drilled cuttings bed cross sectional area, and the force of the weight of the drilled cuttings can be related by the following equation (Ergun 1952):

$$\Delta P = h(1 - \text{Ø})(\rho_s - \rho_f)g = \left(\frac{gM_s}{A}\right)\left(\frac{\rho_s - \rho_f}{\rho_s}\right) \qquad \text{Eqn. 2.11}$$

Where:

ΔP = Pressure drop across the drilled cuttings bed

h = height of the drilled cuttings bed

Ø = Drilled cuttings bed voidage (in a drilling scenario, the degree of packing, and the voidage can be assumed)

$M_s$ = Total mass of drilled solids in the cuttings bed (this may be estimated from the volume of cuttings a particular bit may be able to generate

A = Drilled cuttings bed cross-section area

With reference to the Geldart groupings (Geldart 1973), drilled solids may be assumed to fall into group "C" & "D"

- Group C: Contains extremely fine and highly cohesive solids. These groups of solids are difficult to fluidize once settled. They may require mechanical agitation

- Group D: Typically sized above 600μm with significant densities. They require light fluid flow to fluidize and can be abrasive

To predict the critical annular velocity for fluidization, one half of eqn. 2.11 may be used such that:

$$\Delta P = h(1 - \emptyset_m)(\rho_s - \rho_f)g \qquad \text{Eqn. 2.12}$$

Equation 2.12 implies that the pressure-drop experienced equals the effective weight per unit area of the drilled cuttings bed. $\emptyset_m$, the drilled cuttings bed voidage, may be considered as the bed voidage at incipient or critical fluid velocity. The voidage may be estimated by assuming a particular lattice packing structure for the drilled cuttings bed.

Following on from above, the Ergun's equation (Ergun 1952) for spherical particles in packed beds can thus be used to estimate the pressure drop, $\Delta P$, as follows:

$$\frac{\Delta P}{h} = \left\{\frac{150\mu U_{mf}}{D_p^2}\frac{(1-\emptyset_m)^2}{\emptyset_m^3}\right\} + \left\{\frac{1.75\rho_f U_{mf}^2}{D_p}\frac{(1-\emptyset_m)}{\emptyset_m^3}\right\} \qquad \text{Eqn. 2.13}$$

Note:

$\emptyset_m$ = minimum voidage or porosity of the cuttings bed for fluidization to occur

$\mu$ = fluid viscosity

$D_p$ = particle diameter

$U_{mf}$ = critical annular velocity for fluidization (as defined by Ergun)

To account for the fact that the drilled cuttings would not be spherical in shape, a "sphericity factor, ϕ, is introduced into eqn. 2.13 such that:

$$\frac{\Delta P}{h} = \left\{\frac{150\mu U_{mf}}{\phi_s^2 D_p^2}\frac{(1-\emptyset_m)^2}{\emptyset_m^3}\right\} + \left\{\frac{1.75\rho_f U_{mf}^2}{\phi_s D_p}\frac{(1-\emptyset_m)}{\emptyset_m^3}\right\} \qquad \text{Eqn. 2.14}$$

Eqn. 2.14 has been found to fit data for spheres, cylinders, and crushed solids over a wide range of flow rates.

#### 2.2.5.1 Conditions for fluidization in a well

Transferring Ergun's theories, the conditions for fluidization in a well are summarized below. The following assumptions are held:

1. At low flow rate, annular velocity $(U)$ is less than the critical annular velocity. Mud will pass through the drilled cuttings bed and over it without causing any solids movement. However, there will be a pressure drop proportional to the superficial velocity.
2. As the flow rate is increased, the annular velocity increases, and the pressure drop increases. However, the drilled cuttings are still immobile. The bed height remains the same, and $(U < critical\ annulus\ velocity, U_{mf})$.
3. At a critical velocity ($U = U_{mf}$) in the annulus, the force of gravity (or the weight of the drilled cuttings is just balanced. At a velocity ($U > U_{mf}$), the drilled cuttings will move but the cuttings bed may not "separate or expand" at this point.
4. With further increases in velocity such that $U \gg U_{mf}$, the cuttings bed will separate enough to begin to exhibit individual motion (albeit somewhat restricted) within the bed. This is the point of fluidization.

5. Once fluidization occurs, the pressure-drop ($\Delta P$) across the drilled cuttings bed remains the same. However, the cuttings bed will continue to separate with increased flow rate
6. If the flow rate is reduced or stopped altogether, the drilled cuttings bed will begin to settle. The final "bed height" will differ each time flow is stopped and may sometimes be greater than the initial bed height. It is theorized that this is the case because solids slowly settling from a fluidized state do not tend to pack so tightly, or in the same way prior to being fluidized. There would however be a tendency for the larger solids to settle faster than the smaller/finer solids due to gravity. The smaller/finer solids will settle later if the system is left long enough and undisturbed. Should this be the case, it is believed that there is a significant probability for these finer solids to "cement" the larger solids in place; potentially making it more difficult to fluidize the next time around
7. The cementation mentioned above is suspected to be due to the very strong interstitial, particle-to-particle forces (or Van der Waal's forces) known to be of significant magnitude in very small or fine solids. This needs to be considered in the over-all force equation

Based on point 6 above, it would suggest that the "$\Delta P$" for subsequent fluidization start-ups will be less than the first or initial start-up. Hence it may also be theorized that "the minimum fluidization velocity (or critical annular velocity)" is not constant. It will change each time drilling mud flow is stopped.

## 2.3 Review of Existing Stuck Pipe Prediction Methods and Capabilities

Several major oil and gas operators, oilfield service providers, and drilling rig contractors have invested significant resources in the prevention, mitigation, and prediction of stuck pipe events. Such efforts have been concentrated on well engineering design, operational competence, and the development and implementation of tried and tested field best practices. However, the implementation of these efforts has largely been found to be inconsistent in many instances. There is an element of subjectivity as the human interface is still required to recognize impending stuck pipe symptoms and take certain decisions which may be regarded as being critical to the prevention of a potential stuck pipe event. Unsurprisingly, the frequency of stuck pipe events within the industry remains high, and accounts for a significant proportion of non-productive time. Thus, a need to automate the detection of early stuck pipe indicators to give drilling crews warning alerts, represents a consistent approach to stuck pipe prediction. This approach, when efficiently developed and implemented, can present an accurate and robust method in preventing the occurrence of stuck pipe events.

Several proprietary automated stuck pipe prediction methods exist in the industry. Limited information on some of these may be found in the public domain; but majority of the efforts are held in confidence. As such it is a challenge to fully evaluate the advances that have been made over the years. Section 1.1 of this thesis has discussed the historic work done by previous researchers. The section also differentiated the efforts at automating the prediction of stuck pipe into five main groups as summarized in Table 1.1.

This research proposes to use a statistical approach combined with analytical well design models to predict the onset of a stuck pipe event. The data patterns, rates of change of data from point to point, or deviation change of real-time drilling data from previously observed trends (anomaly detection), or comparison of actual measured data versus a well design model predicted value can be used to identify downhole anomalies indicative of several drilling challenges including stuck pipe events. The combined approach can be enhanced further with any machine learning technique to deliver real-time prediction capabilities.

A review of different statistical analysis techniques (including a brief their associated deficiencies), and statistical methods is presented in the next section.

### 2.3.1 Review of Statistical Analysis Techniques and Methods

There are seven types of statistical analysis. These are described as follows:

- Descriptive statistical analysis: This is the simplest form of statistical analysis and uses numbers to describe qualities of data set. It summarizes characteristics and distribution of values in one or more data sets; and allows analysts to assess the central tendency and variation of data in spatial context (Lee 2020). Data visualization tools such as tables, graphs and charts are used to make analysis and interpretation easier. It is not suited for drawing conclusions; but allows the application of more sophisticated tools to draw inferences (Nisbet et al., 2018).
- Inferential statistical analysis: This type of analysis helps researchers reach conclusions that extend beyond the immediate data set. It allows the ability to draw conclusions based on extrapolations and is fundamentally different from

descriptive statistics that merely summarize the data that has been measured (Chin and Lee, 2008). Inferential statistics analysis is explicitly designed to test hypotheses.

- Associational statistical analysis: This is used by researchers to make predictions and find causation. It is a tool that can be used to identify interdependence among multiple variables in a data set or across data sets. In this technique, a wide range of coefficients of variation, including correlation and regression analysis is used to determine inferences and predictions about a data set from the characteristics of another data or groups of data (Nisbet et al., 2018).
- Predictive analysis: This technique uses historic and current data to make predictions about future unknowns. It relies on a wide range of probabilistic techniques such as data mining algorithms, big data statistics (e.g., logistic regressions, decision trees, time series, etc.), predictive modelling (e.g., well design models), and simulations to guess what is likely to occur in the future (Nisbet et al., 2018; Lepenioti et al., 2020). It is important to note that predictive analysis can only make high quality forecasts depending on the accuracy of the models and underlying data sets from which it refers.
- Prescriptive analysis: This type of analysis helps organizations use data to guide their decision-making process. Prescriptive analysis has two levels of human intervention – decision support (i.e., providing recommendations) and decision automation (i.e., implementing the prescribed action) (Lepenioti et al., 2019). Companies can use tools such as graph analysis, algorithms, machine learning and simulation for this type of analysis. Prescriptive analysis

helps businesses make the best choice from several alternative courses of action.

- Exploratory data analysis: This technique is used to identify patterns and trends in a data set. They can also use it to determine relationships among samples in a population, validate assumptions, test hypotheses, and find missing data points (Nisbet et al., 2018).
- Causal analysis: This technique uses data to determine causation or why things happen the way they do. It is an integral part of quality assurance, accident investigation and other activities that aim to find the underlying factors that led to an event. Companies can use causal analysis to understand the reasons for an event and use this understanding to guide future decisions (Nisbet et al., 2018).

The four common methods for performing statistical analysis are listed below as follows:

- Mean (or average): This is the first method used to perform statistical analysis, and it calculates the central point of the data being analysed. It allows for determining the overall trend of a data set. It is a simplistic and quick calculation which allows users the ability to obtain a fast and concise view of the data. However, the mean is not recommended as a standalone statistical analysis method. It does not give the most representative result especially when dealing with large data points with either a high number of outliers or inaccurate distribution (Calvello 2020).
- Standard deviation: This method of statistical analysis measures the spread of data around the mean. It is useful when determining whether a set of data

points are clustered or not. A low standard deviation will suggest that most data points are in line with the mean, and can be called the expected value set

- Regression: This shows the relationship between a dependent variable (the data to be measured), and an independent variable (the data used to predict the dependent variable). A major disadvantage of regression is that it ignores the reasons for why the outliers exist in a particular data set, and only focuses on the trends in the data.
- Hypothesis testing: This is a technique used to establish if a certain argument or conclusion is true for the data set. It allows for comparing the data against various hypotheses and assumptions. Hypothesis testing can sometimes be skewed by the "placebo effect". This is when the expectations to see a certain outcome clouds the judgement even though the data may be suggesting otherwise.

For statistically detecting an impending stuck pipe event, the outliers in a data set that are different from an observed trend are used as the indicators of a worsening downhole condition. To achieve this, a combination of descriptive, inferential, and predictive analysis techniques is proposed in this research.

In performing the analysis, the z-score (also called the "standard score") method, which is a numerical measurement that describes the relationship between a data point to the mean of a data set is used (Lepenioti et al., 2020). A z-score represents how many standard deviations above or below the mean population the score derived from a z-test is. The z-score method is selected in this research because the drilling data acquired in real-time falls into a normally distributed frequency. Hence, with the z-score method

a. The probability of a score occurring within a normal distribution can be calculated by standardizing the scores. Thus, any data outside that distribution curve is identified as an anomaly which could be indicative of a downhole problem, in this case, a stuck pipe event.
b. Two or more scores that are from different normal distributions can also be compared. This allows the assessment of how real-time drilling data obtained while drilling with a current stand or joint of drill pipe differs from the previous stand or joint of drill pipe that had been drilled
c. A combination of (a) and (b) above is proposed by this research for anomaly detection of the onset of a potential stuck pipe event. Thus, the z-score is a predictive statistics analysis method
d. As descriptive statistics, z-scores describe exactly where each data point is in the distribution. As inferential statistics, z-scores determine whether a specific sample is representative of its population or is extreme and unrepresentative.

Key takeaways for using the z-score method are as follows:

- A z-test is a statistical test to determine whether two population means are different when the variances are known, and the sample size is large.
- A z-test is a hypothesis test in which the z-statistic follows a normal distribution.
- Z-tests are closely related to t-tests, but t-tests are best performed when the data has a small sample size.
- Z-tests assume the standard deviation is known, while t-tests assume it is unknown

## 2.4 Review of Fundamentals Related to Cutting Transport Models

### 2.4.1 Summary of Cuttings Transport Correlations and Models

As previously mentioned, studies involving experimental or empirical observations estimated the cuttings transport efficiency by predicting the cuttings bed height, annular cuttings concentration in the wellbore, area occupied by the cuttings bed, and the ratio of the mass of suspended cuttings to the mass of the originally deposited drilled cuttings. These observations were within the bounds of certain conditions and parameters. Other studies using numerical analysis, or mechanistic models (e.g., two-layer or three-layer) achieved the same objective by predicting the critical velocities (annular, settling, and fluid) required to keep the annular cuttings concentration to a minimum (Li and Luft 2014).

### 2.4.2 Layer Modelling: Two-Layer vs Three-Layer Models

In describing the solids / cuttings transportation process, consideration should be given to the fact that the down-hole environment in which the process is occurring is rapidly changing and varies in time. Hence it can be expected that the concentration and velocity of solids in the wellbore will vary in time, and along the length of the said wellbore.

As a result, understanding and describing the concentration and velocity profiles can be considered as critical, if not more than simply calculating a CSV or CRV value. It should also be pointed out that the solids / cuttings transport process is an unsteady state process; and therein lies the challenge. The problem posed by the solids / cuttings transport process is also a three-dimensional problem; and is affected in the longitudinal axial coordinate as well as in the radial coordinate.

Majority of the mechanistic models are based either on the two-layer (Duan et al., 2009, Naganawa and Nomura 2006, Costa et al., 2008), or the three-layer approach (Guo et al., 2010, Wang et al., 2010). A few others have based their approach on the "kinematic two-layer models" (Aitken and Li 2013). The governing equations for layer modelling constitute

- Mass conservation equations for both solids and liquid phases
- Momentum equations for the different layers
- Related closure equations

The two-layer and three-layer models are "transient models"; and they make a distinction between solids moving with liquids and solids in a stationary or moving bed. The inadequacy of this approach is that there is a significant level of generality introduced to the solid transport analysis. This is supported by Li and Luft (2014) who point out that it introduces all the "well-known problems of transient two-fluid models such as the need for a well-posed problem and the need to deal with the propagation of pressure waves". It is on this basis that the kinematic two-layer approach is favored. The kinematic two-layer approach neither distinguishes between solids moving with liquid and solids contained in a stationary bed nor solids moving with liquid and solids contained in a moving bed. In the kinematic two-layer approach, steady state continuity and momentum equations are used versus the transient forms applied in the two-layer and three-layer models. Assuming a steady state scenario obviously simplifies the problem. In addition, the mass balance equations that ensues from the kinematic two-layer approach can be solved if the fluxes of solids and solids exchange rate can be defined in terms of the total true area occupied by the solids in the annulus; and the total true cross-sectional area occupied by the solids in the bed layer.

#### 2.4.2.1 Two-Layer Modelling

With the CSV, CRV, and AAV estimated, a comparison can be made to a defined critical minimum fluid velocity such as the CTFV or CAFV to establish whether drilled cuttings may deposit in the annulus or not. Together with the removable cutting concentration profile, an assessment or prediction of the hole cleaning efficiency can be made using the cutting transport ratio. At this stage, the methodology developed by Larsen et al. (1997) for estimating the CTFV is thought to be robust.

Two-layer modelling is preferred over three-layer modelling for the following reasons:

a. Two-layer approach is simplistic compared to the three-layer approach. It considers a suspension and bed layer each. In comparison, the three-layer approach considers a cuttings bed, suspension layer, and a liquid or fluid layer
b. In simplifying the approach, Gavignet and Sobey (1989) assumed the following for the two-layer model:
    i. All the cuttings fall to the low side because of wellbore inclination
    ii. The cuttings bed is closely packed. Hence the cuttings concentration ranges between 50 – 60%
    iii. Saltation, the mechanism for dispersing particles at high flow rates and in wells with low wellbore deviations, is neglected

iv. Hydrostatic pressure is neglected because the cuttings bed is closely packed and mechanically support each other. Hence, the hydrostatic pressures in both layers are the same. Thus, if a pressure gradient is eliminated, an equation that relates the stresses at the wellbore walls to the interfacial stress can be obtained.

v. The cuttings wall stress is assumed to be the sum of the fluid friction effect, and the sliding friction of cuttings in the bed

c. As a result of the simplifying assumptions in b(i) – b(v), there are fewer variables and equations to resolve in the two-layer approach in comparison to the three-layer approach. This introduces errors in the calculation. However, as stated by Gavignet and Sobey (1989), a representation of the dominant effects in the two-layer model is a sufficient approach in providing meaningful estimations of the force and momentum balance during solids transport predictions. The agreements they reported for their model in comparison to experimental work justified that in highly deviated wellbores, the criterion for thick-bed formation should be based on a simple momentum exchange between the fluid and cuttings bed layer.

d. Even though the two-layer approach is less complex, the resulting models still effectively describe the solid-liquid flow problem. This conclusion is supported by Figure 2.2 which shows that in a two-phase solid -liquid flow, the modes of solids transport progress from a three-layer to a two-layer, and finally to a fully suspended flow (or single-layer flow). Hence, neglecting the saltation process is a reasonable approximation

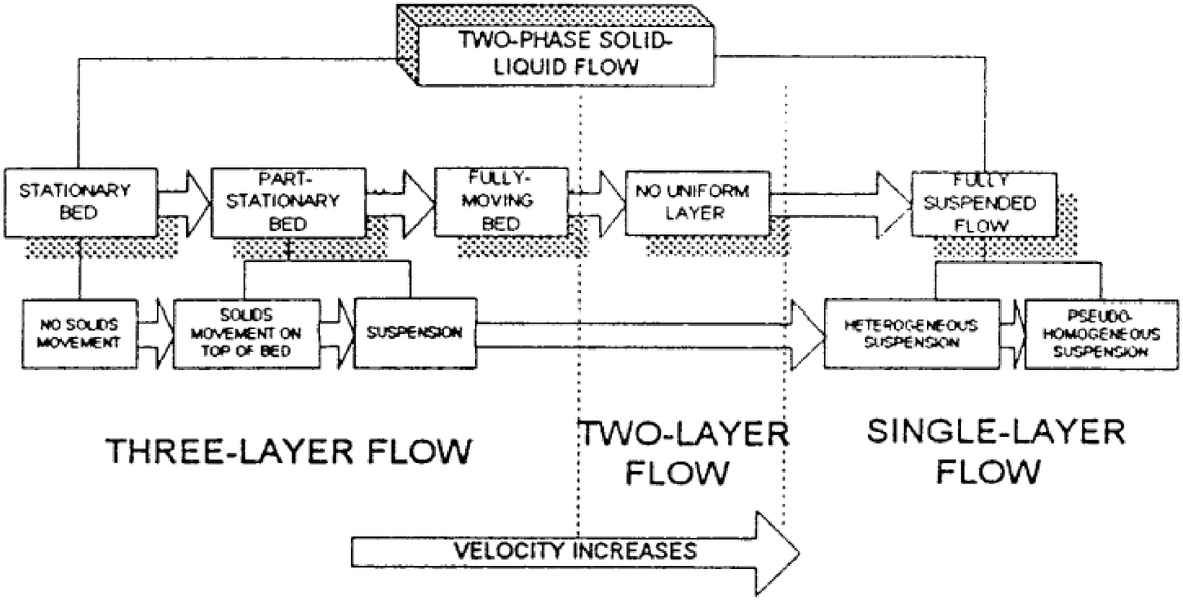


Figure 2.2: Modes of Transport in a Two-Phase Solid-Liquid Flow (Nguyen and Rahman, 1998)

Thus, at the field level, where fast and easy-to-use applications would be preferred, a two-layer model is judged to be sufficient to diagnose a hole cleaning problem. Thus, it is concluded that a realistic hole cleaning prediction approach for oilfield application would be one based on the following:

- 1-D layer modelling along the length of the wellbore
- 2-D modelling across various intervals of the wellbore cross sections for velocity and cuttings concentration profiles
- Cuttings bed height prediction models.

Table 2.2 summarizes some mechanistic models developed based on the two-layer approach. Table 2.3 summarizes some mechanistic models based on the three-layer approach.

Table 2.2 Previous Models Using Two Layer Approach (Kelin et al., 2013)

| **Researchers** | **Objective of Study** | **Summary of Work and Factors Considered** | **Limitations** |
|---|---|---|---|
| Lu (2008) | Cuttings bed height | Formation of cuttings bed in inclined wellbores | • Drill string rotation is ignored<br>• Drilled cutting size, shape, and distribution are assumed uniform<br>• Cutting bed concentration is assumed constant<br>• Mud density, rheological properties are assumed constant<br>• Rate of penetration (ROP) is assumed constant<br>• Isothermal process is assumed<br>• There is mass and energy exchange between the wellbore and drilled formation |
| Gavignet and Sobey (1989) | | Mud rheology, pipe eccentricity, wellbore inclination | |
| Santana et al. (1998) | | Slippage between drilled cuttings and fluid | |
| Kamp and Rivero (1999) | | Cuttings settling velocity and cuttings re-suspension | |
| Martins et al. (1999) | | Wellbore cave-in | |
| Li et al. (2007) | | Cuttings and fluids exchange between layers | |
| Suzana et al. (2008) | | Solids-fluid interaction. Slippage between fluid and cuttings, diffusion, mass exchange between layers | |
| Doan et al. (2003) | Cuttings bed height<br><br>Cutting concentration | Cutting deposition and re-suspension, interaction between fluid and solid phase in suspended layer, interaction between cuttings bed and suspended layer | |
| Martins and Santana (1992) | Cutting concentration | Diffusion equation | |

Table 2.3 Previous Models Developed Using Three Layer Approach

| Researchers | Objective of Study | Summary of Work and Factors Considered | Limitations |
|---|---|---|---|
| Lu (2008) | Cuttings bed height | Formation of cuttings bed in inclined wellbores | Drilled cutting size, shape, and distribution are assumed uniform<br>• Mud density, rheological properties are assumed constant<br>• Cutting bed velocity is estimated based on mechanical equilibrium<br>• Isothermal process is assumed<br>• There is mass and energy exchange between the wellbore and drilled formation |
| Nguyen and Rahman (1996) | | Based on effective thickness expression | |
| Cho et al. (2000) | | Diffusion equation, drilled cuttings settling, variations in ROP) | |
| Wang et al. (2010) | | Based on cutting suspension, rolling, slippage, drill string rotation, mass exchange between layers | |
| Ozbayoglu et al. (2009) | Cuttings bed area | Based on slip between fluids and drilled cuttings, in-situ concentration of mobile drilled cuttings | |

Previous works used flow loop experiments and computational fluid dynamics (CFD) to develop empirical correlations and models. These experiments considered parameters such as drilling fluids rheology, string eccentricity, flow rate, string rotation, well-bore inclination, variations in ROP, different string size, and annuli size.

Tables 2.4 and 2.5 present a summary of some published empirical studies for determining cuttings bed height and critical annular fluid velocity required to prevent cuttings bed formation.

Table 2.4 Empirical Models Developed to Estimate Annular Cuttings Concentration and bed height

| Researchers | Objective of Study | Summary of Work and Factors Considered |
|---|---|---|
| Wang et al. (1995) | Cuttings bed height | Based on flow rate, cuttings injection rate, mud density and viscosity, string eccentricity and rotation |
| Bassal (1996)<br>Li et al. (2010) | | Based on flow rate, variations in ROP, string rotation, mud density and rheology, annuli size, cuttings size and density, wellbore inclination |
| Duan et al. (2008) | Cuttings bed height<br>Cutting concentration | Based on flow rate, wellbore inclination, cuttings size, and string rotation |
| Ozbayoglu et al. (2008) | Cuttings bed area | Based on flow rate, variations in ROP, annuli size, wellbore inclination, mud density and rheology, string rotation |
| Loureiro et al. (2010) | Ratio between mass of suspended cuttings versus initial mass of deposited cuttings | Based on annuli size, cuttings density, mud density and rheology, string rotation, initial cuttings bed height and cuttings mass |

Table 2.5 Empirical / Mechanical Models Developed to Estimate Critical Velocities for Hole Cleaning

| Researchers | Objective of Study | Summary of Work and Factors Considered |
|---|---|---|
| Peden et al. (1998) | Minimum transport velocity (MTV) | Mechanical correlations based on drag force, friction force, gravity force, and lift force. Applicable in inclined wells |
| Clark and Bickham (1994) | | Mechanical correlations based on buoyancy force, plastic force, gravity force, lift force, drag force, and pressure force. Applicable in vertical, deviated, and horizontal wells |
| Mirhaj et al. (2007) | | Empirical correlations based on flow rate, ROP, string rotation, mud density and rheology, annuli size, cuttings size and density, wellbore inclination. Applicable in deviated and horizontal wells |
| Duan et al. (2009) | Critical re-suspension velocity (CRV) | Mechanical correlations based on static force, drag force, lift force, and Van der Waal's force. Applicable in high angle and horizontal wells |
| Ozbayoglu et al. (2010) | Critical flow velocity (CFV) | Empirical correlations based on flow rate, variations in ROP, annuli size, wellbore inclination, mud density and rheology. Applicable in inclined and horizontal wells |
| Luo et al. (1992) | Critical flow rate (CFR) | Empirical correlations based on annuli size, cuttings density, mud density and rheology, flow rate, gravity, string eccentricity. Applicable in deviated wells |
| Mohammadsalehi and Malekzadeh (2011) | Minimum flow rate | Empirical correlations based on flow rate, ROP, string rotation, mud density and rheology, annuli size, cuttings size and density, wellbore inclination. Applicable in deviated and horizontal wells |
| Larsen et al. (1997) | Critical Transport Fluid Velocity (CTFV) | Mechanical correlations based on mass conservation of drilled cuttings. Applicable in high angle and horizontal wells |

### 2.4.3 Determining Flow Regime (Reynolds Number vs Taylor Number)

Conventionally the dimensionless Reynold's number ($R_e$) has been used to determine laminar or turbulent flow regime in hole cleaning estimations. The critical Reynold's number is accepted in most literature to be 2,300. Where a flow regime is concluded to be laminar or turbulent if the estimated Reynold's number is lower or higher than the critical Reynold's number, respectively.

The Taylor-Couette flow has been discussed and referenced in section 2.2.3. The dimensionless Taylor number ($T_a$), describes the resultant inertial forces due to fluid rotation about an axis, and relative to the present viscous forces. Based on the previously referenced research efforts, and the analogy made apparent earlier, this research concludes that the Taylor number is a more appropriate criteria for defining turbulence in drilling operations when there is drill string rotation. This is supported by Philip et al. (1998) who demonstrated from experiments that Taylor vortices formed in all fluids tested at string rotations as low as 40 RPM. When there is no string rotation, the Taylor vortices are absent. Thus, in such cases the axial (non-rotational) Reynolds number will be used. Equation 2.15 (Taylor, 1923) will be used to estimate the dimensionless Taylor number when there is string rotation.

$$T_a = \frac{\omega^2 r_i (r_o - r_i)^3}{\gamma^2} \qquad \text{Eqn. 2.15}$$

Where;

$\omega$ = Angular velocity (revolution/sec)

$r_i$ = Drill string radius (m)

$r_o$ = Wellbore radius (m)

$\gamma$ = Kinematic viscosity ($m^2/s$)

Figure 2.3 shows the four possible flow regimes that can exist for a combined axial and rotary flow in an annulus.

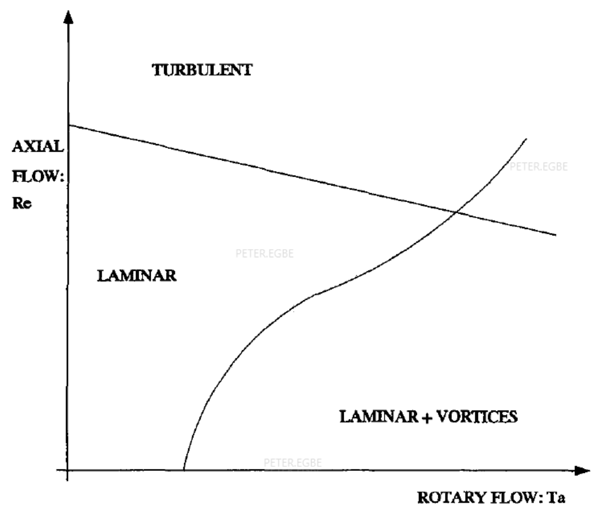


Figure 2.3: Four Regimes Possible for Combined Axial and Rotary Flow in an Annuli (Lockett et al., 1993)

### 2.4.4 Taylor Vortices and Azimuthal Annulus Velocity

The Taylor-Couette flow creates toroidal vortices which exist in pairs (see Figure 2.4). Lockett et al. (1993) established through computer modelling, the presence of Taylor toroidal vortices which regardless of whether the flow regime was laminar or turbulent provided a regular re-circulation of the fluids from the drill string to the wellbore, and back to the drill string. In horizontal cases, they determined that this re-circulation of fluids can, and does provide a lift force to drilled cuttings like instantaneous action of eddies in a turbulent flow.

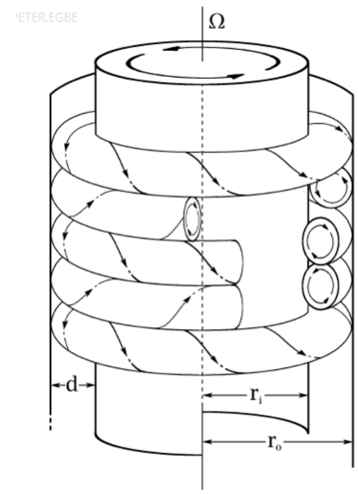


Figure 2.4: Illustration of Taylor-Couette flow resulting from shear flow between concentric rotating inner cylinder and a stationary outer cylinder (Taylor, 1923)

For the computer simulations, Lockett et al. (1993) reproduced the conditions used by Ford et al. (1990). A summary of their findings is presented below:

- The critical Taylor's number is influenced by eccentricity. The higher the eccentricity, the higher the critical Taylor's number required for the onset of toroidal vortices
- In vertical and high angle wells (including horizontal wells), the probability of any cuttings or drilled solids to be lifted, and entrained in the fluid flow is determined by the ratio of the vortex (or radial) velocity to the cutting terminal / settling velocity (which is defined as the "CSV" in this research)
- Vortex velocity is defined by Lockett et al. (1993) as

$$V_{vortex} \cong m(Ta - Ta_{cr})^{1/2} \qquad \text{Eqn. 2.16}$$

And the following conditions were established:

$$\frac{CSV}{V_{vortex}} \gg 1, cuttings\ will\ not\ be\ captured\ by\ the\ vortices \qquad \text{Eqn. 2.17}$$

$$\frac{CSV}{V_{vortex}} \ll 1, cuttings\ will\ be\ captured\ by\ the\ vortices \qquad \text{Eqn. 2.18}$$

- The rate of increase of the Taylor's number due to eccentricity is marginally dependent on the non-Newtonian character of the fluid (Power Law index, n). This is illustrated in Figure 2.5

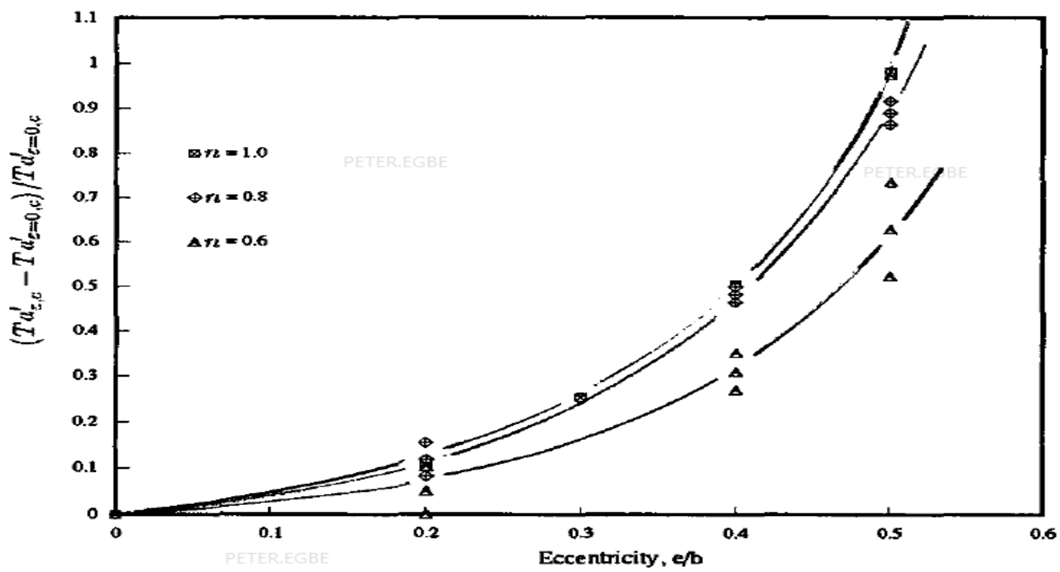


Figure 2.5: Sensitivity of critical Taylor's number to eccentricity & non-Newtonian fluids (Lockett et al., 1993)

- Drilled cuttings or particles can be suspended indefinitely by Taylor vortices, even without axial flow. By inference, Taylor vortices can capture cuttings at all angles between vertical and horizontal. This is qualitatively in agreement with the work of Ford et al. (1990)
- The force acting in the radial direction determines if a particle will be lifted away from the wall of the wellbore. If the net force is positive, lift will be achieved, and vice-versa

- The density ratio of the cuttings to the drilling fluid influences how easily the said cuttings will be lifted by the vortices. This is the case for ${CSV}/{V_{vortex}} \sim 1$.
- For a given vortex velocity (or by extension string revolutions per minute, RPM), the peak of the vortex oscillation is enough to lift drilled cuttings of a mass less than a critical mass value, away from the wall of the wellbore. Thus, validating that cutting may be removed from the low side of the annulus by action of vortices

The annulus velocity profile in the annulus may be best described in cylindrical coordinates in the radial, azimuthal, and axial directions. Wereley and Lueptow (1998) established that the axial and radial velocity components are relatively small compared to the azimuthal velocity component. Typically, they argued, the axial and radial velocities are only a few percent of the inner cylinder surface rotating speed. This will seem to contradict the findings of Lockett et al. (1993). However, the work by Philip et al. (1998) does appear to suggest that there is indeed a significant contribution by the azimuthal velocity in lifting the drilled cuttings. They (Philip et al., 1998) concluded that "although the magnitude of the computed vortex velocity was significant, it was difficult to quantify its effect on particle lift due to the superimposed azimuthal velocity". Other conclusions reached from experiments conducted by Philip et al. (1998) are as follows:

- Taylor vortices formed in all the fluids tested (water, glycerine, and xanvis polymer solutions) even at lower string rotations of 40 RPM
- Newtonian fluids with higher viscosities showed better cuttings lift at lower RPMs. However, better cuttings lift from a stationary bed was observed in

Power law fluids as the “n” values increased. Also, as the “k” values increased, better cuttings suspension for longer periods was observed

- Newtonian fluids exhibited better lifting properties compared to Power Law fluids of similar apparent viscosity because higher velocities are obtained close to the wellbore wall. However, irrespective of the nature of the lift, Power Law fluids showed better cuttings transport with higher “n” values
- The improved cuttings suspension and transport capabilities of Power Law fluids is because as the “k” and “n” values increase, the fluid becomes more viscous. As the fluid becomes more viscous, its ability to suspend and transport cuttings is improved. Philip et al. (1998) state that the vortices were stronger, and fluid velocities were higher close to the wellbore walls in fluids that had a higher flow index (“n”). Ramadan (2001) illustrated that typical drilling fluids exhibit a fair agreement with Power Law fluid model. However, Shakers (2005) and Huang et al. (2020) argue that when fitted to high shear rate viscosity measurements, the Power Law model underestimates the low shear rate viscosity. They also argued that Bingham Plastic fluid model overestimates the low shear rate viscosity. Huang et al. (2020) reports that the Herschel-Bulkley model had the best fitting accuracy over a wide range of shear rates. This research will use a Herschel-Bulkley fluid model
- Although the magnitude of vortex velocity was significant, it was difficult to assess its effect on the particle lift due to the superimposed azimuthal velocity. In horizontal wells, the ability of Taylor vortices to pile cuttings in bands (the dune effect) on the low side of the hole will assist in cuttings

entrainment by axial flow. This implies a complimentary effect (illustrated in Figure 2.6(a) below) where the superimposed azimuthal velocity yields a net lift force. In other locations of the wellbore, the Taylor vortices could be non-complimentary to the cuttings lift process as shown in Figure 2.6(b), where the vortex velocity forces particles that are in the path of its downward direction to remain so until the next wave of "complimentary" vortices come along. This pattern of the vortex velocity was observed to create bands (or dunes) in the cuttings bed. Similar observations have been reported by previous researchers (Duan et al., 2009). In the presence of sufficient axial flow above a critical value, this banding will assist in significantly lifting and aiding the transport of the cuttings to surface (Philip et al., 1998).

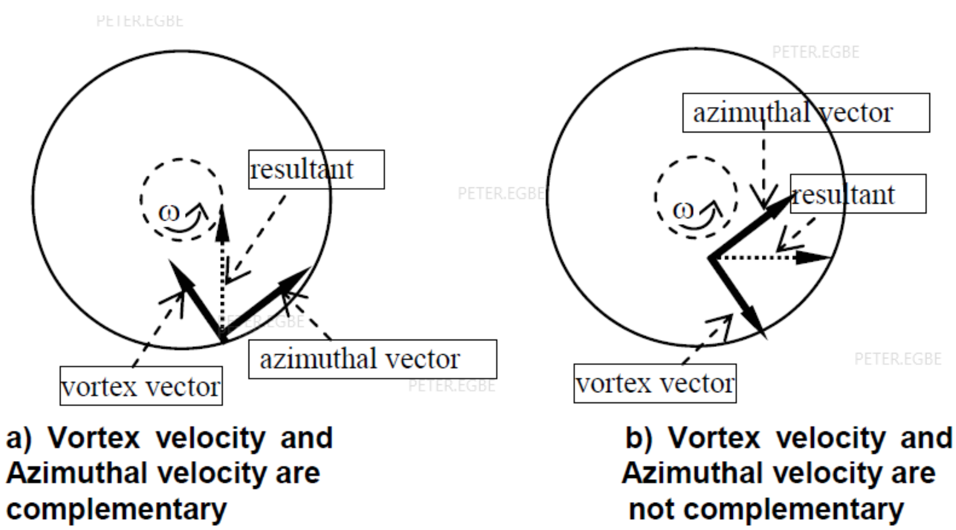


Figure 2.6: Vectoral Sum of the Vortex and Azimuthal Velocities (Philip et al., 1998)

Wavy vortex flow, as described by Taylor-Couette flow is characterized by azimuthally wavy deformation of the toroidal vortices both axially and radially. Significant transfer of fluid between neighboring vortices occurs cyclically, almost cancelling out each other. Such that as one vortex grows, the adjacent vortices shrink, and vice-versa. On this basis, it is theorized that the main component of the velocity profile during rotation of the drill string is largely going to be due to the azimuthal velocity as it is directly related to the magnitude of string rotation; with a maximum value ($V_{\theta max}$) obtained at the surface of the rotating string and decaying exponentially towards the wall of the wellbore.

# 3. METHODOLOGY

Cuttings transport studies by previous researchers have involved empirical observations (from flow loop experiments), numerical analysis, mechanistic models (sometimes involving computational fluid dynamics simulations), and in some instances a combination of these methods. Regardless of the method, the focus has been to define a critical velocity to prevent the formation of cuttings bed in the wellbore annulus.

A method for real-time stuck pipe detection is proposed. The method is based on regression analysis of real-time data for anomaly detection (rate of change), and deviation change (actual versus well design model simulation). A weighted risk calculation and ranking approach is combined with the statistical method to significantly predict ahead of time the probable risk of a stuck pipe event occurring.

The fluid rheology model is important, and majority of the previous works have based their models on the Power Law model. Section 2.4.4 (page 77) of this thesis, highlights the challenges with using the Power Law and Bingham Plastic fluid models at high shear rate viscosity measurements. Agwu et al. (2021) conducted a critical review of 21 drilling mud rheological models. Majority of the models are reported as having limited field usage due to complexities in determining model parameters. Agwu et al. (2021) state the following for the most popular typical models used to describe drilling fluids behavior:

a. Bingham Plastic model (2-parameter model): Predictions deviate at high temperatures, and has the tendency to overestimate the yield stress

b. Power Law model (2-parameter model): Does not adequately account for the yield stress of drilling muds, thus leading to inaccuracies
c. Herschel-Bulkley model (3-parameter model): Challenges exist in performing hydraulic calculations due to the extra rheological parameter (i.e., the yield stress)

However, where adequate experimental data are available, and especially for water-based fluids and at low shear rates, the Herschel-Bulkley fluid model is preferred to Power Law or Bingham Plastic because it has been demonstrated to give more accurate models of rheological behavior (Huang et al.,2020). The 3-RPM reading is typically taken as the yield stress. The consistency index (k) and flow index (n) are calculated from the 300-RPM and 600-RPM values. Figure 3.1 shows X-Y plots of the Newtonian, Power Law, Bingham Plastic, and Herschel-Bulkley fluid models. As can be inferred, the Herschel-Bulkley model is a good combination of the Power Law model (which under predicts the low shear stress of drilling fluids), and the Bingham Plastic model (which over predicts the low shear).

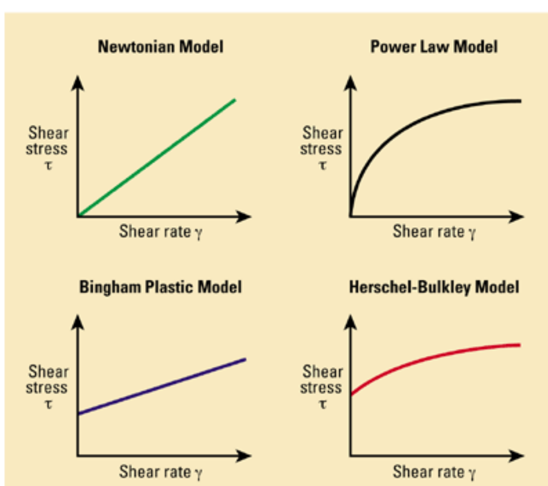


Figure 3.1: X-Y Plots of Rheological Models (Schlumberger)

### 3.1 Research Methodology for Developing Cuttings Transport Models

In the literature review, several concepts were identified for consideration in defining the physics of the hole cleaning process. These concepts include:

- Effect of centrifugal forces on drilled cuttings settling velocity
- Hindered settling in stirred tanks
- Taylor-Couette flow in concentric and eccentric cylinders
- Particle-to-particle Van Der Waals forces
- Fluidized beds

In this research, these concepts have been incorporated in the development of the following models using numerical analysis methods:

- Estimating annular cuttings concentration
- Cuttings settling velocity (CSV)
- Critical re-suspension velocity (CRV)
- Azimuthal annulus velocity profile (AAV)
- Critical annular fluid velocity (CAFV) or critical transport fluid velocity (CTFV)

The models are based on equilibrium between static forces (e.g., gravity, drag, lift, particle-particle), and the Heschel-Bulkley rheology model. The models are summarized as follows:

1. Annular cuttings concentration profile: Is developed based on a mass balance, and the Buckingham pi-theorem. Because of the complexity of cuttings transport problems, it is believed that dimensionless analysis provides a means to investigate the relationship among the variables. The

variables used in this research to develop the cuttings concentration model are shown in Table 3.1.

2. Cuttings settling velocity (CSV): The proposed expression for CSV considers the influence of hindered centrifugal settling, and an application of the Richardson-Zaki equation (R-Z equation). The R-Z equation is a modification of the Maude and Whitmore (1958) empirical relationship. Renzo and Ralf (2000) and Spearman and Manning (2017) have also presented modifications to the R-Z equation.
3. Critical re-suspension velocity (CRV):
    a. The concept of equilibrium of moments around a particle just as it is about to experience motion is adopted. The influence of the Van der Waals forces is explored; and an expression for the Van der Waals force is developed based on the works of Derjaguin (1934), Hamaker (1937), Duan et al. (2009), and Nguyen et al. (2012)
    b. A model for the near-bed velocity profile is presented. The work done by Taylor (1923) using two concentric cylinders in which the outer was held stationary while the inner cylinder was in rotation, is instrumental to understanding the fluid instabilities that develop in the wellbore annulus, including an application of the Taylors number criterion to define instances of laminar and turbulent flow regimes
    c. With the near-bed velocity profile, and all balance forces in the equilibrium moments equation obtained, a step-by-step procedure to estimate the CRV is presented

4. Azimuthal annulus velocity profile (AAV): An expression is developed considering a Herschel-Bulkley rheological model, and Taylor-Couette flow to determine turbulence (as opposed the Reynold's number criterion)
5. Critical transport fluid velocity (CTFV) or critical annular fluid velocity (CAFV): The minimum velocity below which a cuttings bed may form is subsequently determined based on #1 - #4 above.
6. Cuttings bed height prediction: Is based on geometrical analysis, and the resulting expression is a typical transcendental equation that is solved by iteration
7. Estimate the hole cleaning efficiency from the cuttings transport ratio

The results from the above models are validated against published models and data. The results are discussed in chapter 4, and limitations of the models highlighted.

## 3.2 Assumptions for Model Development

To develop the models, several simplifying assumptions have been made. The main assumptions are listed below:

- Isothermal transient 2-D flow of solid-liquid phases in the wellbore annulus
- The fluid under consideration is an incompressible Herschel-Bulkley fluid
- The cuttings bed has a uniform thickness
- The cuttings are spherical with same diameter, and in a hexagonal packing structure.
- Rolling is the dominant re-suspension mechanism
- Van der Waal forces between similar cuttings in proximity are not negligible

- Hindered settling effects are not negligible
- Cuttings and liquid have a constant density
- There is drill string rotation
- The drill string torque and drag is done using the soft string model

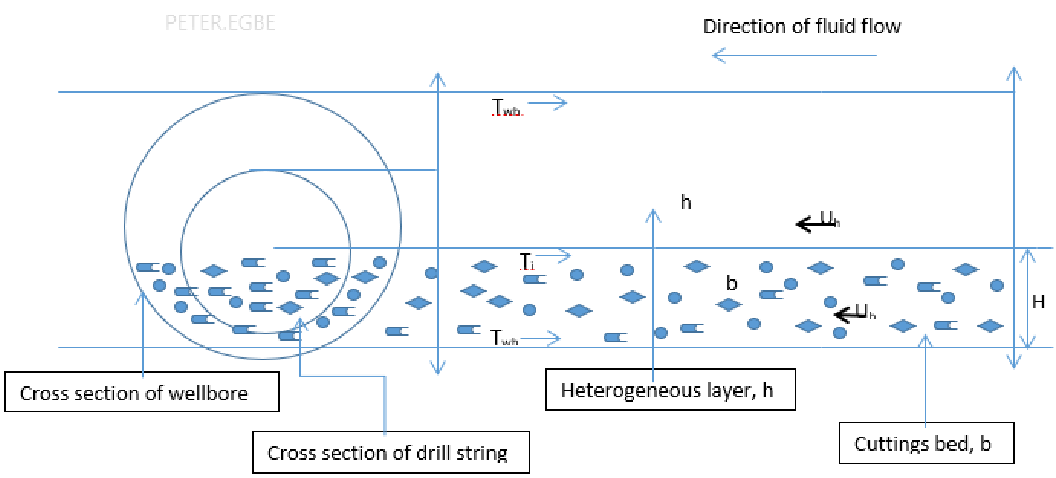


Figure 3.2: Cross section of well bore showing heterogeneous and cuttings bed layers.

Based on Figure 3.2, mass and momentum conservation equations are presented as follows (Kamp and Rivero 1999):

$$\frac{d}{dz}(\rho_s C_h U_h A_h) = -\emptyset_s A_i \qquad \text{Eqn. 3.1}$$

$$\frac{d}{dz}(\rho_l (1 - C_h) U_h A_h) = -\emptyset_s A_i \qquad \text{Eqn. 3.2}$$

$$\frac{d}{dz}(\rho_b U_b A_b) = (\emptyset_s + \emptyset_l) A_i \qquad \text{Eqn. 3.3}$$

Where:

$$\emptyset_s \equiv \emptyset_{s,dep} - \emptyset_{s,susp}$$

$$\emptyset_l \equiv \emptyset_{l,dep} - \emptyset_{l,susp}$$

$\emptyset_{s,dep}$= Mass flux of cuttings deposit per unit interface

$\emptyset_{s,susp}$= Mass flux of cuttings re-suspended

$\emptyset_s$= Cutting deposition and re-suspension flux

$\emptyset_l$= Liquid deposition and re-suspension flux

$\emptyset_s$ & $\emptyset_l$ are related as follows:

$$\emptyset_l = \frac{1-C_b}{C_b}\frac{\rho_l}{\rho_s}\emptyset_s \qquad \text{Eqn. 3.4}$$

$C_h$= Concentration of cuttings in the heterogeneous layer = 1 - $C_b$

$C_b$= Concentration of cuttings in the bed layer = 0.74 (assuming a hexagonal packing structure) (Duan et al., 2009)

$A_i$ = Interfacial area between the heterogeneous layer and the cuttings bed

$U_h$= Velocity of the heterogeneous layer (average annulus velocity)

$U_b$= Cuttings bed velocity (derived as follows):

The relative velocity between fluid and cuttings bed ($U_h - U_b$), is defined below (Zhang et al., 2013):

$$U_h - U_b = 0.4U_{critical}$$

$$\therefore U_b = U_h - 0.4U_{critical} \qquad \text{Eqn. 3.5}$$

Kamp and Rivero (1999) define the cuttings bed density ($\rho_b$) and heterogeneous layer density ($\rho_h$) as follows:

$$\rho_b = C_b\rho_s + (1 - C_b)\rho_l \qquad \text{Eqn. 3.6}$$

$$\rho_h = C_h\rho_h - (1 - C_h)\rho_l \qquad \text{Eqn. 3.7}$$

The following is the momentum equation for the heterogeneous layer and bed layer (Kamp and Rivero 1999):

$$\frac{d}{dz}\left\{\rho_h U_h^2 A_h\right\} = -A_h\frac{dp}{dz} - A_h\rho_h g cos\theta - \tau_{wh} - \tau_i - (\emptyset_s + \emptyset_l)(U_h - U_b) \qquad \text{Eqn. 3.8}$$

$$\frac{d}{dz}\left\{\rho_b U_b^2 A_b\right\} = -A_b\frac{dp}{dz} - A_b\rho_b g cos\theta - \tau_{wb} + \tau_i + (\emptyset_s + \emptyset_l)(U_h - U_b) \qquad \text{Eqn. 3.9}$$

Note that "$(\emptyset_s + \emptyset_l)(U_h - U_b)$" represents the momentum exchange through particle deposition and re-suspension. As would physically be the case, the heterogeneous phase can be expected to have a significantly faster velocity than the sliding cuttings bed. It can thus be expected that as more cuttings deposit, the additional mass of cuttings would add momentum to the sliding cuttings bed as per the effect of the interfacial shear stress ($\tau_i$). Consequently, to satisfy the laws of conservation, the heterogeneous layer loses that momentum. Kamp and Rivero (1999) agree with this assumption. Hence adding equations 3.8 to 3.9 simplifies both momentum equations to the following:

$$\frac{d}{dz}\left\{\rho_h U_h^2 A_h\right\} + \frac{d}{dz}\left\{\rho_b U_b^2 A_b\right\} = -\frac{dp}{dz}(A_h + A_b) - g\cos\theta\,(A_h\rho_h + A_b\rho_b) - (\tau_{wh} + \tau_{wb}) \text{Eqn. 3.10}$$

As a result, five variables exist ($C_h$, $U_h, U_b, p\ and\ h$); and five equations. The terms $\emptyset_{s,dep}$,$\emptyset_{s,susp}$,$\tau_{wb}, \tau_{wh}$, and $\tau_i$ are the closure terms to be determined.

Where;

$\tau_{wb}$ = Bed shear stress between cuttings bed and wellbore = $\frac{f_b\rho_b U_b^2}{2}$ Eqn. 3.11

$\tau_{wh}$ = Wall shear stress between heterogeneous layer and the wellbore = $\frac{f_h \rho_h U_h^2}{2}$

Eqn. 3.12

$\tau_i$ = Interfacial shear stress at the boundary between cuttings bed and heterogeneous layer = $\frac{f_{bh} \rho_h (U_h - U_b)^2}{2}$ Eqn. 3.13

$f_{bh}$ = Interfacial friction factor. The correlation of Televantos et al. (1979) is used

## 3.3 Annular Cuttings Volumetric Concentration ($C_c$)

The following variables in Table 3.1 are considered for the development of the cutting concentration model:

Table 3.1 Variables Used to Develop Annular Cuttings Volumetric Concentration Model

| | |
|---|---|
| Fluid Properties | • Density ($\rho_l$)<br>• Dynamic viscosity ($\mu$)<br>• Kinematic viscosity ($\gamma$) |
| Drilled cuttings properties | • Cutting diameter ($d_p$)<br>• Cutting density ($\rho_p$ $or$ $\rho_s$) is assumed constant<br>• Cutting shape is assumed spherical. This will influence cuttings bed packing structure (cubic or hexagonal), and thus the cuttings bed concentration |
| Drilling parameters | • Rate of penetration (ROP)<br>• Wellbore diameter ($D_o$ $or$ $d_o$)<br>• Drill pipe diameter ($D_i$ $or$ $d_i$)<br>• Drill string revolutions per minute (RPM)<br>• Angular velocity (ω)<br>• Drill string eccentricity (ε) |

The mathematical or numerical relationship between these variables can be expressed as:

$$f_1(C_c,\ \rho_l, \gamma, d_p, ROP, \omega, D_o, D_i, \varepsilon, V) = 0 \qquad \text{Eqn. 3.14}$$

Where:

$$f_1\ = Unknown\ function$$

$$\omega\ = 6\ \times RPM$$

$$\gamma\ = \frac{\mu}{\rho} \qquad \text{Eqn. 3.15}$$

Dimensionless analysis can offer the most direct control in exploring the relationships between these variables. The Buckingham Pi-theorem is applied to combine the variables into dimensionless groups (Busch et al., 2020; Gupta et al., 2014; Rubenstein et al., 2021). These dimensionless groups reduce the complexity of the problem to a simple study of relationships between a reduced number of variables. Martins and Santana (1992), Ozbayoglu et al. (2002, 2007, 2008), Yu et al. (2007), Duan et al. (2008), and Ahmed et al. (2010) have all utilized dimensionless models to study and predict the cuttings volumetric concentration, cuttings bed height, critical fluid velocity, and frictional pressure drop.

Based on equation 3.14, there are

n = 10 variables

j = 3 different dimensions (Mass - M / Length – L / Time – T)

K = Number of $\pi$ groups = 10 – 3 = 7

Table 3.2 shows the 10 variables.

Table 3.2 Variables for Dimensionless Analysis

| | | | Dimensions | | |
|---|---|---|---|---|---|
| **Variables** | **Symbol** | **Unit** | **M** | **L** | **T** |
| Cuttings Concentration | $C_c$ | - | 0 | 0 | 0 |
| Fluid density | $\rho_l$ | $kg/_{m^3}$ | 1 | -3 | 0 |
| Kinematic viscosity | $\gamma$ | $m^2/_s$ | 0 | 2 | -1 |
| Cutting diameter | $d_p$ | m | 0 | 1 | 0 |
| Rate of penetration | ROP | $m/_s$ | 0 | 1 | -1 |
| Angular velocity | $\omega$ | $1/_s$ | 0 | 0 | -1 |
| Wellbore diameter | $D_0$ | m | 0 | 1 | 0 |
| Drill pipe diameter | $D_i$ | m | 0 | 1 | 0 |
| Eccentricity | $\varepsilon$ | - | 0 | 0 | 0 |
| Mean Annular Fluid Velocity | V | $m/_s$ | 0 | 1 | -1 |

### 3.3.1 Dimensionless Groups

Each dimensionless group that is developed has a physical meaning. One of the dimensionless groups, the Taylors number, already exists, and does not need to be re-generated. The first two $\pi$ dimensionless groups are as follows:

- $\pi_1 = C_c$ = Annular cuttings volumetric concentration = the dependent variable

- $\pi_2 = T_a$ = Taylor's number defining stability of flow in an annulus surrounding a rotating inner cylinder (such as the drill pipe) = $\frac{\omega^2 R_i (R_o - R_i)^3}{\gamma}$ Eqn. 3.16
- Where $R_i$ and $R_o$ are related to the drill pipe and wellbore diameters as follows:

$$R_i = {}^{D_i}/_2 \text{ and } R_o = {}^{D_o}/_2$$

Other dimensionless groups are summarized as follows:

$$\pi_3 = \omega^a \rho_l^b D_o^c D_i = (T^{-1})^a (M^1 L^{-3})^b (L^1)^c L^1 = M^0 L^0 T^0 \quad \text{Eqn. 3.17}$$

$$Mass\ (M): b = 0$$

$$Length\ (L): -3b + c + 1 = 0$$

$$Time\ (T): -a = 0$$

$$\therefore a = b = 0; and\ c = -1$$

Eqn. 3.17 becomes

$$\pi_3 = {}^{D_i}/_{D_o} = Dimensionless\ drill\ pipe - wellbore\ ratio \quad \text{Eqn. 3.18}$$

$$\pi_4 = \omega^a \rho_l^b D_o^c \varepsilon = (T^{-1})^a (M^1 L^{-3})^b (L^1)^c = M^0 L^0 T^0 \quad \text{Eqn. 3.19}$$

Based on Eqn. 3.19; a = b = c = 0. Eqn. 3.19 becomes $\pi_4 = \varepsilon$

For convenience, equation 3.20 is used

$$\pi_4 = 1 - \varepsilon \quad \text{Eqn. 3.20}$$

$$\pi_5 = \omega^a \rho_l^b D_o^c ROP = (T^{-1})^a (M^1 L^{-3})^b (L^1)^c (L^1 T^{-1}) = M^0 L^0 T^0 \quad \text{Eqn. 3.21}$$

Based on Eqn. 3.21; a = -1, b = 0, and c = -1.

Eqn. 3.21 becomes

$$\pi_5 = \frac{ROP}{\omega D_o}$$

$\pi_5$ above is the dimensionless ROP (or dimensionless cuttings-injection rate) based on the wellbore diameter. However, it also has a direct effect on the cutting volumetric concentration and the mean velocity in the annular space between the wellbore and the drill string. Hence, to make it representative for annular flows, and direct comparison with existing non-dimensional numbers, Eqn. 3.21 is re-written in the form proposed by Song et al. (2017) and Yu et al. 2007. Eqn. 3.22 is dimensionally the same as Eqn. 3.21.

$$\pi_5 = \frac{ROP D_o}{\omega\left(D_o^2 - D_i^2\right)} \qquad \text{Eqn. 3.22}$$

$$\pi_6 = \omega^a \rho_l^b D_o^c d_p = (T^{-1})^a (M^1 L^{-3})^b (L^1)^c (L^1) = M^0 L^0 T^0 \qquad \text{Eqn. 3.23}$$

Based on Eqn. 3.23; a = b = 0, and c = -1.

Eqn. 3.23 becomes

$$\pi_6 = \frac{d_p}{D_o} \qquad \text{Eqn. 3.24}$$

$$\pi_7 = \omega^a \rho_l^b D_o^c V = (T^{-1})^a (M^1 L^{-3})^b (L^1)^c (L^1 T^{-1}) = M^0 L^0 T^0 \qquad \text{Eqn. 3.25}$$

Based on Eqn. 3.25; a = c = -1, and b = 0

Eqn. 3.25 becomes

$$\pi_7 = \frac{V}{\omega D_o} \qquad \text{Eqn. 3.26}$$

Table 3.3 summarizes the seven (7) dimensionless groups.

Table 3.3 Summary of Dimensionless Groups

| $\pi$ Group | Dimensionless Group | Remark |
|---|---|---|
| $\pi_1$ | $C_c$ | Dimensionless Cuttings Volumetric Concentration in the annulus. This is the dependent variable |
| $\pi_2$ | $\frac{\omega^2 R_i (R_o - R_i)^3}{\gamma}$ | Taylor's Number which represents the effect of flow, and its stability in the annulus |
| $\pi_3$ | ${D_i}/{D_o}$ | Drill Pipe / Wellbore Diameter Ratio |
| $\pi_4$ | $1 - \varepsilon$ | Wellbore Eccentricity. For the case of a concentric annulus, the eccentricity is zero |
| $\pi_5$ | $\frac{ROPD_o}{\omega\left(D_o^2 - D_i^2\right)}$ | Dimensionless ROP (dimensionless cuttings injection rate) |
| $\pi_6$ | $\frac{d_p}{D_o}$ | Dimensionless Cuttings Diameter |
| $\pi_7$ | $\frac{V}{\omega D_o}$ | Dimensionless Annular Fluid Velocity |

A mathematical relationship among the dimensionless groups may be expressed as proposed by Song et al. (2017):

$$C_c = \pi_1 = f_2\left(\pi_2, \pi_3, \pi_4, \pi_5, \pi_6, \pi_{7,}\right) = 0 \qquad \text{Eqn. 3.27}$$

Where "$f_2$" is an unknown function representing the relationships between the dependent variable ($C_c$), and the six independent variables.

Song et al. (2017) have already established these relationships. Based on their experimental work, they demonstrated that the cuttings volumetric concentration

- Decreases as the Reynolds number, and the drill pipe / wellbore diameter ratio increases. Although their work used the Reynolds number, the relationship is applicable to the Taylors number criterion being used in this research because the Taylors number does similarly represent the effect of flow in the annulus.
- Increases as the dimensionless ROP, and the drill string eccentricity increases
- Initially decreases, then increases as the dimensionless cutting diameter increases

Song et al. (2017) found that because the effect of the Reynolds number, dimensionless ROP, and drill pipe / wellbore diameter ratio changed monotonously as the dimensionless groups changed, the formulas of these groups in the correlations were power functions.

With regards to the effect of the cutting diameter, Song et al. (2017) established two different formulas below from which the best fit was chosen.

$$\pi_6 + e_6.\ln(\pi_6) \qquad \text{Eqn. 3.28}$$

$$(1 + c_6.\pi_6)^{d_6} \qquad \text{Eqn. 3.29}$$

In terms of the effect of eccentricity, Song et al. (2017) also proposed two different formulas below from which the best fit to the experimental data is selected.

$$\pi_4^{c_4} \qquad \text{Eqn. 3.30}$$

$$1 + a_4.\pi_4^{b_4} \qquad \text{Eqn. 3.31}$$

Consequently, four correlations for estimating the cuttings volumetric concentration ($C_c$) are expressed as follows:

$$C_c = (a_1.\pi_2{}^{a_2})(\pi_3^{a_3})(1 + a_4.\pi_4)^{b_4}(\pi_5^{a_5})(\pi_6 + a_6.\ln(\pi_6))(\pi_7^{a_7}) \qquad \text{Eqn. 3.32}$$

$$C_c = (c_1.\pi_2^{c_2})(\pi_3^{c_3})(\pi_4^{c_4})(\pi_5^{c_5})(1 + c_6.\pi_6)^{d_6}(\pi_7^{c_7}) \qquad \text{Eqn. 3.33}$$

$$C_c = (e_1.\pi_2^{e_2})(\pi_3^{e_3})(\pi_4^{e_4})(\pi_5^{e_5})(\pi_6 + e_6.\ln(\pi_6))(\pi_7^{e_7}) \qquad \text{Eqn. 3.34}$$

$$C_c = (f_1.\pi_2^{f_2})\left(\pi_3^{f_3}\right)(1 + f_4.\pi_4)^{g_4}\left(\pi_5^{f_5}\right)(1 + f_6.\pi_6)^{g_6}(\pi_7^{f_7}) \qquad \text{Eqn. 3.35}$$

The coefficients (a, b, c, d, e, f, and g,) are obtained from regression analysis.

Note that the Taylors number is used instead of the Reynolds number. As per section 2.2.3 of this thesis, the dimensionless Taylors number has been used because the phenomena of two concentric (or eccentric) cylinders where the outer cylinder is held stationary, while the inner cylinder rotates about its axis very closely describes what obtains in drilling operations.

The Taylors number also introduces the angular velocity due to the drill string rotation into consideration. The influence of the string rotation (RPM) is well known and documented in hole cleaning efficiency studies. An increase in RPM typically aids the agitation of the cuttings bed, as the generated vortices sweep the cuttings into the flow stream to be transported to surface. Thus, confirming that RPM can be a good indicator or factor to consider in cuttings transport efficiency.

In comparison to the work done by Song et al. (2017), below is a summary of the contribution of this research:

1. Correlations have been developed to estimate cuttings concentration in the wellbore annulus during conventional drilling mode with string rotation
2. The correlations have considered Taylor number instead of the Reynolds number.
3. Consequently, the angular velocity component (and by extension the string rotation, RPM), and its effect on hole cleaning is thus considered in the correlations for estimating the annular cuttings concentration profile
4. For conventional drilling operations, and at low ROP (35 ft/hr and lower), the effects of cutting diameter in the correlations was found to be better with a linear expression, not a natural logarithmic or exponential expression as previously proposed by Song et al. (2017). This is further discussed in section 4.2.1 (validation of annular cuttings concentration model).

The experimental data from Song et al. (2017) was based on micro-hole drilling using coiled tubing. As such there is no string rotation. The application of Taylors number which has a string rotation (RPM), or angular velocity component has no application in the Song et al. (2017) dataset. Hence the experimental data from Larsen et al. (1997) has been used to test the numerical correlations developed in this research and obtain the associated coefficients by regression analysis.

## 3.4 Cuttings Settling Velocity (CSV)

A knowledge of cuttings settling velocity in drilling operations is important for establishing critical flow rates to avoid a bed build up. Previously, the settling or slip velocity for cuttings in the annulus have largely been determined using the Stokes law equation given below

$$V_s = \frac{(\rho_s - \rho_l) g d_p^2}{18\mu} \qquad \text{Eqn. 3.36}$$

Where;

$V_s$ = Settling velocity (CSV)

$\rho_s$ = Solids or cuttings density

$\rho_l$ = Fluid density

$d_p$ = Solids or cuttings diameter

$\mu$ = Fluid viscosity

Equation 3.36 however is for a single cutting particle experiencing free fall in a quiescent (or still) fluid; such that the flow induced by the falling cuttings particle is laminar in nature. This applies for a particle Reynold's number ($R_{ep}$) that is less than approximately unity (Spearman and Manning, 2017). In cases where the particle Reynold's number is greater than around 100, the flow around the falling cuttings particle is turbulent, and the terminal settling velocity is expressed as below (Spearman and Manning, 2017)

$$F_D = {}^{1}/_{2}\, \rho_w V_s^2 C_D A \qquad \text{Eqn. 3.37}$$

The above describes an unhindered particle settling process. In drilling operations however, hindered settling is what occurs due to the wellbore annulus being occupied by drilled cuttings existing in suspension by the mud at various times of the process. Additionally, the rotational effect of the drill string rotating at a given revolution per minute (RPM) cannot be ignored.

Consequently, hindered settling is an important consideration in developing a usable settling or slip velocity relationship. Hindered settling has been studied extensively in other fields such as Chemical Engineering, in the modeling of debris flow, study of turbidites, piping of slurries, etc. (Spearman and Manning, 2017).

The well-known Richardson and Zaki (R-Z) equation is the starting point to be modified for application in this research. It is similar to the Maude and Whitmore (1958) equation presented in section 2.2.2 of this research. For the sake of this research, it is referred to as the "R-Z" equation, and is expressed below (Renzo and Ralf, 2000)

$$V_s = V_{s,o}\varepsilon^n \qquad \text{Eqn. 3.38}$$

Equation 3.38 is the result of extensive experimental liquid studies, where the dependency of settling velocities ($V_s$) on the voidage fraction ($\varepsilon$) was investigated by Richardson and Zaki. The simplicity of equation 3.38 is unique as it condenses into only two parameters the complex influence of fluid and particle physical characteristics on the particle-fluid interaction forces. Several researchers have sought to replicate or challenge the work of Richardson-Zaki but have all largely agreed on its application in describing the characteristics of sedimenting concentrated suspensions (Renzo and Ralf, 2000). "n" in equation 3.38 is the R-Z exponent. $V_{s,o}$ is the settling velocity of a single particle in a quiescent or still fluid.

Richardson and Zaki obtained correlations for the "n" exponent as a function of the particle Reynold's number. The correlations however are a function of the particle to wall diameter ratio, and several flow regimes. If it is assumed that the particle diameter is significantly less than the container diameter as is obtained in drilling operations, the effect of the particle to wall diameter ratio can be ignored. Consequently, the R-Z exponent (n) is wholly a function of the flow regime (Felice and Kehlenbeck, 2000). For ease, this research will consider the correlations of Rowe (1987) or Khan and Richardson (1989) because both correlations cover the entire flow regime. The correlation of Rowe (1987) is however preferred because the Reynold's number can easily be related to the Taylor's number, and without a need for the particle to wall diameter ratio.

Rowe (1987)'s correlation is expressed below

$$n = \frac{4.7+0.41R_e^{0.75}}{1+0.175R_e^{0.75}} \qquad \text{Eqn. 3.39}$$

The role of Taylor vortices is identified as being critical by this research. This is because the concept is directly representative of what occurs in drilling operations. The Taylor vortices are formed when the drill string rotates at a critical rotation RPM. Philip et al. (1998) confirms that under typical drilling RPMs, the Taylor vortices do form.

In the application of the R-Z equation in Drilling Operations, the following are assumed:

- Hindered settling
- Non-cohesive settling.
- Wall effects are negligible (i.e., the effect of the ratio ${d_p}/{D_o}$ is ignored. $d_p$ = cuttings diameter. $D_o$ = wellbore diameter)
- There is string rotation at, or above magnitudes required for the formation of Taylor's vortices

- At high cuttings volume concentration, segregation is increasingly suppressed
- Settling velocities of any resulting flocs do not follow Stoke's law; but is a function of their size, and is treated as a single cutting
- Drilled cuttings experience turbulent flow as they fall through the fluid ($Re_p > 100$). Fluid drag force is considered

Equation 3.38 can be re-written as follows,

$$V_s = V_{s,o}(1 - C_c)^n \qquad \text{Eqn. 3.40}$$

Where $C_c$ is the cuttings volume concentration as obtained in section 3.3

Equation 3.40 does not reach zero at the maximum volume fraction concentration. This thus implies the volume fraction concentration becomes unphysically large. This challenge stems mainly from the fact that the R-Z relationship does not account for mono-dispersed suspensions in which the maximum volume fraction concentration is not unity. This is because the R-Z hindrance function represented by $(1 - C_c)^n$, assumes a "hard-sphere" which suggests an infinite repulsion of cuttings upon contact. However, inter-particle interactions exist. The R-Z hindrance function assumes that there are no restrictions on the minimum separation distance between two colloidal particles, and the maximum volume fraction is determined by random sphere packing theory. This assumption may hold for larger non-colloidal particles but may not be suitable for highly charged colloidal particles which exists in drilling operations.

Consequently, to account for highly charged colloidal particles such as the clays encountered in drilling operations, the Acrivos hindered settling function (Rao et al., 2002) is used. Equation 3.40 thus becomes

$$V_s = V_{s,o}\left(\frac{\mu_c(1-C_c)}{\mu}\right) \qquad \text{Eqn. 3.41}$$

Where;

$\mu_c$ = Fluid viscosity

$\mu$ = Mixture viscosity

The use of the mixture viscosity thus considers hindered settling effects; and eliminates the need to specify the R-Z "n" exponent which is dependent on so many other parameters.

Furthermore, due to inter-particle interactions, random sphere packing theory for colloidal particles does not properly describe the max volume fraction of the cuttings in the drilling fluid. Thus, an effective maximum volume fraction concentration ($C_{c,max}^{eff}$), is defined by the Quemada model (Quemada 1977).

$$\mu = \mu_c\left(1 - \frac{C_c}{C_{c,max}^{eff}}\right)^{-2} \qquad \text{Eqn. 3.42}$$

Equation 3.42 has been shown to model the mixture viscosity of silica suspensions adequately (Rhodes, 2008). Equation 3.42 also allows the hindered settling velocity to tend to zero at the effective maximum volume fraction concentration. This eliminates the "hard-sphere" assumption, and accounts for inter-particle interactions.

Metin (2012) provides an expression for effective maximum volume fraction concentration ($C_{c,max}^{eff}$) as follows:

$$C_{c,max}^{eff} = C_{c,max}\left(\frac{d+\bar{s}}{d}\right)^{-3} \qquad \text{Eqn. 3.43}$$

Where;

$\bar{s}$ = Minimum separation distance between the surfaces of two particles

$C_{c,max}$ = Maximum volume fraction concentration; and is dependent on randomly packed hard spheres (0.639) (Qi and Tanner 2012); or 0.74 - hexagonal packing, or 0.59

$d = d_p =$ Dispersed phase diameter (in this case, the cuttings diameter, $d_p$)

Substituting equation 3.42 into equation 3.41 yields

$$V_s = V_{s,o}(1 - C_c)\left(1 - \frac{C_c}{C_{c,max}^{eff}}\right)^2 \qquad \text{Eqn. 3.44}$$

With reference to the expression by Metin (2012) for the effective maximum volume fraction concentration, this research assumes the term $\left(\frac{d+\bar{s}}{d}\right)^{-3}$ tends to unity as "$\bar{s}$" is very small compared to "$d_p$".

Hence for this research, equation 3.43 reduces to

$$C_{c,max}^{eff} = C_{c,max} \qquad \text{Eqn. 3.45}$$

Equation 3.44 can subsequently be re-written as

$$V_s = V_{s,o}(1 - C_c)\left(1 - \frac{C_c}{C_{c,max}}\right)^2 \qquad \text{Eqn. 3.46}$$

Equation 3.46 can also be written in a form analogous to the Richardson-Zaki equation as follows

$$V_s = V_{s,0}\xi \qquad \text{Eqn. 3.47}$$

Where;

$$\xi = (1 - C_c)\left(1 - \frac{C_c}{C_{c,max}}\right)^2 \qquad \text{Eqn. 3.48}$$

For a single cutting particle falling through the drilling fluid, the flow induced by the cutting particle could be laminar ($R_{ep} < \sim 1$), or turbulent ($R_{ep} > 100$). In drilling operations, it is very rarely the case that $R_{ep} < \sim 1$; hence the effect of the fluid drag force is considered.

Formulae for $V_{s,0}$ that covers the whole range of viscous drag, intermediate, and inertial regions have been developed by several previous researchers (Soulsby 1997, Schiller and Naumann, 1933, Coulson and Richardson 1955). Smith and Friedrichs (2011) established that all these equations predicted very similar settling velocities. The empirical constants in the Soulsby (1997) equation were determined experimentally. The Soulsby (1997) settling equation was shown to be valid for particle aspect ratios less than 2 and reduces to Stokes law for small particle Reynolds number (< 1). At higher particle Reynolds number (>1), the Soulsby (1997) equation showed close agreement with Stokes law modified with the Schiller-Naumann drag coefficient (Coulson and Richardson, 1955). It was also reported to agree closely with Winterwerp (1998, 2002) at particle Reynolds number greater than 1. Hence, the Coulson and Richardson equation is preferred for its simplicity; and is given as follows

$$V_{s,0} = \frac{g d_p^2 (\rho_s - \rho_f)}{18\mu} \frac{1}{1 + 0.15 R_{ep}^{0.687}} \qquad \text{Eqn. 3.49}$$

Recall that there is string rotation. Hence, equation 3.49 can be re-written as follows:

$$V_{s,0} = \frac{\omega^2 r d_p^2(\rho_s - \rho_f)}{18\mu} \frac{1}{1+0.15R_{ep}^{0.687}} \qquad \text{Eqn. 3.50}$$

Where;

r = centrifuge radius of curvature, in this case, the wellbore radius ($r_o$)

Equation 3.50 considers centrifuge sedimentation for two phase systems, and assumes the following:

- Uniform circular motion (i.e., a constant rate of rotation)
- Centrifuge radius of curvature does not change in time
- Angular velocity, ω, is constant

Recall equations 3.47 and 3.48 respectively as follows

$$V_s = V_{s,0}\xi \qquad \text{Eqn. 3.47}$$

$$\xi = (1 - C_c)\left(1 - \frac{C_c}{C_{c,max}}\right)^2 \qquad \text{Eqn. 3.48}$$

Substituting for $V_{s,0}$ modified for wellbore diameter, equation 3.47 becomes

$$V_s = \left(\frac{\omega^2 d_o d_p^2(\rho_s - \rho_f)}{18\mu} \frac{1}{1+0.15R_{ep}^{0.687}}\right)\left((1 - C_c)\left(1 - \frac{C_c}{C_{c,max}}\right)^2\right) \qquad \text{Eqn. 3.51}$$

Equation 3.51 is proposed by this research for estimation of cutting settling velocity (CSV) based on hindered settling.

Where;

$V_s$ = Hindered cutting settling velocity, CSV (m/s)

ω = Angular velocity (rev/sec)

$d_o$ = Wellbore diameter (m)

$d_p$ = Particle or cutting diameter (m)

$\rho_s$ = Solid or cutting density ($kg/m^3$)

$\rho_f$ = Fluid density ($kg/m^3$)

$\mu$ = Fluid dynamic viscosity ($kg/m.s$)

$C_c$ = Annular cuttings concentration (%)

$R_{ep}$ = Particle Reynolds number (Kamp and Rivero, 1999) =

$$\left(\frac{\rho_s - \rho_l}{\rho_l} g d_p\right)^{0.5} \frac{\rho_l d_p}{\mu_l} \quad \text{Eqn. 3.52}$$

Equation 3.51 is proposed by this research to be used for the estimation of the critical transport fluid velocity (CTFV) or the critical annular fluid velocity (CAFV). For simplicity, its form ($V_s = V_{s,0}\xi$) as represented by equation 3.47 is retained.

"$\xi$" is a function of the annular cuttings volume concentration at critical flow rate ($C_c$), and the maximum annular cuttings volume concentration ($C_{c,max}$). It thus represents the cuttings concentration interaction, and directly influences the hindered settling velocity profile.

Consequently, it is proposed that log-log charts can be plotted for quick cuttings settling velocity references in the field as shown below in Figure 3.3.

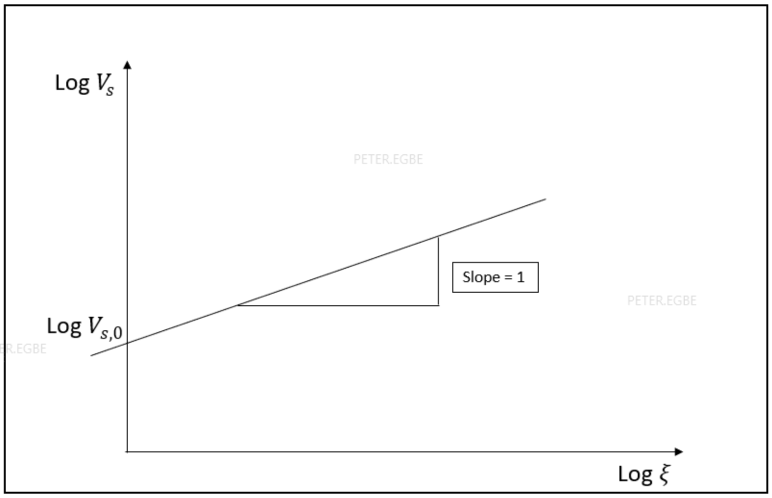


Figure 3.3: Cuttings Settling Velocity "Log-Log" Plot for Field Reference

## 3.5 Critical Re-Suspension Velocity (CRV)

An understanding of the mechanism which influences the ease of entraining a drilled cutting / solid to be transported out of the hole is important. It has been demonstrated by previous researchers that a particle may be entrained by "lifting" or "rolling" (Clark and Bickham, 1994). Duan et al. (2009) established that the relationship between the solids angle of repose (∅) and the wellbore inclination influenced which of the mechanisms was at play. The angle of repose is defined as the maximum angle of slope measured from a horizontal plane at which the particle comes to rest on a pile. At wellbore inclinations that are less than the angle of repose, "lifting" was the dominant resuspension mechanism; and at wellbore inclinations that are higher than the angle of repose, "rolling" along the cuttings or solids bed is the dominant mechanism (Clark and Bickham, 1994). Results from empirical studies demonstrated that the angle of repose for sand-sized particles soaked in a drilling fluid ranged from around 15 - 30° (Duan et al., 2009). For development of the critical resuspension velocity (CRV) in this research, the rolling mechanism is assumed to be dominant because the research is focused on high angle or horizontal wells, and as such hole inclination would be higher than the angle of repose.

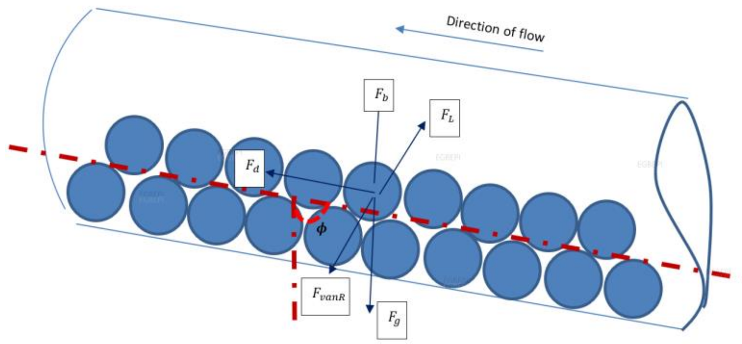


Figure 3.4: Typical Force Diagram of a Particle on a Cuttings Bed

As referenced from the work done by Liang et al (1996), solids or particle arrangements can significantly influence the drag coefficient. For spherical particles in Newtonian fluids, the drag force, $C_D$ is a function of the Reynolds number ($R_e$), and dimensionless shear rate (η). But for non-Newtonian fluids, as is the case in drilling operations, $C_D$, is a function of a host of factors. Of interest is the impact of hindered settling and drill string rotation.

In drilling operations, a cutting can hardly be said to be experiencing free fall, and this has been discussed extensively in section 3.4. To gain a deeper insight into how hindered settling and drill string rotation affect the drag force, advances in the Chemical Process Industries were referenced. It is proposed that the principles of solids suspension in a stirred tank are analogous to hindered settling with drill string rotation in a turbulent flow regime in drilling operations.

Within the Chemical Process Industries, significant research has been done in this regard; and as such, correlations relating the inter-phase drag force with solid volume fraction in turbulent flow are available. Reference is made to the works of Ranade and Sardeshpande (2012), Schiller and Neumann (1933), and Brucato et al. (1998).

It is important to make the comparison apparent. In stirred tanks, turbulence is controlled using mechanically powered impellers which mix tanks filled with solids and liquids mixtures. This is analogous to what obtains in a well bore during a drilling operation where a top drive system provides drill string rotation. It is therefore important that just as different drag correlations are used to depict this in stirred tanks, a similar idea may be applied in the drilling operations process. The Chemical Process Industries have developed computational fluid dynamic (CFD) models that relate impeller rotations (analogous to drill string RPM), multi-phase turbulence (i.e., turbulent flow regime of mud and drilled cuttings), and effective drag coefficient. And of all three parameters, the critical parameter of interest is the effective drag coefficient, $C_D$ (Ranade and Sardeshpande, 2012). It is believed that the effect of bulk turbulence created in a well bore due to drill string rotation, and of hindered settling and interaction of drilled cuttings should not be ignored. This research proposes to use the correlations of Brucato et al. (1998) and Schiller and Neumann (1933) to provide a reasonable approximation of the above effects.

With reference to Brucato et al. (1998), the ratio of effective $C_D$ is given as follows:

$$\frac{C_D}{C_{D0}} = \left[1 + 8.76 \times 10^{-4}\left(\frac{d_p}{\lambda}\right)^3\right] \qquad \text{Eqn. 3.53}$$

Where;

λ = Kolmogorov length scale of turbulence. Defined as the scale at which the particle Reynold's number ($R_{ep}$) equals unity.

The Kolmogorov length scale of turbulence is defined as follows (Brucato et al., 1998):

$$\lambda = \frac{(\eta/\tau_\eta)\eta}{\gamma} \qquad \text{Eqn. 3.54}$$

η = Dimensionless shear rate for a particle on a solids bed. Defined as (Duan et al., 2009) = $\frac{dV_r}{dy}\frac{y}{V_r}$ Eqn. 3.55

$\tau_\eta$ = Dimensionless shear stress. The correlations of Duan et al. (2009) will be used to estimate the dimensionless bed shear stress

$\gamma$ = Kinematic viscosity of fluid

y = Distance from the mean bed surface to the center of the cutting

$V_r$ = the local particle velocity profile

Equation 3.53 has been corroborated by Khopkar et al. (2006), Pinelli et al. (2001), and Magelli et al. (1990). Schiller and Naumann (1933) presented a correlation for $C_{D0}$ (the effective drag in a quiescent fluid) as follows:

$$C_{D0} = \frac{24}{R_{ep}}\left(1 + 0.15R_{ep}^{0.687}\right) \qquad \text{Eqn. 3.56}$$

Recall the particle Reynolds number, $R_{ep}$, from equation 3.52, is defined as follows (Kamp and Rivero, 1999):

$$R_{ep} = \left(\frac{\rho_s - \rho_l}{\rho_l} g d_p\right)^{0.5} \frac{\rho_l d_p}{\mu_l} \qquad \text{Eqn. 3.52}$$

The correlations of Brucato et al. (1998) and Schiller and Naumann (1933) will be used in this research for estimating the drag coefficient ($C_D$).

Naganawa and Nomura (2006) provide expressions for the three forces (gravity, drag, and lift) acting on a single particle about to move at the surface of a deposited bed in terms of the friction velocity ($U_{bh}$) as follows:

$$F_g = (\rho_s - \rho_l) g \frac{\pi d_p^3}{6} \qquad \text{Eqn. 3.57}$$

$$F_D = C_D' \rho_l U_{bh}^2 \frac{\pi d_p^2}{4} \qquad \text{Eqn. 3.58}$$

$$F_L = C_L' \rho_l U_{bh}^2 \frac{\pi d_p^2}{4} \qquad \text{Eqn. 3.59}$$

The drag and lift coefficients are redefined by Naganawa (2006) as:

$$C_D' = \frac{C_D}{f_{bh}} \qquad \text{Eqn. 3.60}$$

$$C_L' = \frac{C_L}{f_{bh}} \qquad \text{Eqn. 3.61}$$

$f_{bh}$ = The interfacial friction coefficient. The correlations of Televantos et al. (1979) will be used.

$$\frac{1}{\sqrt{2f_{bh}}} = -0.86 ln\left(\frac{d_p/D_{hyd}}{3.7} + \frac{2.51}{R_{e,bh}\sqrt{2f_{bh}}}\right) \qquad \text{Eqn. 3.62}$$

$R_{e,bh}$ = Reynolds number for interfacial friction factor (or the generalized Reynold's number) = $\frac{D_{hyd}^n \rho_h U^{2-n}}{8^{n-1} K}$ Eqn. 3.63

$D_{hyd}$ = Hydraulic diameter. Note that a hydraulic diameter definition is utilized because it has been established to give a better estimate under laminar conditions (Anifowoshe and Osisanya, 2012).

U = Average annulus fluid velocity

n = Fluid behavior index

K = Fluid consistency index

As proposed by Naganawa and Nomura (2006), where "rolling" is the dominant re-suspension mechanism, the equilibrium of moments around the contact point of a particle that is just about to move is as follows (Naganawa 2006):

$$\frac{d_p}{2} F_D Cos\emptyset + \frac{d_p}{2} F_L Sin\emptyset - \frac{d_p}{2} F_g Sin\left(\frac{\pi}{2} - \theta + \emptyset\right) = 0 \qquad \text{Eqn. 3.64}$$

$\emptyset$ = Particle angle of repose (in radians)

$\theta$ = Wellbore inclination (in radians)

Where "lifting" is the dominant re-suspension mechanism, Naganawa and Nomura (2006) proposed the following:

$$F_L - F_g Sin\theta = 0 \qquad \text{Eqn. 3.65}$$

Substituting equations (3.57) to (3.59) in the equilibrium equations (3.64) & (3.65), and assuming the boundary angle to be equal to the complementary angle of repose (β), and continuity of the critical friction velocity at the boundary angle is achieved, the critical friction velocity ($U_{bh}^{*}$) was obtained for each case where the re-suspension mechanism is rolling or lifting respectively as follows Naganawa and Nomura (2006):

$$C'_L = \frac{C'_D}{tan\emptyset} \qquad \text{Eqn. 3.66}$$

$$U^*_{bh} = \begin{cases} \left[\frac{d_p g(\rho_s - \rho_l)}{3\rho_l C'_D}(Cos\theta + tan\emptyset Sin\theta)\right]^{1/2}, & \theta \geq \beta \\ \left[\frac{2d_p g(\rho_s - \rho_l)}{3\rho_l C'_D} tan\emptyset Sin\theta\right]^{1/2}, & \theta < \beta \end{cases} \qquad \text{Eqn. 3.67}$$

Duan et al. (2009) presents an expression for a lift coefficient ($C_L$) based on Saffman (1965) and assuming a wall correction factor of 0.6 as follows:

$$C_L = 2.47\sqrt{\frac{d_p}{R_{ep}V_r}\frac{dV_r}{dy}}, \quad R_{ep} < 1 \qquad \text{Eqn. 3.68}$$

For $R_{ep} > 1$, the expression proposed by Kurose and Komori (1999) is commonly used.

$$C_L = K_0\eta^{0.9} + K_1\eta^{1.1}, \quad R_{ep} > 1 \qquad \text{Eqn. 3.69}$$

$K_0$ and $K_1$ are dependent on $R_{ep}$. Duan et al. (2009) present expressions for $K_0$ and $K_1$ by curve fitting.

By adopting the analogy of the principles of solids suspension in a stirred tank, this research proposes an opportunity to extend the current understanding of how hindered settling and drill string rotation affect the drag forces in a turbulent flow regime. Arguments have been presented to use correlations from the chemical process industries to estimate the effective drag coefficient, which is important for calculating the drag force ($F_D$).

### 3.5.1 Van Der Waal Forces

Solids or particles near each other experience inter-particle forces. As the solids or particles diminish in size, so does the magnitude of the inter-particle force increase due to the increase in surface area per unit volume. It has been established that for fine particles or solids in close contact, the Van Der Waals forces are the dominant forces (Hiemenz, 1986). Van De Ven (1989) further found that the forces are attractive if the solids or particles are made of the same material.

To account for the existence of the Van Der Waals forces at play between particles, this research proposes an equilibrium of moment equation for a single particle resting on a pile of inclined cuttings bed, and just about to experience motion as follows:

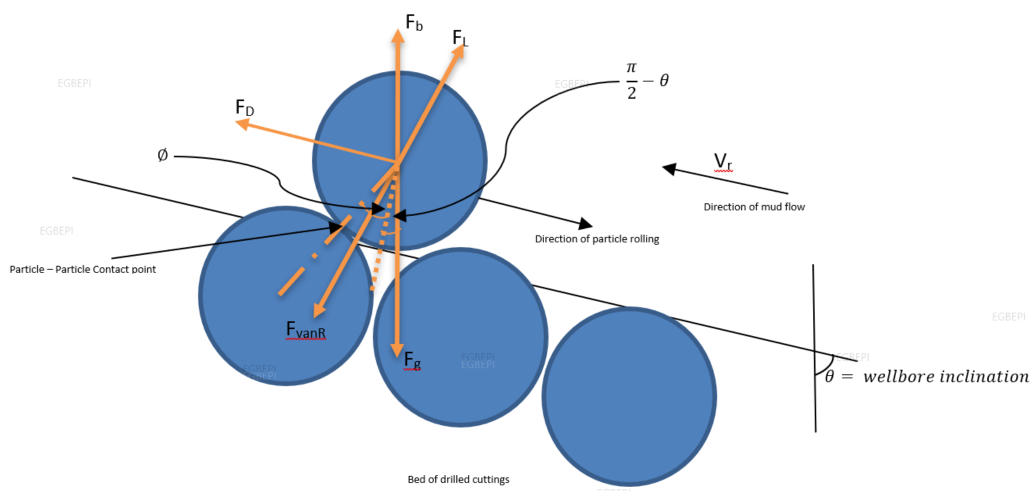


Figure 3.5: Moment-Balance of a Cuttings Particle at Rest and About to Experience Motion

Based on Figure 3.5, the proposed moment-balance equation is given as:

$$\frac{d_p}{2} F_D Cos\emptyset + \frac{d_p}{2} F_L Sin\emptyset - \frac{d_p}{2} F_{vanR} Sin\emptyset - \frac{d_p}{2} F_g Sin\left(\frac{\pi}{2} - \theta + \emptyset\right) + \frac{d_p}{2} F_b Sin\left(\frac{\pi}{2} - \theta + \emptyset\right) = 0$$

Above is simplified as follows:

$$\frac{d_p}{2}\left[F_D Cos\emptyset + (F_L - F_{vanR})Sin\emptyset + (F_b - F_g)Sin\left(\frac{\pi}{2} - \theta + \emptyset\right)\right] = 0 \qquad \text{Eqn. 3.70}$$

Where;

$F_{vanR}$ = Resultant Van Der Waals forces

$F_b$ = Buoyancy forces = $\frac{\pi d_p^3}{6}\rho_h g$ Eqn. 3.71

Duan et al. (2009) proposed a moment-balance equation like Eqn. 3.70 above except that it is missing the drag force component. The moment balance equation by Naganawa and Nomura (2006) does not account for the Van Der Waals force component either. The drag force and Van Der Waals force comes into play as the cutting is about to roll. Both forces cannot be ignored. Eqn. 3.70 proposed by this research will be used going forward in this thesis.

Work done by previous research have proposed several models to approximate the Van Der Waals energy ($E_{van}$) between two spherical particles and subsequently the Van Der Waals force. Derjaguin (1934) estimated the Van Der Waals force ($F_{van}$) between two spherical particles or curved surfaces in terms of an interaction Van Der Waals energy per unit area as follows:

$$F_{van} = 2\pi \frac{R_1 R_2}{R_1 + R_2} E_{van} \qquad \text{Eqn. 3.72}$$

Where;

$R_1$ and $R_2$ = Radii of two solids or particles or spheres

To estimate the Van Der Waals energy ($E_{van}$), the Hamaker (1937) approach for sphere – sphere interactions is referenced. For two spheres separated by the inter-surface shortest distance, j, is described as follows:

$$E_{van} = -\frac{A}{6}\left\{\frac{2R_1R_2}{r^2-(R_1+R_2)^2} + \frac{2R_1R_2}{r^2-(R_1-R_2)^2} + ln\frac{r^2-(R_1+R_2)^2}{r^2-(R_1-R_2)^2}\right\} \quad \text{Eqn. 3.73}$$

Where;

r = Inter-center distance = $R_1 + R_2$ + j (Nguyen, 2000)

A = Hamaker constant = 4.14 x $10^{-20}$ N.m for quartz (Duan et al., 2009). This value is used for sand

There exists a simpler form of Eqn. 3.73 for sphere - to - sphere interactions. However, Eqn. 3.73 has been shown in Figure 3.6 to have a better approximation to the exact solution for Van Der Waals energy for two polystyrene spheres of radius = 250 nm in water as demonstrated by Nguyen et al. (2012). Figure 3.6 also shows other model approximations (e.g., Derjaguin approximation and non-retarded interaction) to significantly deviate from the exact solution as the inter-surface separation distance, j, increased.

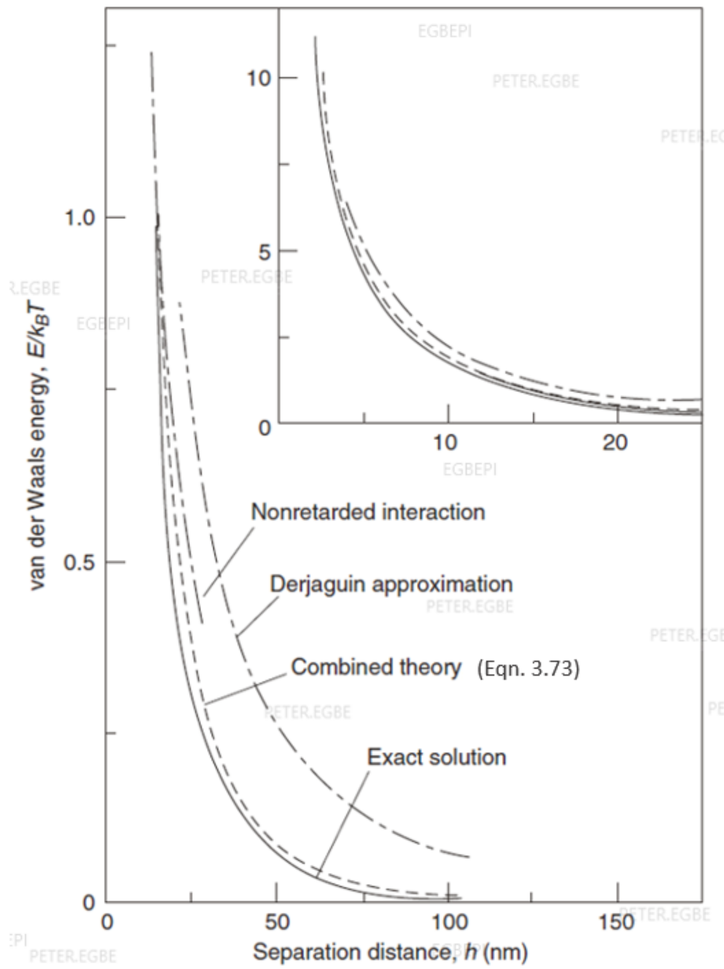


Figure 3.6: Comparison between approximate models and the exact solution for the Van Der Waals energy for two polystyrene spheres of radius R = 250 nm in water (Nguyen, 2000)

Eqn. 3.73 is valid for where the inter-surface shortest distance between the particles or spheres is significantly smaller than the radius of the spheres. This is important to satisfy a fundamental condition of the Van Der Waals forces theory, which is that the particles must be in very close proximity to experience the effect of the inter-particle forces.

To estimate the Van Der Waals force, substitute Eqn. 3.73 into Eqn. 3.72 to obtain the following:

$$F_{van} = \left[2\pi \frac{R_1 R_2}{R_1 + R_2}\right]\left[-\frac{A}{6}\left\{\frac{2R_1R_2}{r^2-(R_1+R_2)^2} + \frac{2R_1R_2}{r^2-(R_1-R_2)^2} + ln\frac{r^2-(R_1+R_2)^2}{r^2-(R_1-R_2)^2}\right\}\right] \qquad \text{Eqn. 3.74}$$

To simplify Eqn. 4.74, it is assumed that $R_1 = R_2 = \frac{d_p}{2}$ for homogeneously sized drilled particles. Eqn. 3.74 thus reduces to

$$F_{van} = -\frac{\pi A d_p}{24}\left\{\frac{d_p^2}{r^2-d_p^2} + \frac{d_p^2}{r^2} + 2ln\left(\frac{r^2-d_p^2}{r^2}\right)\right\} \qquad \text{Eqn. 3.75}$$

The relationship between inter-particle shortest distance, j, and particle diameter, $d_p$, was established based on experimental observations by Yu et al. (2003). Thus, r, the inter-center distance is further simplified because of the above assumption.

$$r = R_1 + R_2 + j = d_p + j$$

$$r = d_p + 1.78 \times 10^{-5} d_p^{0.77} \qquad \text{Eqn. 3.76}$$

To be able to estimate the resultant Van Der Waals forces, $F_{vanR}$, it is important to understand how particles cluster together. The particle surrounded by the cluster experiences a resultant Van Der Waals force as each surrounding particle in the cluster applies a Van Der Waals force to the particle in the middle. Duan et al. (2009) observed experimentally that the average number of sand particles neighboring a single particle is six (i.e., a hexagonal packing structure). As per Duan et al. (2009), the magnitude of the resultant Van Der Waals forces in terms of the angle of repose, ∅, is given as per Eqn. 3.77; and the resultant Van Der Waals force acts in a direction perpendicular to the mean bed surface according to the particle arrangement:

$$F_{vanR} = 6F_{van} \sin \emptyset \qquad \text{Eqn. 3.77}$$

Substituting Eqn. 3.75 into 3.77 results in the proposed estimate for the resultant Van Der Waals forces to be substituted into Eqn. 3.70.

$$F_{vanR} = -\frac{\pi A d_p}{4}\left\{\frac{d_p^2}{r^2-d_p^2} + \frac{d_p^2}{r^2} + 2ln\left(\frac{r^2-d_p^2}{r^2}\right)\right\}\sin \emptyset \qquad \text{Eqn. 3.78}$$

### 3.5.2 Near Bed Velocity Profile

Based on the work by Schlichting (1955), the velocity profile in the viscous layer closest to the cuttings bed is given as follows:

$$u^+ = y^+ \qquad \text{Eqn. 3.79}$$

$$y^+ \leq 5 \qquad \text{Eqn. 3.80}$$

Where;

- $u^+ = \frac{V_r}{U_{bh}}$ = Dimensionless local velocity Eqn. 3.81
- $y^+$ = Dimensionless distance from the mean bed surface
- $V_r$ = Local velocity profile
- $U_{bh}$ = Bed friction velocity = $\left(\frac{\tau_{wb}}{\rho_h}\right)^{0.5}$ Eqn. 3.82

  The heterogeneous layer density ($\rho_h$), is used in this research instead of the fluid density ($\rho_l$ or $\rho_f$) as defined in the original relationships proposed by Schlichting (1955). This is because the density of the fluid in the wellbore is a heterogeneous mixture of drilled cuttings and the initial homogeneous fluid. When that heterogeneous mixture is in circulation, the density of the fluid is referred to as the "equivalent circulating density (ECD)" and considers the friction pressure in the wellbore annulus. When the heterogeneous mixture is static, the density of the fluid is referred to as the "equivalent static density (ESD)". No friction pressure losses are considered in ESD calculations, but the concentration of drilled solids influence the effective weight of the initial homogeneous fluid in the wellbore. Invariably, both the ECD and the ESD values will differ from the homogeneous fluid density. Due to the distribution of drilled solids in the wellbore annulus, the density of that heterogeneous mixture is not constant along the wellbore but will change as the cutting concentration ($C_c$) changes in the heterogeneous layer.

Drilling fluids exhibit more non-Newtonian rheological fluid behaviors. For Power Law fluids, Dodge and Metzner (1958) proposed the below expression for the dimensionless distance from the mean bed surface:

$$y^+ = yU_{bh}^{\frac{2-n}{n}}\left(\frac{\rho_f}{K}\right)^{1/n} \qquad \text{Eqn. 3.83}$$

For a Herschel-Bulkley fluid, this research derives the dimensionless distance from the mean bed surface as follows:

$$\tau_{wb} = \tau_0 + K\left(\frac{dV_r}{dy}\right)^n$$

$$\frac{\tau_{wb} - \tau_0}{K} = \left(\frac{dV_r}{dy}\right)^n$$

$$\frac{dV_r}{dy} = \left(\frac{\tau_{wb} - \tau_0}{K}\right)^{1/n}$$

$$dV_r = \left(\frac{\tau_{wb} - \tau_0}{K}\right)^{1/n} dy$$

$$V_r = y\left(\frac{\tau_{wb}-\tau_0}{K}\right)^{1/n} \qquad \text{Eqn. 3.84}$$

Recall Eqn. 3.79, $y^+ = u^+ = \frac{V_r}{U_{bh}}$. Hence, the dimensionless distance from the mean bed surface is proposed as follows:

$$y^+ = \frac{y}{U_{bh}}\left(\frac{\tau_{wb}-\tau_0}{K}\right)^{1/n} \qquad \text{Eqn. 3.85}$$

Where;

- $\tau_{wb}$ = Bed shear stress
- $\tau_0$ = Yield stress (normally taken as the 3-RPM reading)
- K = Fluid consistency index
- y = Distance from the mean bed surface
- n = Flow index (a Power-Law exponent)

As derived, the local particle velocity profile for a Herschel-Bulkley fluid is mathematically described in equation 3.84 as follows:

$$V_r = y\left(\frac{\tau_{wb}-\tau_0}{K}\right)^{1/n} \qquad \text{Eqn. 3.84}$$

Eqn. 3.84 can also be re-written as

$$dV_r = \left(\frac{\tau_{wb}-\tau_0}{K}\right)^{1/n} dy \qquad \text{Eqn. 3.86}$$

Based on the work by Ahmed (2001), when the viscous sub-layer ceases to exist, the dimensionless velocity profile is as follows:

$$u^+ = 2.44 \ln\left\{\frac{y}{\varepsilon_{bed}}\right\} + 8.5 \qquad \text{Eqn. 3.87}$$

Recall Eqn. 3.79:

$$u^+ = y^+$$

Substituting equation 3.85 into equation 3.87 yields,

$$\frac{y}{U_{bh}}\left(\frac{\tau_{wb}-\tau_0}{K}\right)^{1/n} = 2.44\ln\left\{\frac{y}{\varepsilon_{bed}}\right\} + 8.5 \qquad \text{Eqn. 3.88}$$

Re-arranging, and substituting for $V_r$ and $U_{bh}$ results in the following

$$V_r = \left(\frac{\tau_{wb}}{\rho_h}\right)^{0.5}\left[2.44\ln\left\{\frac{y}{\varepsilon_{bed}}\right\} + 8.5\right] \qquad \text{Eqn. 3.89}$$

$\tau_{wb}$, the bed shear stress (between the cuttings-fluid interface and the wellbore), influences the local velocity; and can be predicted by (Martins et al., 1996):

$$\tau_{wb} = \frac{f_b \rho_b U_b^2}{2} \qquad \text{Eqn. 3.90}$$

$\varepsilon_{bed}$ = Absolute mean cuttings bed roughness (Duan et al., 2009) = $\frac{d_p}{2}(1 + \sin \emptyset)$

Eqn. 3.91

$U_b$ = Cuttings bed velocity

$f_b$ = Bed friction factor, and is defined as follows (Duan et al., 2009):

$$f_b = \frac{16}{R_e^g},\ (Laminar\ Flow) \qquad \text{Eqn. 3.92}$$

And for turbulent flow,

$$\frac{1}{\sqrt{f_b}} = -4\log\left(\frac{0.27\varepsilon_{bed}}{D_{hyd}} + \frac{1.26^{n^{-1.2}}}{\left[R_e^g f_b^{1-n/2}\right]^{n^{-0.75}}}\right),\ (turbulent\ flow) \qquad \text{Eqn. 3.93}$$

$D_{hyd}$ = Hydraulic diameter for an annulus with a bed (Duan et al., 2009) = $\frac{4A_f}{S_o+S_i+S_b}$

Eqn. 3.94

$A_f$ =Fluid open flow area

$S_o, S_i, S_b$=Wetted perimeters of the wellbore, drill pipe, and cuttings bed respectively.

$R_e^g$=Generalized Reynolds number (Duan et al., 2009) = $\frac{D_{hyd}^n \rho_h U^{2-n}}{8^{n-1} K}$ Eqn. 3.95

Eccentricity (e) is estimated as (Duan et al., 2009) = $\frac{a}{R-r}$ Eqn. 3.96

Where "a", "R", and "r" are the offset distance between the center of the wellbore and center of the drill pipe, the wellbore radius, and the drill pipe radius respectively.

Duan et al. (2009) also presents an expression relating the particle Reynold's number to the local velocity profile along the particle center as follows:

$$R_{ep} = \frac{\rho_l V_r^{2-n} d_p^n}{K} \qquad \text{Eqn. 3.97}$$

Recall Eqn. 3.70, the equilibrium of moments around the contact point of a particle that is just about to move,

$$\frac{d_p}{2}\left[F_D Cos\emptyset + (F_L - F_{vanR})Sin\emptyset + (F_b - F_g)Sin\left(\frac{\pi}{2} - \theta + \emptyset\right)\right] = 0$$

The procedure for computing the re-suspension velocity is as follows:

- At a given fluid flow rate Q, into the wellbore, estimate the average annular fluid velocity (U) considering the wellbore geometry
- Estimate the hydraulic diameter ($D_{hyd}$); and the generalized Reynolds number, $R_e^g$. Use the equivalent circulating density (ECD) or heterogeneous layer density ($\rho_h$), and not the original drilling fluid density ($\rho_l$)
- Determine the flow regime (laminar or turbulent flow). Calculate the bed friction factor ($f_b$) using Eqn. 3.92 or 3.93

- Estimate the bed shear stress ($\tau_{wb}$) using Eqn. 3.90
- Estimate the particle Reynolds number ($R_{ep}$) using Eqn. 3.52, and dimensionless shear rate (η)
- Calculate the local particle velocity, $V_r$ using Eqn. 3.97; and the local velocity gradient $\frac{dV_r}{dy}$ using Eqn. 3.86
- Estimate the drag coefficient ($C_D$), and the lift coefficient ($C_L$). Estimate the re-defined $C_D'$ and $C_L'$
- Calculate the drag, lift, buoyant, and gravity forces. Use the estimated local particle velocity ($V_r$) as the velocity term in the calculations for the drag and lift forces. Use the ECD or heterogeneous layer density ($\rho_h$) as the density term in the calculations for the drag, lift and buoyant forces
- Estimate the resultant Van Der Waals force using Eqn. 3.78
- Substitute all the forces into Eqn. 3.70. If the resultant moment is greater than zero (0), decrease the flow rate. If it is less than zero, increase the flow rate; and repeat the above procedure until the resultant moment converges to zero (or within an acceptable tolerance). When the solution converges to zero, the average fluid velocity calculated at that point is the critical re-suspension velocity (CRV). The flow chart shown in Figure 3.7 summarizes the proposed procedure for estimating the CRV.

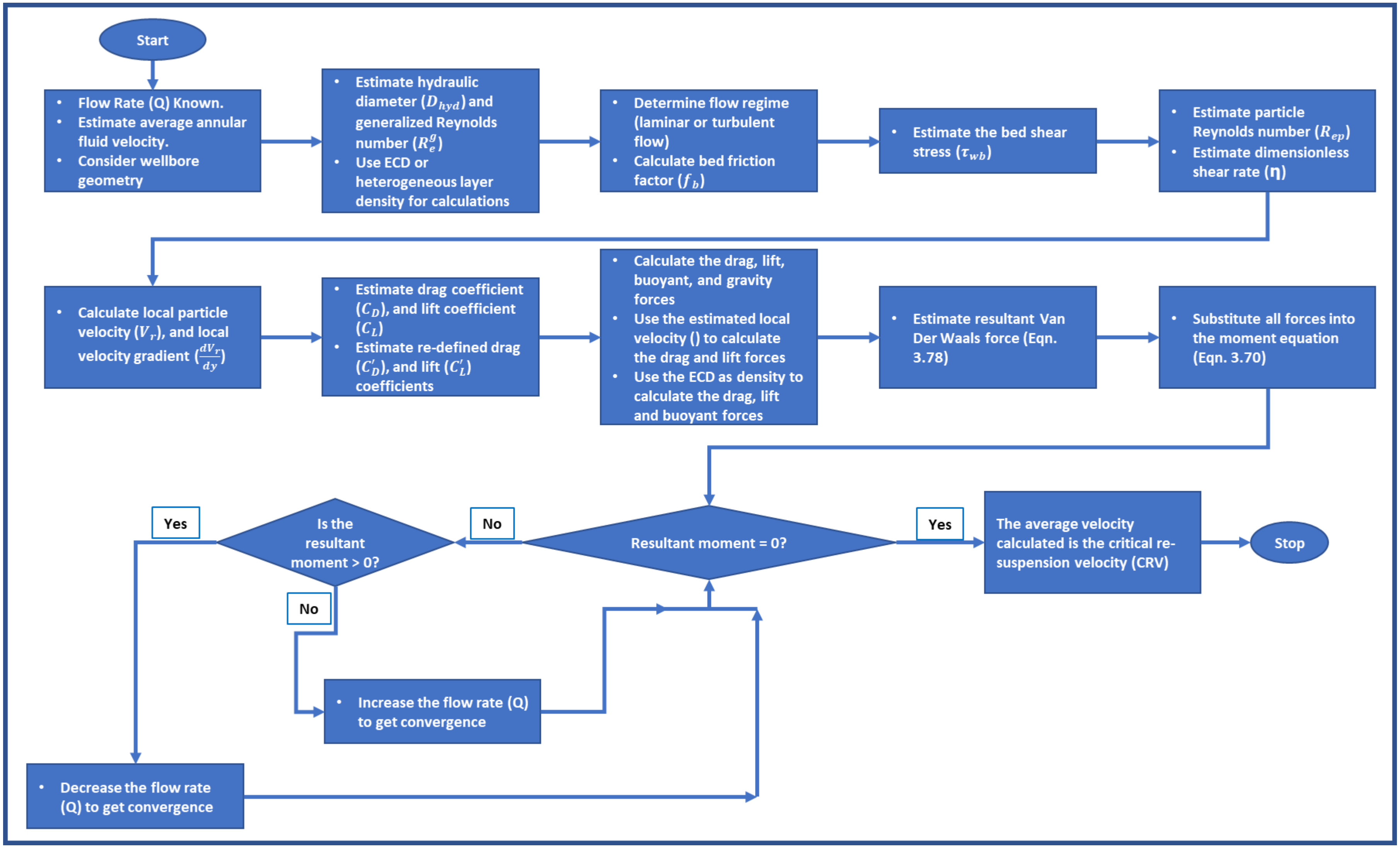


Figure 3.7: Flow Chart for Estimating Critical Re-Suspension Velocity (CRV)

## 3.6 Azimuthal Annulus Velocity (AAV) Profile

With reference to section 2.4.4, the annular velocity profile will be developed based on the azimuthal velocity; and the following boundary conditions

$$V_r = V_z = 0 \; at \; r = r_o$$

$$V_r = V_z = 0 \; at \; r = r_i$$

$$V_\theta = 0 \; at \; r = \; r_o$$

The conditions in Eqn. 2.17 and 2.18 are re-defined in terms of the azimuthal velocity ($V_\theta$) as follows:

$$\frac{CSV}{V_\theta} \gg 1, cuttings \; will \; not \; be \; captured \; by \; the \; vortices$$

$$\frac{CSV}{V_\theta} \ll 1, cuttings \; will \; be \; captured \; by \; the \; vortices$$

A relationship for the azimuthal velocity is obtained from the Herschel-Bulkley fluid model in terms of the Power Law index (n). The relationship is obtained by equating the expressions for shear stress as a function of the following:

i. The azimuthal velocity gradient in the direction normal to the string rotation ($\frac{dV_\theta}{dr}$)
ii. The radius and torque of the string (which is equivalent to the inner rotating cylinder in Taylor's experimental setup)

The following are assumed:

- Flow is steady, isothermal, and laminar
- The fluid is a Herschel-Bulkley fluid

- The drill string is rotating at a constant revolution per minute (RPM), and by extension, a constant angular velocity
- Flow is axi-symmetric, and end effects are negligible or eliminated by geometrical configuration
- Gravity effects are negligible

The listed assumptions reduce the flow problem in cylindrical coordinates to a one-dimensional problem, and $\frac{dV_\theta}{dr} \neq 0$

As discussed at the beginning of this chapter-3, the Herschel-Bulkley fluid model is being used in this research, and its constitutive equation is given as follows:

$$\tau = \tau_o + K\dot{\gamma}^n \qquad \text{Eqn. 3.98}$$

Where:

$\tau$ = Shear stress

$\tau_o$= Yield stress or true yield. Usually taken as the 3-RPM reading

$K$= Consistency index

$n$= Power law exponent (or fluid index)

$\dot{\gamma}$= Shear rate = $-\frac{dV_\theta}{dr}$ Eqn. 3.99

Equation 3.98 becomes

$$\tau = \tau_o + K\left(-\frac{dV_\theta}{dr}\right)^n$$

$$|\tau| = |\tau_o| + K\left(\frac{dV_\theta}{dr}\right)^n \qquad \text{Eqn. 3.100}$$

At r = $r_i$ (i.e., the radius of the inner rotating string)

$$\text{Torque, } T = \tau_{r\theta|r=r_i}(2\pi r_i \times L r_i)$$

$$\tau_{r\theta} = \frac{T}{2\pi L r^2}$$

$$\tau_{r\theta} = \frac{C}{r^2}$$

The governing "θ – momentum" equation becomes

$$\tau = \frac{C}{r^2} \qquad \text{Eqn. 3.101}$$

Where;

T = Torque = $\tau \times 2\pi r \times Lr = 2\pi L r^2 \tau$ Eqn. 3.102

Based on Eqn. 3.102,

$$\tau = \frac{T}{2\pi L r^2} \qquad \text{Eqn. 3.103}$$

Equating Eqn. 3.100 to 3.103

$$\tau_o + K\left(\frac{dV_\theta}{dr}\right)^n = \frac{T}{2\pi L r^2} \qquad \text{Eqn. 3.104}$$

Re-arranging, integrating, and making $V_\theta$ subject of the equation yields the following

$$V_\theta = \left(\frac{T}{2\pi K L}\right)^{1/n} \frac{r^{1-2/n}}{(1-2/n)} - r\left(\frac{\tau_o}{K}\right)^{1/n} + C \qquad \text{Eqn. 3.105}$$

Applying boundary conditions of $V_\theta = 0, at\ r = r_o$ yields the following

$$C = r_o\left(\frac{\tau_o}{K}\right)^{1/n} - \left(\frac{T}{2\pi K L}\right)^{1/n} \frac{r_o^{1-2/n}}{(1-2/n)} \qquad \text{Eqn. 3.106}$$

Substituting in Eqn. 3.105, and re-arranging results in the following

$$V_\theta = \frac{1}{1-{}^2/_n}\left(\frac{T}{2\pi KL}\right)^{1/n}\left(r^{1-2/n} - r_o^{\,1-2/n}\right) - \left(\frac{\tau_o}{K}\right)^{1/n}(r - r_o) \qquad \text{Eqn. 3.107}$$

Eqn. 3.107 is differentiated, and results in the proposed azimuthal velocity profile in terms of n, K, r, and T at any depth (L) along the wellbore as follows

$$\frac{dV_\theta}{dL} = \frac{1}{1-{}^2/_n}\left(\frac{T}{2\pi K}\right)^{1/n} {}^1/_n\left(\frac{1}{L^{1+1/n}}\right)\left(r^{1-2/n} - r_o^{\,1-2/n}\right) \qquad \text{Eqn. 3.108}$$

Eqn. 3.108 is wholly a function of the Power Law fluid and consistency indices ("n" and "k"), and the drill string rotating torque (T).

Where;

$V_\theta$ = Azimuthal velocity at any radial point "r" between (m/s)

$r_o$ = Wellbore radius (m)

$r_i$ = Drill string outer radius (m)

$r$ = Any radial distance from the center of the drill string (m)

$K$ = Power Law fluid consistency index $= \frac{\theta_{300}}{511^n}$, $\theta_{300} = PV + YP$ Eqn. 3.109

$n$ = Power Law fluid index $= 3.32\ \log\frac{\theta_{600}}{\theta_{300}}$, $\theta_{600} = \theta_{300} + PV$ Eqn. 3.110

$T$ = Drill string rotating torque

$L$ = Wellbore length in measured depth (m)

PV = Plastic viscosity, YP = Yield point

A relationship for the maximum azimuthal velocity ($V_{\theta max}$) can be obtained using Eqn. 3.107, and the following boundary condition

$$V_\theta = V_{\theta max} \; at \; r = r_i$$

Eqn. 3.107 thus becomes

$$V_{\theta max} = \frac{1}{1-{}^2/_n}\left(\frac{T}{2\pi KL}\right)^{1/n}\left(r_i^{1-{}^2/_n} - r_o^{1-{}^2/_n}\right) - \left(\frac{\tau_o}{K}\right)^{1/n}(r_i - r_o) \qquad \text{Eqn. 3.111}$$

Given the above, the azimuthal velocity ($V_\theta$) at any radial point (r) from the surface of the rotating drill string can be obtained as a function of the maximum azimuthal velocity ($V_{\theta max}$). Dividing Eqn. 3.107 by Eqn. 3.111, and eliminating similar terms yields the following:

$$\frac{V_\theta}{V_{\theta max}} = \frac{\left[r^{1-{}^2/_n} - r_o^{1-{}^2/_n}\right] - (r - r_o)\left({}^{\tau_o}/_K\right)^{1/n}}{\left[r_i^{1-{}^2/_n} - r_o^{1-{}^2/_n}\right] - (r_i - r_o)\left({}^{\tau_o}/_K\right)^{1/n}} \qquad \text{Eqn. 3.112}$$

The azimuthal velocity profile at any radial point (r), from the surface of a rotating drill string is obtained (as a function of "n", the yield Power Law fluid index) from Eqn. 3.112. The profile will be the same at any depth "L" along the wellbore.

As determined by Philip et al. (1998), the influence of the vortex velocity, and the azimuthal velocity yield a net lift force. They added that in some locations, the Taylor vortices may aid the lift forces generated due to the azimuthal velocity; and in some other instance, may act negatively to minimize the impact of the azimuthal velocity lift force. Regardless, and by way of experimental observations, they established that the cuttings bed showed a banded structure (like sand dune formations) resulting from the action of Taylor vortices and azimuthal velocity. In the presence of axial, and/or rotational flow, this cuttings banding will positively influence the lifting and cuttings transportation efficiency out of the wellbore.

### 3.7 Real-Time Stuck Pipe Prediction

A technique to reliably predict the probability of a drill string getting stuck well ahead of time is proposed as part of this research. The technique evaluates changing wellbore conditions in real-time and detects the onset of conditions that may result in a stuck drill pipe. It does this by applying the “ROW” technique described in section 1.1 and illustrated in Figure 1.1 of this thesis. The philosophy of using the “ROW” technique proposed by this research to predict stuck pipe events is seen as robust because it considers current well bore conditions (i.e., real-time data), previous historical events (i.e., offset wells), and engineering simulation predictions (i.e., well design models). It is applicable to wells of all types, and for all operational activities such as, but not limited to drilling, tripping, reaming, and deployment of tubulars.

The numerical workflow (i.e., a combination of different models) developed in this research are used to analyse and predict the hole cleaning efficiency. In combination with other available industry well design models (e.g., torque & drag and fluid hydraulics), it provides an early warning capability based on a non-subjective risk probability. The risk profile is displayed in real-time to warn the user of changing wellbore conditions that could result in a potential stuck pipe situation. The risk alert increases in the time leading up to the stuck pipe event and remains relatively low during normal drilling operations. The alerts are expected to occur sufficiently ahead of the event so that drilling teams have time to proactively respond and avert the potential stuck pipe events.

### 3.7.1 Determination of Stuck Pipe Leading Indicators in Real-Time

Based on the analysis of several historical stuck-pipe events, stuck pipe events are not preceded by a single leading indicator. It usually is a combination of various data points that is required to reliably predict the onset of the event. The adopted approach in this research is to analyze the trends of the real-time data streams, as well as independently compared to pre-determined thresholds. Trends that exceed the defined thresholds either individually, or in combination form the basis of the flags that indicate an impending stuck pipe event. Thus, in terms of real-time data analysis, the stuck pipe predictive tool is designed to achieve the following minimum capabilities:

- Generate valid alerts based on evolution of real-time data from point to point
- Use well design model predictions (e.g., hole cleaning, torque & drag, hydraulics) as guided road maps to which evolving real-time data are constantly compared to. Deviations from such road maps may indicate a potential downhole problem
- Compare evolving real-time data trends to offset wells historical data for pattern recognition
- Generate valid alerts with sufficient warning time ahead of the actual event
- Generate a minimum number of false alerts

To achieve the above capabilities, the type, frequency, and quality of data streamed via the Wellsite Information Transfer Markup Language (WITSML) needs to be consistent in all wells (Salminen et al., 2017). Ideally, the more high-quality real-time data streams available, the higher the accuracy of the prediction. However, many drilling operations transmit only the basic data available from the Martin Decker instruments, and sometimes at poor data frequency. Hence, any predictive algorithm must also be able to generate the required valid alerts using this bare minimum information. Below are the basic rig data used in the proposed method:

- Mud flow rate into the well
- Surface drill string rotary speed (revolutions per minute, RPM)
- Weight-on-bit (WOB) at surface
- Stand-pipe pressure (secondary data derived from the magnitude of mud flow rate)
- Drill string torque (secondary data derived from the applied drill string surface rotary speed)
- Hook-load (secondary data derived from the applied weight-on-bit, string weight, fluid buoyancy effect, wellbore trajectory & tortuosity)
- Rate of penetration (secondary data derived from applied weight-on-bit, and string rotation. It is also indicative of the formation lithology being drilled)

### 3.7.2 Regression Analysis for Real-Time Data Trends

The predictive method proposed in this research identifies the start of a potential stuck-pipe event based on real-time data trends. Regression analysis of data to detect anomalies in real time is thus critical. The below regression analysis methods are used to evaluate trends in the transmitted real-time data:

1. “Deviation” of real-time data from the well design model predicted values: This will compare what is measured by the rig sensors to what has been generated by hole cleaning, hydraulics, or torque and drag (T&D) models. If the deviation between actual and predicted data approaches or exceeds a defined threshold, the risk of an impending stuck pipe is assessed to be increasing. Figure 3.8 is an example of actual on and off bottom torque values are compared to model predicted on and off bottom torque values. In this example, the actual data and model predictions show a very good correlation.

$$Deviation = \frac{Data_{actual} - Data_{predicted}}{Data_{predicted}} \qquad \text{Eqn. 3.113}$$

The numerical workflow for hole cleaning and hydraulics models developed in this research have been used. These are presented in sections 3.3 to 3.6 of this thesis. T&D analysis was done with Halliburton Landmark software utilizing the “soft-string” model. Soft-string T&D modeling was initially developed with Johancsik et al. (1984), and later adapted in a standard differential form by Sheppard et al. (1987). Because of its simplicity, and the fact of being user friendly, it has found extensive use and preference in the industry unless it introduces considerable errors in the calculations. The soft-string model by Sheppard et al. (1987) is considered by many in the industry to be the standard model for T&D analysis (Ohia et al., 2021). The general belief in the industry is that for majority of the cases, the soft-string model predictions are sufficient; and in other instances, a combination of the soft and stiff-string model can be used (Mirhaj et al., 2016). Such instances may include wells with highly tortuous trajectories, high dog-leg severities, and with narrow radial clearances (Ohia et al., 2021).

Hole cleaning, hydraulics, or T&D models predict results on a set frequency (usually per 100 ft). Real-time data on the other hand is generated on a higher frequency. This thus presents a problem where most of the actual data will fall in the interval between model predicted results. To resolve this challenge, a direct interpolation of the predicted data for each depth is used to plug the gaps, and there is a prediction for each depth for comparison.

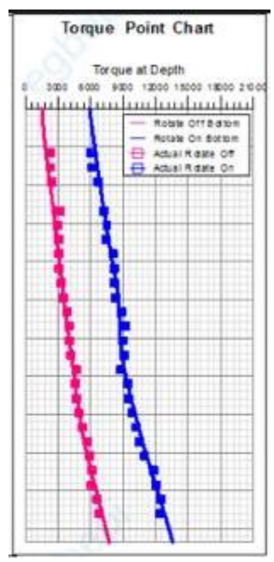


Figure 3.8: Example of model vs. actual real-time data

2. Rate of change ("RoC data"): This focuses only on the rate of change of a single data variable from point to point. No reference is made to well design model predictions; but is used to track rapid, "single point" changes or trends (i.e., anomaly detection) which may be indicative of evolving downhole wellbore conditions.

Various statistical methods for anomaly detection or regression analysis such as moving averages, and the z-score were considered. Section 2.3.1 of this thesis presents a review of different statistical techniques and methods. Salminen et al. (2017) used the simple moving average method with good success. Although moving averages are a good method to analyze trend cycles, the “m” order of the moving average must be accurate, and symmetric to be representative of the data being analyzed. The z-score method in anomaly detection works on the basis that the value of the data is in a Gaussian distribution with some skewness and shape of the probability distribution (Zhang, 2019). Consequently, the anomalies present in a data set will be the points located by some order of standard deviation away from the mean of the data set (Nisbet et al., 2018; Lepenioti et al., 2020). The larger the number of standard deviations away from the mean, the more of an anomaly that data point is, and the higher the probability that it is an outlier (see Figure 3.9 where the red dots are outliers relative to the distribution curve). Z-scores are also recommended for use as benchmarks in supervised and unsupervised learning systems. Z-score techniques are applied in other “data heavy” disciplines such as mobile telephone networks to ensure that a user’s mobile connection syncs with the nearest network signal; and financial fraud detection to review credit card usage to identify fraudulent purchases.

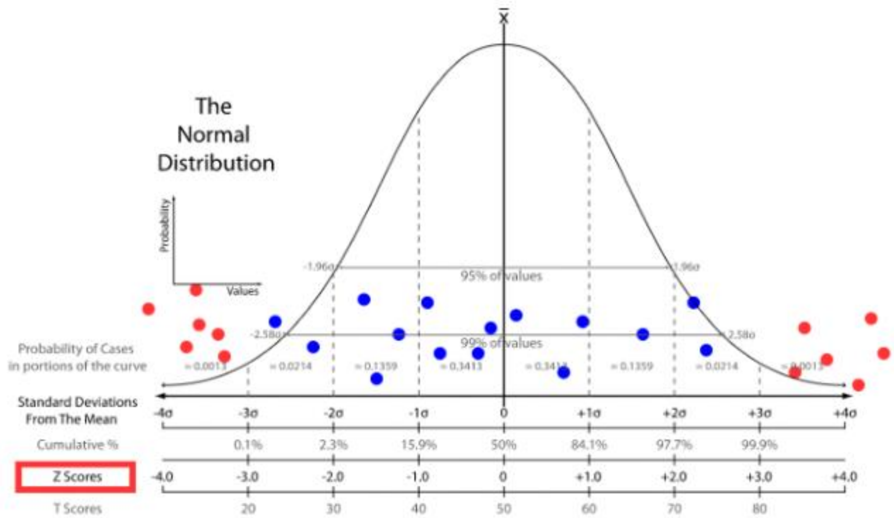


Figure 3.9: z-Score Method for Anomaly Detection (Zhang, 2019)

Thus, for increased accuracy, the RoC data is calculated in this research by using a "z-score" statistical method. It is used to compare the data obtained while drilling the current stand or joint of drill pipe to the previously drilled one or more stands, or joints of drill pipe to evaluate if an outlier from a normal trend has occurred or not. The idea is that while drilling a stand or joint of drill pipe with constant parameters (of WOB, RPM, and GPM), the output in drilling mechanics variables (e.g., HKLD, TRQ, and SPP) should be stable, unless something changes downhole (e.g., the formation strata being drilled, presence of a cuttings bed, etc.). That change could be indicative of evolving downhole conditions (e.g., increased risk of stuck pipe, a kick, etc.) if the z-score correlation falls outside of a defined statistical range compared to previous data windows. The data windows for comparison could be one, two, or more windows depending on the level of accuracy desired. In this case a data window is defined as 30 ft or 93 ft, the average length of a joint or stand of drill pipe, respectively. Depending on user preferences, the data window can also be smaller sizes (e.g., 5, 10, or 15 ft). This assessment provides an additional layer of sensitivity and accuracy. For this research, the z-score ranges from -3 to 3, and is defined as follows:

$$z_i = \frac{x_i - \mu_i}{\sigma_i} \qquad \text{Eqn. 3.114}$$

where μ and σ refer to the mean and standard deviation for the $i^{th}$ drilling parameter and x is the drilling parameter value that will be normalized. This research proposes the following steps for assessing the real-time data rate of change:

a. Generate the z-score using raw transmitted WITSML data per depth in each defined data window
b. Calculate the average of z-score for each data window such that
   i. Window 1 = $Z_{1\,(avg)}$
   ii. Window 2 = $Z_{2\,(avg)}$
   iii. Window "n" = $Z_{n\,(avg)}$
c. Calculate the absolute rate of change (RoC) from one window to the next using the average z-score as follows
   i. $RoC_1 = \frac{Z_{1(avg)} - Z_{0(avg)}}{Z_{0\,(avg)}}$
   ii. $RoC_2 = \frac{Z_{2(avg)} - Z_{1(avg)}}{Z_{1(avg)}}$ Eqn. 3.115
   iii. $RoC_n = \frac{Z_{n(avg)} - Z_{n-1(avg)}}{Z_{n-1(avg)}}$
d. Compare the calculated RoC to a threshold to assess if an alert should be generated

With reference to appendix A, Table 3.4 presents results of a typical RoC calculation for four equally spaced 5 ft data windows of a sample well

Table 3.4 Sample RoC Calculation

| Data Window (n) | Average z-Score ($Z_{n\,(avg)}$) | Rate of Change ($RoC_n$) |
|---|---|---|
| 1 | 5.3187 E-15 | 0 |
| 2 | 5.7425 E-15 | $\frac{(5.7425\ E{-}15)-(5.3187\ E1{-}15)}{(5.3187\ E1{-}15)} = 0.0797$ |
| 3 | 5.4741 E-15 | $\frac{(5.4741\ E{-}15)-(5.7425\ E{-}15)}{(5.7425\ E{-}15)} = -0.0467$ |
| 4 | -8.7139 E-15 | $\frac{(-8.7139\ E{-}15)-(5.4741\ E{-}15)}{(5.4741\ E{-}15)} = -2.5918$ |

3. Threshold definition: For the real-time data regression analysis, the threshold is defined based on an assessment of offset wells with stuck pipe case histories. As a result, the threshold can be field or well specific. The ability to be able to adjust the thresholds per field and well type is seen as an advantage since it provides a level of adaptability for users fit-for-purpose thresholds, as opposed generic thresholds. The alerts will be generated based on:

    a. When the correlation of the "deviation change" falls outside of a defined threshold, or

    b. When the correlation of the absolute RoC falls outside of a defined threshold, or

c. When both "a" and "b" above occur simultaneously

Thus, using the above logic a deviation change of 10% should flag an alert if for example the threshold (based on offset historic wells) was defined as 5%. Likewise, the opposite (i.e., no flags) should be true if the change is less than the threshold.

4. Data normalization and smoothening: Outliers in rig sensor data output is a common occurrence. These may be due to calibration issues, sensor offsets, or data transmission quality issues. To account for these, moving averages are used to smoothen the data and provide better prediction accuracy. Moving averages acts as a low-pass filter to smoothen noisy data.

#### 3.7.2.1 Data Preparation and Classification

Data preparation and classification to define the operations logic is required. Identifying the maximum, minimum, and mean values for critical parameters is key to enabling any predictive tool to select the correct data points for analysis.

The logic for the stuck pipe prediction tool works as follows:

1. Hole cleaning and hydraulics models are prepared using planned mud weights, well / section total depths (measured & true vertical), and fluid rheology. This will estimate the expected standpipe pressures, equivalent circulation densities (ECDs), minimum/critical flow velocity, and bed heights at corresponding measured depths
2. Torque and drag (T&D) simulations are prepared for the subject well at the design phase using well specific info, and friction factors from offset wells.

The T&D charts are prepared using several "open hole" and "cased hole" friction factors. The range of the friction factors are field dependent. If no offset field data is available, the friction factors can be calibrated in real-time

3. During drilling, the model versus actual deviation change, and / or the rate of change from point to point are evaluated as described in section 3.7.2 for the following data variables
    a. The pick-up, slack-off, rotating weights based on the hook-load data
    b. The "on" and "off" bottom rotating torque based on the surface torque data
    c. The critical velocities, stand-pipe pressure, ECD, and bed heights based on the flow rate data, and fluid rheology
    d. Deviation of the following parameters from well design predictions are evaluated:
        i. Stand-pipe pressure (SPP)
        ii. Surface rotary torque (TRQ)
        iii. Hook-load data (HKLD) including pick-up weight (PU_WT) and slack-off weight (SO_WT)
    e. Rate of change of the following parameters as the well is drilled is evaluated:
        i. Stand-pipe pressure (SPP_RoC)
        ii. Surface rotary torque (TRQ_RoC)

iii. Hook-load data (HKLD_RoC)

iv. A delta (Hook-load, HKLD) plotted against time is used to further compare the wellbore "aging"; and compare / identify degrees of wellbore deterioration

f. A "deviation change" and / or a "rate of change" outside a permitted range will flag that there is an impending stuck pipe; or a deteriorating wellbore condition

Note that the above described is applicable to all rig operation activities, and not only for "rotary drilling" activity where the hole depth increases as the wellbore is deepened progressively. Thus, the real-time data needs to be grouped per other activities that occur after a stand has been drilled down such as ream in, back ream, trip in, trip out, and slide drill, etc. (Salminen et al., 2017, Al Shaikh et al., 2019). Hence, an algorithm to automatically detect the start of each rig operation activity is necessary. This is important for three main reasons:

- To assign the incoming real-time data correctly to each phase of rig operation activity
- To ensure that all incoming data are grouped and classified together for ease of evaluating change which could be either RoC, or deviation change
- Well design models (e.g., torque & drag, hydraulics, trajectory, etc) predict an expected value for a specific parameter versus the bit depth. Hence, if we know the bit depth, and the associated rig operation activity for each real-time transmitted data, we can correctly assign and compare the relevant data to the corresponding predicted value from the models

An example of how the logic works for the pick-up (PU_WT) and slack-off (SO_WT) is presented in Table 3.5. Similar logics are defined for other rig operations activities.

Table 3.5 Example Data Classification

| **Data Class** | **Rate of Change (RoC)** | **Deviation Change (DeC)** |
|---|---|---|
| Pick-Up Weight | • Identify Kelly down (rate of penetration, ROP = 0, and hook height above rotary table, HKHT = ±2 ft)<br>• Bit Moving Up<br>• Window ends when the bit starts moving down<br>• Calculate the z-score between two or more windows<br>• Assess hole condition using z-score<br>• Compare to thresholds and raise alert if necessary | • Interpolate planned data over every interval of depth<br>• Compare the actual data in a window vs interpolated planned window<br>• Assess deviation change<br>• Compare to thresholds and raise alert if necessary |
| Slack-Off Weight | • Starts immediately after PU window<br>• Stops when the hook-load (HKLD) drops significantly (~20%)<br>• Calculate the z-score between two or more windows<br>• Assess hole condition using z-score<br>• Compare to thresholds and raise alert if necessary | Same as above |

#### 3.7.2.2 Challenges with Stuck Pipe Tool Automation

A summary of challenges faced in trying to automate the logic are as follows:

1. Single point versus multiple point data comparison with the simulated T&D and hydraulics results: The manual logic utilized single point comparison. The use of multiple points for comparison is believed to provide better accuracy; and with the added ability to be able to reflect the operational stages (i.e., drilling / wash-up / ream-up / wash-down / ream-down)

2. A method or means of getting the real-time tool to compare data for a given interval drilled.

    a. It is easy to pick a data point and compare that data point to a single value from the simulated data at a particular depth.

    b. However, evaluating the rate of change of a "group" of data points obtained in real-time over a 30 ft or 93 ft interval as the drill string is manipulated up and/or down proved to be a challenge in terms of how to ascribe the acquired data to the correct period given that a particular depth may be transversed several times while the hole depth remains unchanged. To solve this challenge, Salminen et al. (2017) presented a solution by introducing the "bit velocity" term to convert the data from a "depth" domain to a "time" domain. Salminen et. al. (2017) found that by including the bit velocity term, the same thresholds that were found to be accurate in a "depth" domain could be utilized with the same accuracy. The bit velocity can be positive (tripping in or drilling), or negative (picking up or tripping out).

$$RoC\ threshold = \frac{Change\ in\ Parameter}{Depth\ (m)} = \frac{Change\ in\ Parameter}{Bit\ Velocity\ (m/s) \times time\ (s)} \qquad \text{Eqn. 3.116}$$

c. For comparison purposes, the "bit depth" rather than the "hole depth" is used. This is because as the drill string is pulled out or lowered into the wellbore, real-time data (such as hook-load, SPP, TRQ, etc.) is continuously being transmitted and written into the WITSML database against a reference time and depth. In this time however, only the "bit depth" changes while the "hole depth" remains constant until the wellbore is deepened further. Thus, a means of identifying, and "grouping" the real-time data acquired during each phase of the string going up or down was necessary – as well as associating it the correct wellbore interval. The application of the bit velocity term again proved useful in switching from a "depth" to a "time" domain

### 3.7.3 Method of Risk Ranking

The method of risk calculation and ranking (low, medium, or high risk) is based on a semi-qualitative, and weighted risk approach. A weighted risk scoring approach is used because of its simplicity, and consistency (with limited bias) in evaluating a potential risk.

The weighted risk scoring model used is broken down into a set of pre-established criteria highlighted in Table 3.6. Each criterion is given a unique risk weight which determines the level of the criterion's influence on the overall stuck pipe risk score.

Table 3.6 Weighted Risk Scoring Model

| Risk Criteria | Weighted Risk Score | Remarks |
|---|---|---|
| **R**eal-time drilling data rate of change (RoC) for:<br>• Flow rate in<br>• Surface rotary speed (RPM)<br>• Surface weight on bit (WOB)<br>• Surface rotary torque<br>• Stand-pipe pressure changes<br>• Hook-load | 60% | The real-time data is allocated the highest score as it is representative of the conditions of the well under construction. It is considered the source of highest risk influence. Each of the real-time parameters contribute a fraction of the allotted 60% weighted risk score |
| **O**ffset wells data pattern such as:<br>• Known wellbore instability zones<br>• Intervals of anticipated high over-balance pressures<br>• Wells with historic stuck pipe events | 20% | Assessment of real-time data trends are used in combination with statistical analysis to identify similar trends from offset wells in which stuck pipe events have occurred historically. Each pattern contributes a fraction of the allotted 20% weighted risk score |
| **W**ell design & planning analysis deviation change (model vs actual data) such as:<br>• Hydraulics & hole cleaning models (e.g., critical velocity models, equivalent circulating density, ECD)<br>• Torque & Drag models (e.g., Pick-up & Slack-off weights changes<br>• Planned trajectory | 20% | These will form the basis for real-time comparison. The deviation from which may signal an alert warning to the crew. Each parameter contributes a fraction of the allotted 20% weighted risk score |

Offset wells analysis involves review of drilling troubles encountered in similar formation intervals. This could range from loss of circulation, wellbore instability, intervals of high over-balance pressure, historic stuck pipe events, etc. The formation intervals at which these historic drilling troubles were encountered are pre-populated in the stuck pipe predictive tool. This is important for the tool's weighted risk scoring model to account for the possibility of such potential drilling troubles in the alerting system.

Three advantages of the weighted risk approach are as follows:

- It allows for a layer of flexibility for future evolution of the logic. For example, an additional risk criterion can be added (or removed) and awarded a weighting for use in evaluating the probability for a stuck pipe event.
- Depending on the peculiar challenges faced in a particular field, and / or well type, the risk weighting for the criterion considered most important can be amended as required by the drilling team.
- Can be applied across a large dataset without a loss of consistency

The above advantages mean the proposed stuck pipe index prediction tool is adaptable to a variety of conditions without a loss of sensitivity, reliability, and repeatability in its output. Based on the risk criteria and weighted score, the risk probability indices are calculated as follows:

$$
\begin{aligned}
&Stuck\ Pipe\ Index \\
&\qquad = Weighted\ risk\ due\ to\ Real\ Time\ Well\ Conditions \\
&\qquad + Weighted\ risk\ due\ to\ offset\ wells \\
&\qquad + Weighted\ risk\ due\ to\ deviation\ from\ well\ design\ \&\ planning\ models
\end{aligned}
$$

A traffic light scheme indicated by a scale ranging from 0 – 100% is used to visually represent the increasing risk of a potential stuck pipe event such that:

- Green (low risk of stuck pipe): 0 to <25%
- Amber (medium risk of stuck pipe): 25 to <50%
- Red (high risk of stuck pipe): >50%

The logic described in section 3.7 (and sub-sections) was coded into a tool called the stuck pipe index (SPI) tool. The logic was coded using TIBCO Spotfire® data visualization and predictive analytics software. The software allows the combination of several statistical data in a single analysis. TIBCO Spotfire® was selected because it offers seamless connection to the traditional WITSML rig-site data and is known within the industry to offer high confidence real-time data driven intelligence analytics. It is also recognized across different industries as a leading integration, data management and analytics software platform. Case histories with known stuck pipe events in the South Ghawar field of Saudi Arabia were replayed using WITSML recorded data. The results demonstrated the efficiency of the SPI tool and are presented in chapter 4.

# 4. APPLICATION AND VALIDATION OF NUMERICAL MODELS AND STUCK PIPE PREDICTION CONCEPT

Improved cuttings transport equations for the annular cutting volumetric concentration ($C_c$), cutting settling velocity (CSV), critical re-suspension velocity (CRV), and the azimuthal annulus velocity (AAV) have been developed in sections 3.3, 3.4, 3.5, and 3.6, respectively. The equations are necessary to obtain the:

1. Critical Transport Fluid Velocity (CTFV)
2. Estimate the cuttings transport ratio and the “vortex” transport ratio
3. Establish the ease with which a settled cuttings bed may be re-suspended (i.e., the CRV)

The steps in section 5.1 below summarize how the numerical equations developed in this research are applied. Sample experimental data sets from Larsen et al. (1997) and Duan et al. (2009) are used to test and validate the numerical models, and the results analyzed accordingly. Also based on Larsen et al. (1997) experimental data set, results of the settling velocity and the transport ratio estimated from numerical models of this research were compared with the models of Moore (1974), Chien (1971), and Walker and Mayes (1975) for validation.

The above is used to assess the hole cleaning efficiency in the wellbore. The hole cleaning efficiency is coded into the stuck pipe index (SPI) tool. In combination with real-time data trends (anomaly detection), deviation changes of drilling parameters from well design simulations, and offset well histories, the SPI tool is used to predict potential stuck pipe risk in four case history wells using the “ROW” method proposed in this research. Figure 4.1 shows a typical process flow chart.

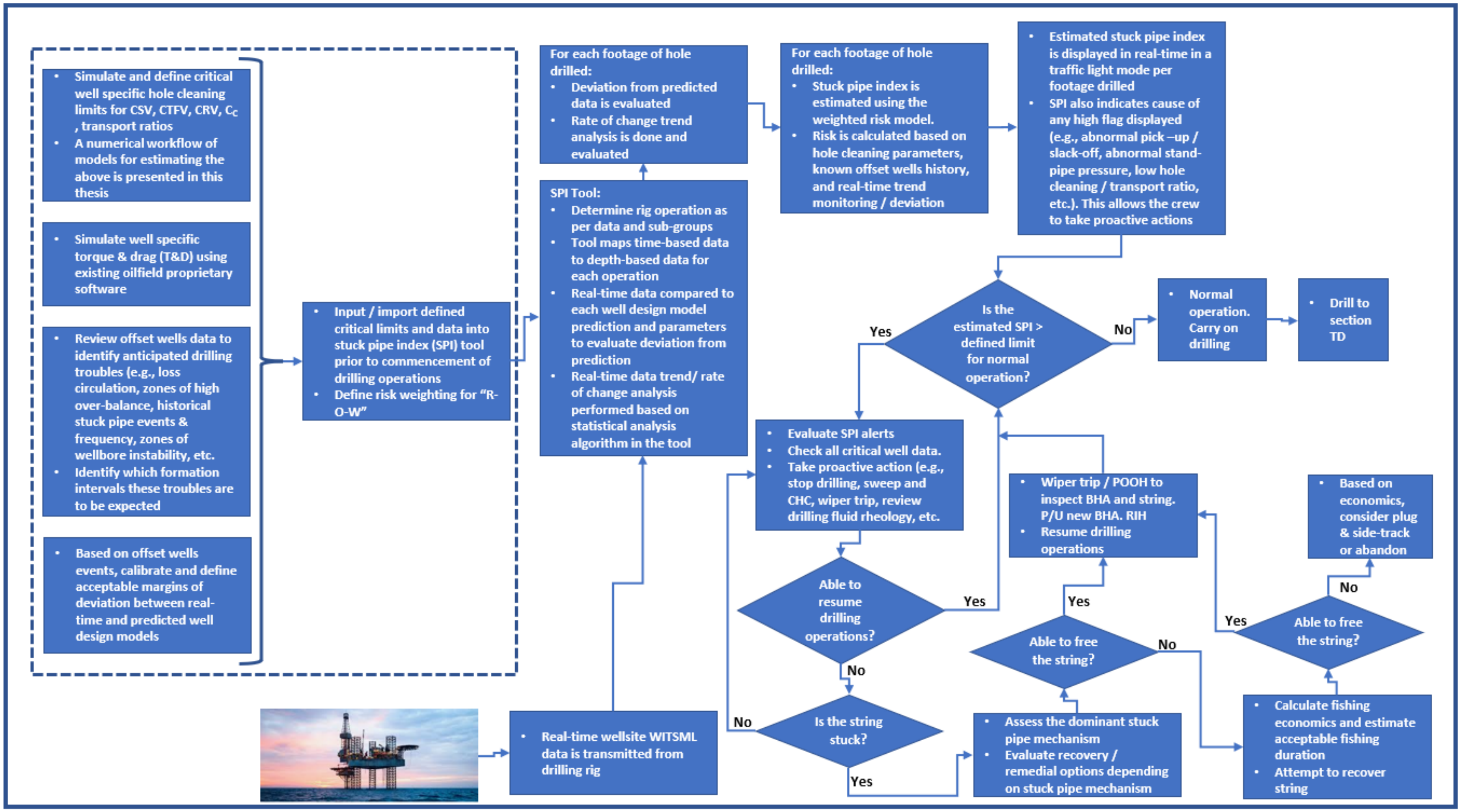


Figure 4.1: Process Flow Chart Showing Application of R-O-W Method

## 4.1 Steps for the Application of Numerical Workflow Models

1. Estimate the annular cuttings volumetric concentration in percent using equation 3.34
2. Estimate cuttings settling velocity ($CSV\ or\ V_s$) using the derived hindered settling equation 3.51
3. Estimate the cuttings transport velocity (CTV) using Larsen (1990) equation

$$CTV = \frac{ROP}{36\left[1 - \left(\frac{D_{pipe}}{D_{hole}}\right)^2\right] C_{conc}} \qquad \text{Eqn. 4.1}$$

$$Where\ C_{conc} = C_c$$

4. Estimate the CTFV as follows:

$$CTFV = V_s + CTV \qquad \text{Eqn. 4.2}$$

5. Estimate the cutting transport ratio ($F_T$) (Bourgoyne et al., 1986) as follows:

$$F_T = 1 - \frac{V_s}{U_h} \qquad \text{Eqn. 4.3}$$

$$U_h = \frac{Q}{A_{ann}} \qquad \text{Eqn. 4.4}$$

Where;

- $U_h$ = Average annulus fluid velocity ($m/s$)
- $Q$ = Annulus flow rate ($m^3/s$)
- $A_{ann}$ = Cross sectional area of annulus ($m^2$)

6. Estimate the vortex (or azimuthal) velocity ($V_\theta$) using equation 3.112
7. Estimate the vortex cutting transport ratio ($F_\theta$) as follows:

$$F_\theta = \frac{CSV}{V_\theta} \qquad \text{Eqn. 4.5}$$

8. Estimate the critical re-suspension velocity (CRV) using equation 3.70

## 4.2 Model Validation (Using Larsen et al., 1997 Experimental Data)

Table 4.1 is experimental data from Larsen et al. (1997). The data set has been used to test the numerical equations developed by this research.

Table 4.1 Larsen et al. (1997) Experimental Data

| Parameters | Field Units | S.I Units |
|---|---|---|
| 600 dial reading | 24 $lbf/100\ ft^2$ | 1.173 $kg/100\ m^2$ |
| 300 dial reading | 16 $lbf/100\ ft^2$ | 0.782 $kg/100\ m^2$ |
| 3 dial reading | 2 $lbf/100\ ft^2$ | 0.098 $kg/100\ m^2$ |
| Plastic Viscosity | 8 $lbf/100\ ft^2$ | 0.391 $kg/100\ m^2$ |
| Apparent Viscosity | 26.9 cp | 0.0269 $kg/m.s$ |
| Yield Point | 8 $lbf/100\ ft^2$ | 0.391 $kg/100\ m^2$ |
| Mud / Fluid Density | 8.57 $lbm/gal$ | 1026.9 $kg/m^3$ |
| Cutting / Solid Density | 22.13 $lbm/gal$ | 2651 $kg/m^3$ |
| Flow rate | 110 GPM | 0.00694 $m^3/s$ |
| Wellbore Inclination | 65 degrees | |
| Cutting diameter | 0.175 inches | 0.00445 m |
| Rate of Penetration (ROP) | 54 ft/hr | 0.004572 m/s (16.46 m/hr) |
| Wellbore Diameter | 5 inches | 0.127 m |
| Drill Pipe Diameter | 2.375 inches | 0.060 m |
| Drill Pipe RPM | 50 RPM | |
| Angular Velocity | 300 RPM | 5 rad/sec |
| Acceleration Due to Gravity | | 9.81 $m/s^2$ |
| Cuttings bed porosity (Φ) | 36% | 36% |

### 4.2.1 Validation of Annular Cuttings Concentration Model

Based on regression analysis, equation 3.34 was found to be the best fit. It predicted the annular cuttings concentration by volume at an ROP of 54 ft/hr (0.00457 m/s) to be 1.65% versus the experimentally measured value of 1.58%. This represents a margin of error of 4.42%. Equation 3.34 was further modified by substituting a linear expression for the natural logarithmic expression used to describe the effects of cuttings diameter. This was done because it was found that at rates of penetration of 35 ft/hr and lower, the margins of error of the predicted cuttings concentration compared to the experimentally measured values exceeded 30%. The linear expression $(\pi_6 + (e_6 \cdot \pi_6))$, was used to achieve a better fit to the experimental data. The modification was based on findings from previous researchers who establish that the relationship between the cuttings size and the concentration is linear (Larsen et al., 1997). The modified equation is presented below

$$C_c = \left(e_1.\pi_2^{e_2}\right)\left(\pi_3^{e_3}\right)\left(\pi_4^{e_4}\right)\left(\pi_5^{e_5}\right)(\pi_6 + (e_6.\pi_6))\left(\pi_7^{e_7}\right) \qquad \text{Eqn. 4.6}$$

Using the modified equation 4.6, the annular cuttings concentration by volume at 54 ft/hr is predicted to be 1.57% versus the experimentally measured value of 1.58%. Thus, representing a margin of error of approximately 1%.

Equations 3.34 and 4.6 were then used over a range of ROP values to correlate with the other experimentally measured data reported by Larsen et al. (1997). The modified model (equation. 4.6) largely predicted the annular cuttings concentration by volume to within approximately 24% margin of error compared to the Larsen et al. (1997) experimental data. Using the same dataset, equation 3.34 predicted the annular cuttings concentration to within approximately 28% margin of error. Table 4.2 summarizes the results of equation 3.34 versus eqn. 4.6.

Table 4.2 Summary of Model Predicted Cuttings Volume vs Larsen et al (1997) Experimental Data

| ROP (ft/hr) | ROP (m/s) | Predicted Cuttings Vol Conc (%) - Eqn. 3.34 | Predicted Cuttings Vol Conc. (%) - Eqn. 4.6 | Larsen Experimental Measurements | % Margin of Error (Predicted Cuttings Vol vs Larsen Experimental Measurements) | |
|---|---|---|---|---|---|---|
| | | | | | Eqn. 3.34 vs Larsen Experimental Measurements | Eqn. 4.6 vs Larsen Experimental Measurements |
| 90 | 0.00762 | 1.81 | 1.72 | 2.25 | 19.64 | 23.56 |
| 85 | 0.00720 | 1.79 | 1.72 | 1.92 | 6.61 | 10.26 |
| 75 | 0.00635 | 1.75 | 1.69 | 1.50 | -16.73 | -12.33 |
| 70 | 0.00593 | 1.73 | 1.65 | 1.75 | 1.14 | 5.94 |
| 65 | 0.00550 | 1.71 | 1.63 | 1.54 | -10.79 | -5.41 |
| 60 | 0.00508 | 1.68 | 1.60 | 1.63 | -3.63 | 1.42 |
| 55 | 0.00466 | 1.66 | 1.58 | 1.38 | -20.58 | -14.76 |
| 54 | 0.00457 | 1.65 | 1.57 | 1.58 | -4.42 | 0.63 |
| 50 | 0.00423 | 1.63 | 1.55 | 1.38 | -18.62 | -12.87 |
| 45 | 0.00381 | 1.60 | 1.52 | 1.50 | -6.73 | -1.60 |
| 35 | 0.00296 | 1.53 | 1.46 | 1.25 | -22.56 | -16.64 |
| 34 | 0.00288 | 1.53 | 1.45 | 1.25 | -22.00 | -16.00 |
| 30 | 0.00254 | 1.49 | 1.42 | 1.25 | -19.28 | -13.52 |
| 17.5 | 0.00148 | 1.36 | 1.29 | 1.06 | -27.72 | -21.51 |

As several factors affect and influence the accurate prediction of cuttings concentration in an annulus (Larsen et al., 1997; Tomren et al, 1986; Luo et al. 1992), this research proposes that the numerical models developed be used to estimate a range of annular cuttings concentration rather than a single value. This is to account for uncertainties such as eccentricity, effectiveness of rheological properties of the drilling fluids, cuttings characteristics (e.g., size, density, and shape etc.). The estimated range of values can serve as input for sensitivity assessments to optimize drilling operations, including the evaluation of the maximum possible annular cutting concentration values that could impact the drilling operations adversely.

Figure 4.2 is a graphical representation of Table 4.2. Eqn. 4.6 (orange curve) is seen to demonstrate a better correlation with the experimental data.

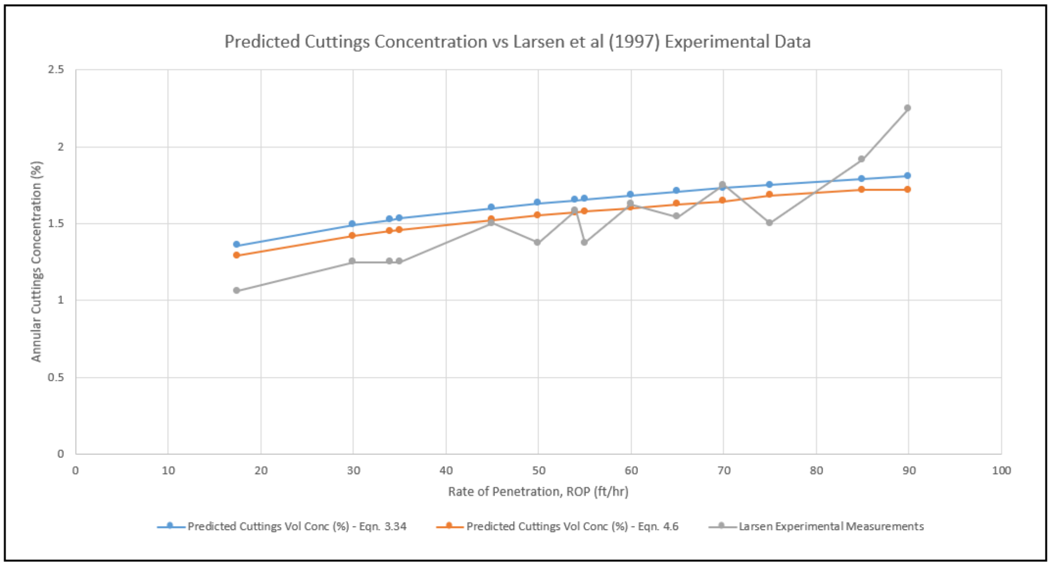


Figure 4.2: Predicted Cuttings Concentration vs Experimental Data

Based on the experimental measurements, Larsen et al. (1997) had derived a linear correlation from empirical data to estimate the annular cuttings concentration by volume. The linear correlation is given below:

$$C_c = 0.01778ROP + 0.505 \qquad \text{Eqn. 4.7}$$

Compared to Larsen et al. (1997) linear empirical correlation (i.e., eqn. 4.7), a margin of error between ±29 – 58% is observed at rates of penetration of 35 ft/hr and lower for eqn. 4.6. A similar comparison for equation 3.34 shows a margin of error between ±22 – 66% but for rates of penetration of 45 ft/hr and lower. It is believed that this difference is because Larsen et al. (1997)'s linear empirical correlation is an approximate line of best fit used to describe a large scatter group of experimental data (see Figure 4.3).

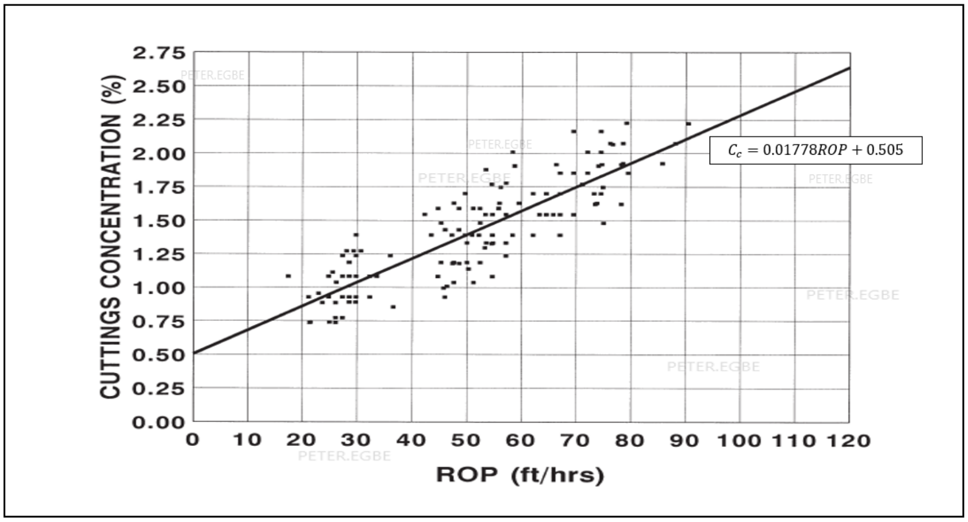


Figure 4.3: Larsen et al. (1997) Experimental Data (Cuttings Concentration vs ROP) at Critical Transport Flow Velocity

Figure 4.4 shows a comparison between equations 3.34 and 4.6 versus the line of best fit as presented by Larsen et al. (1997).

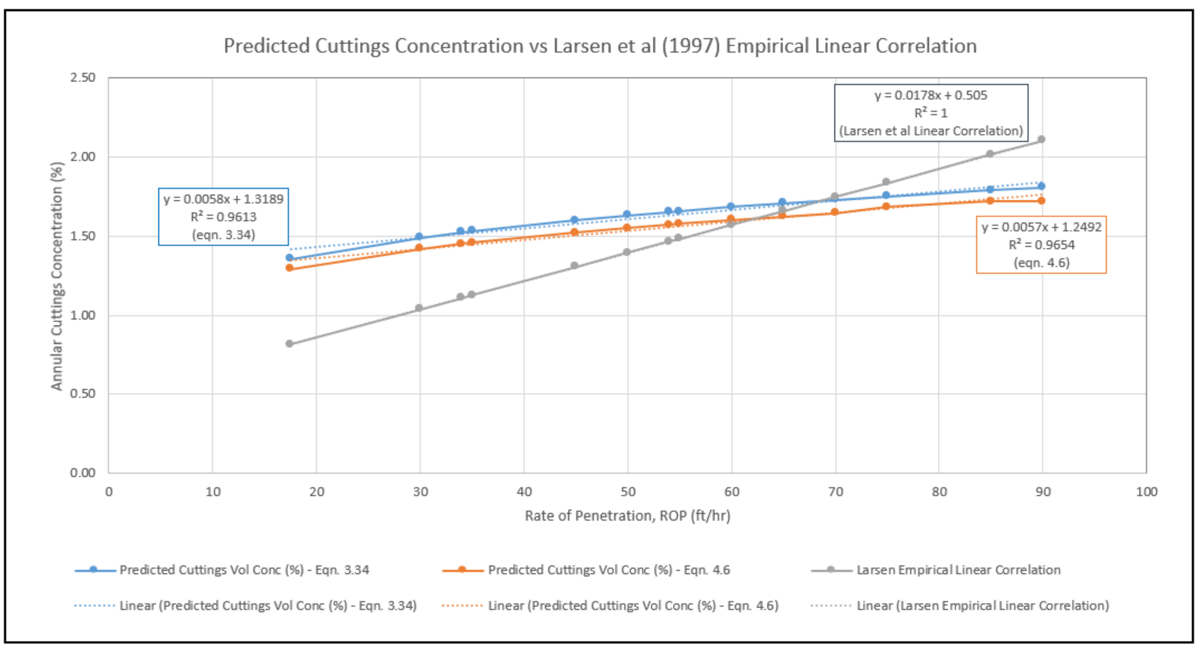


Figure 4.4: Comparison Between Research Model Equations and Larsen et al. (1997) Empirical Linear Correlation

The results of cuttings concentration at critical transport fluid velocity from equation 4.6 was used to compare with a leading Oilfield Services (Schlumberger, SLB) provider prediction software. For a 12,000 ft MD (3,937 m) well at a critical transport flow rate of 280 GPM (0.0177 $m^3/s$). The model agreed to within 10 - 25% margin of error for rates of penetration between 50 – 100 ft/hr (15 – 30 m/hr), and 90% eccentricity ($\varepsilon$). At rates of penetration ≤40 ft/hr (12.5 m/hr) and ≥105 ft/hr (32.8 m/hr), the cuttings concentration predicted by equation 4.6 showed significant differences up to ±37%. Figure 4.5 shows the comparison between equation 4.6 and the SLB prediction model.

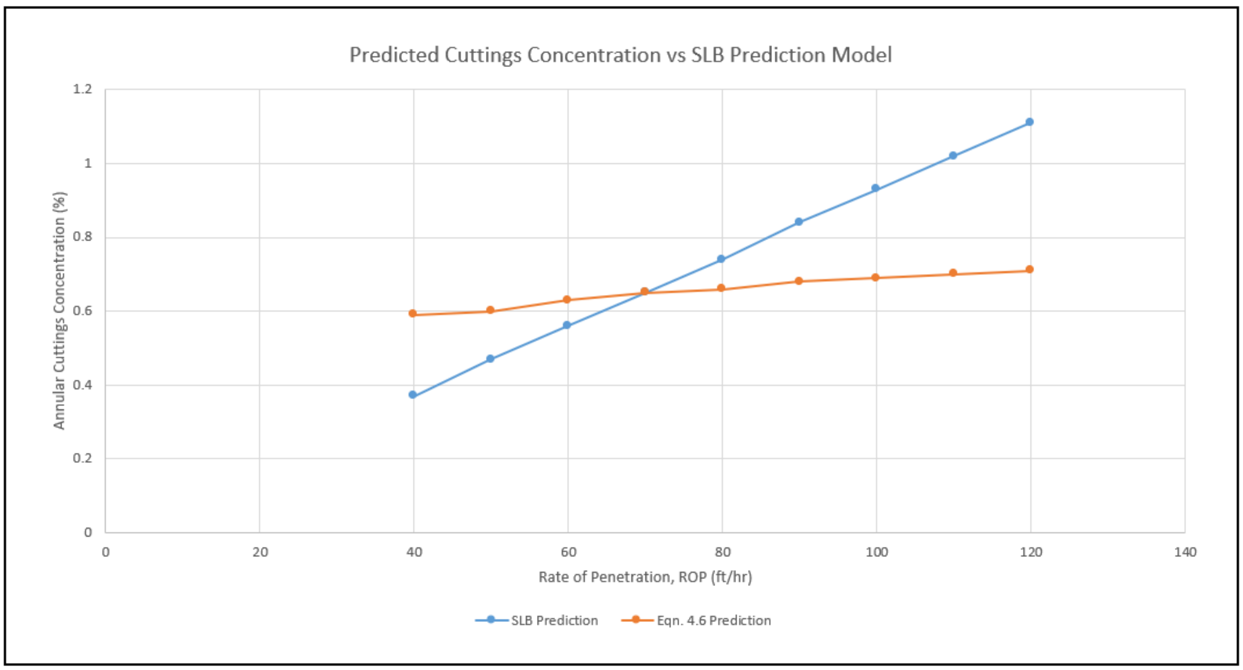


Figure 4.5: Comparison Between Research Equation and SLB Prediction Model

The SLB prediction model was used to test Larsen et al. (1997) experimental data and was found to significantly under-predict the cuttings concentration. The highest differences (72 – 84%) also occurred at ROPs of 45 ft/hr and lower. Table 4.3 and Figure 4.6 summarizes these differences.

Relative to the model proposed by this research (i.e., eqn. 4.6), and the empirical correlations by Larsen et al. (1997), the SLB model predicted the lowest annular cuttings concentration by volume. This is shown in Figure 4.6. It is believed that this under-prediction by the SLB model is because it does not fully consider the effect of wellbore inclination, drill string eccentricity, and Taylor vortices due to drill string rotation.

Table 4.3 Summary of Differences Between Cuttings Concentration Predicted by SLB Model vs Larsen et al. (1997) Experimental Data

| ROP (ft/hr) | SLB Predicted Volumetric Cuttings Concentration (%) | Larsen Experimental Measurements | Differences (%) |
|---|---|---|---|
| 90 | 0.834 | 2.25 | 62.93 |
| 85 | 0.788 | 1.92 | 58.89 |
| 75 | 0.696 | 1.50 | 53.60 |
| 70 | 0.65 | 1.75 | 62.86 |
| 65 | 0.604 | 1.54 | 60.82 |
| 60 | 0.558 | 1.63 | 65.66 |
| 55 | 0.512 | 1.38 | 62.76 |
| 54 | 0.5028 | 1.58 | 68.24 |
| 50 | 0.466 | 1.38 | 66.11 |
| 45 | 0.42 | 1.50 | 72.00 |
| 35 | 0.328 | 1.25 | 73.76 |
| 34 | 0.3188 | 1.25 | 74.50 |
| 30 | 0.282 | 1.25 | 77.44 |
| 17.5 | 0.167 | 1.06 | 84.28 |

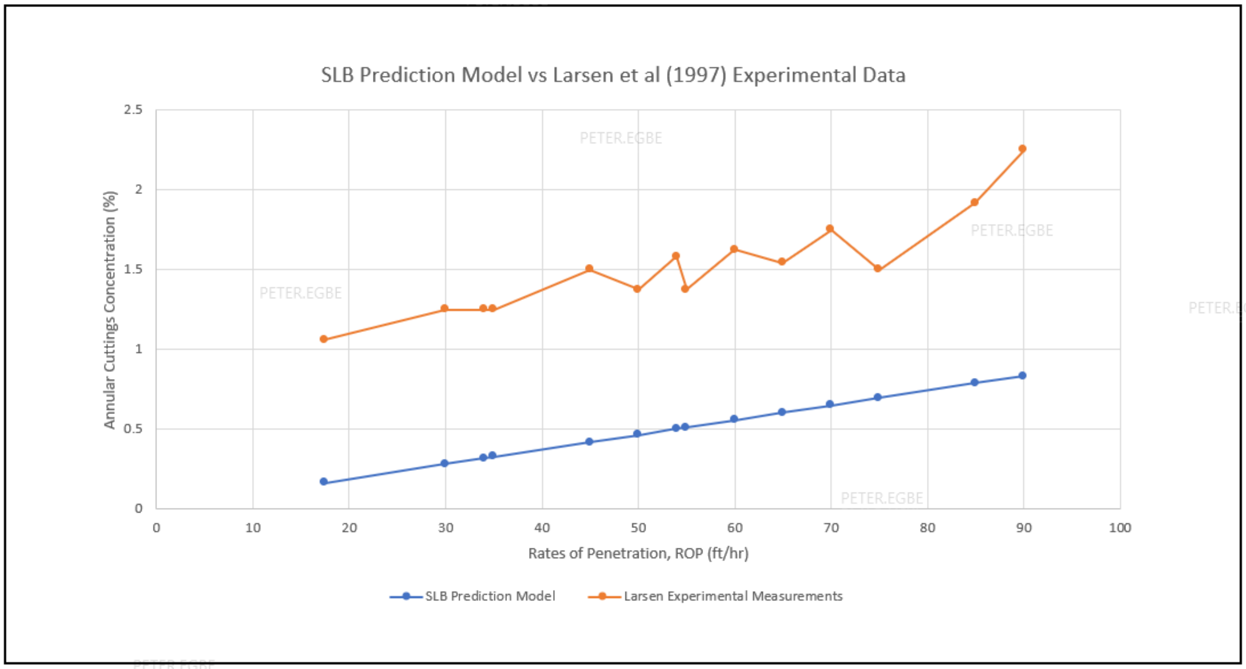


Figure 4.6: SLB Prediction Model vs Larsen et al. (1997) Experimental Data

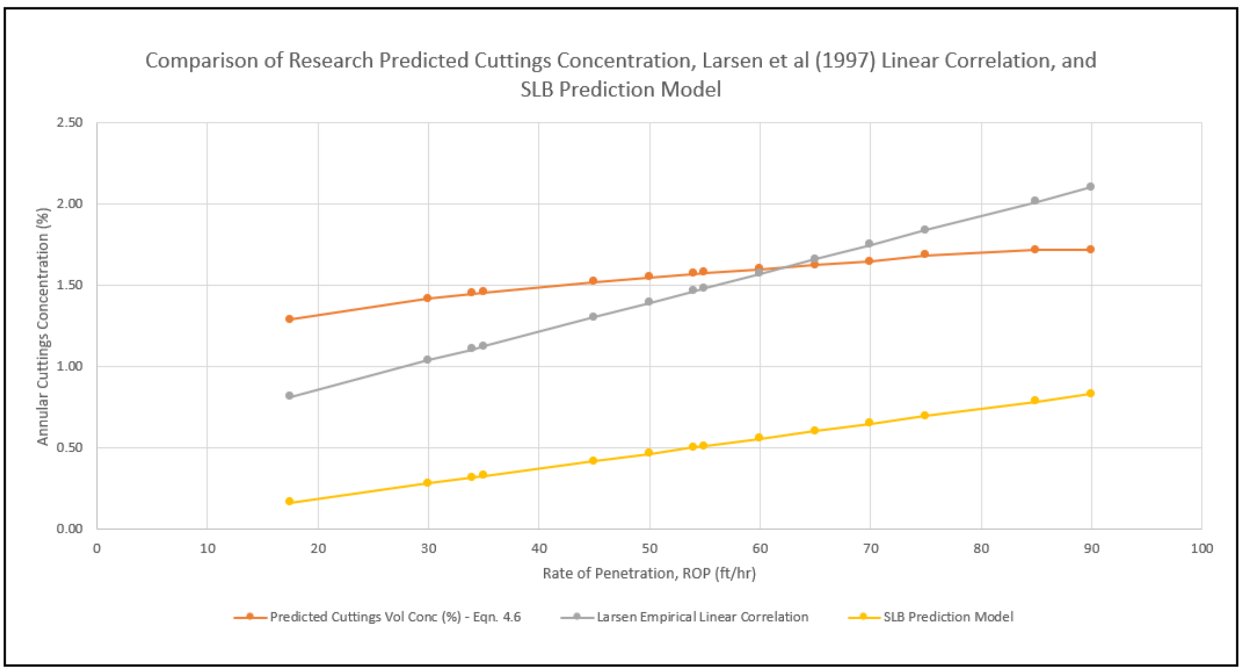


Figure 4.7: Comparison Between Research Model (Eqn. 4.6), Larsen et al. (1997) Empirical Linear Correlation, and SLB Model

Based on the validation results presented in this section, equation 4.6 is considered suitable, and proposed for use in estimating the annular cuttings concentration at a critical transport flow rate. The values of the constants ($e_1, e_2, e_{3,}\ e_{4,}\ e_{5,}\ e_{6,}\ and\ e_7$) are obtained via regression analysis and presented in Table 4.4 below:

Table 4.4 Research Model Table of Constants

| $e_1$ | $e_2$ | $e_3$ | $e_4$ | $e_5$ | $e_6$ | $e_7$ |
|---|---|---|---|---|---|---|
| 10,574 | -0.753 | 0.095 | 0.469 | 0.175 | -0.295 | 0.005 |

### 4.2.2 Validation of Cutting Settling Velocity and Critical Transport Fluid Velocity Models

Following the steps in section 4.1, and Larsen et al. (1997) data in Table 4.1:

1. Annular cuttings concentration ($C_c$) is estimated as 0.01557 (or 1.557%) using equation 4.6
2. The cutting settling velocity (CSV or $V_s$) is calculated using equation 3.51 given below

$$V_s = \left(\frac{\omega^2 d_o d_p^2(\rho_s - \rho_f)}{18\mu}\frac{1}{1+0.15R_{ep}^{0.687}}\right)\left((1-C_c)\left(1-\frac{C_c}{C_{c,max}}\right)^2\right)$$

Where:

$$R_{ep} = \left(\frac{\rho_s - \rho_f}{\rho_f} g d_p\right)^{0.5} \frac{\rho_f d_p}{\mu}$$

$$C_{c,max} = 0.74\ (assuming\ hexagonal\ packing\ structure, Duan\ et\ al., 2009)$$

Substituting for all variables, estimates the cutting settling velocity (CSV or $V_s$) as 3.90 ft/s (or 1.19 m/s). This compared to Larsen et al. (1997) empirical correlation of 3.56 ft/s (or 1.09 m/s) represents a margin of error of 9.2%

Equation 3.46 developed by this research for the estimation of the settling velocity is interestingly very similar to that obtained by Spearman and Manning (2017).

$$w_s = w_{s,0}(1-\emptyset)^m \left(1 - {\emptyset}/{\emptyset_{max}}\right)^{\acute{n}} \qquad \text{Eqn. 4.8}$$

Where;

$w_s = V_s$ = Hindered cutting settling velocity of the cutting / particle (m/s)

$w_{s,0}$ = $V_{s,o}$ = Terminal settling velocity of a single cutting / particle without the influence of other cuttings / particles in a still fluid (m/s)

$\emptyset$ = $C_c$ = Cutting volume concentration (%)

$\emptyset_{max}$ = $C_{c,max}$ = Maximum cuttings volume concentration = 0.74 (depending on packing structure)

Comparing equation 3.46 (developed by this research) and equation 4.8 (developed by Spearman and Manning, 2017), the Spearman and Manning (2017) exponents estimated by equation 3.46 of this research are as follows

$$m = 1, and\ \acute{n} = 2$$

Based on their research work, Spearman and Manning (2017) had proposed the following expressions to obtain both the "$m$" and "$\acute{n}$" exponents as follows

$$m = 2.7 - 0.15n\ (accounts\ for\ the\ contribution\ to\ hinderance\ of\ the\ non - viscosity\ terms)$$

$$\acute{n} = 0.6n - 1.46$$

$$n = R - Z\ exponent\ (which\ can\ be\ obtained\ from\ correlations\ in\ literature$$

Spearman and Manning (2017) established that $\acute{n} = 0$ in the inertial regime, and $\acute{n} \approx 1.5\ (and\ R - Z\ exponent, n = 4.93)$ in the Stokes regime which they claim corroborates with the Krieger-Dougherty viscosity law.

Based on the above comparisons with the work of Spearman and Manning (2017), the estimations of "$m$" and "$\acute{n}$" exponents from the model developed by this research is in the range predicted by Spearman and Manning (2017).

As such, the numerical model for the cutting settling velocity (CSV) (i.e., equation 3.51) proposed by this research is thus validated

3. The cutting transport velocity (CTV) is estimated as 1.25 ft/s (or 0.38 m/s).
4. The critical transport fluid velocity (CTFV) is estimated as

   CTFV = CTV + $V_s$ = 0.38 + 1.19 = 1.57 m/s (or 4.79 ft/s)

   i. Compared to a CTFV of 1.60 m/s (or 4.88 ft/s) estimated by Larsen et al. (1997). This represents a margin of error of 1.8%
   ii. With an annulus cross-sectional area ($A_{ann}$) of 0.0098 $m^2$, the corresponding flow rate to the CTFV is calculated as 0.0154 $m^3/s$ (or 244 GPM)
   iii. The flow rate (244 GPM) calculated using the CTFV estimated from the numerical models proposed in this research is 5.5% higher than the predicted flow rate of 231 GPM reported by Larsen et al. (1997)
   iv. Compared to the flow rate of 110 GPM used in the experimental setup, cuttings will accumulate in the annulus. Results from this research, and Larsen et al. (1997) experimental work agree. Thus, validating the models proposed by the research
5. The cutting transport ratio ($F_T$) is estimated using equation 4.3 as follows:
   i. At 110 GPM, $F_T$ = -0.676 (i.e., cuttings will accumulate)
   ii. At 244 GPM, $F_T$ = 0.242 (i.e., cuttings are transported to surface)
6. The vortex (or azimuthal) velocity ($V_\theta$) is estimated using equation 3.112

$$\frac{V_\theta}{V_{\theta max}} = \frac{\left[r^{1-2/n} - r_o^{1-2/n}\right] - (r - r_o)\left(\tau_o/K\right)^{1/n}}{\left[r_i^{1-2/n} - r_o^{1-2/n}\right] - (r_i - r_o)\left(\tau_o/K\right)^{1/n}}$$

Where:

$\tau_o$ = 3 RPM dial reading

n = $3.32 \log \frac{\theta_{600}}{\theta_{300}}$ = 0.584

K = $\frac{\theta_{300}}{511^n}$ = 0.419 $Pa.s^n$

$V_{\theta max}$ = $\frac{\pi D_i RPM}{60}$ = The drill string rotation (in RPM) converted to m/s. $D_i$ is the string diameter

Substituting into equation 3.112 estimates $V_\theta$ = 0.10 ft/s (or 0.034 m/s) at r = 0.04675m.

7. The vortex transport ratio ($F_\theta$) at r = 0.04675m is estimated as 35 at RPM = 50 using equation 4.5. The following conclusions can be drawn from this:
   i. In the experimental setup by Larsen et al. (1997) and based on the results of the vortex transport ratio at string RPM = 50, the hole cleaning efficiency was predominantly by the mud flow rate. The Taylors vortices played no active role.
   ii. To initiate powerful enough Taylor vortices with the fluid type used in the experiment, and to achieve $F_\theta$ <<1, a critical inner string rotation of 494 RPM is required. The critical string RPM for the initiation of Taylor vortices is estimated using equation 4.9 proposed by Philip et al. (1998)

$$Critical\ RPM = \left[\frac{T_{a,cr}\left(r_o^2 - r_i^2\right)\mu_a^2}{4\rho_f r_i^2 (r_o - r_i)^4}\right]\frac{60}{2\pi} \qquad \text{Eqn. 4.9}$$

   With a string rotation of 494 RPM, the vortex velocity ($V_\theta$) in the setup of Larsen et al. (1997) would have been 5.51 ft/s (or 1.68 m/s); and accordingly, $F_\theta$ is calculated to be 0.57.

Alternatively, as a string rotation of 494 RPM is not practical, the fluid characteristics (n and K) may be modified for improved cuttings transport. Figure 4.8 shows the azimuthal velocity profile for five different fluids rheology taken from Larsen et al. (1997) experimental data. The shape of the profile becomes more linear as the "n" value increases. The "red" line is for "n = 0.75 and K = 0.409" (Larsen et al., 1997 mud data #5). As can be seen in Figure 4.8, the azimuthal velocity profile for "n = 0.75" appears to become more linear relative to mud #1 (n = 0.584). Philip et al. (1998) concluded from their studies that higher "n" and "k" values resulted in better cuttings lift and suspension. Their findings are also supported by Zhang et al. (2017) and Saasen and Løklingholm (2002), who state that the flow behaviour index (n) is reflective of the drilling fluid cutting-carrying ability.

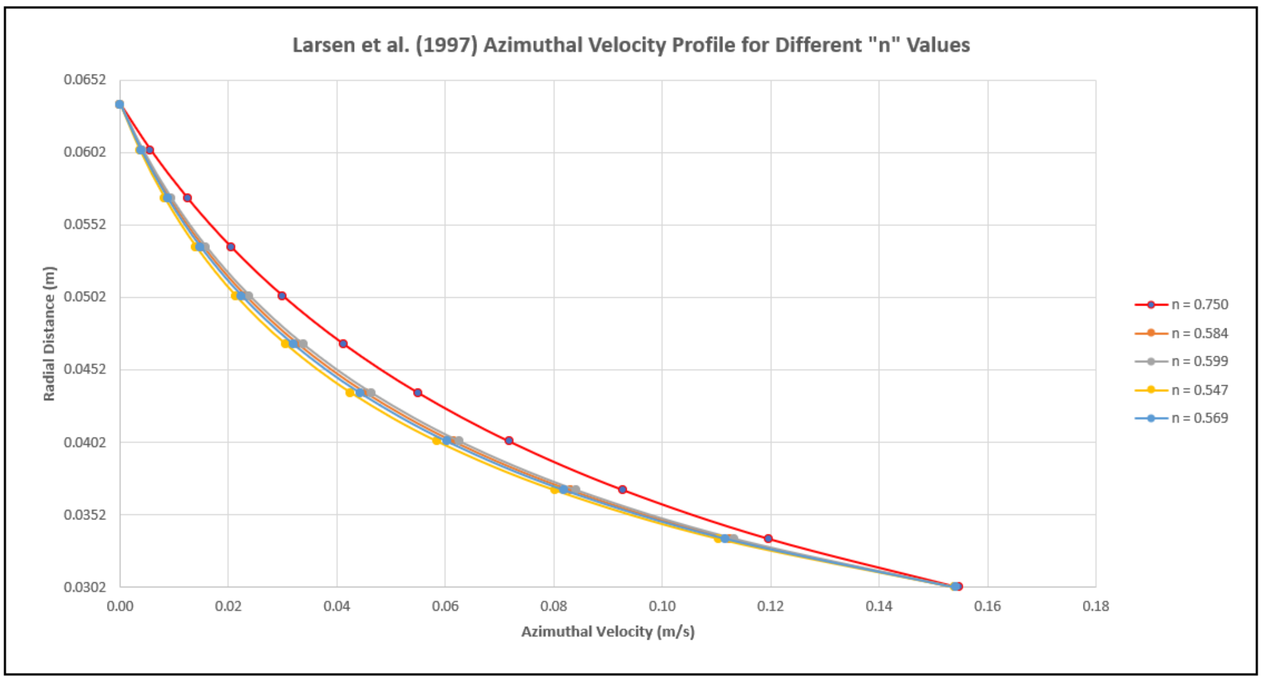


Figure 4.8: Azimuthal Velocity Profile for Larsen et al. (1997) Experimental Data

i. This research proposes the vortex transport ratio as an additional check that can be used to estimate the fraction of cuttings lifted into the flow stream versus the string rotation rate (RPM). Considering fluid and drilling parameters, it is a useful tool for engineers and field personnel to assess and optimize for cutting / hole cleaning efficiency. A chart of vortex transport ratio ($F_\theta$) can be plotted against string rotation (RPM) and used as a quick guide to determine which drilling fluid system might offer the most efficient drilled cutting lift at various string RPM. Figure 4.9 shows how such a plot may look like using vortex transport ratios estimated from Larsen et al. (1997) fluids data. Based on Figure 4.9, mud #1 (n = 0.584) and mud #5 (n = 0.75) appear to offer the best vortex transport ratio for hole cleaning. Additionally, as mud #5 has a higher fluid behaviour index, it would be the better of the two fluids. This also aligns with Figure 4.8, and the findings of Philip et al. (1998), Zhang et al. (2017), and Saasen and Løklingholm (2002). Table 4.5 shows the properties of the fluids used to generate Figure 4.9.

Table 4.5 Mud Rheology Data for Sample Calculations (Larsen et al., 1997)

| | Mud 1 | Mud 2 | Mud 3 | Mud 4 | Mud 5 |
|---|---|---|---|---|---|
| At 600 rev/min, ° | 20 to 24 | 41 to 46 | 72 to 76 | 46 to 50 | 70 to 74 |
| At 300 rev/min, ° | 13 to 16 | 27 to 31 | 48 to 52 | 29 to 33 | 41 to 44 |
| At 200 rev/min, ° | 11 to 13 | 22 to 25 | 39 to 41 | 24 to 26 | 31 to 33 |
| At 100 rev/min, ° | 7 to 9 | 14 to 17 | 27 to 29 | 14 to 16 | 20 to 22 |
| At 6 rev/min, ° | 2 to 3 | 4 to 5 | 12 to 13 | 3 to 4 | 4 to 5 |
| At 3 rev/min, ° | 1 to 2 | 3 to 4 | 11 to 12 | 2 to 3 | 3 to 4 |
| 10-second gel, lbf/100 $ft^2$ | 3 to 4 | 5 to 7 | 16 to 18 | 3 to 4 | 5 to 6 |
| 10-minute gel, lbf/100 $ft^2$ | 4 to 5 | 8 to 10 | 45 to 50 | 11 to 12 | 20 to 22 |
| $Y_p$, lbf/100 $ft^2$ | 6 to 8 | 14 to 16 | 24 to 26 | 14 to 16 | 14 to 16 |
| $\mu_p$, cp | 7 to 10 | 13 to 16 | 24 to 27 | 15 to 17 | 27 to 29 |
| Mud weight, lbm/gal | 8.57 | 8.65 | 8.7 | 11.0 | 15.0 |

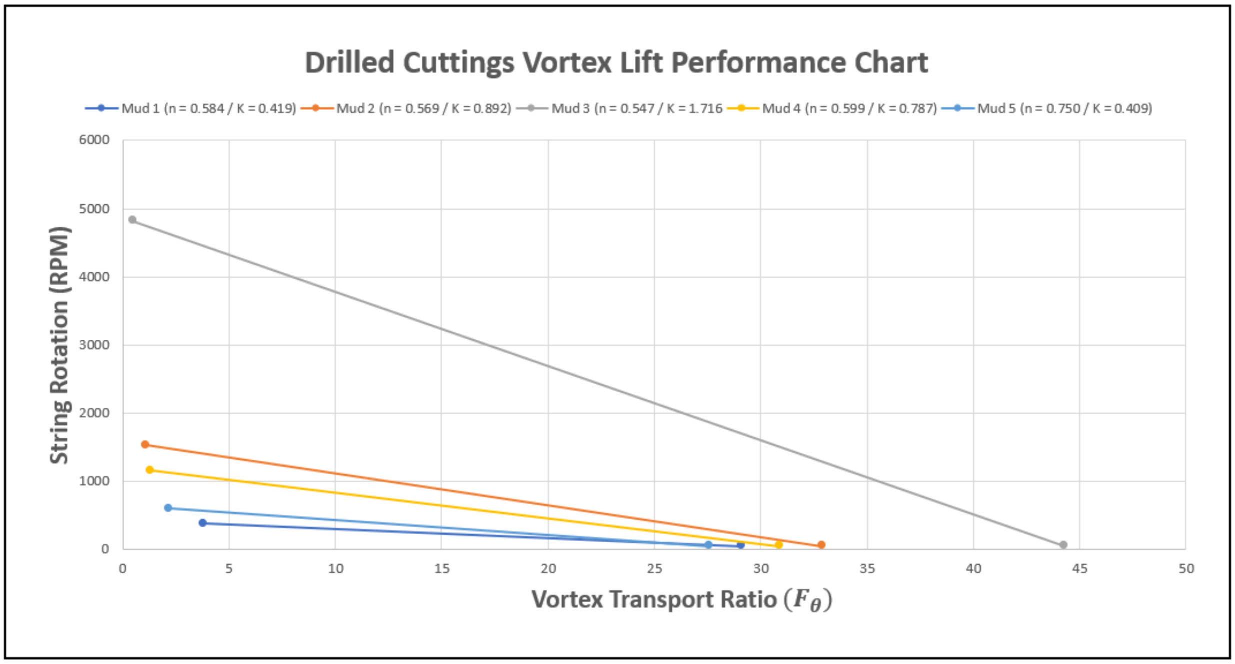


Figure 4.9: Sample Drilled Cuttings Vortex Lift Performance Chart (Developed Using Larsen et al., 1997 Fluids Data)

## 4.3 Validation of CSV, CTFV, and CRV Models Using Duan et al. (2009) Experimental Data

A second validation is done using the experimental data (Table 4.6) obtained by Duan et al. (2009) using the low-pressure / ambient-temperature (LP/AT) flow loop at the University of Tulsa. The same set of equations used to validate the Larsen et al. (1997) data are applied.

Table 4.6 Parameters for Sample Calculations (Duan et al., 2009)

| Parameters | Field Units | S.I Units |
|---|---|---|
| Apparent Viscosity | 26.9 cp | 0.0269 $kg/m.s$ |
| Mud / Fluid Density | 8.35 $lbm/gal$ | 1000 $kg/m^3$ (water) |
| Flow Behaviour Index, n | | 0.72 |
| Fluid Consistency Index, K | | 0.0254 $Pa.s^n$ |
| Yield Stress, $\tau_0$ | | 0 |
| Cutting / Solid Density | 22.95 $lbm/gal$ | 2630 $kg/m^3$ |
| Flow rate | 700 GPM | 0.044163 $m^3/s$ |
| Wellbore Inclination | 70 – 90 degrees | 70 - 90 degrees |
| Cutting diameter | 0.45 mm<br>1.4 mm | 0.00045 m<br>0.0014 m |
| Rate of Penetration (ROP) | | 9 m/hr |
| Wellbore Diameter | 8 inches | 0.203 m |
| Drill Pipe Diameter | 4.5 inches | 0.114 m |
| Drill Pipe RPM | 140 RPM | |
| Angular Velocity | 840 RPM | 14.66 rad/sec |
| Acceleration Due to Gravity | | 9.81 $m/s^2$ |

1. Annular cuttings concentration ($C_c$) is estimated as 1.417%
2. The cutting settling velocity (CSV or $V_s$) for the 0.45mm sand is estimated as 5.61 ft/s (or 1.71 m/s)
3. The cutting transport velocity (CTV) is estimated as 0.85 ft/s (or 0.26 m/s)
4. The critical transport fluid velocity (CTFV) or critical deposition velocity (CDV) is estimated as

   CTFV = CTV + $V_s$ = 0.26 + 1.71 = 1.97 m/s (or 6.46 ft/s)

   a. The predicted CTFV of 1.97 m/s is within 4.8% of the experimentally measured value of 1.88 m/s by Duan et al. (2009) at 70 degrees hole inclination.
   b. As the CTFV predicted by this research is independent of bed height, it is a flat profile.
      i. For dimensionless bed heights between 0.5 to about 0.7, the CTFV (1.97 m/s) predicted by this research is within 1.5 – 7.5% compared to the measured values of 1.88 m/s, 2 m/s, and 2.13 m/s respectively. This represents a higher accuracy compared to the values predicted using Larsen et al. (1997) empirical models. Duan et al. (2009) state that for the same dimensionless bed heights, the empirical models of Larsen et al. (1997) predicted 25% lower than their measured experimental values
      ii. Above 0.7 dimensionless bed height, the value (1.97 m/s) predicted by this research was lower compared with the measured values (2.5 m/s and 2.63 m/s respectively). The margin of error was higher at ±21.2 – 25.1%. This, however, still

agrees with the findings of Duan et al. (2009) who confirmed that compared with other test data, the predicted equivalent CTFVs are mostly 25% lower than measured values

c. With an annulus cross-sectional area ($A_{ann}$) of 0.0222 $m^2$, the corresponding flow rate to the CTFV is calculated as 0.0437 $m^3/s$ (or 693 GPM). Based on the proposed models in this research, this is the minimum flow rate to prevent the formation of a cuttings bed

5. The cutting transport ratio ($F_T$) is estimated to be 0.14 (14%)
6. The vortex (or azimuthal) velocity ($V_\theta$) is estimated as 0.30 m/s (or 0.91 ft/s) at r = 0.07925m.
7. The vortex transport ratio ($F_\theta$) at r = 0.07925m is estimated to be 5.7. indicating hole cleaning efficiency was mainly by the mud flow rate. Figure 4.10 shows the azimuthal velocity profile.

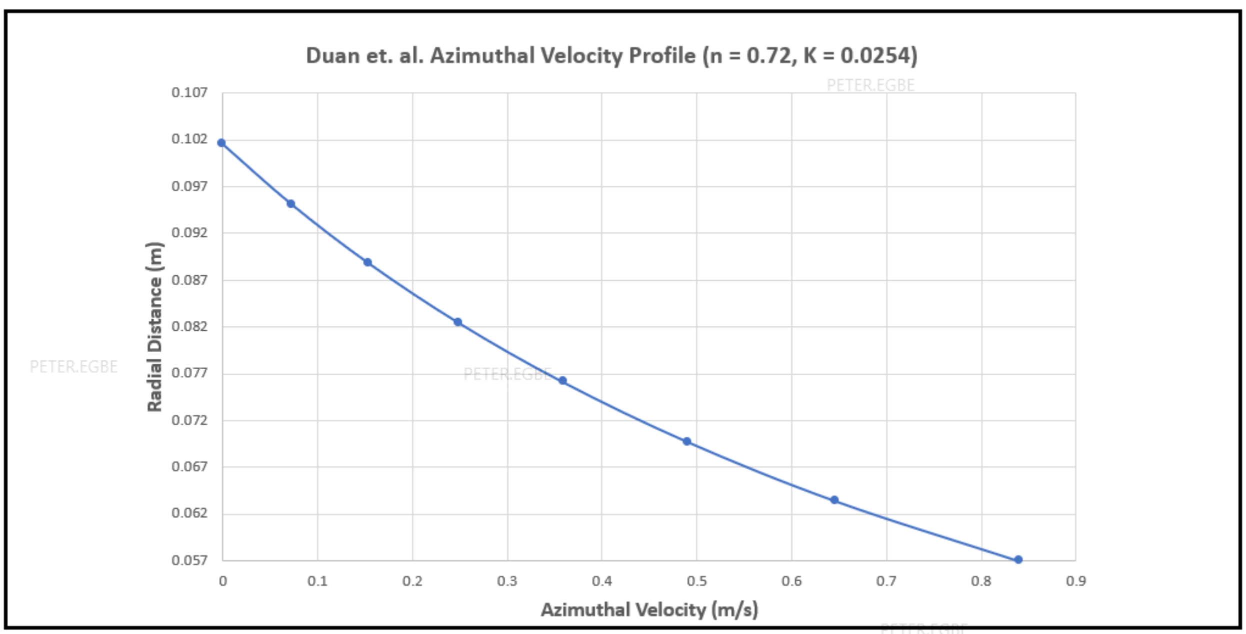


Figure 4.10: Azimuthal Velocity Profile for Duan et al. (2009) Experimental Data

8. Duan et al. (2009) measured the critical re-suspension velocity (CRV) as part of their experiments. They did this at various dimensionless bed heights and hole inclinations of 70 and 90 degrees respectively for 0.45mm and 1.4mm sized sand. For comparison, the steps described in section 4.1, and the models developed in this research were used to estimate the CRV for a 0.45mm sand at 70 degrees inclination and a 50% eccentricity. The equilibrium of moments (equation 3.70) around the contact point of a sand particle that is just about to experience motion converges to zero at the flow rate and average fluid velocity that corresponds to a CRV = 0.57 m/s. The calculations are presented in appendix-D. The following conclusions are drawn
   i. For a 0.45 mm sand, 70 degrees wellbore inclination, 50% eccentricity, water as test fluid, and a dimensionless bed height of 0.55, the CRV of 0.57 m/s predicted by this research is:
      a. 5% lower than the ±0.6 m/s experimentally measured CRV value by Duan et al. (2009).
      b. 12.3% lower than the ±0.65 m/s predicted by Duan et al. (2009) numerical correlations. Note that Duan et. al. (2009)'s equilibrium of moments model does not include the drag force. This could be the reason why Duan et al. (2009)'s correlation predicts higher values than their experimentally measured values
   ii. The corresponding flow rate for the CRV predicted by this research at a CRV = 0.57 m/s is 0.0126 $m^3/s$ (or 200 GPM)

a. Compared to the experimentally reported flow rate (0.0077 $m^3/s$ or 125 GPM) by Duan et al. (2009), the predicted flow rate (200 GPM) by this research is approximately 60% higher

b. At a flow rate of 0.0077 $m^3/s$ (125 GPM), the models proposed by this research predict a CRV = 0.36 m/s which is 40% lower than the experimentally measured value reported at the same flow rate. Similarly, a divergence of 33 – 40% was observed between experimental and predicted data reported by Duan et al. (2009)

## 4.4 Comparison of Research CSV Model with Moore (1974), Chien (1971), and Walker & Mayes (1975)

Within the industry, the correlations of Moore (1974), Chien (1971), and Walker and Mayes (1975) have achieved the most widespread acceptance (Bourgoyne et al., 1986; Philip et al., 1998). All the major service providers use one or more of these three correlations. Hence, the result of the cuttings settling velocity (CSV) model developed in this research was compared to the settling velocities obtained from the three correlations mentioned above. Larsen et al. (1997) experimental data was used.

### 4.4.1 Moore's correlation

Moore (1974)'s correlation is based on applying the slip velocity equation for static fluids to the average flowing conditions experienced during drilling operations. Moore (1974) proposed the following set of equations (in field units):

$$\mu_a = \frac{K}{144}\left(\frac{d_2-d_1}{\bar{v}_a}\right)^{1-n}\left(\frac{2+\frac{1}{n}}{0.0208}\right)^n \qquad \text{Eqn. 4.10}$$

$$\bar{v}_{sl} = \begin{cases} 1.54\sqrt{d_s\frac{\rho_s-\rho_f}{\rho_f}}, & N_{Re} > 300 \\ \frac{2.90 d_s\left(\rho_s-\rho_f\right)^{0.667}}{\rho_f^{0.333}\mu_a^{0.333}}, & 300 \geq N_{Re} \geq 3 \\ 82.87\frac{d_s^2}{\mu_a}\left(\rho_s-\rho_f\right), & N_{Re} \leq 3 \end{cases} \qquad \text{Eqn. 4.11}$$

Where;

$\mu_a$ = apparent viscosity

K = fluid consistency index

n = flow behavior index

$d_2$ = wellbore diameter

$d_1$ = drill pipe diameter

$d_s$ = particle or cutting diameter

$\bar{v}_a$ = average annular fluid velocity

$\bar{v}_{sl}$ = particle slip or settling velocity

$\rho_s$ = cutting or solid density

$\rho_f$ = fluid density

$N_{Re}$ = particle Reynold's number

### 5.4.2 Chien's correlation

For polymer-type drilling fluids, Chien (1971)'s correlation is similar to Moore (1974) as it involves the estimation of an apparent Newtonian viscosity for use in determining the particle Reynold's number (Bourgoyne et al., 1986). In suspensions of bentonite in water, Chien (1971) recommends the use of the plastic viscosity in place of the apparent viscosity. Chien (1971) proposed the following set of equations (in field units)

$$\mu_a = \mu_p + 5\frac{\tau_y d_s}{\bar{v}_a} \quad \text{Eqn. 4.12}$$

$$\bar{v}_{sl} = 0.0075\left(\frac{\mu_a}{\rho_f d_s}\right)\left[\sqrt{\frac{36{,}800 d_s}{\left(\frac{\mu_a}{\rho_f d_s}\right)^2}\left(\frac{\rho_s-\rho_f}{\rho_f}\right)+1}-1\right], N_{Re} < 100 \quad \text{Eqn. 4.13}$$

Where;

$\mu_p$ = plastic viscosity

$\tau_y$ = shear stress

### 4.4.3 Walker and Mayes Correlation

Walker and Mayes (1975) proposed a correlation based on a circular disk in flat horizontal fall rather than for a sphere. They proposed the following set of equations (in field units):

$$\bar{v}_{sl} = \begin{cases} 2.19\sqrt{h\left(\frac{\rho_s - \rho_f}{\rho_f}\right)}, \ N_{Re} > 100 \\ 0.0203\tau_s\sqrt{\frac{d_s\dot{\gamma}}{\sqrt{\rho_f}}}, \ N_{Re} < 100 \end{cases} \qquad \text{Eqn. 4.14}$$

$$\tau_s = 7.9\sqrt{h(\rho_s - \rho_f)} \qquad \text{Eqn. 4.15}$$

$$\mu_a = 479\frac{\tau_s}{\dot{\gamma}_s} \qquad \text{Eqn. 4.16}$$

The shear rate ($\dot{\gamma}_s$) corresponding to the shear stress ($\tau_s$) is determined from a plot of shear stress vs shear rate using a standard rotational viscometer.

Using Larsen et al. (1997) experimental data presented in Table 4.1, cutting settling velocities are estimated using the models of Moore (1974), Chien (1971), and Walker and Mayes (1975). Table 4.7 is a comparison of the estimated settling velocities with that calculated from the CSV models developed in this research and estimated from Larsen et al. (1997) empirical correlations. The corresponding transport ratio (the measure of a fluid’s cutting carrying capacity, Bourgoyne et al., 1986) is also estimated for comparison.

Table 4.7 Comparison with Models of Moore (1974), Chien (1971), and Walker and Mayes (1975) Using Larsen et. al. (1997) Empirical Data

| | **Moore's Correlation** | **Chien's Correlation** | **Walker and Mayes Correlation** | **Larsen et. al. (1997) Empirical Correlation** | **Research Model** |
|---|---|---|---|---|---|
| **Cutting Settling Velocity (CSV or $v_{sl}$)** | 0.14 m/s | 0.23 m/s | 0.36 m/s | 1.09 m/s | 1.19 m/s |
| **Transport Ratio ($F_T$)** | 0.806 (**80.6%**) | 0.683 (**68.3%**) | 0.493 (**49.3%**) | -0.535 | -0.676 |

Based on Table 4.7, and as previously highlighted, the CSV ($V_s$) predicted by this research is within 9.2% of the results obtained by Larsen et al. (1997) empirical correlation. The CSV estimated using correlations of Moore, Chien, and Walker and Mayes deviate significantly from Larsen et al. (1997) empirical correlation, and under-predicts by margins of 87.2%, 78.9%, and 67% respectively.

The under-prediction is because the assumptions of Moore, Chien, and Walker and Mayes do not consider hindered settling in the estimation of the cutting settling or slip velocity. The implication of this is that the settling velocities predicted by these models are comparatively lower to what is occurring in the annulus. In contrast, this research has incorporated the process by which the settling of a cutting is impacted or impeded due to the proximity of other cuttings in its vicinity. This research has also considered the influence of Van der Waal's forces in the settling process. Both assumptions were not considered in the equations previously put forward by Moore, Chien, and Walker and Mayes. The result is the significant deviations of between 3 – 8 times below what the cuttings settling velocity should be as shown in Table 4.7.

In terms of the transport ratio, the prediction of this research was that cuttings will accumulate because a sub-critical flow rate (110 GPM) was being used. Thus, a negative transport ratio is estimated using equation 4.3 as follows:

$$F_T = 1 - \frac{V_s}{U_h}$$

At 110 GPM, average annular velocity ($U_h$) is 0.71 m/s. The transport ratio is estimated as

$$F_T = 1 - \frac{1.19}{0.71} = 1 - 1.676 = -0.676 \text{ (i.e., cuttings will accumulate)}$$

Similarly, a negative transport ratio of -0.535 is estimated at the flow rate of 110 GPM using the empirical correlations of Larsen et al. (1997).

Consequently, the cuttings accumulation in the annulus due to the sub-critical flow of 110 GPM is estimated to be 35.15% using a cuttings bed porosity of 36%.

$$\left(1 - \frac{110}{244}\right)(1 - 0.36)100 = 35.15\%$$

Larsen et al. (1997) estimates uncorrected and corrected cuttings concentration of 33.5% and 30.4% respectively.

In contrast, the correlations of Moore, Chien, and Walker and Mayes predicted significantly positive transport ratios, and thus suggest overly optimistic hole cleaning efficiencies at the sub-critical flow rate of 110 GPM. This is because their correlations significantly under-predict the slip velocity. As the slip velocity increases, the transport ratio decreases and becomes negative, implying that the concentration of cuttings in the annulus increases (Bourgoyne et al., 1986).

At the critical transport flow rate of 244 GPM, a positive transport ratio of 24.2% is predicted by this research. Larsen et al. (1997) predicts a transport ratio of 27%. This is because the annular fluid velocity is doubled, and subsequently higher than the estimated cuttings settling velocity. Thus, implying a positive transportation of the cuttings to surface.

## 4.5 Validation of Stuck Pipe Prediction Tool with Stuck Pipe Case Histories

A sample well drilled in the South Ghawar field of Saudi Arabia was used to test the models developed in this research. Table 4.8 summarizes Well-A (HRDH-1476) data.

Table 4.8 Sample Well-A Data

| **Parameters** | **Field Units** | **S.I Units** |
|---|---|---|
| Apparent Viscosity | 30 cp | 0.03 $kg/m.s$ |
| Mud / Fluid Density | 10.96 $lbm/gal$ | 1313.5 $kg/m^3$ (WBM) |
| Flow Behaviour Index, n | | 0.575 |
| Fluid Consistency Index, K | | 1.3362 $Pa.s^n$ |
| Yield Stress, $\tau_0$ | 2.3 | 0.1127 kg/100 m-2 |
| Cutting / Solid Density | 21.7 $lbm/gal$ | 2600 $kg/m^3$ |
| Flow rate | 280 GPM | 0.0177 $m^3/s$ |
| Wellbore Inclination | 90 degrees | 1.57 rad |
| Cutting diameter | 0.07 inches | 0.001778 m |
| Rate of Penetration (ROP) | 60 ft/hr | 18.29 m/hr |
| Wellbore Diameter | 6.125 inches | 0.156 m |
| Drill Pipe Diameter | 4 inches | 0.102 m |
| Drill Pipe RPM | 160 RPM | |
| Angular Velocity | | 44 rad/sec |
| Acceleration Due to Gravity | | 9.81 $m/s^2$ |

Following the steps in section 4.1, and data in Table 4.8:

1. Annular cuttings concentration ($C_c$) is estimated as 0.015912 (or 1.5912% by volume). Larsen et al. (1997) estimates 1.5718% by volume, and a reputable service company software estimates 0.56% by volume
2. The cutting settling velocity (CSV or $V_s$) is calculated as 1.065 m/s. Larsen et al. (1997) method estimates 1.122 m/s.
3. The cutting transport velocity (CTV) is estimated as 0.557 m/s.
4. The critical transport fluid velocity (CTFV) is estimated as

   CTFV = CTV + $V_s$ = 0.557 + 1.065 = 1.622 m/s (or 5.322 ft/s)

   i. Compared to a CTFV of 1.679 m/s (or 5.506 ft/s) estimated by Larsen et al. (1997), this represents a difference of 3.4%
   ii. With an annulus cross-sectional area ($A_{ann}$) of 0.0109 $m^2$, the corresponding flow rate to the CTFV is calculated as 0.0177 $m^3/s$ (or 280 GPM). Larsen et al. (1997) estimates 0.0183 $m^3/s$ (or 290 GPM), and represents 3.4% margin of error
   iii. The critical flow rate predicted by the service company software package is 0.0139 $m^3/s$ (220 GPM). See Figure 5.11. This is 21% lower than the predictions from the numerical models of this research, and 24% lower than Larsen et al. (1997) predictions.
   iv. For Well-A, the flow rate planned to be used during drilling was 280 GPM. The average annular velocity ($U_h$) in the open hole section at this flow rate is estimated to be 1.62 m/s.
   v. The transport ratio ($F_T$) at 280 GPM is estimated as 0.344 (or 34.4%).

## HYDRAULICS - SUMMARY

| | | | | |
|---|---|---|---|---|
| Company Name: | | | | |
| Field: | | | | |
| Structure: | | | | |
| Well: | | | | |
| Location: | | | | |
| Borehole: | | | | |
| Operator: | | | | |
| District: | | | | |
| BHA Data: | | | | |
| Wellbore Data: | | | | |
| Survey Data: | | | | |
| Activity: | 6.125" BHA Run | | | |
| Depth In: | 9500.0 | ft | | |
| Depth Out: | 14416.0 | ft | | |
| Report Date: | Apr-26-2020 16:29 | | | |

**Mud Properties**

| | | |
|---|---|---|
| Type: | Water-based mud (Inhibitive) | |
| Mud Wt: | 82.000 | lbm/ft3 |
| API PV: | 19.0 | cP |
| API YP: | 22.0 | lbf/100ft2 |
| Model: | Power Law / Bingham | |
| H-B K: | 549.2 | eq.cP |
| H-B n: | 0.575 | |
| H-B YS: | 2.3 | lbf/100ft2 |
| P-T: | Off | |
| Fann 3: | 4.9 | lbf/100ft2 |
| Fann 6: | 6.3 | lbf/100ft2 |
| Fann 100: | 22.8 | lbf/100ft2 |
| Fann 200: | 32.9 | lbf/100ft2 |
| Fann 300: | 41.0 | lbf/100ft2 |
| Fann 600: | 60.0 | lbf/100ft2 |

**Pressure Drop Summary**

| | | |
|---|---|---|
| Surf. Eqpt: | 11 | psi |
| Inside Drillstr. | 1001 | psi |
| Tools: | 840 | psi |
| Motor: | 0 | psi |
| RSS / Turbine: | 59 | psi |
| Flow Restrictor: | 165 | psi |
| Bit Nozzles: | 466 | psi |
| Annulus*: | 799 | psi |
| Chokeline: | 0 | psi |
| Hyd. Imbalance: | -20 | psi |
| Ann. Back-Pres: | 0 | psi |
| TOTAL: | 3321 | psi |
| (Actual): | | |

*Including cutting weight & tool joint

| | | |
|---|---|---|
| Tool Joint: | 10 | % (length) |

| | | | | | | | | |
|---|---|---|---|---|---|---|---|---|
| Flowrate: | 280.0 | gal/min | Bit MD: | 14416.0 | ft | ECD at Bit: | 97.530 | lbm/ft3 |
| ROP: | 60.00 | ft/h | Bit TVD: | 7217.0 | ft | ECD at Shoe: | 89.508 | lbm/ft3 |
| RPM: | 140.0 | | Casing Shoe: | 9498.0 | ft | ECD at 14416ft: | 97.530 | lbm/ft3 |

**BHA Description**

| Element | Length ft | ID in | OD in | Cum Len ft | Press Drop psi |
|---|---|---|---|---|---|
| 6 1/8" PDC Bit (TD406) (n | 0.00 | 1.25 | 3.88 | 0.00 | 465.9 |
| 6 1/8" PDC Bit (TD406) (s | 0.52 | 1.25 | 3.88 | 0.52 | 2.9 |
| PD 475 Orbit AA 6 1/8" St | 0.00 | 3.64 | 4.75 | 0.52 | 165.2 |
| PD 475 Orbit AA 6 1/8" St | 13.30 | 3.64 | 4.75 | 13.82 | 59.3 |
| PD X-Over | 2.00 | 2.25 | 4.75 | 15.82 | 0.9 |
| SHORT HOP | 7.24 | 2.50 | 4.75 | 23.06 | 1.4 |
| IMPulse 20k Medium Flow | 32.33 | 2.25 | 4.75 | 55.39 | 708.0 |
| In-Line Stabilizer | 1.42 | 2.25 | 4.75 | 56.81 | 0.6 |
| ADN-4 w/ 5 3/4" Stabilizer | 23.32 | 2.25 | 4.75 | 80.13 | 108.8 |
| 4 3/4" NMDC | 30.90 | 2.25 | 4.75 | 111.03 | 13.7 |
| Crossover | 2.63 | 2.50 | 4.75 | 113.66 | 0.7 |
| 3 Jnts X4" HWDP | 92.49 | 2.56 | 4.00 | 206.15 | 22.5 |
| 4 3/4" Drilling Jar | 29.15 | 2.00 | 4.75 | 235.30 | 21.6 |
| 2 Jnts X4" HWDP | 61.86 | 2.56 | 4.00 | 297.16 | 15.0 |
| 330 Jnts x 4" 14.00 DPG | 9870.09 | 3.34 | 3.87 | 10167.25 | 876.2 |
| Crossover | 2.35 | 2.50 | 4.75 | 10169.60 | 0.7 |
| 5-1/2 " 24.70 DPG, to Sur | 4246.40 | 4.67 | 5.33 | 14416.00 | 68.2 |

**Borehole description**

| Element | Length ft | ID in | Cum Len ft |
|---|---|---|---|
| Air | 35.50 | | 35.50 |
| 9.625" Casing Ru | 5563.50 | 8.84 | 5599.00 |
| 7" Casing Run | 3899.00 | 6.28 | 9498.00 |
| 6.125" BHA Run | 4918.00 | 6.13 | 14416.00 |

**Nozzle Details**

| | Bit |
|---|---|
| Type: | PDC |
| Hole Size: in | 6.125 |
| TFA: in2 | 0.389 |
| Nozzles: 1/32 in | 3 x 13 |

**RSS Details: PD 475 Orbit AA 6 1/8" Stabilized CC**

| | | |
|---|---|---|
| RSS Flowrate: | 280.0 | gal/min |
| RSS Actuator Flow: | 2.7 | % |
| Flow Restrictor Diameter: | 26 | 1/32 in |
| Pad Pressure Drop: | 631.1 | psi |

**Nozzle Optimization**

| | Bit |
|---|---|
| Nozzle Flowrate: gal/min | 272.5 |
| Nozzle Pressure Drop: psi | 465.9 |
| Jet Velocity: ft/s | 224.9 |
| Jet Imp.Force: lbf | 348.0 |
| Hydraulic Power: hhp | 74.1 |
| HSI: hp/in2 | 2.5 |

**Motor Details**

| |
|---|
| Differential Pressure: |
| On-Bottom RPM: |
| DTOR: |
| WOB: |
| Power-Section Flowrate: |
| Rotor Nozzle Flowrate: |
| Bearing Flowrate: |
| Maximum WOB: |
| Maximum Overpull: |

*On-Bottom RPM exclude drillstring surface RPM

**Cuttings**

| | | |
|---|---|---|
| Cuttings Diameter: | 0.07 | in |
| Cuttings Density: | 2.60 | g/cm3 |
| Cutt. Concentration: | 0.56 | % by vol |
| Cuttings Weight: | 22 | psi |
| Bit ECD Increase: | 0.43 | lbm/ft3 |

**Hole Cleaning**

| | | |
|---|---|---|
| Critical Rate: | 219.8 | gal/min |
| Annular Flow: | 272.5 | gal/min |
| Critical MD: | 11137.3 | ft |
| Hole Inclination: | 89.0 | deg |
| Riser Boost Flow: | 0.00 | gal/min |

| Quality Control: | Date: |
|---|---|
| Created By: | |
| Checked By: | |

Drilling Office ver. 2.10.794.0

Figure 4.11: Service Company Hydraulics Modeling Results

The torque & drag, and hydraulics simulations were generated by the service company. Open hole and cased hole friction factors of 0.2 – 0.3 were anticipated based on offset well data.

### 4.5.1 Assessment of Well-A Hook-load Deviation Change

During drilling, the rate of change (from point to point) and deviation change (actual vs model predicted) of each drilling parameter were monitored using the methods described in section 3.7.2. This was done to evaluate the downhole conditions and identify the start of any potential stuck pipe event. As an example, the rate of change and deviation change of the hook-load data for this sample well is discussed. The deviation of the pick-up (PU_WT) and slack-off (SO_WT) weights from well design simulation results are assessed.

Using the logic developed in this research, the "expected" actual PU_WT and SO_WT at the end of each stand drilled is automatically detected and recorded and are highlighted by the yellow and blue columns of Figures 4.12, 4.13, and 4.14 respectively. These values are analogous to what the directional drilling engineer would have manually recorded at the end of each stand drilled to "kelly down". As the "expected" PU_WT and SO_WT were not generated at the exact same depth that the directional drilling engineer records their values, a direct comparison cannot be made. However, Figures 4.12, 4.13, and 4.14 respectively show a visual correlation between both sets of data. Table 4.9 is the "actual" PU_WT and SO_WT manually recorded and reported by the service company directional drilling engineer.

Table 4.9 Actual PU_WT and SO_WT Reported by Directional Drilling Engineer

Drilling Parameter Record Sheet

*data will be plotted in Drilling Loads Plot and Torque Plot

| Depth | Slack Off Weight | Rotating Weight | Pick/Up Weight | Rotary RPM | Off-btm Torque | Break Off Torque | On-btm Torque |
|---|---|---|---|---|---|---|---|
| 9584.00 | **140.00** | **152.00** | **165.00** | 80.00 | 5.00 | 7.00 | 9.00 |
| 9677.00 | **140.00** | **152.00** | **165.00** | 140.00 | 5.00 | 7.00 | 9.00 |
| 9771.00 | **140.00** | **152.00** | **165.00** | 140.00 | 5.00 | 7.00 | 9.00 |
| 9866.00 | **130.00** | **150.00** | **165.00** | 150.00 | 5.00 | 7.00 | 9.50 |
| 9960.00 | **130.00** | **150.00** | **170.00** | 160.00 | 5.00 | 7.00 | 9.50 |
| 10055.00 | **130.00** | **150.00** | **170.00** | 160.00 | 5.00 | 7.00 | 9.50 |
| 10151.00 | **130.00** | **154.00** | **170.00** | 160.00 | 5.00 | 7.00 | 9.50 |
| 10246.00 | 130.00 | 154.00 | 170.00 | 160.00 | 5.00 | 7.00 | 9.00 |
| 10341.00 | 133.00 | 154.00 | 173.00 | 160.00 | 5.00 | 7.00 | 10.00 |
| 10432.00 | 135.00 | 154.00 | 175.00 | 160.00 | 5.00 | 7.00 | 10.00 |
| 10516.00 | 133.00 | 155.00 | 175.00 | 160.00 | 5.00 | 7.00 | 10.00 |
| 10620.00 | 130.00 | 155.00 | 175.00 | 160.00 | 5.00 | 7.00 | 10.00 |
| 10715.00 | 130.00 | 155.00 | 175.00 | 160.00 | 5.00 | 7.00 | 10.00 |
| 10809.00 | 130.00 | 155.00 | 175.00 | 160.00 | 5.00 | 7.00 | 10.00 |
| 10904.00 | 130.00 | 155.00 | 175.00 | 160.00 | 5.00 | 7.00 | 10.00 |
| 10999.00 | 140.00 | 158.00 | 180.00 | 160.00 | 5.00 | 7.00 | 10.00 |
| 11092.00 | 140.00 | 158.00 | 180.00 | 160.00 | 5.00 | 7.00 | 10.00 |
| 11185.00 | 120.00 | 160.00 | 180.00 | 160.00 | 5.00 | 7.00 | 10.00 |
| 11279.00 | 140.00 | 160.00 | 180.00 | 160.00 | 5.00 | 7.00 | 9.00 |
| 11376.00 | 140.00 | 162.00 | 180.00 | 160.00 | 5.00 | 7.00 | 9.50 |
| 11465.00 | 140.00 | 162.00 | 180.00 | 160.00 | 5.00 | 7.00 | 9.50 |
| 11559.00 | 140.00 | 163.00 | 180.00 | 160.00 | 5.00 | 7.00 | 9.50 |
| 11662.00 | 140.00 | 164.00 | 180.00 | 160.00 | 5.00 | 7.00 | 10.00 |
| 11748.00 | 140.00 | 164.00 | 180.00 | 160.00 | 5.00 | 7.00 | 10.00 |
| 11842.00 | 140.00 | 164.00 | 180.00 | 160.00 | 5.00 | 7.00 | 10.00 |
| 11936.00 | 140.00 | 164.00 | 180.00 | 160.00 | 5.00 | 7.00 | 10.00 |
| 12032.00 | 140.00 | 165.00 | 180.00 | 160.00 | 5.00 | 7.00 | 10.00 |
| 12046.00 | | 155.00 | 170.00 | 160.00 | 5.00 | 6.50 | 8.00 |
| 12142.00 | | 155.00 | 170.00 | 160.00 | 5.00 | 6.50 | 8.00 |
| 12236.00 | 110.00 | 155.00 | 170.00 | 160.00 | 5.00 | 6.50 | 8.00 |
| 12332.00 | 110.00 | 150.00 | 170.00 | 150.00 | 5.50 | 6.50 | 8.00 |
| 12426.00 | 120.00 | 150.00 | 175.00 | 150.00 | 5.50 | 6.50 | 8.00 |
| 12515.00 | 100.00 | 150.00 | 175.00 | 150.00 | 5.50 | 6.50 | 8.00 |
| 12609.00 | 100.00 | 150.00 | 175.00 | 150.00 | 5.50 | 6.50 | 8.00 |
| 12711.00 | 130.00 | 150.00 | 180.00 | 150.00 | 5.50 | 6.50 | 8.00 |
| 12801.00 | 130.00 | 154.00 | 180.00 | 150.00 | 6.00 | 7.00 | 9.00 |
| 12894.00 | 135.00 | 153.00 | 180.00 | 155.00 | 6.00 | 7.00 | 9.00 |
| 12989.00 | 133.00 | 155.00 | 180.00 | 155.00 | 6.00 | 7.00 | 9.00 |
| 13088.00 | 130.00 | 155.00 | 180.00 | 160.00 | 6.00 | 7.00 | 9.00 |
| 13176.00 | 128.00 | 156.00 | 181.00 | 160.00 | 6.00 | 7.00 | 9.00 |
| 13271.00 | 128.00 | 156.00 | 182.00 | 160.00 | 6.00 | 7.00 | 9.00 |
| 13371.00 | 128.00 | 156.00 | 184.00 | 160.00 | 6.00 | 7.00 | 9.00 |
| 13463.00 | | 156.00 | 185.00 | 160.00 | 6.00 | 7.00 | 9.60 |
| 13552.00 | | 162.00 | 185.00 | 160.00 | 6.00 | 7.00 | 9.60 |
| 13646.00 | 115.00 | 164.00 | 185.00 | 160.00 | 6.00 | 7.00 | 9.60 |
| 13740.00 | 115.00 | 164.00 | 185.00 | 160.00 | 6.00 | 7.00 | 9.60 |
| 13835.00 | 125.00 | 164.00 | 185.00 | 160.00 | 6.00 | 7.00 | 9.60 |
| 13929.00 | 130.00 | 164.00 | 190.00 | 160.00 | 6.00 | 7.00 | 9.60 |
| 14023.00 | 130.00 | 164.00 | 190.00 | 160.00 | 6.00 | 7.00 | 9.60 |
| 14116.00 | 125.00 | 166.00 | 190.00 | 160.00 | 6.00 | 7.00 | 9.60 |

Based on a 5% threshold for PU_WT and SO_WT respectively, Figures 4.12 and 4.14 show flags from 12,037 ft MD for the PU_WT, and from start of drilling operations for SO_WT. These flags were based on deviation change (actual vs model predicted). Comparing the simulated data versus the actual reported PU_WT, and the logic "predicted" PU_WT does also show a deviation change the from start of the drilling operations. The reason why it is not flagged is because the threshold is set to 5%. If the threshold is reduced to 3%, then all deviation changes >3% become apparent and is automatically flagged at shallower depths (see Figure 4.13). It should be noted that the deviation change highlighted here was not apparent to the directional drilling engineer on site at the time of real-time drilling operations.

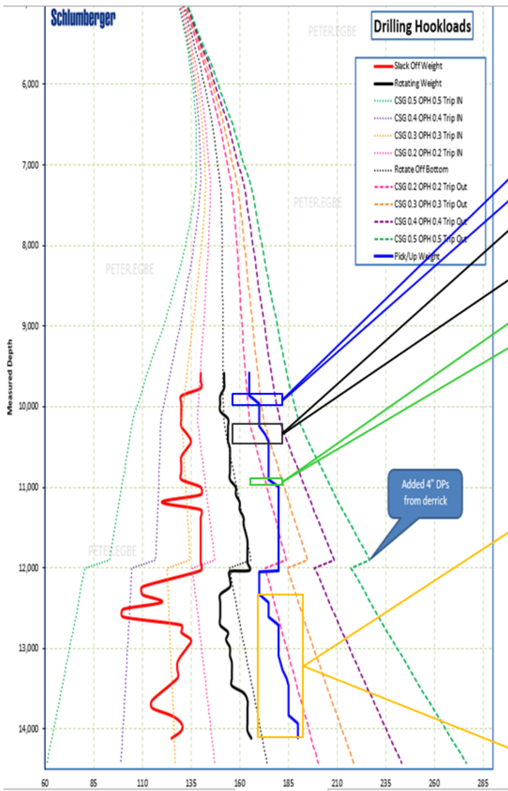


| pickup_window | DEPTH_max | SPI Predicted P/U_WT | Well Design Simulated_Value | footage | ROC_1W_correlation | ROC_2W_correlation | DEV_delta_pct |
|---|---|---|---|---|---|---|---|
| 1 | 9505.85 | 150.25 | | | 0.2 | | 0.05 |
| 2 | 9591.11 | 155.42 | 162.92 | 85.27 | 0.24 | 0.00 | 4.83% |
| 3 | 9683.55 | 157.70 | 163.24 | 92.44 | 0.47 | 0.68 | 3.51% |
| 4 | 9776.67 | 163.01 | 163.53 | 93.12 | 0.37 | 0.09 | 0.32% |
| 5 | 9871.44 | 158.09 | 163.83 | 94.76 | 0.18 | 0.36 | 3.63% |
| 6 | 9965.41 | 166.52 | 164.12 | 93.98 | -0.19 | -0.08 | 1.44% |
| 7 | 10060.94 | 154.39 | 164.44 | 95.53 | -0.01 | 0.17 | 6.51% |
| 8 | 10158.01 | 164.81 | 164.92 | 97.06 | 0.14 | 0.03 | 0.07% |
| 9 | 10252.14 | 163.65 | 165.75 | 94.13 | 0.51 | 0.61 | 1.28% |
| 10 | 10346.09 | 163.99 | 166.77 | 93.96 | 0.64 | 0.33 | 1.70% |
| 11 | 10438.76 | 166.23 | 167.78 | 92.67 | 0.51 | 0.06 | 0.93% |
| 12 | 10531.09 | 164.13 | 168.79 | 92.33 | 0.16 | 0.27 | 2.84% |
| 13 | 10626.29 | 164.77 | 169.84 | 95.21 | 0.38 | -0.28 | 3.08% |
| 14 | 10719.77 | 165.01 | 170.86 | 93.47 | 0.70 | 0.16 | 3.54% |
| 15 | 10815.25 | 169.64 | 171.90 | 95.49 | 0.72 | 0.24 | 1.33% |
| 16 | 10909.27 | 170.12 | 172.94 | 94.02 | 0.71 | 0.69 | 1.65% |
| 17 | 11002.82 | 170.76 | 173.96 | 93.55 | 0.81 | 0.26 | 1.88% |
| 18 | 11097.04 | 175.33 | 175.00 | 94.22 | 0.29 | -0.05 | 0.19% |
| 19 | 11191.11 | 175.09 | 176.04 | 94.07 | 0.26 | -0.01 | 0.54% |
| 20 | 11284.96 | 175.19 | 177.08 | 93.86 | 0.36 | -0.11 | 1.08% |
| 21 | 11378.04 | 173.24 | 178.11 | 93.08 | 0.42 | 0.07 | 2.81% |
| 22 | 11472.62 | 174.94 | 179.16 | 94.58 | 0.26 | -0.11 | 2.41% |
| 23 | 11566.83 | 180.25 | 180.20 | 94.21 | 0.21 | 0.01 | 0.03% |
| 24 | 11662.30 | 174.51 | 181.26 | 95.47 | 0.45 | 0.01 | 3.87% |
| 25 | 11755.58 | 171.24 | 182.31 | 93.28 | 0.07 | -0.15 | 6.46% |
| 26 | 11847.94 | 181.47 | 183.33 | 92.35 | 0.07 | 0.02 | 1.02% |
| 27 | 11942.67 | 179.33 | 179.22 | 94.74 | 0.13 | 0.42 | 0.06% |
| 28 | 12037.00 | 184.44 | 173.43 | 94.33 | 0.53 | 0.08 | 5.97% |
| 29 | 12146.77 | 164.08 | 174.64 | 109.77 | 0.26 | 0.36 | 6.43% |
| 30 | 12441.30 | 163.79 | 177.92 | 294.53 | 0.22 | -0.65 | 8.63% |
| 31 | 12524.40 | 163.69 | 178.84 | 83.10 | 0.60 | 0.29 | 9.25% |
| 32 | 12616.09 | 164.91 | 179.86 | 91.68 | 0.26 | 0.16 | 9.06% |
| 33 | 12712.95 | 163.01 | 180.95 | 96.86 | 0.52 | 0.03 | 11.01% |
| 34 | 12806.47 | 167.69 | 181.98 | 93.52 | 0.18 | -0.33 | 8.52% |
| 35 | 12901.09 | 169.25 | 183.04 | 94.62 | 0.57 | 0.40 | 8.15% |
| 36 | 12996.34 | 168.08 | 184.11 | 95.25 | 0.41 | 0.35 | 9.54% |
| 37 | 13089.40 | 164.86 | 185.17 | 93.06 | 0.42 | 0.23 | 12.31% |
| 38 | 13182.72 | 172.90 | 186.24 | 93.32 | 0.42 | 0.11 | 7.71% |
| 39 | 13276.75 | 167.59 | 187.29 | 94.03 | 0.52 | 0.58 | 11.76% |
| 40 | 13370.51 | 170.66 | 188.35 | 93.76 | 0.40 | 0.15 | 10.36% |
| 41 | 13463.82 | 169.49 | 189.39 | 93.31 | 0.42 | 0.16 | 11.74% |
| 42 | 13558.36 | 176.11 | 190.46 | 94.54 | 0.16 | 0.14 | 8.14% |
| 43 | 13652.16 | 170.85 | 191.52 | 93.80 | 0.72 | 0.14 | 12.09% |
| 44 | 13841.64 | 175.14 | 193.71 | 189.49 | 0.55 | 0.18 | 10.61% |
| 45 | 13934.90 | 170.90 | 194.77 | 93.25 | 0.30 | 0.54 | 13.97% |
| 46 | 14029.81 | 177.96 | 195.85 | 94.92 | 0.30 | -0.16 | 10.05% |
| 47 | 14124.84 | 174.90 | 196.95 | 95.03 | 0.08 | 0.30 | 12.61% |
| 48 | 14218.33 | 171.29 | 198.01 | 93.49 | 0.29 | 0.13 | 15.60% |
| 49 | 14313.07 | 172.31 | 199.11 | 94.74 | 0.45 | -0.03 | 15.55% |
| 50 | 14408.57 | 176.16 | 200.18 | 95.50 | 0.32 | 0.08 | 13.63% |

Figure 4.12: Well-A Correlation for Pick-up Weight (RoC Threshold = 0.20 & Deviation Threshold = 5%). PU_WT Deviation Flagged at 12,037 ft MD

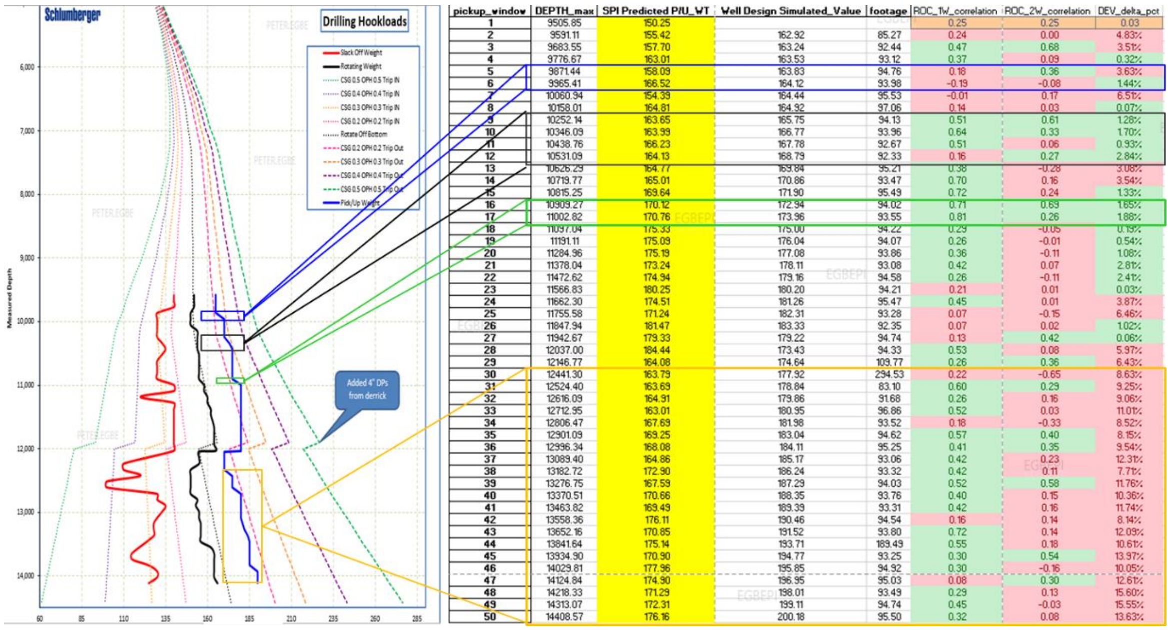


Figure 4.13: Well-A Correlation for Pick-up Weight (RoC Threshold = 0.25 & Deviation Threshold = 3%). PU_WT Deviation Flagged Shallower at 9,591 ft MD

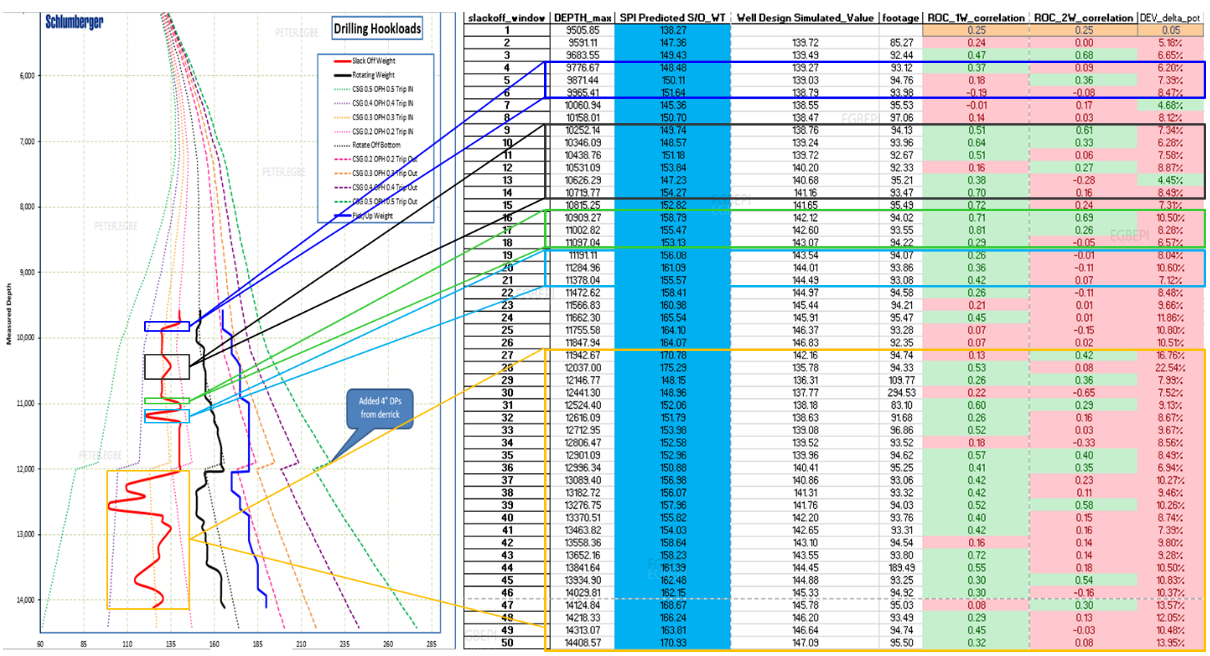


Figure 4.14: Well-A Correlation for Slack-Off Weight (RoC Threshold = 0.25 & Deviation Threshold = 5%). SO_WT Deviation Flagged from Start of Section as Expected

### 4.5.2 Assessment of Well-A Hook-load Rate of Change

Evaluating the rate of change (RoC) for the hook-load data in real-time is more cumbersome because of the volume of the data involved. For ease of this discussion, a data window is regarded as 93 ft (i.e., one stand of drill pipe). The window size can be 30 ft (i.e., one joint of drill pipe), or 15 ft windows (depending on preference). Assuming a 93 ft data window, and at an average rate of penetration (ROP) of 60 ft/hr, it will take approximately 1.55 hours to drill the stand down. At a data transmission rate of 1 data point per second (i.e., 1 Hz frequency), and if considering rotary drilling data alone, that is a lot of data points (5,580) to evaluate for change as each footage is drilled. Using the rate of change logic described in section 3.7.2 (i.e., the z-score), the RoC was estimated using the previous one and two data windows. With a threshold of 0.2 and 0.25 respectively, and relative to the one-window correlation, the two-window RoC correlation appears to agree with the changing hook-load data as shown in Figures 4.12, 4.13, and 4.14. This assessment is based on the z-score statistical method of anomaly detection as described in section 3.7.2 of this thesis. In this case, the color change is associated with a z-score correlation falling outside of the defined statistical range or threshold compared to the previous data window.

### 4.5.3 Assessment of Well-A Stuck Pipe Risk Based on Hook-load Real-Time Data

With reference to the weighted risk structure described in section 3.7.3, and depending on the number of variables being monitored, the deviation change, and rate of change contribute a certain percentage of that weighted risk based on their associated risk group. For example, the pick-up and slack-off hook-load deviation change (actual vs. model predicted) falls under the well design group of data which is allotted a 20% weighting.

For the discussed example, and assuming there are a total of five variables of torque, pick-up weight, slack-off weights, stand-pipe pressure, and ECD being monitored in the group, each of the variable will account for a maximum of 4% risk contribution (i.e., 20% divided by 5 variables). If only one variable is being monitored, it accounts for all the 20% risk allotted to well design model group. In this case for Well-A, as the deviation change is observed in the pick-up weight and slack-off weight, both variables contribute 4% each of 20% (i.e., 4% + 4% = 8%) to the overall stuck pipe risk weighting for that group of data.

Similarly, the stuck pipe risk associated with the rate of change (RoC) calculations apply to all real-time data streams being transmitted by the WITSML system. In the SPI algorithm, real-time data rate of change analysis has been allotted the highest weighting of 60%. As was the case with the deviation change, each RoC variable contributes a risk factor dependent on the number of variables being monitored. If four real-time variables of flow rate, torque, hook-load, and stand-pipe pressure are being transmitted, each contributes 15% to the 60% allotment being used to estimate the average stuck pipe risk. Thus, in this case, the hook-load RoC contributes 15% of 60% to the overall stuck pipe risk weighting for that group of data.

RoC (anomaly detection) and deviation change (actual vs model predicted) of other real-time data sets (e.g., surface torque, stand-pipe pressure, etc.) for various rig operation activities (e.g., ream in, back ream, trip in, trip out, slide drill, etc.) are processed in the same manner as described. A risk contribution is calculated based on the weight allotted to their associated data classification group. The method of risk calculation and ranking is as described in section 4.7.3 to compute the final stuck pipe risk probability index as drilling operations progress.

Well-A was analyzed using the coded stuck pipe index (SPI) tool. The real-time stuck pipe risk index trend is plotted in "red" on the first track from the right. In Figure 4.15, the first consistent medium (>25%) to high (>50%) stuck pipe risk alerts (blue colored ovals) were flagged at 19:39hrs on the 16$^{th}$ of April 2020 and at 10:07hrs on the 17$^{th}$ of April 2020, respectively. Prior to that, the alerts were mainly low risk flags (i.e., <20%). The string got stuck 24hrs later at 19:37hrs on the 17$^{th}$ of April 2020. This prediction was done using only real-time data anomaly detection. No well design model analysis was used as part of this prediction.

For this case of Well-A, the SPI tool detected an anomaly in the hook-load trend and flagged an "abnormal hook-load" alert. Based on this alert, the crew should have considered the following operational recommendations:

- Stop drilling. Sweep and circulate the hole clean with tandem (low viscosity / weighted hi-vis) sweep pills. More than one bottoms-up is recommended

- Perform a wiper trip to the previous casing shoe to confirm the hole condition
- Assess the drilling fluid rheology. Confirm all properties are in the correct range; and if not make the necessary adjustments
- Assess the drilling parameters and confirm via sensitivity analysis if sufficient for hole cleaning considering the rate of penetration, etc.
- If not previously done, the Drilling Engineer should run his/her well design models (T&D, hole cleaning, etc.) and compare with the actual well data to further fine-tune the above recommendations to the rig crew

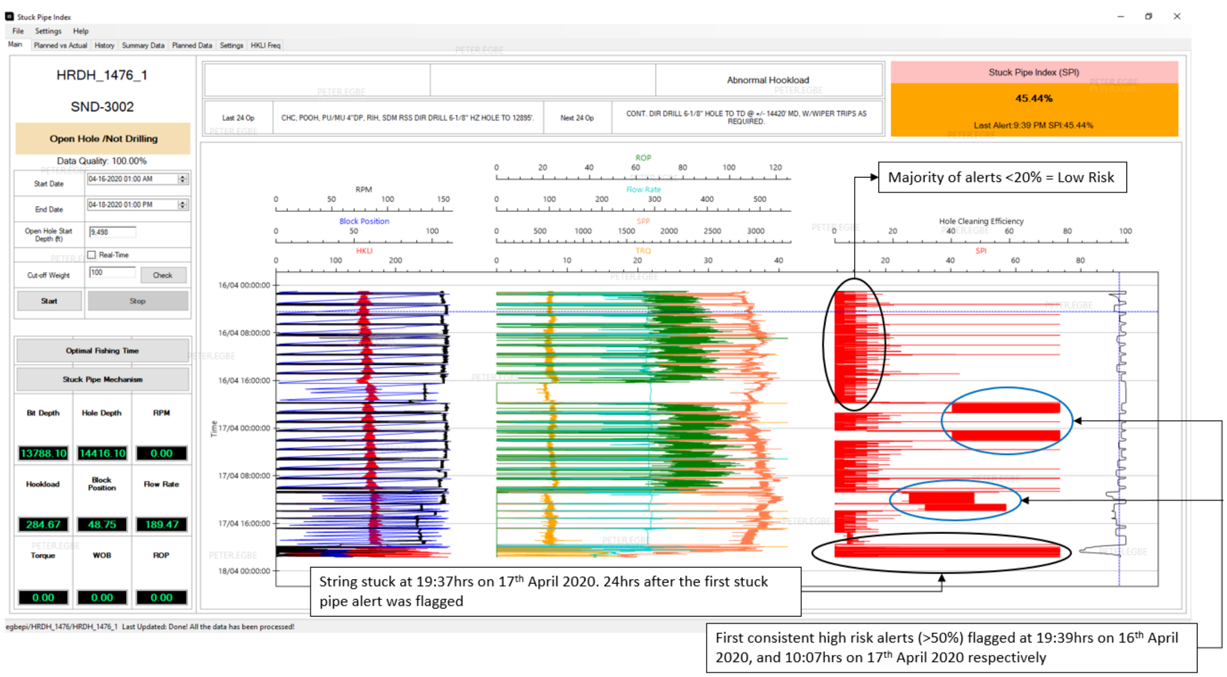


Figure 4.15: Well-A Stuck Pipe Risk Index Trend Using Real-Time Data Only (No Well Design Models)

Figure 4.16 shows the same prediction but with torque & drag well design simulation loaded into the SPI tool to be used as part of the monitoring criteria to evaluate a deviation change of actual versus model analysis for the PU_WT and

SO_WT. It was observed that the real-time SPI risk trend increased by an additional 15 – 20 percentage points and flagged "medium (>25%)" compared to the SPI risk trend without the T&D well design simulation which flagged "low risk (<20%) for the same time and depth interval. Recall that in Figure 4.14 (manual analysis), it was highlighted that a flag should be raised from the beginning of the hole section because the actual slack-off weight (SO_WT) measured at the end of each drilled stand showed a deviation change of more than 5% compared to the expected values predicted by the T&D model. Thus, the real-time SPI prediction with the T&D simulation results validates the manual analysis and indicate a relatively higher degree of accuracy. If the crew had an alert system like SPI actively monitoring the well in real-time, a medium risk flag from the beginning of the section may have alerted them significantly earlier to an impending stuck pipe situation.

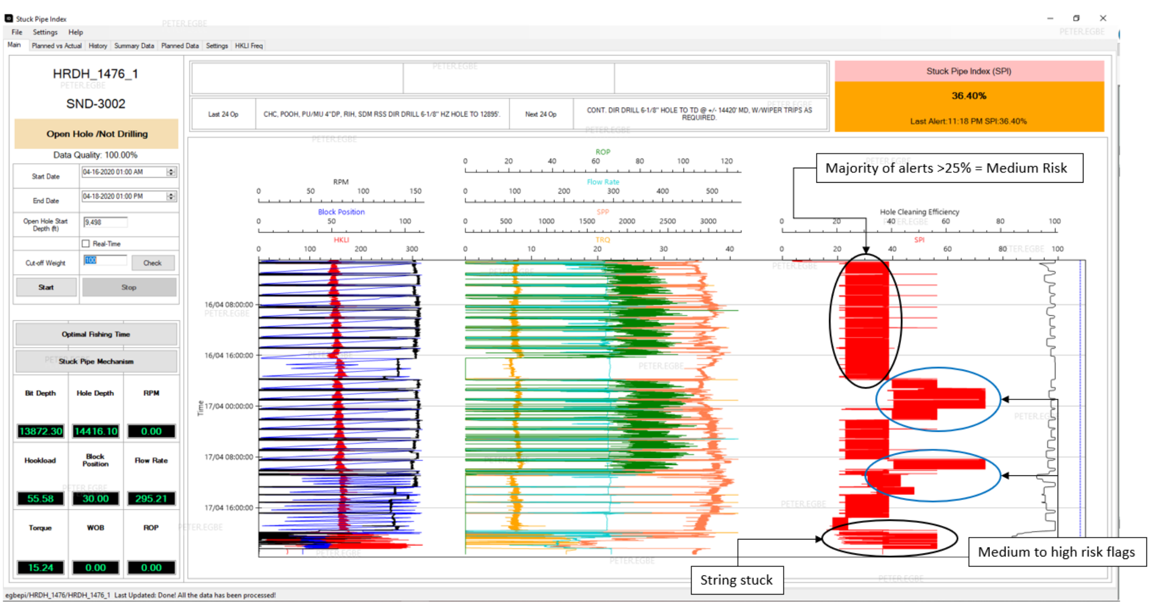


Figure 4.16: Well-A Stuck Pipe Risk Index Trend Using Real-Time Data with T&D Model Simulation

Figure 4.17 shows a snapshot of the results for PU_WT and SO_WT deviation change computed by the SPI tool. It highlights the deviation change flags in the same intervals as the manual analysis (Figures 4.12, 4.13, and 4.14). Note that "manual analysis" here refers to the non-automated logic programmed into a tool, where the Drilling Engineer analyzes the events, and detect any anomaly changes.

Appendix-A and Appendix-B show the full SPI tool report for the two scenarios presented in Figures 4.15 and 4.16, respectively. Figure 4.18 is a snapshot of the daily drilling report corroborating the stuck pipe event details.

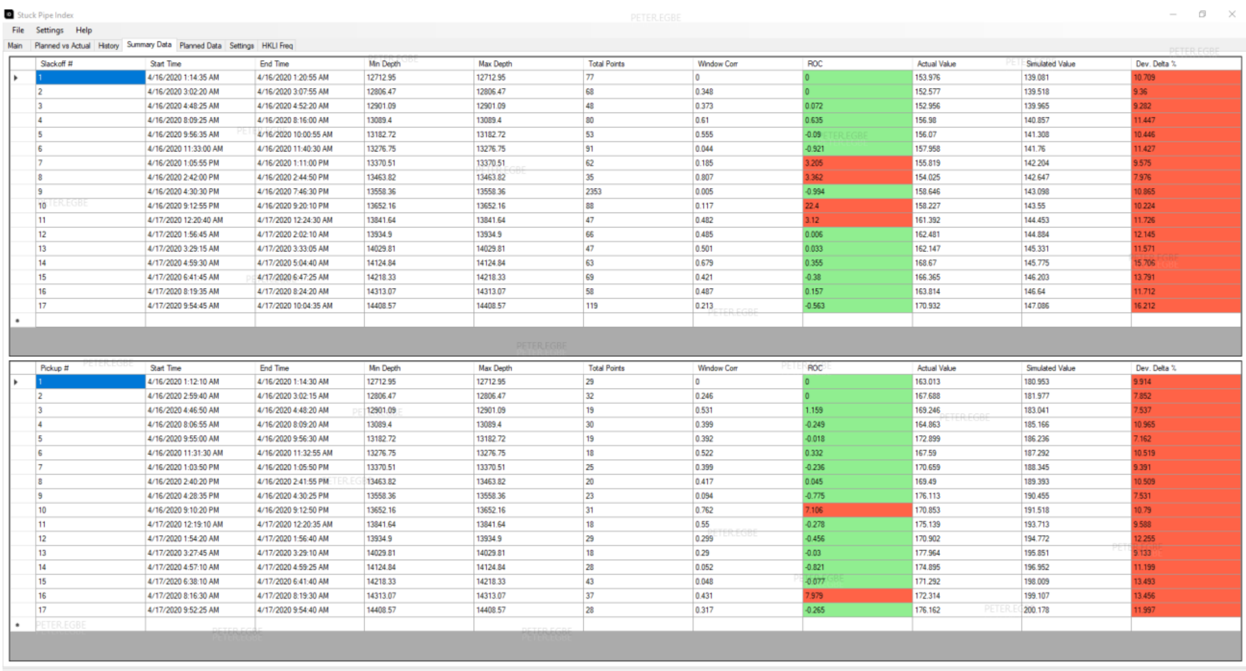


| Slackoff # | Start Time | End Time | Min Depth | Max Depth | Total Points | Window Corr | ROC | Actual Value | Simulated Value | Dev. Delta % |
|---|---|---|---|---|---|---|---|---|---|---|
| 1 | 4/16/2020 1:14:35 AM | 4/16/2020 1:20:55 AM | 12712.95 | 12712.95 | 77 | 0 | 0 | 153.976 | 139.081 | 10.709 |
| 2 | 4/16/2020 3:02:20 AM | 4/16/2020 3:07:55 AM | 12806.47 | 12806.47 | 68 | 0.348 | 0 | 152.577 | 139.518 | 9.36 |
| 3 | 4/16/2020 4:48:25 AM | 4/16/2020 4:52:20 AM | 12901.09 | 12901.09 | 48 | 0.373 | 0.072 | 152.956 | 139.965 | 9.282 |
| 4 | 4/16/2020 8:09:25 AM | 4/16/2020 8:16:00 AM | 13089.4 | 13089.4 | 80 | 0.61 | 0.635 | 156.98 | 140.857 | 11.447 |
| 5 | 4/16/2020 9:56:35 AM | 4/16/2020 10:00:55 AM | 13182.72 | 13182.72 | 53 | 0.555 | -0.09 | 156.07 | 141.308 | 10.446 |
| 6 | 4/16/2020 11:33:00 AM | 4/16/2020 11:40:30 AM | 13276.75 | 13276.75 | 91 | 0.044 | -0.921 | 157.958 | 141.76 | 11.427 |
| 7 | 4/16/2020 1:05:55 PM | 4/16/2020 1:11:00 PM | 13370.51 | 13370.51 | 62 | 0.185 | 3.205 | 155.819 | 142.204 | 9.575 |
| 8 | 4/16/2020 2:42:00 PM | 4/16/2020 2:44:50 PM | 13463.82 | 13463.82 | 35 | 0.807 | 3.362 | 154.025 | 142.647 | 7.976 |
| 9 | 4/16/2020 4:30:30 PM | 4/16/2020 7:46:30 PM | 13558.36 | 13558.36 | 2353 | 0.005 | -0.994 | 158.646 | 143.098 | 10.865 |
| 10 | 4/16/2020 9:12:55 PM | 4/16/2020 9:20:10 PM | 13652.16 | 13652.16 | 88 | 0.117 | 22.4 | 158.227 | 143.55 | 10.224 |
| 11 | 4/17/2020 12:20:40 AM | 4/17/2020 12:24:30 AM | 13841.64 | 13841.64 | 47 | 0.482 | 3.12 | 161.392 | 144.453 | 11.726 |
| 12 | 4/17/2020 1:56:45 AM | 4/17/2020 2:02:10 AM | 13934.9 | 13934.9 | 66 | 0.485 | 0.006 | 162.481 | 144.884 | 12.145 |
| 13 | 4/17/2020 3:29:15 AM | 4/17/2020 3:33:05 AM | 14029.81 | 14029.81 | 47 | 0.501 | 0.033 | 162.147 | 145.331 | 11.571 |
| 14 | 4/17/2020 4:59:30 AM | 4/17/2020 5:04:40 AM | 14124.84 | 14124.84 | 63 | 0.679 | 0.355 | 168.67 | 145.775 | 15.706 |
| 15 | 4/17/2020 6:41:45 AM | 4/17/2020 6:47:25 AM | 14218.33 | 14218.33 | 69 | 0.421 | -0.38 | 166.365 | 146.203 | 13.791 |
| 16 | 4/17/2020 8:19:35 AM | 4/17/2020 8:24:20 AM | 14313.07 | 14313.07 | 58 | 0.487 | 0.157 | 163.814 | 146.64 | 11.712 |
| 17 | 4/17/2020 9:54:45 AM | 4/17/2020 10:04:35 AM | 14408.57 | 14408.57 | 119 | 0.213 | -0.563 | 170.932 | 147.086 | 16.212 |

| Pickup # | Start Time | End Time | Min Depth | Max Depth | Total Points | Window Corr | ROC | Actual Value | Simulated Value | Dev. Delta % |
|---|---|---|---|---|---|---|---|---|---|---|
| 1 | 4/16/2020 1:12:10 AM | 4/16/2020 1:14:30 AM | 12712.95 | 12712.95 | 29 | 0 | 0 | 163.013 | 180.953 | 9.914 |
| 2 | 4/16/2020 2:59:40 AM | 4/16/2020 3:02:15 AM | 12806.47 | 12806.47 | 32 | 0.246 | 0 | 167.688 | 181.977 | 7.852 |
| 3 | 4/16/2020 4:46:50 AM | 4/16/2020 4:48:20 AM | 12901.09 | 12901.09 | 19 | 0.531 | 1.159 | 169.246 | 183.041 | 7.537 |
| 4 | 4/16/2020 8:06:55 AM | 4/16/2020 8:09:20 AM | 13089.4 | 13089.4 | 30 | 0.399 | -0.249 | 164.863 | 185.166 | 10.965 |
| 5 | 4/16/2020 9:55:00 AM | 4/16/2020 9:56:30 AM | 13182.72 | 13182.72 | 19 | 0.392 | -0.018 | 172.899 | 186.236 | 7.162 |
| 6 | 4/16/2020 11:31:30 AM | 4/16/2020 11:32:55 AM | 13276.75 | 13276.75 | 18 | 0.522 | 0.332 | 167.59 | 187.292 | 10.519 |
| 7 | 4/16/2020 1:03:50 PM | 4/16/2020 1:05:50 PM | 13370.51 | 13370.51 | 25 | 0.399 | -0.236 | 170.659 | 188.345 | 9.391 |
| 8 | 4/16/2020 2:40:20 PM | 4/16/2020 2:41:55 PM | 13463.82 | 13463.82 | 20 | 0.417 | 0.045 | 169.49 | 189.393 | 10.509 |
| 9 | 4/16/2020 4:28:35 PM | 4/16/2020 4:30:25 PM | 13558.36 | 13558.36 | 23 | 0.094 | -0.775 | 176.113 | 190.455 | 7.531 |
| 10 | 4/16/2020 9:10:20 PM | 4/16/2020 9:12:50 PM | 13652.16 | 13652.16 | 31 | 0.762 | 7.106 | 170.853 | 191.518 | 10.79 |
| 11 | 4/17/2020 12:19:10 AM | 4/17/2020 12:20:35 AM | 13841.64 | 13841.64 | 18 | 0.55 | -0.278 | 175.139 | 193.713 | 9.588 |
| 12 | 4/17/2020 1:54:20 AM | 4/17/2020 1:56:40 AM | 13934.9 | 13934.9 | 29 | 0.299 | -0.456 | 170.902 | 194.772 | 12.255 |
| 13 | 4/17/2020 3:27:45 AM | 4/17/2020 3:29:10 AM | 14029.81 | 14029.81 | 18 | 0.29 | -0.03 | 177.964 | 195.851 | 9.133 |
| 14 | 4/17/2020 4:57:10 AM | 4/17/2020 4:59:25 AM | 14124.84 | 14124.84 | 28 | 0.052 | -0.821 | 174.895 | 196.952 | 11.199 |
| 15 | 4/17/2020 6:38:10 AM | 4/17/2020 6:41:40 AM | 14218.33 | 14218.33 | 43 | 0.048 | -0.077 | 171.292 | 198.009 | 13.493 |
| 16 | 4/17/2020 8:16:30 AM | 4/17/2020 8:19:30 AM | 14313.07 | 14313.07 | 37 | 0.431 | 7.979 | 172.314 | 199.107 | 13.456 |
| 17 | 4/17/2020 9:52:25 AM | 4/17/2020 9:54:40 AM | 14408.57 | 14408.57 | 28 | 0.317 | -0.265 | 176.162 | 200.178 | 11.997 |

egbepi/HRDH_1476/HRDH_1476_1 Last Updated: Done! All the data has been processed!

Figure 4.17: Example of Well-A PU_WT and SO_WT Deviation Change Analysis by Stuck Pipe Risk Index Tool

**Daily Onshore Drilling Report**
**(0500-0500) Saudi Aramco**
**Date: Saturday 04/18/2020**
Southern Area 911 Emergency Center
(013) 572-0911

| Rig | Charge # | Operation Type | Well Type |
|---|---|---|---|
| SND-3002 | (66- 19058- 1476) | NEW WELL | PRODUCER |

Well: HRDH-1476
Wellbores: (0-1) HRDH_1476_1
BI: (60) DEVELOPMENT DRILLING AND WORKOVERS
Objective: OIL PRODUCER SINGLE LATERAL
Drilling Date: 05/02/2020
Decimal Degrees Latitude: 24.0991221
Decimal Degrees Longitude: 49.1256898
UTM Easting: 309477.44
UTM Northing: 2666508.95

Foreman(s): CHIBANI, FOUZI/ IBRAHIM, MOSTAFA ABDOU/
Engineer: SHAMMARI, NAWAF SAUD/
Superintendent: HUAIMLI, AHMED ABDULAZIZ

| THURAYA | RIG FORMAN VSAT | OTHER VSAT | CONTRACTOR/CLERK VSAT |
|---|---|---|---|
| 88-216-777-12-717 | 013-87-65-182 | 013-87-65-149 | 013-87-65-189 |

Last 24 hr operations: SDM DIR DRILL 6-1/8" HZ HOLE TO TD @ 14416',CHC,STUCK PIPE,GLYCOL PILL.

Next 24 hr plan: FREE STUCK PIPE, POOH & L/D SDM DIR. BHA, PU/MU & RIH W/6-1/8" REAM ASSY.

| Depth | Lost Hrs. | Footage Hrs. | Non Footage Hrs | 30 PPM H2S RER (M) | 100 PPM H2S RER (M) | Max GOR (scf/stb) | Distance from Dhahran M/Gate (KM) | Location |
|---|---|---|---|---|---|---|---|---|
| 14416 | 9.25 | 5.75 | 18.25 | 663 | 396 | 475 | 267 | 267 KM FROM DAHRAN MAIN GATE |

| Prev. Depth | Last Csg Size | Landing Point MD | Landing Point TVD | Liner Size | TOL | MD | TVD | Circ % | Days Since Spud/Comm (Date) |
|---|---|---|---|---|---|---|---|---|---|
| 14118 | 9 5/8 | 6172 | 6068 | 7 | 5599 | 9498 | 7054 | 100 | 50.5 (02/27/2020@1700) |

Footage: 298
Total Operations Lost Time Hours: 316.75
Total UPRATime Hours: 00.00

| | | | | |
|---|---|---|---|---|
| Hrs | 33.25 | 195.50 | 78.75 | 09.25 |
| Lateral | 0 | 0 | 0-1 | 0-1 |
| Phase | 12 1/4 | 8 1/2 | 8 1/2 | 6 1/8 |

Compl.: Hrs
Ev.: Hrs
Rig Move KPI: 18.12 Days
Actual Rig Move: 14.5 DAYS
ROP: 51.83 Feet/Hrs
Target Days: 45

Formation tops

| | | |
|---|---|---|
| UMER | 490 | 27' DEEPER AS PER RCC |
| ARUM | 1195 | |
| LAMS | 1805 | 75' DEEPER AS PER RCC |
| AHMD | 2320 | 24' SHALLOWER AS PER RCC |
| SFNY | 2635 | 35' SHALLOWER AS PER RCC |
| SHUB | 3480 | 35' SHALLOWER AS PER RCC |
| BYDH | 3730 | 18' SHALLOWER AS PER RCC |
| MDTM | 4818 | 18' SHALLOWER AS PER GOC |
| SULY | 5400 | 40' SHALLOWER AS PER GOC |
| HITH | 6028 | 40' SHALLOWER AS PER GOC |
| ABAR | 6461 | 61' SHALLOWER AS PER GOC |
| ARBB | 6508 | 60' SHALLOWER AS PER GOC |
| ABBR | 6618 | 36' SHALLOWER AS PER GOC |
| ARBC | 6648 | 34' SHALLOWER AS PER GOC |
| ABCR | 6747 | 33' SHALLOWER AS PER GOC |
| ARBD | 6908 | 24' SHALLOWER AS PER GOC |
| PADS | 7034 | 8' SHALLOWER AS PER GOC |
| BPDS | 7046 | 2' SHALLOWER AS PER GOC |
| ABD1 | 7092 | 28' DEEPER AS PER GOC |
| AD2A | 7108 | 26' DEEPER AS PER GOC |

| (From - To) | Hrs | Lateral | Phase | Cat. | Major OP | Action | Object | Resp. Co | Hole depth Start | Hole depth End | Event depth Start | Event depth End | LT TYPE | LT ID | Summary of Operations |
|---|---|---|---|---|---|---|---|---|---|---|---|---|---|---|---|
| 0500 - 1045 | 05.75 | 0-1 | 6 1/8 | N | DRLG | D | RSS | SDM | 14118 | 14416 | | | | | SDM RSS DIR. DRLG 6-1/8" HZ HOLE W/82 PCF NACL MUD & 100% CIRC. TO TD @ 14,416' MD CONFIRMED BY GOC.<br>* REAM UP / DOWN PRIOR EACH CONNECTION.<br>* SWEEP HOLE W/15/30 BBLS LV/HW PILL EVERY STAND DRILLED.<br>* SEND DOWNLINK AS REQUIRED, TAKE SURVEY 30' OFF BTM AFTER EVERY STAND DRILLED.<br>* FOLLOWING DIREC. PLAN HRDH-1476 L_0_1_PROJECTION & GOC INSTRUCTION. |
| 1045 - 1945 | 09.00 | 0-1 | 6 1/8 | N | DRLG | CIRC | MPMP | RIG | 14416 | 14416 | | | | | SWEPT HOLE TWICE W/15/30 BBLS LV/HW PILL, CIRC. 6 BTMS UP TILL SHAKERS CLEAN.<br>* FLOW CHECK -WELL STATIC.<br>* RACK BACK ONE STAND AFTER EACH BTM UP. |
| 1945 - 0300 | 07.25 | 0-1 | 6 1/8 | N | DRLG | WOS | STRG | RIG | 14416 | 14416 | 13869 | 13869 | STUK | 832257 | HELD PJSM, POOH 1ST STD W/SOFT BACK RAMING AND WHILE CONNECTION FOR 2ND STD STRING GOT STUCK, P/U ONE SINGLE & WORK STRING DOWN W/MAX S/O WEIGHT & TORQUE -NO SUCCESS.<br>* CONT WORK STRING DOWN W/MAX S/O WEIGHT & TORQUE WHILE PREPARING GLYCOL PILL. |
| 0300 - 0415 | 01.25 | 0-1 | 6 1/8 | N | DRLG | CIRC | MPMP | RIG | 14416 | 14416 | | | STUK | 832257 | HELD PJSM, SPOT GLYCOL PILL AS FOLLOWS:<br>* PUMP 100 BBLS 92 PCF HI-WT PILL AHEAD.<br>* PUMP 100 BBLS 65 PCF GLYCOL.<br>* PUMP 50 BBLS 92 PCF HI-WT PILL BEHIND. |

Figure 4.18: Well-A Daily Drilling Report Highlighting Stuck Pipe Event

### 4.5.4 Review of Other Case Histories Using SPI Real-Time Alerts

#### 4.5.4.1 Well-B (BRRI-462)

Well-B was a 6.125-inch horizontal well section drilled offshore of Saudi Arabia. The section was successfully geo-steered in the carbonate reservoir and drilled to planned total depth (TD) with full circulation using oil-based mud (OBM). Rate of penetration was in the range of 80 – 90 ft/hr and with a flow rate of 310 GPM. Approximately 2,000 ft to planned total depth, it is highlighted in the daily drilling report that over-pulls of up to 15 k-lbs. were observed during connection, and the hole was circulated clean with tandem sweep pills. No mention was made about how many bottoms up the well was circulated clean. At well TD, a short 2,000 ft trip was made to mid-way in the open hole. The string was run-in-hole (RIH) back to bottom. The hole was reported to have been circulated clean for 2.25hrs, confirmed to be in good condition, and afterwards displaced to viscous brine. Thereafter the string became stuck at 19:37hrs. on the 5$^{th}$ of October 2020. The SPI tool was used to play-back the recorded real-time data, and the results are discussed as follows:

- First indications of a potential stuck pipe were flagged at 14:00hrs. on the 5$^{th}$ of October 2020. This is approximately 5.5 hrs. ahead of the stuck pipe event
- From 14:00hrs. onwards, the estimated stuck pipe risk index showed an increasing risk trend until the string got stuck (see Figure 4.19)
- Probable stuck pipe mechanism is assessed to be a pack-off either due to formation, or a cuttings bed avalanche. This assessment is based on
    - Pipe motion before sticking: Rotating down

- Pipe motion after sticking: Impossible to go down
- Pipe rotation after sticking: Restricted rotation observed
- Circulation pressure after sticking: Restricted circulation observed

- 10 minutes prior to the actual stuck pipe event, a review of the WITSML transmitted real-time data indicates a sudden increase and step-change in the stand-pipe pressure (see Figure 4.20). This is further support that there may have been a sudden cuttings bed avalanche or formation pack-off

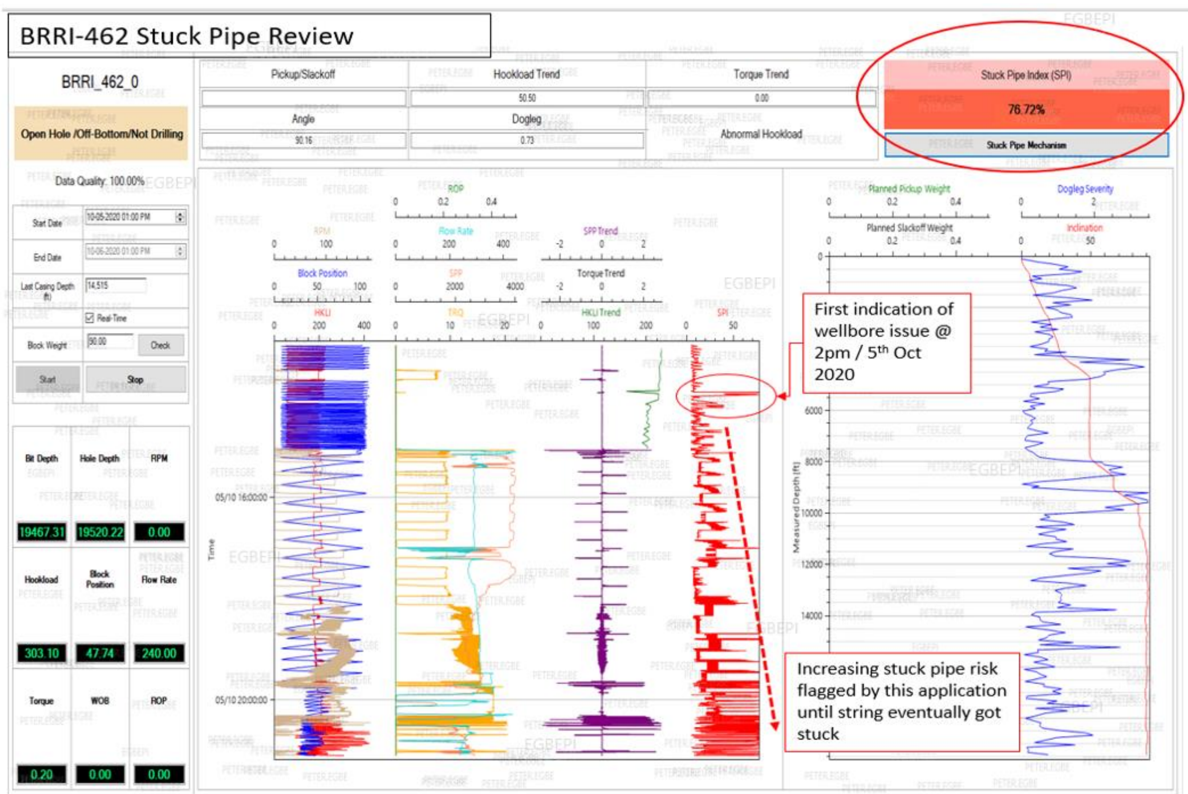


Figure 4.19: Well-B Stuck Pipe Risk Index Trend

BRRI-462 Stuck Pipe Review

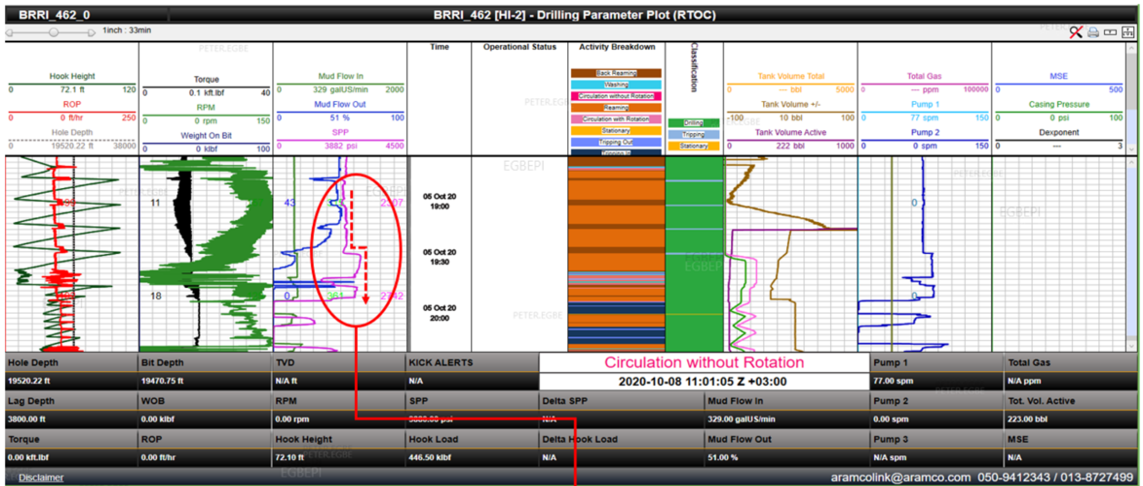


Sudden increase in stand-pipe pressure at 5th Oct 2020 / 19:27 hrs (10 minutes prior to stuck)
String stuck at 19:37 hrs
Stuck pipe predictive tool flagged that there was a developing issue at 14:00 hrs on 5th Oct 2020 (5 ½" hours prior to stuck)

Figure 4.20: Well-B Sudden Step Change in Stand-Pipe Pressure

Operational recommendations for Well-B:

1. SPI flagged an alert of "abnormal hook-load" which suggests that the drag profile in the wellbore had changed possibly due to a cuttings bed accumulation in the annulus or a formation pack-off. This is even though a reasonable flow rate was being used to drill, the hole had been circulated, and a short trip had been performed
2. Based on the events, the following should have been considered when the first alert was raised
    a. Review the drilling fluid properties and evaluate if in the correct range for cuttings transport. As this was a horizontal section, it is critical to ensure that the low shear rheology of the mud is in the right window such as

i. 6-RPM should be ≥ 1.2 – 1.5 times the hole size (in inches)
ii. 3-RPM should be at a value between hole size and 1.5 times the hole size
iii. Low shear yield point (LSYP: 2*3-RPM minus 6-RPM) and should be ≥ hole size

b. Optimize drill string rotation to be in the range of between 100 – 150 RPM. This is important to enhance hole cleaning in terms of the azimuthal velocity profile and vortex transport ratio
c. Tandem sweep pills: These should only be used as hole cleaning indicators; and optimized as follows for wellbore inclination > 35° inclination
    i. High density sweeps should be 15 – 30 PCF > active drilling mud weight.
    ii. Consider sweeps containing fibres for better sweep efficiency
    iii. Volume of sweeps should be at least 200 – 500 ft of the largest annular clearance
    iv. At least 2 – 3 bottoms-up is recommended. A single bottoms-up is not sufficient
d. Wiper trips
    i. should not be done blindly. Evaluate hole condition during trips against a well calibrated torque and drag model
    ii. should be done to the previous casing shoe as a first consideration
    iii. should include clear communication regarding circulating times, maximum over-pulls, tripping speed, and any trouble intervals

#### 4.5.4.2 Well-C (KRSN-155)

Well-C was an 8.5-inch horizontal well section drilled onshore of Saudi Arabia. The section was drilled until a loss circulation zone (LCZ) was encountered. Attempts were made to regain circulation but without success. The decision was made to continue drilling ahead with zero returns and fly-mixed mud. While reaming down, the string stalled at 58 ft off-bottom, and the string got stuck at 02:00hrs. on 12$^{th}$ of October 2020. The daily drilling report recorded that no up and down movement was possible afterwards. It was also reported that string rotation was not possible. The SPI tool was used to play-back the recorded real-time data, and the results are discussed as follows:

- First indications of a potential stuck pipe were flagged at 00:30hrs. on the 12$^{th}$ of October 2020. This is approximately 1.5 hrs. ahead of the stuck pipe event
- From then onwards, the estimated stuck pipe risk index remained steady at medium to high risk (25% - 50%) until the string got stuck (see Figure 5.21)
- Probable stuck pipe mechanism is assessed to be wellbore geometry. This assessment is based on
    - Pipe motion before sticking: Rotating down
    - Pipe motion after sticking: Impossible to go down or up
    - Pipe rotation after sticking: String rotation not possible
    - Circulation pressure after sticking: No change in stand-pipe pressure

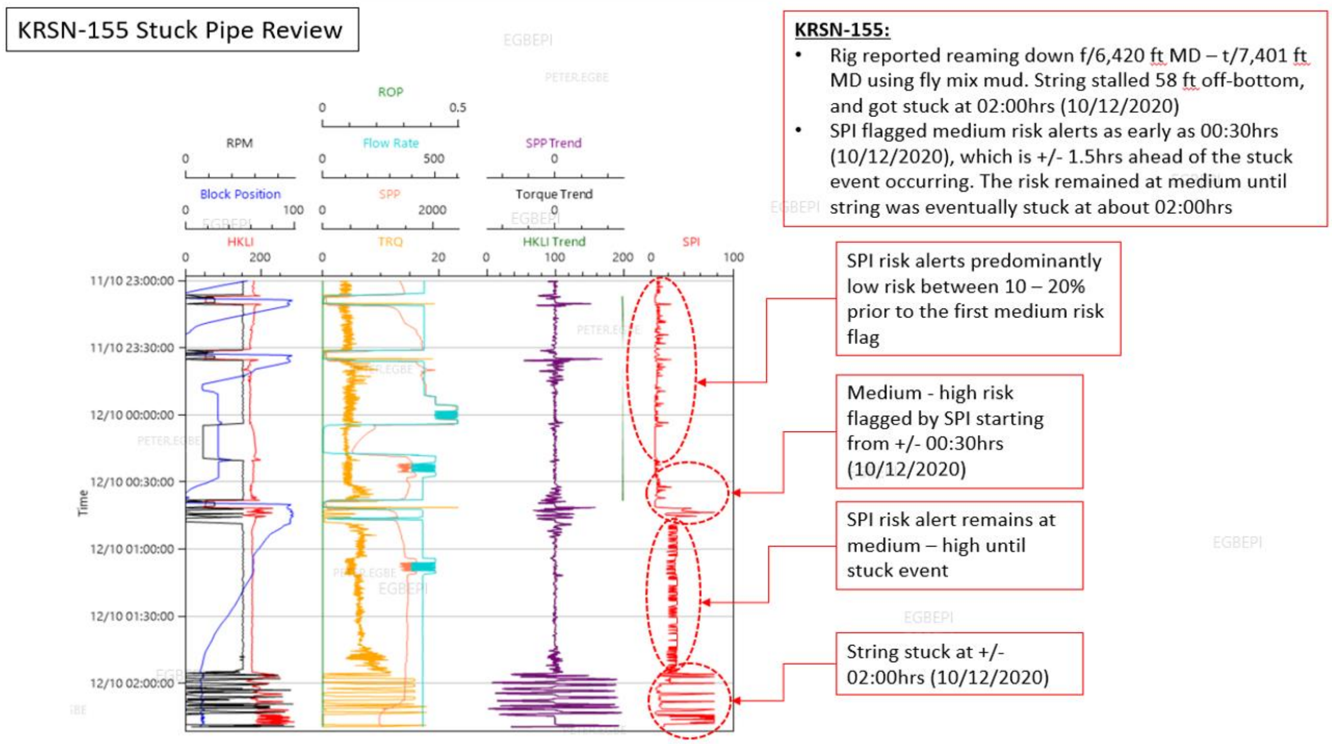


Figure 4.21: Well-C Stuck Pipe Risk Index Trend

Operational recommendations for Well-C:

1. After first indications of potential stuck pipe were flagged, stop drilling, sweep, and circulate the hole clean to the loss circulation zone. The fly-mixed mud could be enhanced with fibrous additives which may also help with curing losses as well as hole cleaning
2. A wiper trip should have been planned to the previous shoe. This would also have ensured that any cuttings accumulation in the annulus is removed. Wiper trips
    a. should not be done blindly. Evaluate hole condition during trips against a well calibrated torque and drag model

b. should be done to the previous casing shoe as a first consideration; and should not be avoided in a bid to save drilling cost

3. During the wiper trip
    a. The Drilling Engineer should re-calibrate the torque and drag models with the most representative friction factors.
    b. The directional drilling engineer should take regular pick-up and slack-off weights for use in updating the T&D model.
    c. The directional engineer should also avoid sudden directional changes that will induce significant doglegs that worsen the wellbore geometry issue. Where a significant dogleg is created, it should be carefully reamed to wipe it out
    d. Rotating time off-bottom should be minimized because the side load against a possible dogleg increases as hook-load increases
    e. The driller must be aware of the position of the bottom-hole assembly relative to the wellbore geometry, and pull through this section cautiously
4. At the end of every stand, the driller should ensure that the string is free in the up and down direction prior to proceeding to make a connection
5. The following should also be considered
    a. Review the drilling fluid properties and evaluate if in the correct range for cuttings transport. As much as possible, ensure that the low shear rheology of the mud is in the right window as per below
        i. 6-RPM should be ≥ 1.2 – 1.5 times the hole size (in inches)

ii. 3-RPM should be at a value between hole size and 1.5 times the hole size

iii. Low shear yield point (LSYP: 2*3-RPM minus 6-RPM) and should be ≥ hole size

b. Optimize the drilling parameters to stabilize the wellbore

i. String rotation to be in a range that results in stable parameters. As loss circulation was encountered, a range of between 100 – 150 RPM may be too severe. Instead, a range that results in stable downhole conditions and a reasonable hole cleaning efficiency should be targeted

ii. Rates of penetration should be adjusted to allow for efficient hole cleaning as much as possible

c. Tandem sweep pills: These should only be used as hole cleaning indicators; and optimized as follows for wellbore inclination > 35° inclination

i. High density sweeps should be 15 – 30 PCF > active drilling mud weight.

ii. Consider sweeps containing fibres for better sweep efficiency

iii. Volume of sweeps should be at least 200 – 500 ft of the largest annular clearance

iv. At least 2 – 3 bottoms-up is recommended. A single bottoms-up is not sufficient

v. Bottoms up in this scenario should be calculated to the loss circulation zone

### 4.5.4.3 Well-D (UTMN-4058)

Well-D was a 6.125-inch horizontal well section drilled onshore of Saudi Arabia. The section was successfully geo-steered in the carbonate reservoir and drilled to planned well total depth (TD) with full circulation using water-based mud (WBM). At well TD, the well was swept and circulated hole clean (CHC) with four bottoms up, however the wellbore was unstable. The SPI tool was used in real-time to monitor the well while tripping the bottom hole assembly (BHA) to surface. The tool flagged stuck pipe risk in real-time across tight spots, alerting the rig site crew to implement best practices to sweep and CHC to avoid a stuck pipe event. Figures 4.22, 4.23, 4.24, and 4.25 highlight the various stuck pipe risk indices flagged by the tool at various tight spots. The daily drilling report also records tight spots within the same intervals (see Figure 4.26).

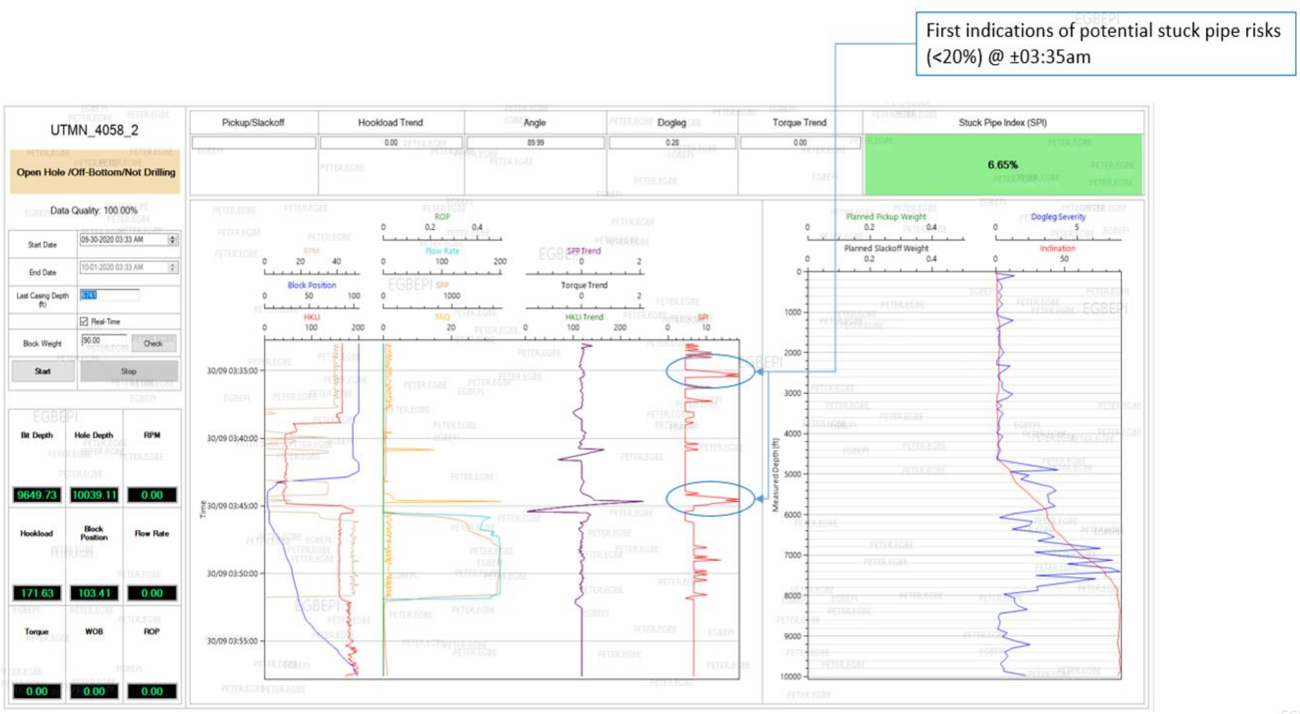


Figure 4.22: Well-D First Indication of Stuck Pipe Risk

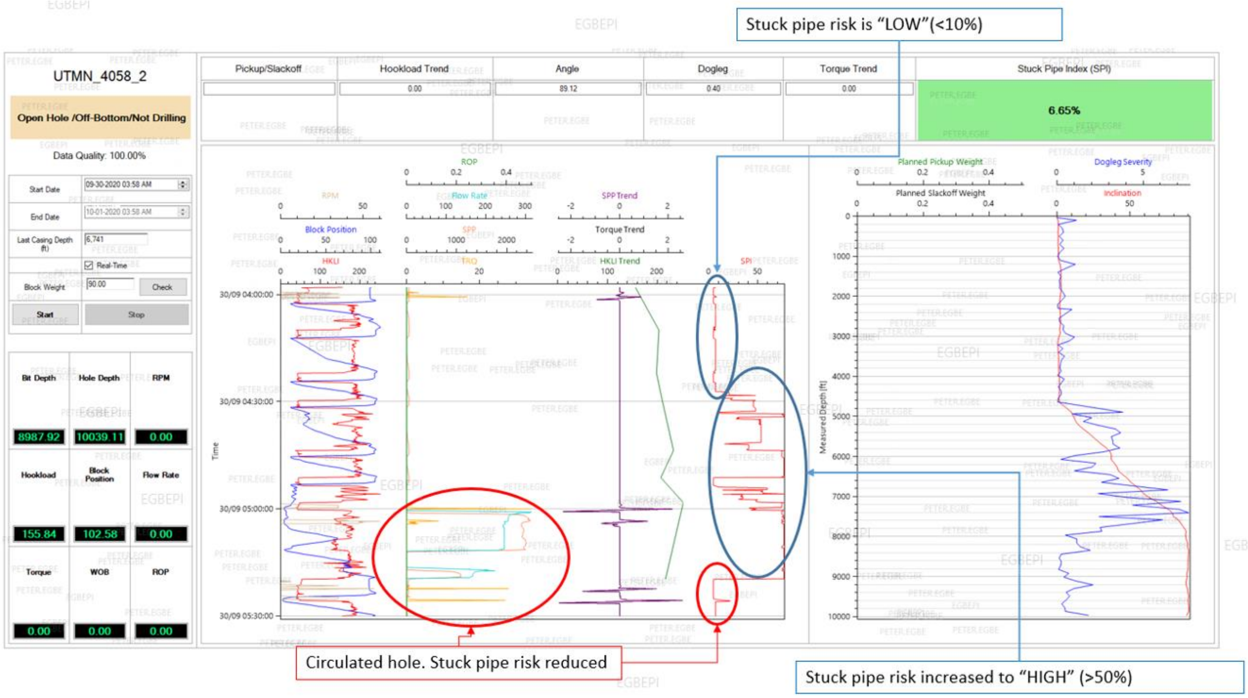


Figure 4.23: Well-D Stuck Pipe Risk Reduced from >50% (High Risk) to 6.65% (Low Risk) After Crew Alerted to Circulate Hole Clean

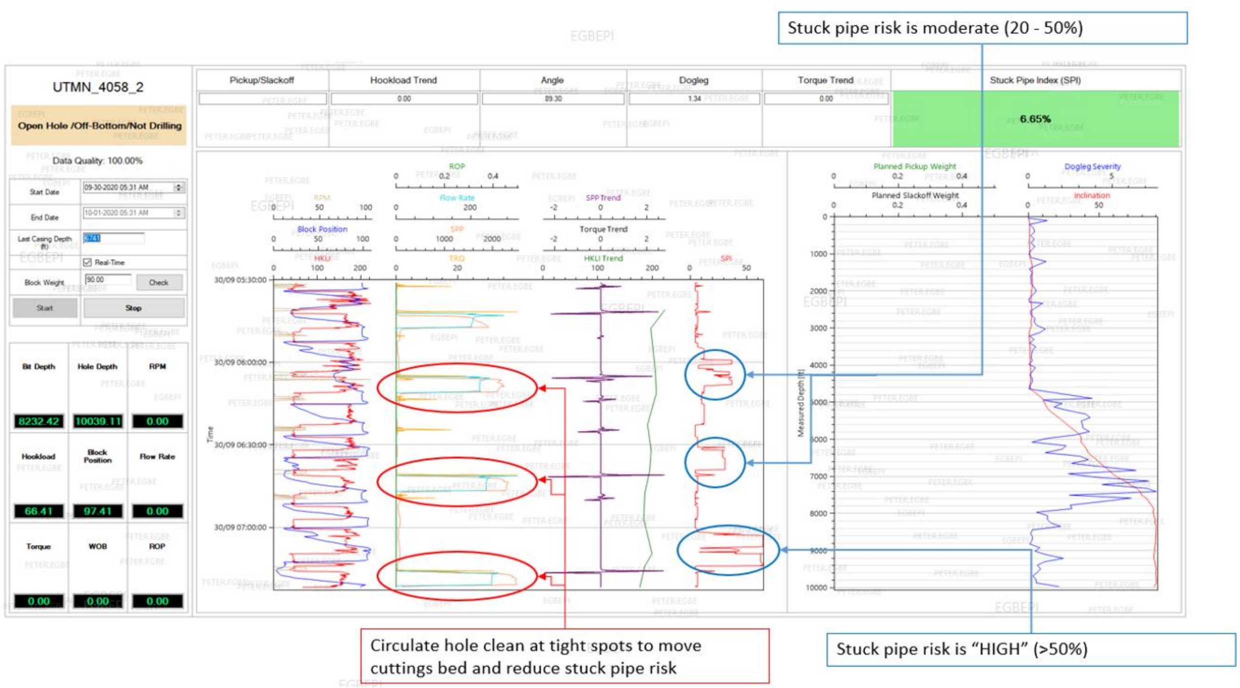


Figure 4.24: Well-D Stuck Pipe Risk Trend Alerted Crew to Circulate Hole Clean

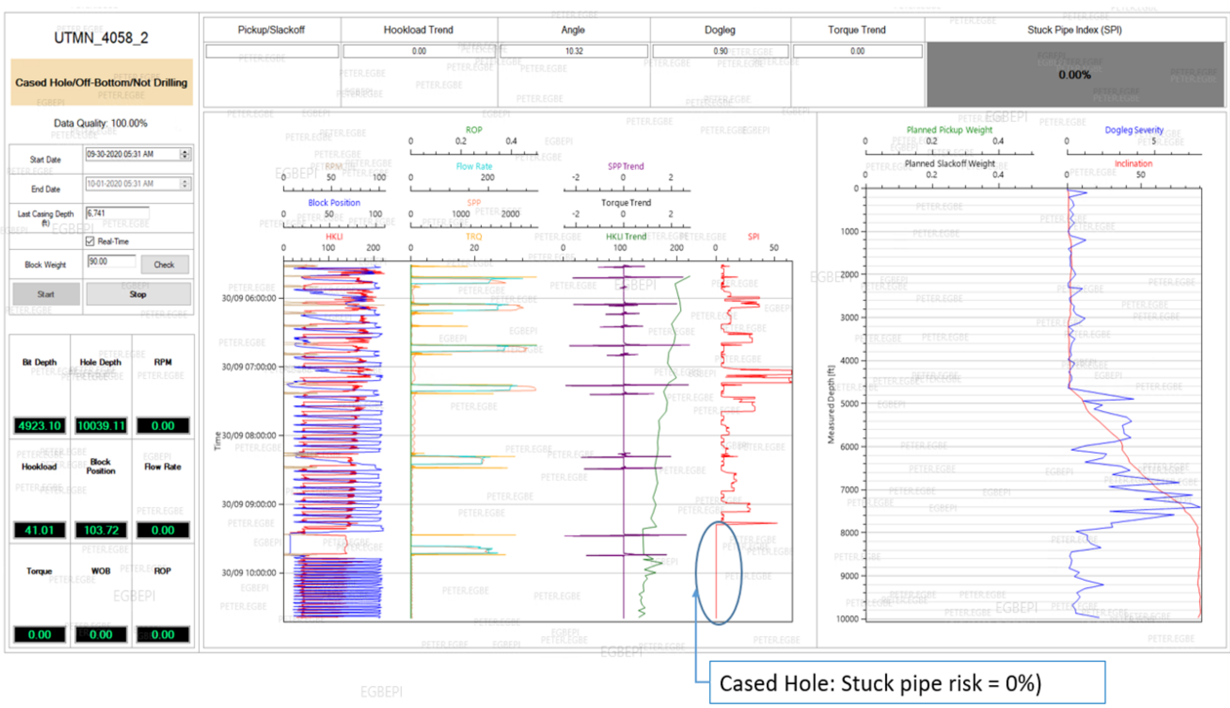


Figure 4.25: Well-D BHA Successfully Tripped into Cased Hole and Stuck Pipe Event Avoided

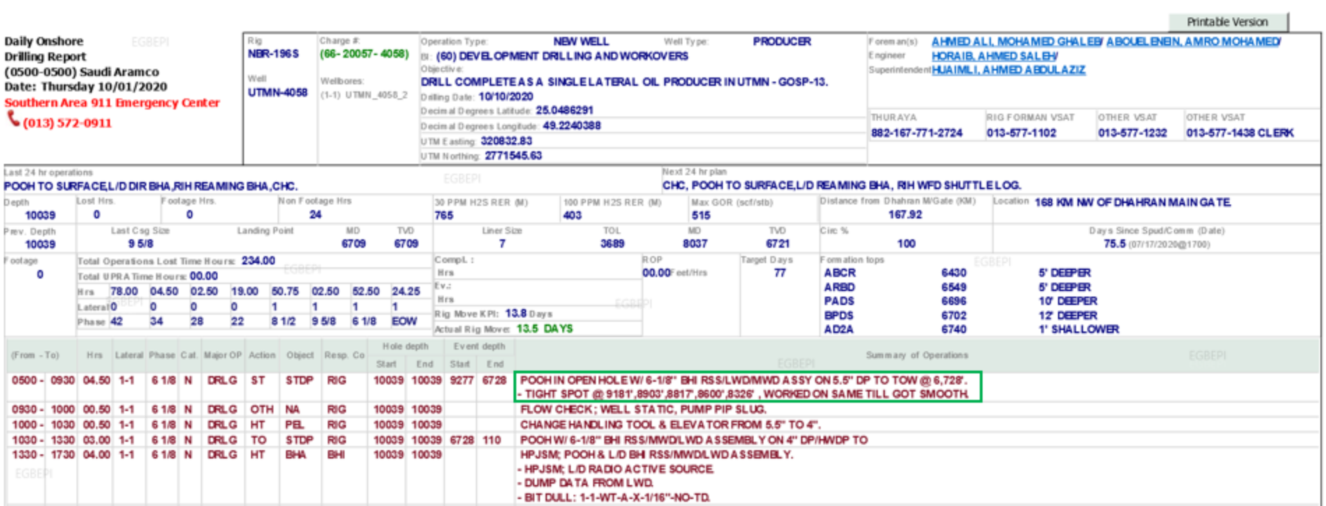

Printable Version

**Daily Onshore Drilling Report (0500-0500) Saudi Aramco**
**Date: Thursday 10/01/2020**
Southern Area 911 Emergency Center (013) 572-0911

Rig: NBR-196S | Charge #: (66- 20057- 4058) | Operation Type: NEW WELL | Well Type: PRODUCER
Well: UTMN-4058 | Wellbores: (1-1) UTMN_4058_2
BI: (60) DEVELOPMENT DRILLING AND WORKOVERS
Objective: DRILL COMPLETE AS A SINGLE LATERAL OIL PRODUCER IN UTMN - GOSP-13.
Drilling Date: 10/10/2020
Decimal Degrees Latitude: 25.0486291
Decimal Degrees Longitude: 49.2240388
UTM Easting: 320832.83
UTM Northing: 2771545.63
Foreman(s): AHMED ALI, MOHAMED GHALEB/ ABOUELENEIN, AMRO MOHAMED/
Engineer: HORAIB, AHMED SALEH/
Superintendent: HUAIMLI, AHMED ABDULAZIZ

| THURAYA | RIG FORMAN VSAT | OTHER VSAT | OTHER VSAT |
|---|---|---|---|
| 882-167-771-2724 | 013-577-1102 | 013-577-1232 | 013-577-1438 CLERK |

Last 24 hr operations: POOH TO SURFACE,L/D DIR BHA,RIH REAMING BHA,CHC.
Next 24 hr plan: CHC, POOH TO SURFACE,L/D REAMING BHA, RIH WFD SHUTTLE LOG.

Depth: 10039 | Lost Hrs.: 0 | Footage Hrs.: 0 | Non Footage Hrs: 24 | 30 PPM H2S RER (M): 765 | 100 PPM H2S RER (M): 403 | Max GOR (scf/stb): 515 | Distance from Dhahran M/Gate (KM): 167.92 | Location: 168 KM NW OF DHAHRAN MAIN GATE.
Prev. Depth: 10039 | Last Csg Size: 9 5/8 | Landing Point MD: 6709 | TVD: 6709 | Liner Size: 7 | TOL: 3689 | MD: 8037 | TVD: 6721 | Circ %: 100 | Days Since Spud/Comm (Date): 75.5 (07/17/2020@1700)
Footage: 0 | Total Operations Lost Time Hours: 234.00 | Total UPRA Time Hours: 00.00 | Compl.: Hrs | Ev.: Hrs | ROP: 00.00 Feet/Hrs | Target Days: 77
Rig Move KPI: 13.8 Days
Actual Rig Move: 13.5 DAYS

| Hrs | 78.00 | 04.50 | 02.50 | 19.00 | 50.75 | 02.50 | 52.50 | 24.25 |
|---|---|---|---|---|---|---|---|---|
| Lateral | 0 | 0 | 0 | 0 | 1 | 1 | 1 | 1 |
| Phase | 42 | 34 | 28 | 22 | 8 1/2 | 9 5/8 | 6 1/8 | EOW |

| Formation tops | | |
|---|---|---|
| ABCR | 6430 | 5' DEEPER |
| ARBD | 6549 | 5' DEEPER |
| PADS | 6696 | 10' DEEPER |
| BPDS | 6702 | 12' DEEPER |
| AD2A | 6740 | 1' SHALLOWER |

| (From - To) | Hrs | Lateral | Phase | Cat. | Major OP | Action | Object | Resp. Co | Hole depth Start | Hole depth End | Event depth Start | Event depth End | Summary of Operations |
|---|---|---|---|---|---|---|---|---|---|---|---|---|---|
| 0500 - 0930 | 04.50 | 1-1 | 6 1/8 | N | DRLG | ST | STDP | RIG | 10039 | 10039 | 9277 | 6728 | POOH IN OPEN HOLE W/ 6-1/8" BHI RSS/LWD/MWD ASSY ON 5.5" DP TO TOW @ 6,728'.<br>- TIGHT SPOT @ 9181',8903',8817',8600',8326' , WORKED ON SAME TILL GOT SMOOTH. |
| 0930 - 1000 | 00.50 | 1-1 | 6 1/8 | N | DRLG | OTH | NA | RIG | 10039 | 10039 | | | FLOW CHECK; WELL STATIC, PUMP PIP SLUG. |
| 1000 - 1030 | 00.50 | 1-1 | 6 1/8 | N | DRLG | HT | PEL | RIG | 10039 | 10039 | | | CHANGE HANDLING TOOL & ELEVATOR FROM 5.5" TO 4". |
| 1030 - 1330 | 03.00 | 1-1 | 6 1/8 | N | DRLG | TO | STDP | RIG | 10039 | 10039 | 6728 | 110 | POOH W/ 6-1/8" BHI RSS/MWD/LWD ASSEMBLY ON 4" DP/HWDP TO |
| 1330 - 1730 | 04.00 | 1-1 | 6 1/8 | N | DRLG | HT | BHA | BHI | 10039 | 10039 | | | HPJSM; POOH & L/D BHI RSS/MWD/LWD ASSEMBLY.<br>- HPJSM; L/D RADIO ACTIVE SOURCE.<br>- DUMP DATA FROM LWD.<br>- BIT DULL: 1-1-WT-A-X-1/16"-NO-TD. |

Figure 4.26: Well-D Daily Drilling Report Highlighting Tight Spots at Corresponding Depths Flagged by the Stuck Pipe Index Tool

Recently, Meor Hashim et al. (2021) published a similar approach to the proposed "ROW" method called the Wells Augmented Stuck Pipe (WASP) indicator. Their technique splits into three separate modules (differential sticking module, wellbore geometry module, and hole cleaning module), where each module is used to predict stuck pipe only for a specific defined applicable rig operation. Notably, they report that their technique has prediction look-ahead limitations which are summarized in Table 4.10. The implication is that any wellbore conditions evolving earlier than these look-ahead limitations may not be detected. In contrast, the "ROW" method in this research combines real-time, offset wells data, and well design model analysis continuously and simultaneously for stuck pipe predictions irrespective of the rig operations (e.g., drilling, tripping, reaming, etc.), and without any limitations to how early (i.e., look-ahead) the predictions can be made.

Table 4.10 Summary of Meor Hashim et al. (2021) Approach

| **WASP Modules** | **Sub-Module** | **Machine Learning Prediction Look-ahead Capability** |
|---|---|---|
| Differential Sticking Module (DSM) | Tripping | 6 stands / joints and 10 stands / joints |
| | Drilling | 2 stands |
| | System Static | Real-time trigger |
| Wellbore Geometry Module (WGM) | Tripping | 6 stands / joints and 10 stands / joints |
| Hole Cleaning Module (HCM) | Drilling | 20 minutes |
| | Non-Drilling | 20 minutes |
| | Flow vs SPP | Real-time trigger |

# 5. CONCLUSION AND RECOMMENDATION

This thesis presents improved cuttings transport numerical models and an integrated approach for the prediction of stuck pipe events.

The research incorporates physical concepts not previously considered in existing cuttings transport numerical models. The new concepts applied in developing the improved cuttings transport numerical models include hindered centrifugal settling, effect of Taylor vortices, and particle-to-particle Van der Waals forces. Hole cleaning efficiency (i.e., cutting transport ratio) is subsequently determined using the improved cuttings transport models.

In combination with the improved cuttings transport models, an integrated real-time stuck pipe prediction concept called the “ROW” approach is also presented. The core of the prediction concept relies on

- Estimating the probable risk of a stuck pipe event while drilling based on statistical analysis of how real-time data changes from point to point (anomaly detection) using the z-score statistical method to identify outliers which may be indicative of deteriorating downhole conditions
- Using previous events from offset wells case histories for statistical analysis to highlight problematic intervals,
- The deviation changes of specific drilling parameters based on a comparison of actual drilling data versus well design model simulation (e.g., hole cleaning, torque & drag, hydraulics, etc.) is used to evaluate if downhole conditions are deviating from pre-drill design expectations.

## 5.1 Summary of Findings and Limitations

### 5.1.1 Cuttings Transport (Hole Cleaning) Numerical Models

The following is a summary of pertinent findings:

1. Effect of hindered centrifugal settling:
    a. The presence of other cuttings in the annulus affects the cuttings settling process. However, several slip velocity models currently used in the industry by leading industry service providers were found to assume "free settling" which is not the case in drilling operations.
    b. This research has developed a cutting settling velocity model (equation 3.51) that considers the influence of hindered centrifugal settling, and an application of the Richardson-Zaki equation as basis. The model was successfully tested and validated to within 10% of Larsen et al. (1997) empirical measurements.
    c. For the same dataset, models of Moore (1974), Chien (1971), and Walker and Mayes (1975) deviate significantly (up to 87% with Moore's correlation) compared to the experimental data of Larsen et al. (1997). This deviation is because the models of Moore (1974), Chien (1971), and Walker and Mayes (1975) do not account for hindered transport and settling effect. The particle-to-particle interactions and impediments which occur due to proximity in the annulus influences the way such particles or cuttings settle or are being transported in the annulus. Due to these interactions, cuttings may settle or be transported in flocs rather than as single individual particles even if non-cohesive particles

are considered (the effect is magnified if considering cohesive settling / transportation). The effect of Van der Waals forces also requires consideration due to the proximity of the particles. The settling velocity of flocs can be a few orders of magnitude higher than that of the primary particle itself. Thus, this means that the physics governing the settling and transportation process changes. This research has considered these factors in the numerical models that have been presented. In the models of Moore, Chien, and Walker and Mayes, these considerations are not reflected. The implication of this is that the critical transport flow rate required to move drilled cuttings out of the hole is under-predicted by their models. Thus, increasing the potential for poor hole cleaning, and the associated challenges such as stuck pipe events

d. In terms of transport ratio (a measure of hole cleaning efficiency), the prediction of this research agrees with Larsen et al. (1997) empirical data also to approximately 10%. The correlations of Moore (1974), Chien (1971), and Walker and Mayes (1975) over-predict the transport ratio even when a sub-critical flow rate was used in the empirical data. This also implies that hole cleaning efficiency predictions vary significantly, are not entirely accurate, and may potentially inadvertently result in stuck pipe events. Hence this research has placed a greater emphasis on real-time data analysis in the case studies

e. The proposed cuttings settling velocity can be used to estimate the critical transport fluid velocity (CTFV) to prevent a cuttings bed build up. Compared to experimental data from Larsen et al. (1997), it estimated a CTFV within <10%, and predicted a critical flow rate that was within 6% of the empirical data

f. A cutting settling velocity “log-log” chart based on annular cuttings concentration and fluid properties is also proposed by this research for ease of quick reference for field personnel

2. Taylor-Couette flow in concentric and eccentric cylinders:

   a. Based on the analogy of drilling operations to the work done by Taylor (1923), this research challenges the basis of defining fluid regimes solely on the Reynolds number alone. Taylor (1923) demonstrated that although the flow regime may be laminar in the axial direction, it may be turbulent in the rotational direction. Potter et al. (2002) agrees

   b. This research has proposed a numerical model to estimate the azimuthal velocity (equation 3.112) and has demonstrated that a “vortex transport ratio” can be used to evaluate the efficiency of hole cleaning based on the toroidal vortices created when the drill string exceeds a critical value. Philip et al. (1998), and Lockett et al. (1993) all agree that depending on the fluid properties, as little as 40 RPM can create vortices strong enough to aid hole cleaning

   c. The importance of adequate string rotation in hole cleaning is already well documented in the industry. The findings of this research provide further support, and highlights the need for more focus to azimuthal or vortex velocity effects in enhancing hole cleaning process during drilling operations

d. Subsequently, this research proposes the use of "drilled cuttings vortex lift performance chart" as a tool for evaluating which drilling fluid will provide a better azimuthal annulus velocity to support efficient hole cleaning. It is envisaged that such a tool will be useful to Drilling Engineers at the well design and planning stage

3. Particle-to-particle Van Der Waals forces:

   a. This research proposed a moment balance equation (equation 3.70) that accounts for all the forces acting on a particle just about to move from rest on a pile of an inclined cuttings bed. The drag force and Van der Waals force come into play when the particle is about to roll. Hence, both cannot be ignored. Duan et al. (2009) proposed a moment balance equation without the drag force, and Naganawa and Nomura (2006) proposed a moment balance equation without the effect of Van der Waals force. This research incorporates both effects

   b. The moment balance equation is used to estimate the cuttings re-suspension velocity (CRV) and was validated against empirical data by Duan et al. (2009). The CRV predicted by this research is 5% lower than the empirical measurement by Duan et al. (2009). Compared to Duan et al. (2009) numerical models, the CRV from this research is 12.3% lower. This difference is believed to be due to Duan et al. (2009) numerical correlations not accounting for the drag force

   c. It is a known fact that the smaller sized drilled cuttings are harder to suspend. Hence, the implication of the CRV in hole cleaning operations is that it defines the minimum flow velocity required to re-suspend settled drilled cuttings into the flow stream to be transported to surface.

4. Annulus cutting concentration by volume:
    a. Dimensionless analysis using the Buckingham Pi-theorem is used to develop a numerical model (equation 4.6) for the estimation of annular cuttings concentration by volume. Coefficients were obtained using regression analysis
    b. Compared to Larsen et al. (1997) empirical data, the research model predicts the annulus cutting volumetric concentration to within 25% at rates of penetration (ROP) >35 ft/hr.
    c. However, at ROP ≤35 ft/hr, a margin of error of ±29 – 58% is estimated compared to Larsen et al. (1997) linear correlation. It is believed that this relatively large error margin is because Larsen et al. (1997) linear correlation is an approximate line of best fit used to describe a large scatter group of data.
    d. Applying a leading oilfield service company model to Larsen et al. (1997) under predicts the annulus cuttings volumetric concentration by up to 72% - 84% at ROP ≤45 ft/hr (Table 4.3). The results of the service company model however do show a profile (Figure 4.7) like the results obtained by this research model. As the service company model is proprietary, the reason for the difference is not fully understood. However, the implication that wellbore annulus cuttings concentration is being under-predicted suggest that the hole cleaning predictions may not be as accurate as previously thought

### 5.1.2 Real-Time Stuck Pipe Prediction Concept

The R-O-W prediction concept is based on numerical and statistical analysis, and was coded into a tool called the stuck pipe index (SPI) to enhance its real-time capability and achieve the following requirements:

1. Generate real-time stuck-pipe index (SPI) alerts, and such alerts should remain low when no risk of a stuck-pipe event exists
2. Prior to a potential stuck pipe, the predicted SPI alert should increase
3. The predicted SPI alert should occur early enough ahead of the impending stuck pipe event to ensure the rig crews have enough time to take evasive/mitigating actions
4. The SPI tool should be future proof such that it can be programmed with well design models that may become available in the future. Hence, the framework of the SPI tool is flexible and adaptive

A proof of concept is demonstrated and proven in this research using four sample wells. Table 5.1 is a summary of the look-ahead capability predicted by the SPI tool in three of the four case history wells presented in this research. In the fourth case study (well-D), the SPI tool is used in in real-time predictive mode, and it flagged high risk intervals requiring the drilling crew attention. Consequently, it helped prevent a potential stuck pipe event.

Table 5.1 Summary of SPI Tool Look-Ahead Capability in Sample Wells

| **Well Name** | **Stuck Pipe Event?** | **SPI Alert Time** | **Stuck Pipe Event Time** | **SPI Alert Level** | **Look-Ahead Warning Time** |
|---|---|---|---|---|---|
| Well-A | Yes | 19:39 hrs / 16$^{th}$ Apr 2020 | 19:37 hrs / 17$^{th}$ Apr 2020 | >50% | 24 hrs |
| Well-B | Yes | 14:00 hrs / 5$^{th}$ Oct 2020 | 19:37 hrs / 5$^{th}$ Oct 2020 | >50% | 5.5 hrs |
| Well-C | Yes | 00:30 hrs / 12$^{th}$ Oct 2020 | 02:00 hrs / 12$^{th}$ Oct 2020 | >50% | 1.5 hrs |
| Well-D | No | SPI Tool used in real-time to prevent stuck pipe event | | | |

The SPI tool is currently undergoing further field trial and validation by the Drilling & Work-Over department of Saudi Aramco. It is being utilized as a proactive stuck pipe prevention tool on majority of its rigs including the real-time operations center (RTOC). To date, the SPI tool has recorded >90% detection rate in over 150 offshore and onshore wells since field testing began in Q4 2019. Challenges currently experienced with the tool are as follows:

- Building end-user confidence in the tool (technology adoption cycle) and training Drilling Engineers and rig site personnel to use the tool
- Well design models must be loaded into the SPI tool platform each time a model is updated. The goal is to have well design models updated automatically within the tool and in real-time
- Consistency of high-quality real-time data transmission from the rig site

## 5.2 Recommendations for Future Work

Based on the findings of this research, the following recommendations for future work are made:

1. Cuttings transport (hole cleaning) models:
    a. Annulus cuttings volumetric concentration model should be further verified using flow loop experiments and / or computational fluid dynamics (CFD) techniques to investigate the significant divergence of this research model's prediction from empirical data at rates of penetration (ROP) ≤35 ft/hr
    b. This research considered the effect of non-cohesive hindered settling in developing the improved cuttings settling velocity model. However, the drilled cuttings will experience cohesion and settle in clusters. To account for cohesion in this research, the term $\left(1 - \frac{C_c}{C_{c,max}}\right)$ was introduced. It is possible however, that this may not fully account for when the cuttings flocculate together, with a higher mass, and take up much more volume than a similar mass of non-cohesive cuttings. As the settling velocity significantly influences the critical transport flow rate required for hole cleaning, the proposed settling velocity model by this research may require additional modification. This may be further investigated using CFD or flow loop studies.
2. Real-time stuck pipe prediction concept
    a. As part of predicting the stuck pipe risk, the SPI tool should be modified to not only detect that there is a risk of a stuck pipe event unfolding,

but to additionally detect the potential stuck-pipe mechanism (i.e., mechanical, differential, or wellbore geometry), and recommend the step-by-step preventative actions to be implemented in real-time by the team to remedy the problem

b. Although primarily targeted to real-time operations, the SPI tool may be utilized by drilling teams to play back archived real-time data of historic stuck pipe events to learn from such events. Applied in this manner, the SPI tool may be considered as part of a well design / planning tool kit for defining a "design stuck pipe index, (d-SPI)". In the design phase, d-SPI will be used to develop guidance for minimum and maximum drilling parameters to avoid a stuck-pipe event based on the available offset wells data. For example

    i. Maximum allowable surface torque
    ii. Maximum allowable surface drag
    iii. Minimum required flow rate to prevent cuttings bed

c. Incorporate the use of CFD technique as part of the well design model road map to which real-time data is compared for stuck pipe prediction

## REFERENCES

ADARI, R. B. et al., 2000. Selecting Drilling Fluid Properties and Flow Rates for Effective Hole Cleaning in High Angle and Horizontal Wells. In: Proceedings of the SPE Annual Technical Conference and Exhibition, 1 – 4 October 2000. Dallas, Texas, USA: Society of Petroleum Engineers.

AGWU, O. E., AKPABIO, J. U., EKPENYONG, M. E., INYANG, U. G., ASUQUO, D. E., EYOH, I. J., and ADEOYE, O. S., 2021. A Critical Review of Drilling Mud Rheological Model. Journal of Petroleum Science and Engineering. 203 (2021) 108659. https://doi.org/10.1016/j.petrol.2021.108659

AHMED, R. M. et al., 2010. Experimental Studies on the Effect of Mechanical Cleaning Devices on Annular Cuttings Concentrations and Applications for Optimizing ERD Systems. In: Proceedings of the SPE Annual Technical Conference and Exhibition, 19 – 22 September 2010. Florence, Italy: Society of Petroleum Engineers.

AITKEN, B. and LI, J., 2013. Solids Cleanout Analysis Reduces Screen-Out risk. In: Proceedings of the SPE/ICoTA Coiled Tubing & Well Intervention Conference & Exhibition, 26 – 27 March 2013. The Woodlands, Texas, USA: Society of Petroleum Engineers.

AL SHAIKH, A. et al., 2019. Machine Learning for Detecting Stuck Pipe Incidents: Data Analytics and Model Evaluation. In: Proceedings of the International Petroleum Technology Conference, 26 – 28 March 2019. Beijing, China: Society of Petroleum Engineers.

AL AWAMI, M. et al., 2019. A Real-Time Indicator for the Evaluation of Hole Cleaning Efficiency. In: Proceedings of the SPE/IATMI Asia Pacific Oil & Gas Conference and Exhibition, 29 – 31 October 2019. Bali, Indonesia: Society of Petroleum Engineers.

BASSAL, A., 1995. The Effect of Drill Pipe Rotation on Cuttings Transport in Inclined Wellbores, M.Sc. thesis, University of Tulsa.

BECKER, T. E., 1987. Correlations for Drill Cuttings Transport in Directional Well Drilling, Ph.D. thesis, University of Tulsa.

BERDUGO ARIAS, C. A., LEON TORRADO, A. T. and LLANO CARVAJAL, J. S., 2020. Data Boosted Stuck Pipe Event Prevention: Integrating Machine Learning Models into the Mud Plan Design Workflow. In: Proceedings of the SPE Latin American and Caribbean Petroleum Engineering Conference, 27 – 31 July 2020. Bogota, Colombia: Society of Petroleum Engineers.

BIEGLER, M. W. and KUHN, G. R., 1994. Advances in Prediction of Stuck Pipe Using Multivariate Statistical Analysis. In: Proceedings of the IADC/SPE Drilling Conference, 15 – 18 February 1994. Dallas, Texas, USA: Society of Petroleum Engineers.

BIZHANI, M and KURU, E., 2017. Critical Review of Mechanistic and Empirical (Semi-Mechanistic) Models for Particle Removal From Sand bed Deposits in Horizontal Annuli With Water, *SPE Journal,* 23 (02), pp. 237–255.

BIZHANI, M. and KURU, E., 2018. Particle Removal from Sand Bed Deposits in Horizontal Annuli Using Viscoelastic Fluids, *SPE Journal,* 23 (02), pp. 256 – 273.

BOURGOYNE, A. T. et al., 1986. Applied Drilling Engineering. Richardson, TX: SPE Textbook Series

BRUCATO, A., GRISAFI, F. and MONTANTE, G., 1998. Particle Drag Coefficients in Turbulent Fluids, Chem. Eng. Sci., **53**, 3295.

BUSCH, A., WERNER, B. and JOHANSEN S. T., 2020. Cuttings Transport Modeling – Part 2: Dimensional Analysis and Scaling. Original SPE manuscript received for review 16 May 2019. Revised manuscript received for review 9 July 2019. Paper (SPE 198907) peer approved 15 July 2019: Society of Petroleum Engineers.

CHIEN, S. F., 1971. Annular Velocity for Rotary Drilling Operations, Proc., SPE Fifth Conference on Drilling and Rock Mechanics, Austin, TX, 5 – 16.

CHIN, R. and Lee, B. Y., 2008. Principles and Practice of Clinical Trial Medicine

CHO, H., SHAH, S.N. and OSISANYA, S.O., 2000. A Three-Layer Modelling for Cuttings Transport with Coiled Tubing Horizontal Drilling. In: Proceedings of the SPE Annual Technical Conference and Exhibition, 15 – 18 August 2000. Dallas, Texas, USA: Society of Petroleum Engineers.

CLARK, R. K. and BICKHAM, K. L., 1994. A Mechanistic Model for Cuttings Transport. In: Proceedings of SPE 69th Annual Technical Conference and Exhibition, 25 – 28 September 1994. New Orleans, LA, USA: Society of Petroleum Engineers.

DERJAGUIN, B., 1934. Untersuchungen ueber die Reibung und Adhaesion IV. Theorie des Anhaften kleiner Teilchen. Kolloid-Z, 69, 155 – 166.

DIPRIMA, R. C., 1960. The Stability of a Viscous Fluid Between Rotating Cylinders With an Axial Flow, J. Fluid Mech., Vol. 9 (4), 621 – 631.

DIPLAS, P., DANCEY, C. L., CELIK, A. O., 2008. The Role of Impulse on the Initiation of Particle Movement Under Turbulent Flow Conditions. Science 322 (5902): 717–720. https://doi.org/10.1126/science.1158954.

DOAN, Q. T. et al., 2003. Modelling of Transient Cuttings Transport in Underbalanced Drilling (UBD), SPE J., 8(2), 160-170.

DODGE, D. W. and METZNER, A. B., 1959. Turbulent Flow of Non-Newtonian Systems, AIChE Journal, **5**, (2), pp. 189 – 204. DOI: 10.1002/aic.690050214.

DUAN, M. et al., 2008. Transport of Small Cuttings in Extended Reach Drilling, SPE Drilling and Completion, Vol **23**, No. 3, pp. 258 – 265.

DUAN, M. et al., 2009. Critical Conditions for Effective Sand-Sized Solids Transport in Horizontal and High Angle Wells. In: Proceedings of the SPE Production and Operations Symposium, 31 March – 3 April 2007. Oklahoma City, Oklahoma, USA: Society of Petroleum Engineers.

DUAN, M. et al., 2008. Experimental Study and Modeling of Cuttings Transport using Foam with Drill Pipe Rotation. In: Proceedings of the SPE Annual Technical Conference and Exhibition, 21 – 24 September 2008. Denver, Colorado, USA: Society of Petroleum Engineers.

EGBE, P. I. and ITURRIOS, C., 2020. Mitigating Drilling Hazards in a High Differential Pressure Well Using Managed Pressure Drilling and Cementing Techniques. In: Proceedings of the International Petroleum Technology Conference, 13 – 15 January 2020. Dhahran, Saudi Arabia: Society of Petroleum Engineers.

EGBE, P. I., AL-MOUSA, F. and GADALLA, A., 2020. A Novel Application of Filter Cake Remover to Free Differential Stuck Pipe. In: Proceedings of the SPE Asia Pacific Oil & Gas Conference and Exhibition, 17 – 19 November 2020. Perth, Australia: Society of Petroleum Engineers.

ELGADDAFI, R. et al., 2021. A Mechanistic Model For Wellbore Cleanout in Horizontal and Inclined Wells. In: Proceedings of the SPE/ICoTA Well Intervention Conference and Exhibition, 22 – 25 March 2021. Virtual: Society of Petroleum Engineers.

ELMOUSALAMI, H. H. and ELASKARY, M., 2020. Drilling stuck pipe Classification and Mitigation in the Gulf of Suez Oil Fields Using Artificial Intelligent. Journal of Petroleum Exploration and Production Technology (10), 2055–2068

ERGUN, S., 1952. Chemical Engr. Prog., 48:89.

ESCUDIER, M. P., OLIVEIRA, P. J. and PINHO, F. T., 2002. Fully Developed Lamina Flow of Purely Viscous Non-Newtonian Liquids Through Annuli, Including the Effects of Eccentricity and Inner-Cylinder Rotation, International Journal of Heat and Fluid Flow, 23, 52 – 73.

ESCUDIER, M. P. et al., 2000. Effects of Inner Cylinder Rotation on Laminar Flow of A Newtonian Fluid Through an Eccentric Annulus, Int. J. Heat Fluid Flow, 21, 92 – 103.

ESCUDIER, M. P. et al., 2001. Fully Developed Lamina Flow of Purely Viscous Non-Newtonian Liquids Through Annuli: Comparison of Numerical Calculations with experiments, Experiments in Fluids, Vol. 32, 101 – 111.

FORD, J. T., OYENEYIN, M. B. and PEDEN, J. M., 1990. Comprehensive Experimental Investigation of Drilled Cuttings Transport in Inclined Wells Including the Effects of Rotation and Eccentricity. In: Proceedings of the SPE / Europec 90, 22 – 24 October 1990. The Hague, Netherlands: Society of Petroleum Engineers.

GELDART, D., 1973. Types of Gas Fluidization. Powder Technology, 7 (5) 285 - 292.

GERHART, P. M., GROSS, R. J., and HOCHSTEIN, J. I., 1992. Fundamentals of Fluid Mechanics, 2nd Edition. New York: Addison-Wesley Publishing Company.

GRIEVES, M. and VICKERS, J.: "Digital Twin: Mitigating Unpredictable, Undesirable Emergent Behavior in Complex Systems," in Kahlen, F.J., Flumerfelt, S. and Alves, A. (eds.), Transdisciplinary Perspectives on Complex Systems, Springer, 2016, pp. 85-113.

GUO, X., WANG, Z. and LONG, Z., 2010. Study on Three-Layer Unsteady State Model of Cuttings Transport for Extended Reach Wells, Journal of Petroleum Science and Engineering, Vol **73**, p171 – 180.

GUPTA, G. S., SARKAR, S., CHYCHKO, A., TENG, L. D., NZOTTA, M., and SEETHARAMAN, S., 2014. Chapter 3.1 - Process Concept for Scaling-Up and Plant Studies, Editor(s): Seshadri Seetharaman, Treatise on Process Metallurgy, Elsevier, Pages 1100-1144, ISBN 9780080969886, https://doi.org/10.1016/B978-0-08-096988-6.00040-7.

GUZMAN, J. M. et al., 2012. Stuck Pipe Prevention Solutions in Deep Gas Drilling: New Approaches. In: Proceedings of the SPE Saudi Arabia Section Technical

Symposium and Exhibition, 8 – 11 April 2012. Al-Khobar, Saudi Arabia: Society of Petroleum Engineers.

HALL, H. N., THOMPSON, H. and NUSS, F., 1950. Ability of Drilling Mud to Lift Bit Cuttings, Trans. AIME, **189**, 35 – 46.

HAMAKER, H. C., 1937. The London-Van Der Waals attraction between spherical particles”. Physica, 4, 1058 – 1072.

HEMPKINS, W. B., et al., 1987. Multivariate Statistical Analysis of Stuck Drill Pipe Situations. *SPE Drilling and Completion*, 2(03), pp. 237 - 234

HIEMENZ, P. C., 1986. Principles of Colloid and Surface Chemistry, 2nd Ed.: Marcel Dekker Inc; New York, 611 – 786.

HIRPA, M. M. and KURU, E., 2020. Hole Cleaning in Horizontal Wells Using Viscoelastic Fluids: An Experimental Study of Drilling Fluid Properties on The Bed Erosion Dynamics. In: Proceedings of the IADC/SPE International Drilling Conference and Exhibition, 3 – 5 March 2020. Galveston, Texas, USA: Society of Petroleum Engineers.

HJULSTROM, F., 1935. Studies of the Morphological Activity of Rivers as Illustrated by River Fyris, University of Uppsala Geological Institute Bulletin, **25,** pp. 221 – 557.

HOPKIN, E. A., 1967. Factors Affecting Cuttings Removal During Rotary Drilling. *Journal of Petroleum Technology*, 19(06), pp. 807 - 814

HOUSSAIS, M., ORTIZ, C. P., and DURIAN, D. J., 2015. Onset of Sediment Transport is a Continuous Transition Driven by Fluid Shear and Granular Creep. Nature Commun. 6: Article No. 6527. https://doi.org/10.1038/ncomms7527.

HOWARD, J. A. and GLOVER, S. B., 1994. Tracking Stuck Pipe Probability While Drilling. In: Proceedings of the IADC/SPE Drilling Conference, 15 – 18 February 1994. Dallas, Texas, USA: Society of Petroleum Engineers.

HUANG, Y., ZHENG, W., ZHANG, D. AND XI, Y., 2020. A Modified Herschel-Bulkley Model for Rheological Properties with Temperature Response Characteristics of Poly-Sulfonated Drilling Fluids, Energy Sources, Part A: Recovery, Utilization, and Environmental Effects, 42:12, 1464-1475, HTTPS://doi.10.1080/15567036.2019.1604861

IYOHO, A. W., 1980. Drilled Cuttings Transport by Non-Newtonian Drilling Fluids Through Inclined Eccentric Annuli, Ph.D. thesis, University of Tulsa.

JEREZ, H., DIAS, R. and TILLEY, J., 2013. Offshore West Africa Deepwater ERD: Drilling Optimization Case History. In: Proceedings of the SPE/IADC Drilling Conference and Exhibition, 5 – 7 March 2013. Amsterdam, The Netherlands: Society of Petroleum Engineers.

JOHANCSIK, C. A., FRIESEN, D. B. and DAWSON R., 1984. Torque and Drag in Directional Wells: Prediction and Measurement. *Journal of Petroleum Technology*, 36 (06), 987–992

KAMP, A. M. and RIVERO, M., 1999. Layer Modeling for Cuttings Transport in Highly Inclined Wellbores. In: Proceedings of the SPE Latin American and Caribbean

Petroleum Engineering Conference, 21 – 23 April 19999. Caracas, Venezuela: Society of Petroleum Engineers.

KELIN, W. et al., 2013. Review and Analysis of Cuttings Transport in Complex Structural Wells, The Open Fuels & Energy Science Journal, **6**, pp. 9-17.

KHAN, A. R. and RICHARDSON, J. F., 1989. Fluid-particle Interactions and Flow Characteristics of Fluidized Beds and Settling Suspensions of Spherical Particles. Chem. Eng. Comm. 78, pp. 111

KHAN, M. U., 2008. Transient Cuttings Transport Focused on Bed Erosion for Horizontal Wells, M.Sc. thesis, University of Tulsa.

KHOPKAR, A. R. et al., 2006. Computational Fluid Dynamics Simulation of the Solid Suspension in Stirred Slurry Reactor, Ind. Chem. Res. Des., **45**, 4416.

KIM, Y., HWANG, Y. and WOO, N., 2005. Experimental Study on the Helical Flow in a Concentric Annulus With Rotating Inner Cylinder, J. Fluids Eng, 128 (1), 113 – 117.

KIM, Y. et al., 2006. Vortex Flow Study on Non-Newtonian Fluids in Concentric Annulus With Inner Cylinder Rotation, Proceedings of the 16th International Offshore and Polar Engineering Conference, 835 – 839.

KUROSE, R. and KOMORI, S., 1999. Drag and Lift Forces on a Rotating Sphere in a Linear Shear Flow, J. of Fluid Mechanics, **384**, 183 – 206. DOI: 10.1017/S0022112099004164.

LARSEN, T. I., PILEHVARI, A. A. and AZAR, J. J., 1997. Development of a New Cuttings-Transport Model for High-Angle Wellbores Including Horizontal Wells, *SPE Drill & Completion,* 12 (02), pp. 129–135

LARSEN, T., 1990. A Study of the Critical Fluid Velocity in Cuttings Transport for Inclined Wellbores, M.Sc. thesis, University of Tulsa.

LEE, J., 2020. International Encyclopedia of Human Geography, 2$^{nd}$ ed.

LEPENIOTI, K., BOUSDEKIS, A., APOSTOLOU, D. and MENTZAS, G., 2020. Prescriptive Analytics: Literature Review and Research Challenges, International Journal of Information Management, **50**, 2020, 57 – 70.

LI, J., WILDE, G. and CRABTREE, A., 2005. Do Complex Super Gel Liquids Perform Better Than Simpler Linear Liquids in Hole Cleaning with Coiled Tubing? In: Proceedings of the SPE/ICoTA Coiled Tubing Conference and Exhibition, 12 – 13 April 2005. The Woodlands, Texas, USA: Society of Petroleum Engineers

LI, J. and LUFT, B., 2014. Overview of Solids Transport Study and Application in Oil and Gas Industry. In: Proceedings of the International Petroleum Technology Conference, 10 – 12 December 2014. Kuala Lumpur, Malaysia Society of Petroleum Engineers.

LI, J. and WALKER, S., 1999. Sensitivity Analysis of Hole Cleaning Parameters in Directional Wells. In: Proceedings of the SPE/ICoTA Coiled Tubing Roundtable, 25 – 26 May 1999. Houston, Texas, USA: Society of Petroleum Engineers.

LI, J., WALKER, S. and AITKEN, B., 2002. How to Efficiently Remove Sand from Deviated Wellbores with a Solids Transport Simulator and a Coiled Tubing Cleanout

Tool. In: Proceedings of the SPE Annual Technical Conference and Exhibition, 29 September–2 October 2002. San Antonio, Texas, USA: Society of Petroleum Engineers.

LI, M. et al., 2010. Simulation on the Effect of Drill String Rotation on Hole Cleaning for Extended Reach Well, West-China Exploration. Eng., 5, 51-54.

LI, Y., BJORNDALEN, N. and KURU, E., 2007. Numerical Modelling of Cuttings Transport in Horizontal Wells Using Conventional Drilling Fluids. J. Can. Petrol. Tech., 46(7), 9-14.

LIANG, S.C., HONG, T. and FAN, L.S., 1996. Effect of Particle Arrangement on the Drag Force of a Particle, Intl. J. of Multiphase Flow, **22**, No. 2, 285-306.

LOCKETT, T. J., RICHARDSON, S. M. and WORRAKER, W. J., 1993. The Importance of Rotation Effects For Efficient Cuttings Removal During Drilling. In: Proceedings of the SPE/IADC Drilling Conference, 23 - 25 February 1993. Amsterdam, The Netherlands: Society of Petroleum Engineers.

LU, C.S., 2008. Thesis, China University of Petroleum (East China).

LUO, Y. J., BERN, P. A. and CHAMBERS, B. D., 1992. Flow Rate Predictions for Cleaning Deviated Wells. In: Proceedings of the IADC/SPE Drilling Conference, 18 – 21 February 1992. New Orleans, Louisiana, USA: Society of Petroleum Engineers.

MAGELLI, F. et al., 1990. Solids Distribution in Reactors Stirred with Multiple Impellers, Chem. Eng. Sci., **45**, 615.

MALEKZADEH, N. and MOHAMMADSALEHI, M., 2011. Hole Cleaning Optimization in Horizontal Wells: A New Method to Compensate Negative Hole Inclination Effects.

In: Proceedings of the Offshore Conference and Exhibition, 14 – 17 June 2011. Macaé, Brazil: Society of Petroleum Engineers.

MARTINS, A.L., SANTANA, M.L. and GASPARI, E.F., 1999. Evaluating the Transport of Solids Generated by Shale Instabilities in ERW drilling, SPE Drilling & Completion, 14(4), 254-259.

MAUDE, A. D., and WHITMORE, R. L., 1958. A Generalized Theory of Sedimentation, Journal of Applied Physics, 9:477.

MCCABE, W. L., SMITH, J. C. and HARRIOTT, P., 1993. Unit Operations of Chemical Engineering, 5th ed., McGraw-Hill, New York, 154 – 167.

MEOR HASHIM, M. M. H. et al., 2021. Case Studies for The Successful Deployment of Wells Augmented Stuck Pipe Indicator in Wells Real Time Center. In: Proceedings of the International Petroleum Technology Conference, 23 March - 1 April 2021. Virtual: Society of Petroleum Engineers.

MEOR HASHIM, M. M. H., et al., 2021. Utilizing Artificial Neural Networks for Real-Time Prediction of Differential Sticking Symptoms. In: Proceedings of the International Petroleum Technology Conference, 23 March - 1 April 2021. Virtual: Society of Petroleum Engineers.

METIN, C. O., 2012. Characterization of nanoparticle transport in flow through permeable media, Ph.D. thesis, The University of Texas at Austin.

NISBET, R., MINER, G. and YALE, K., 2018. Handbook of Statistical Analysis and Data Mining Applications, 2nd ed., Elsevier, 783 – 792.

MIRHAJ, S. A., SHADIZADEN, S. R. and FAZAELIZADEH, M., 2007. Cuttings Removal Simulation for Deviated and Horizontal Wellbores. In: Proceedings of the SPE Middle East Oil & Gas Show and Conference, 11 – 14 March 2007. Bahrain: Society of Petroleum Engineers.

MIRHAJ, S. A., KAARSTAD, E. and AADNOY, B. S., 2016. Torque and Drag Modelling: Soft String vs Stiff String Models. In: Proceedings of the SPE/IADC Middle East Drilling Technology Conference and Exhibition, 26 –28 January 2016. Abu Dhabi, UAE: Society of Petroleum Engineers.

MOHAMMADSALEHI, M. and MALEKZADEH, N., 2011. Application of New Hole Cleaning Optimization Method Within All ranges of Hole Inclinations. In: Proceedings of the International Petroleum Technology Conference, 7–9 February 2012. Bangkok, Thailand: Society of Petroleum Engineers.

MOHAMMADSALEHI, M. and MALEKZADEH, N., 2011. Optimization of Hole Cleaning and Cuttings Removal in Vertical, Deviated and Horizontal Wells. In: Proceedings of the SPE Asia Pacific Oil and Gas Conference and Exhibition, 20–22 September 2011. Jakarta, Indonesia: Society of Petroleum Engineers.

MOORE, P. L., 1974. Drilling Practices Manual, Petroleum Publishing Co., Tulsa.

MURILLO, A., NEUMAN, J. and SAMUEL, R., 2009. Pipe Sticking Prediction and Avoidance Using Adaptive Fuzzy Logic Modelling. In: Proceedings of the SPE Production and Operations Symposium, 4–8 April 2009. Oklahoma City, Oklahoma, USA: Society of Petroleum Engineers.

NAGANAWA, S. and NOMURA, T., 2006. Simulating Transient Behavior of Cuttings Transport Over Whole Trajectory of Extended Reach Well. In: Proceedings of the IADC/SPE Asia Pacific Drilling Technology Conference and Exhibition, 13–15 November 2006. Bangkok, Thailand: Society of Petroleum Engineers.

NGUYEN, A. V., TRAN, L. T. T. and MILLER, J. D., 2012. Particle-Particle Interaction, Particle Technology and Applications. Sunggyu Lee and Kimberly H. Henthorn. CRC Press, 4, 31 – 50.

NGUYEN, A. V., 2000. Improved Approximation of Water Dielectric Permittivity For Calculation of Hamaker Constants, J. Colloid Interface Sci., 229 (2), 648 – 651.

NGUYEN, D., and RAHMAN, S.S., 1996. A Three-Layer Hydraulic Program for Effective Cuttings Transport and Hole Cleaning in Highly Deviated and Horizontal Wells, *SPE Drill & Completion,* 13 (03), pp. 182–189.

NGUYEN, T. N., 2007. Study on Effective Hole Cleaning Using Conventional and Enhanced Sweeps in Horizontal Wellbores, M.Sc. thesis, University of Tulsa.

OHIA, N. P., EKWUEME, S. T., ACHUMBA, G. I., OKEREKE, N. O., NWANKWO, I. V. and NNWANWE, O. I., 2021. A Comparative Study of Soft String vs. Stiff String Models Application in Torque and Drag Analysis. In: Proceedings of the Annual International Conference and Exhibition, 2 - 4 August 2021. Lagos, Nigeria: Society of Petroleum Engineers.

OZBAYOGLU, E. M. and SORGUN, M., 2010. Frictional Pressure Loss Estimation of water Based Drilling Fluids at Horizontal and Inclined Drilling With Pipe Rotation and

Presence of Cuttings. In: Proceedings of the SPE Oil and Gas India Conference and Exhibition, 20–22 January 2010. Mumbai, India: Society of Petroleum Engineers.

OZBAYOGLU, E.M. et al. 2009. Sensitivity Analysis of Major Drilling Parameters on Cuttings Transport During Drilling Highly Inclined Wells, Petrol. Sci. Technol., 27, 122–133.

OZBAYOGLU, M. E., MISKA, S. Z. and REED, T., 2002. Analysis of Bed Height in Horizontal and Highly Inclined Wellbores by Using Artificial Neural Networks. In: Proceedings of the SPE International Thermal Operations and Heavy Oil Symposium and International Horizontal Well Technology Conference, 4–7 November 2002. Alberta, Canada: Society of Petroleum Engineers.

OZBAYOGLU, M. E., SAASEN, A. and SORGUN, M., 2008. Effect of Pipe Rotation on Hole Cleaning for Water-Based Drilling Fluids in Horizontal and Deviated Wells. In: Proceedings of the IADC/SPE Asia Pacific Drilling Technology Conference and Exhibition, 25–27 August 2008. Jakarta, Indonesia: Society of Petroleum Engineers.

OZBAYOGLU, M. E., SAASEN, A. and Sorgun, M., 2007. Estimating Critical Velocity to Prevent Bed Development for Horizontal Inclined Wellbores. In: Proceedings of the SPE/IADC Middle East Drilling Technology Conference & Exhibition, 22–24 October 2007. Cairo, Egypt: Society of Petroleum Engineers.

OZBAYOGLU, M. E. et al., 2010. Hole Cleaning Performance of Light-Weight Drilling Fluids During Horizontal Underbalanced Drilling, *Journal of Canadian Petroleum Technology,* 49 (04), pp. 21–26.

OZBAYOGLU, M. E., 2002. Cuttings Transport With Foam in Horizontal and Highly Inclined Wellbores, Ph.D. thesis, University of Tulsa.

OZBAYOGLU, M.E. et al., 2008. Effect of Pipe Rotation on Hole Cleaning for Water-Based Drilling Fluids in Horizontal and Deviated Wells. In: Proceedings of the IADC/SPE Asia Pacific Drilling Technology Conference and Exhibition, 25 – 27 August 2008. Jakarta, Indonesia: Society of Petroleum Engineers.

PANDYA, S., AHMED, R., and SHAH, S., 2020. Wellbore Cleanout in Inclined and Horizontal Wellbores: The effect of Flow Rate, Fluid Rheology, and Solids Density, *SPE Drilling & Completions,* 35 (01), pp. 048–068.

PEYSSON, Y., OURIEMI, M., MEDALE, M., 2009. Threshold for Sediment Erosion in Pipe Flow. Int. J. Multiphas. Flow 35 (6): 597–600. https://doi.org/10.1016/j.ijmultiphaseflow.2009.02.007

PHILIP, Z., SHARMA, M. M., and CHENEVERT, M. E., 1998. The Role of Taylor Vortices in the Transport of Drill Cuttings. In: Proceedings of the SPE India Oil and Gas Conference and Exhibition, 7-9 April 1998. New Delhi, India: Society of Petroleum Engineers.

PIGOTT, R., 1941. Mud Flow in Drilling, Drilling and Production Practice.

PINELLI, D., NOCENTINI, M. and MAGELLI, F., 2001. Solids Distribution in Stirred Slurry Reactors: Influence of Some Mixer Configurations and Limits to The Applicability of a Simple Model for predictions, Chem. Eng. Commun., **188**, 91 – 107.

POTTER, C. M. et al., 2002. Internal Flows, Mechanics of Fluids, **7**, 288 – 292.

Qi, F. and Tanner, R. I., 2012. Random close packing and relative viscosity of multimodal suspensions, Rheol. Acta 51, 289. https://doi.org/10.1007/s00397-011-0597-3

QUEMADA, D., 1977. Rheology of Concentrated Disperse Systems and Minimum Energy Dissipation Principle. Rheol Acta 16, 82-94.

RABINOVICH, E. and KALMAN, H., 2007. Pickup, Critical, and Wind Threshold Velocities of Particles. Powder Technology, **176**, pp. 9 – 17

RAMADAN, A., 2001. Mathematical Modelling and Experimental Investigation on Solids and Cuttings Transport, Ph.D. thesis, Norwegian University of Science and Technology.

RANADE, V. V. and SARDESHPANDE, M. V., 2012. Computational Fluid Dynamics Modeling of Solid Suspension in Stirred Tanks, Current Science, Vol 102, No. 11.

RAO, R. et al., 2002. A Numerical and Experimental Study of Batch Sedimentation and Viscous Resuspension. International Journal for Numerical Methods in Fluids **39**, 465-483.

RAO, R. et al., 2007. Instabilities During Batch Sedimentation in geometrics Containing Obstacles: A Numerical and Experimental Study. International Journal for Numerical Methods in Fluids, **55**, 723-735.

RHODES, M., 2008. Introduction to Particle Technology. 2$^{nd}$ Ed. Chichester, UK: John Wiley & Sons.

ROWE, P. N., 1987. A Convenient Empirical Equation for Estimation of the Richardson-Zaki Exponent. Chem. Eng. Sci. 43, pp. 2795ff.

RUBENSTEIN, D. A., YIN, W., and FRAME, M. D., 2021. An Introduction to Fluid Mechanics, Macro circulation, and Microcirculation. 3rd Ed. Elsevier Inc. ISBN 978-0-12-818034-1. https://doi.org/10.1016/C2018-0-02144-1

SAASEN, A. and LøKLINGHOLM, G., 2002. The Effect of Drilling Fluid Rheological Properties on Hole Cleaning. In: Proceedings of the IADC/SPE Drilling Conference, 26–28 February 2002. Dallas, Texas, USA: Society of Petroleum Engineers.

SAINI, G. S., ASHOK, P., and VAN OORT, E., 2020. Predictive Action Planning for Hole Cleaning Optimization and Stuck Pipe Prevention Using Digital Twinning and Reinforcement Learning. In: Proceedings of the IADC/SPE International Drilling Conference and Exhibition, 3–5 March 2020. Galveston, Texas, USA: Society of Petroleum Engineers.

SALMINEN, K. et al., 2017. Stuck-Pipe Prediction by Use of Automated Real-Time Modeling and Data Analysis, *SPE Drilling & Completions,* 32 (03), pp. 184–193

SAMPLE, K. J. and BOURGOYNE, T., 1977. An Experimental Evaluation of Correlations Used For Predicting Cutting Slip Velocity. In: Proceedings of the 52nd Annual Fall Technical Conference and Exhibition, 9 – 12 October 1977. Denver, Colorado, USA: Society of Petroleum Engineers.

SAMPLE, K. J. and BOURGOYNE, T., 1978. Development of An Improved Laboratory and Field Procedures For Determining the Carrying Capacity of Drilling Fluids. In: Proceedings of the 53rd Annual Fall Technical Conference and Exhibition, 1 – 3 October 1978. Houston, Texas, USA: Society of Petroleum Engineers.

SANTANA, M., MARTINS, A.L., and JR, A.S., 1998. Advances in the Modelling of the Stratified Flow of Drilled Cuttings in High Angle and Horizontal Wells. In: Proceedings of the International Petroleum Conference and Exhibition of Mexico, 3 – 5 March 1998. Villahermosa, Mexico: Society of Petroleum Engineers.

SAPRU, A., 2001. Study of Effect of Drill Pipe Rotation on Cuttings Bed Erosion in Horizontal Wells, M.Sc. thesis, University of Tulsa.

SAYINDLA, S. et al., 2017. Hole-Cleaning Performance Comparison of Oil-Based and Water-Based Drilling Fluids. J Pet Sci Eng, 159, pp. 49–57. https://doi.org/10.1016/j.petrol.2017.08.069.

SCHILLER, L. and NEUMANN, A., 1933. Uber die grundlegenden berechungen bei der schwer kraftaufbereitung", Verein Deutscher Ingenieure, **77**, pp. 318.

SCHLICHTING, H., 1955. Boundary Layer Theory. Trans. J. Kestin. New York: McGraw-Hill.

SHAKERS, S., 2005. Drilling Fluids Processing Handbook. Oxford, UK: Gulf Professional Publishing. ISBN: 978-0-7506-7775-2. 34.

SHEPPARD, M. C., WICK, C., and BURGESS, T., 1987. Designing Well Paths to Reduce Drag and Torque, *SPE Drilling & Completions* 2 (04), pp. 344–350.

SMITH, S. J. and FRIEDRICHS, C. T., 2011. Size and Settling Velocities of Cohesive Flocs and Suspended Sediments Aggregates in a Trailing Suction Hopper Dredge Plume. Cont. Shelf Res 31:S50-S63

SONG, X., XU, Z., WAND, M., LI, G., SHAH, S. N. and PANG, Z., 2017. Experimental Study on The Wellbore-Cleaning Efficiency of Micro-hole Horizontal Well Drilling, *Society of Petroleum Engineers Journal*, 22 (04), pp. 1189–1200

SUZANA, S.C., SIDNEY, S., and SERGION, A.B., 2008. Simulation of Transient Cuttings Transportation and ECD in Wellbore Drilling, Europec / EAGE Conference and Exhibition, Rome, Italy.

TAO, F., SUI, F., LIU, A., QI, Q., et al.: "Digital Twin-Driven Product Design Framework," International Journal of Production Research, Vol. 57, Issue 12, 2019, pp. 3935-3953.

TAYLOR, G. I., 1923. Stability of a Viscous Liquid Contained Between Two Rotating Cylinders, Phil. Trans. Royal Society, Series A, Vol. 223, pp. 289 – 343.

TELEVANTOS, Y. et al., 1979. Flow of Slurries of Coarse Particles at High Solids Concentrations, Canadian Journal of Chemical Engineering, **57**(4), pp. 255.

TOMREN, P. H., 1979. The Transport of Drilled Cuttings in an Inclined Eccentric Annulus, M.Sc. thesis, University of Tulsa.

VAN DE VEN, T. G. M., 1989. Colloidal Hydrodynamics. London: Academic Press.

WALKER, R. E. and MAYES, T. M., 1975. Design Muds for Carrying Capacity, J. Pet. Tech., pp. 893 – 900; Trans., **AIME, 259**

WANG, H.G. et al., 1995. An Experimental Study of Transport of Drilling Cuttings in a Horizontal Well. Acta Petrolei Sin., 16(4), pp. 125-132.

WANG, Z. et al., 2010. Numerical Simulation on Three-Layer Dynamic Cutting Transport model and its Application on Extended Well Drilling. In: Proceedings of the IADC/SPE Asia Pacific Drilling Technology Conference and Exhibition, 1–3 November 2010. Ho Chi Minh City, Vietnam: Society of Petroleum Engineers.

WERELEY, S. T. and LUEPTOW, R. M., 1998. Spatio-temporal Character of Non-wavy and Wavy Taylor-Couette Flow, J. Fluid Mech., vol. **364**, pp. 59-80.

WERNER, B., MYRSETH, V. and SAASEN, A. 2017. Viscoelastic Properties of Drilling Fluids and Their Influence on Cuttings Transport, J Pet Sci Eng, 156, pp. 845–851. https://doi.org/10.1016/j.petrol.2017.06.063.

WINTERWERP, J. C., 1998. A Simple Model for Turbulence Induced Flocculation of Cohesive Sediment. IAHR J. Hydraul. Res. 36 (3), 309 – 326

WINTERWERP, J. C., 2002. On the Flocculation and Settling Velocity of Estuarine Mud. Cont. Shelf Res. 22, 1339 - 1360

YADAV, A., AL-TAJAR, T. and ALI, A., 2014. Drilling Technology Taking Drilling Operations to New Frontiers. In: Proceedings of the SPE Bergen One Day Seminar, 2 April 2014. Bergen, Norway: Society of Petroleum Engineers.

YU, H., HANSSON, T. and VAN GUNSTEN, W. F., 2003. Development of a Simple, Self-Consistent Polarizable Model For Liquid Water, J. Chem. Phys., 118, pp. 221 – 234.

YU, M. et al., 2007. An Experimental Study of Hole Cleaning Under Simulated Downhole Conditions. In: Proceedings of the SPE Annual Technical Conference and Exhibition, 11–14 November 2007. Anaheim, California, USA: Society of Petroleum Engineers.

ZARROUGH, R., 1991. Drilled Cuttings Transport in Deviated Wells, M.Sc. thesis, Heriot-Watt University.

ZHANG, A., 2019. Anomaly Detection with Z-Score – Pick the Low Hanging Fruits, Unsupervised Learning in Anomaly Detection Using Python. Anomaly Detection with Z-Score: Pick The Low Hanging Fruits | by Alina Zhang | The Startup | Medium

ZHANG, F. et al., 2019. Real Time Stuck Pipe Prediction by Using a Combination of Physics-Based Model and Data Analytics Approach. In: Proceedings of the International Petroleum Exhibition & Conference, 11 – 14 November 2019. Abu Dhabi, UAE: Society of Petroleum Engineers.

ZHANG, B. et al., 2017. Evaluate Sensitivity and Feasibility of Influencing Factors to Increase the Extreme Hydraulic Extension Length of Horizontal Well. In: Proceedings of the SPE Eastern Regional Meeting, 4-6 October 2017. Lexington, Kentucky, USA: Society of Petroleum Engineers.

ZHANG, H. et al., 2013. Mathematical Modeling of Critical Velocity for Cuttings Transport in Micro-hole Drilling. Proceedings, 4, pp. 39 – 46.

ZHOU, L., 2004. Cuttings Transport With Aerated Mud in Horizontal Annulus Under Elevated Pressure and Temperature Conditions, Ph.D. thesis, University of Tulsa.

**BIBLIOGRAPHY**

AHMED, R., 2001. Mathematical Modeling and Experimental Investigation on Solids and Cuttings Transport, PhD Dissertation, Norwegian U. of Science and Technology, Trondheim, Norway.

ANIFOWOSHE, O. and OSISANYA, S., 2012. The Effect of Equivalent Diameter Definitions on Frictional Pressure Loss Estimation in an Annulus with Pipe Rotation. In: Proceedings of the SPE Deepwater and Completions Conference and Exhibition, 20 - 21 June 2012. Galveston, Texas, USA: Society of Petroleum Engineers.

AVILA, R. J. et al., 2008. Correlations and Analysis of Cuttings Transport With Aerated Fluids in Deviated Wells, *SPE Drilling and Completion*, 23 (02), pp. 132 – 141.

BECKER, T. E., 1982. The Effects of Mud Weight and Hole Geometry Variations on Cuttings Transport in Directional Drilling, M.Sc. thesis, University of Tulsa.

BELASKIE, J. P., MCCANN, D. P. and LESHIKAR, J. F., 1994. A Practical Method to Minimize Stuck Pipe Integrating Surface and MWD Measurements. In: Proceedings of the IADC/SPE Drilling Conference, 15-18 February 1994. Dallas. Texas, USA: Society of Petroleum Engineers.

BIZHANI, M., 2013. Solids Transport With Turbulent Flow of Non-Newtonian Fluid in the Horizontal Annuli, M.Sc. thesis, University of Alberta.

BIZHANI, M., RODRIGUEZ-CORREDOR, F. E. and KURU, E., 2015. Hole Cleaning Performance of Water vs. Polymer-Based Fluids Under Turbulent Flow Conditions.

In: Proceedings of the SPE Canada Heavy Oil Technical Conference, 9 –11 June 2015. Calgary, Alberta, Canada: Society of Petroleum Engineers.

BOURE, J. A. and MATUSZKIEWICZ, A., 1984. Modelisation des Ecoulements Diphasiques. Sur l’Influence des Termes d’Origine Mechanique pour le Calcule du Taux de Vide et des Vitesses en Regime Etablie. Rapport du Commissariat a l’Energie Atomique, CEA-R-5244, Saclay.

CAPO, J. et al., 2006. Cuttings Transport With Aqueous Foam at Intermediate Inclined Wells, *SPE Drilling and Completion*, 21 (02), pp. 99 – 107.

CARTENS, M. R., 1969. Proc. American Society of Chemical Engineers, Hydraulics Division (HY1), 95, pp. 275.

CHAMKALANI, A., SHAHRI, M. P. and POORDAD, S., 2013. Support Vector Machine Model: A New Methodology for Stuck Pipe Prediction. In: Proceedings of the SPE Middle East Unconventional Gas Conference and Exhibition, 28–30 January 2013. Muscat, Oman: Society of Petroleum Engineers.

CHEN, Z. et al., 2007. Experimental Study on Cuttings Transport With foam Under Simulated Horizontal Downhole Conditions, *SPE Drilling and Completion*, 22 (04), pp. 304 – 312.

CORREDOR, F., 2013. Solids Transport with Turbulent Flow of a Drag Reducing Fluid in the Horizontal Annuli, M.Sc. thesis, University of Alberta.

COSTA, S. S. et al., 2008. Simulation of Transient Cuttings Transport and ECD in Wellbore Drilling. In: Proceedings of the SPE Europec/EAGE Annual Conference and Exhibition, 9–12 June 2008. Rome, Italy: Society of Petroleum Engineers.

EDDY, K., 1996. An Experimental Study of the Effect of Mud Weight and Drill Pipe Rotation on Cuttings Transport in Horizontal and Inclined Wells, M.Sc. thesis, University of Tulsa.

EFFIONG, F., 2013. Experimental Cuttings Transport in Horizontal Wellbores – The Determination of Cuttings Bed Height, M.Sc. thesis, Norwegian University of Science and Technology.

FERREIRA, A. P. L. A. et al., 2015. Automated Decision Support and Expert Collaboration Avoid Stuck Pipe and Improve Drilling Operations in Offshore Brazil Subsalt Well. In: Proceedings of the Offshore Technology Conference, 4 –7 May 2015. Houston, Texas, USA: Society of Petroleum Engineers.

GOVIER, G. W. and AZIZ, K., 1972. The Flow of Complex Mixtures in Pipes. Van Nostrand Reinhold. New York.

HARELAND, G., AZAR, J. J. and RAMPERSAD, P. R., 1993. Comparison of Cuttings Transport in Directional Drilling Using Low Toxicity Invert Emulsion Mineral Oil Based and Water Based Muds. In: Proceedings of the SPE Rocky Mountain Regional/Low Permeability Reservoirs Symposium, 12 - 14 April 1993. Denver, Colorado, USA: Society of Petroleum Engineers.

JACOB, A. E., 2013. Investigation of Stationary Cuttings Bed Height in Washout, M.Sc. thesis, Norwegian University of Science and Technology.

JAHANBAKHSHI, R. and KESHAVARZI, R., 2012. Intelligent Prediction of Wellbore Stability in Oil and Gas Wells: An Artificial Neural Network Approach, 46th U.S. Rock Mechanics / Geomechanics Symposium, Chicago, Illinois

JALUKAR, L. S., 1993. A Study of Hole Size effect on Critical and Sub-critical Drilling Fluid Velocities in Cuttings Transport for Inclined Wellbores, M.Sc. thesis, University of Tulsa.

Lourenco, A. et al., 2006. Investigating Solids Carrying Capacity For an Optimized Hydraulics Program in Aerated Polymer Based Drilling Fluid. In: Proceedings of the IADC/SPE Drilling Conference, 21–23 February 2006. Miami, Florida, USA: Society of Petroleum Engineers.

MARTINS, A. L. and LOURENCO, A., 2001. Foam Property Requirements for Proper Hole Cleaning While Drilling Horizontal Wells in Underbalanced Conditions, *SPE Drilling and Completion*, 16 (04), pp. 195 – 200.

MARTINS, A. L. et al., 2002. Evaluation of Solids Carrying Capacity in Aerated Fluid Drilling: Real Scale Tests and Modelling. In: Proceedings of the IADC/SPE Drilling Conference, 26–28 February 2002. Dallas, Texas, USA: Society of Petroleum Engineers.

MARTINS, A. L. et al., 1996. Experimental Determination of Interfacial Friction Factor in Horizontal Drilling With a Bed of Cuttings. In: Proceedings of the 4th Latin American / Caribbean Petroleum Engineering Conference, 23 – 26 April 1996. Port of Spain, Trinidad and Tobago: Society of Petroleum Engineers.

MENDEZ, J., 2002. An Experimental Study of Cuttings Transport in Horizontal Wells with Aerated Fluids and Drill pipe Rotation, M.Sc. thesis, University of Tulsa.

MIRI, R., SAMPAIO, J. H. B. and AFSHAR, M., 2007. Development of Artificial Neural Networks to Predict Differential Pipe Sticking in Iranian Offshore Oil Fields. In:

Proceedings of the International Oil Conference and Exhibition in Mexico, 27–30 June 2007. Veracruz, Mexico: Society of Petroleum Engineers.

NAGANAWA, S. et al., 2002. Cuttings Transport in Directional and Horizontal Wells While Aerated Mud Drilling. In: Proceedings of the IADC/SPE Asia Pacific Drilling Technology, 9–11 September 2002. Jakarta, Indonesia: Society of Petroleum Engineers.

NAJMI, K. et al., 2014. Experimental Study of Low Concentration Sand Transport in Low Liquid Loading Air and Water Flow in Horizontal pipes. In: Proceedings of the 9th North American Conference on Multiphase Technology, 11 – 13 June 2014. Banff, Canada: Society of Petroleum Engineers.

NAKABAYASHI, K., YAMADA, Y., and SEO, K., 1974. Rotational and Axial Flow Through the Gap Between Eccentric Cylinders of Which The Outer One Rotates, Bull. JSME, Vol. 17, No. 114, pp. 1564 – 1571.

NARAGHI, M. E., EZZATYAR, P. and JAMSHIDI, S., 2013. Prediction of Drill Pipe Sticking by Active Learning Method (ALM), Journal of Petroleum and Gas Engineering, 4 (07), pp. 173 – 183. EBB3D3041956 (copyright).

NOURI, J. M. and WHITELAW, J. H., 1994. Flow of Newtonian and Non-Newtonian Fluids in a Concentric Annulus With Rotation of the Inner Cylinder, J. Fluid Eng., 116, pp. 821 – 827.

NOURI, J. M., UMUR, H. and WHITELAW, J. H., 1993. Flow of Newtonian and Non-Newtonian Fluids in Concentric and Eccentric Annuli", J. Fluid Mech., 253, pp. 617 – 641.

OKPOBIRI, G. A., 1982. Experimental Determination of Solids Friction Factors and Minimum Volumetric Requirements in Foam and Mist Drilling and Well Clean-out Operations, Ph.D. thesis, University of Tulsa.

OSGOUEL, R., 2010. Determination of Cuttings Transport properties of Gasified Drilling Fluids", Ph.D. thesis, Middle East Technical University.

OYENEYIN, M. B., BELLO, K. O., and OLUYEMI, G. F., 2011. Minimum Transport Velocity Models for Suspended Particles in Multiphase Flow Revisited. In: Proceedings of the SPE Annual Technical Conference and Exhibition, 30 October–2 November 2011. Denver, Colorado, USA: Society of Petroleum Engineers.

OZBAYOGLU, M. E. et al., 2010. Critical Fluid Velocities for Removing Cuttings Bed Inside Horizontal and Deviated Wells, Petroleum Science and Technology, 28, pp. 594 – 602.

PARKER, D. J., 1987. An Experimental Study on the Effects of Hole Washout and Cutting Size on Annular Hole Cleaning in Highly Deviated Wells, M.Sc. thesis, University of Tulsa.

PEREIRA, E. J., 2003. Experimental Study of Hole Cleaning With an Aerated Fluid at Intermediate Hole Angles, M.Sc. thesis, University of Tulsa.

PERRY, J. H., 1973. Chemical Engineers' Handbook, 5th ed., New York: McGraw-Hill. pp. 3 – 247.

RAMADAN, A., SKALLE, P. and JOHANSEN, S. T., 2003. A Mechanistic Model to Determine the Critical Flow Velocity required to Initiate the Movement of Spherical

Bed Particles in Inclined Channels, Chemical Engineering Science, 58, pp. 2153 – 2163.

SADLIER, A., SAYS, I. and HANSON, R., 2013. Automated Decision Support to Enhance While-Drilling Decision Making. In: Proceedings of the SPE/IADC Drilling Conference and Exhibition, 5–7 March 2013. Amsterdam, The Netherlands: Society of Petroleum Engineers.

SAFFMAN, P.G., 1965. The Lift on Small Sphere in a Slow Shear Flow, J. of Fluid Mechanics, 22, pp. 385-400.

SANCHEZ, R. A. et al., 1997. The Effect of Drill Pipe Rotation on Hole Cleaning During Directional Well Drilling. In: Proceedings of the SPE/IADC Drilling Conference, 4 – 6 March 1997. Amsterdam, The Netherlands: Society of Petroleum Engineers.

SARDESHPANDE, M. V. and RANADE, V. V., 2012. Computational Fluid Dynamics Modelling of Solid Suspension in Stirred tanks, Current Science, Vol 102, No. 11.

SHAH, S. N. and LORD, D. L., 2004. Critical Velocity Correlations for Slurry Transport with Non-Newtonian Fluids, AIChE J. 37 (6), pp. 863 – 870.

SHORAKA, S. A. R., SHADIZADEH, S. R. and SHAHRI, M. P., 2011. Prediction of Stuck Pipe in Iranian South Oil Fields Using Multivariate Statistical Analysis. In: Proceedings of the Annual International Conference and Exhibition, 30 July - 3 August 2011. Abuja, Nigeria: Society of Petroleum Engineers.

SIFFERMAN, T. R. and BECKER, T. E., 1992. Hole Cleaning in Full Scale Inclined Wellbores, *SPE Drilling Engineering*, 7 (02), pp. 115 – 120.

SIFFERMAN, T. R. et al., 1974. Drill Cutting Transport in Full Scale Vertical Annuli, *Journal of Petroleum Technology*, 26 (11), pp. 1295 -1302.

SILVA, M. G. P. and MARTINS, A. L., 1987. Turbulent Flow of Drilling Fluids, Second Latin American Conference of Hydrocarbons – CONEXPO / ARPEL, Rio de Janeiro.

SIRUVURI, C., NAGARANKANTI, S. and SAMUEL, R., 2006. Stuck Pipe Prediction and Avoidance: A Convolutional Neural Network Approach. In: Proceedings of the IADC/SPE Drilling Conference, 21–23 February 2006. Miami, Florida, USA: Society of Petroleum Engineers.

SOEPYAN, F. B. et al., 2014. Confidence in Critical Velocity Predictions for Solids Transport. In: Proceedings of the Annual Technical Conference and Exhibition, 27–29 October 2014. Amsterdam, The Netherlands: Society of Petroleum Engineers.

STUART, J. T., 1958. Non-Linear Mechanics of Hydrodynamic Stability, Journal of Fluid Mechanics, 4(1), pp. 1 – 21.

TOMREN, P. H., IYOHO, A. W. and AZAR, J. J., 1986. Experimental Study of Cuttings Transport in Directional Wells, *SPE Drilling & Completions,* 1 (01), pp. 43–56

VALLURI, S. G. et al., 2006. Experimental Study of Effective Hole Cleaning using Sweeps in Horizontal Wellbores. In: Proceedings of the SPE Annual Technical Conference and Exhibition, 24–27 September 2006. San Antonio, Texas, USA: Society of Petroleum Engineers.

VIEIRA, P. et al., 2002. Minimum Air and Water Flow Rates Required For Effective Cuttings Transport in High Angle and Horizontal Wells. In: Proceedings of the

IADC/SPE Drilling Conference, 26–28 February 2002. Dallas, Texas, USA: Society of Petroleum Engineers.

WALKER, S. and LI, J., 2001. Coiled Tubing Wiper Trip Hole Cleaning in Highly Deviated Wellbores. In: Proceedings of the SPE/ICoTA Coiled Tubing Roundtable, 7–8 March 2001. Houston, Texas, USA: Society of Petroleum Engineers.

WALKER, S. and LI, J., 2000. The Effect of Particle Size, Fluid Rheology, and Pipe Eccentricity on Cuttings Transport. In: Proceedings of the SPE/ICoTA Coiled Tubing Roundtable, 5–6 April 2000. Houston, Texas, USA: Society of Petroleum Engineers.

WILLIAMS, C. E., and BRUCE, G. H., 1951. Carrying Capacity of Drilling Muds, Trans. AIME, 192, pp. 111 – 120.

WILSON, K. C. et al., 2006. Slurry Transport Using Centrifugal Pumps, 3rd Edition.

WISNIE, A. P. and ZHU, Z., 1994. Quantifying Stuck Pipe Risk in Gulf of Mexico Oil and Gas Drilling In: Proceedings of the SPE 69th Annual Technical Conference and Exhibition, 25-28 September 1994. New Orleans, LA, USA: Society of Petroleum Engineers.

XU, J., 2010. Cuttings Transport With Foam Under Simulated Downhole Conditions in Highly Inclined Wellbores, M.Sc. thesis, University of Tulsa.

YATEEM, K. S. et al., 2013. Fill Cleanout operations in offshore Saudi Arabian Fields: Case Histories Toward Improving Economics and Operational Logistics. In: Proceedings of the International Petroleum Technology Conference, 26–28 March 2013. Beijing, China: Society of Petroleum Engineers.

ZEIDLER, H. U., 1970. An Experimental Analysis of the Transport of Drilled Particles, *SPE Journal,* 12 (01), pp. 39–48

ZHANG, F. et al., 2014. Pressure profile in Annulus: Solids Play a Significant Role. *Journal of Energy Resources Technology,* 137 (6): 064502-1-9.

## APPENDIX-A: DATA WINDOWS FOR Z-SCORE SAMPLE CALCULATIONS

Window-1 Data

| RIGTIME | BITDEPTH | DEPTH | FLWPMPS | HKHT | HKLI | Z-Score | Avg Z-Score | RoC-1W |
|---|---|---|---|---|---|---|---|---|
| 2013-11-20 00:52:09 | 5070.105 | 5070.1 | 695.2516 | 13.2384 | 169.5826 | 2.388464641 | | |
| 2013-11-20 00:52:14 | 5070.454 | 5070.454 | 695.2516 | 12.90642 | 162.9081 | 1.316267172 | | |
| 2013-11-20 00:52:19 | 5071.135 | 5071.135 | 695.2516 | 12.22446 | 148.9864 | -0.920126793 | | |
| 2013-11-20 00:52:24 | 5071.468 | 5071.468 | 696.24 | 11.89167 | 155.4904 | 0.124681409 | | |
| 2013-11-20 00:52:29 | 5071.468 | 5071.468 | 640.5404 | 11.89167 | 160.3472 | 0.904881974 | | |
| 2013-11-20 00:52:34 | 5071.468 | 5071.468 | 585.2453 | 11.89167 | 156.344 | 0.261804454 | | |
| 2013-11-20 00:52:39 | 5071.468 | 5071.468 | 537.1115 | 11.89167 | 163.0641 | 1.341327147 | | |
| 2013-11-20 00:52:44 | 5071.468 | 5071.468 | 519.8765 | 11.89167 | 161.4424 | 1.080815852 | | |
| 2013-11-20 00:52:49 | 5071.551 | 5071.551 | 524.0075 | 11.78608 | 158.7582 | 0.649623636 | | |
| 2013-11-20 00:52:54 | 5071.754 | 5071.754 | 524.5608 | 11.57929 | 162.5006 | 1.250806018 | | |
| 2013-11-20 00:52:59 | 5071.963 | 5071.963 | 524.8213 | 11.3569 | 162.6126 | 1.268797795 | | |
| 2013-11-20 00:53:04 | 5072.172 | 5072.172 | 526.4575 | 11.15572 | 159.1019 | 0.704835902 | | |
| 2013-11-20 00:53:09 | 5072.371 | 5072.371 | 525.3762 | 10.95933 | 149.5213 | -0.834199993 | | |
| 2013-11-20 00:53:14 | 5072.49 | 5072.49 | 526.7206 | 10.85133 | 158.4462 | 0.599503685 | | |
| 2013-11-20 00:53:19 | 5072.701 | 5072.701 | 526.132 | 10.73814 | 153.5566 | -0.1859659 | | |
| 2013-11-20 00:53:24 | 5072.795 | 5072.795 | 526.7204 | 10.54295 | 151.3971 | -0.532869853 | | |
| 2013-11-20 00:53:29 | 5072.795 | 5072.795 | 526.457 | 10.54295 | 154.539 | -0.028152312 | | |
| 2013-11-20 00:53:34 | 5072.892 | 5072.892 | 526.4256 | 10.41936 | 152.2377 | -0.39783514 | | |
| 2013-11-20 00:53:39 | 5073.107 | 5073.107 | 526.6895 | 10.32656 | 138.8655 | -2.545956948 | | |
| 2013-11-20 00:53:44 | 5073.107 | 5073.107 | 526.1315 | 10.22537 | 155.2946 | 0.093227927 | | |
| 2013-11-20 00:53:49 | 5073.322 | 5073.322 | 526.1315 | 10.02458 | 155.1405 | 0.06847317 | | |
| 2013-11-20 00:53:54 | 5073.416 | 5073.416 | 526.1315 | 9.916584 | 152.0878 | -0.421915206 | | |
| 2013-11-20 00:53:59 | 5073.626 | 5073.626 | 526.1315 | 9.720194 | 151.3352 | -0.542813523 | | |
| 2013-11-20 00:54:04 | 5073.72 | 5073.72 | 526.689 | 9.617399 | 151.0986 | -0.580821152 | | |
| 2013-11-20 00:54:09 | 5073.825 | 5073.825 | 526.395 | 9.510606 | 151.968 | -0.441159982 | | |
| 2013-11-20 00:54:14 | 5073.929 | 5073.929 | 526.395 | 9.409811 | 152.1551 | -0.411104076 | | |
| 2013-11-20 00:54:19 | 5074.141 | 5074.141 | 526.395 | 9.305017 | 141.9832 | -2.045126915 | | |
| 2013-11-20 00:54:24 | 5074.251 | 5074.251 | 526.3947 | 9.108627 | 152.2259 | -0.399730702 | | |
| 2013-11-20 00:54:29 | 5074.364 | 5074.364 | 526.4246 | 8.995434 | 154.5179 | -0.031541834 | | |
| 2013-11-20 00:54:34 | 5074.669 | 5074.669 | 526.4246 | 8.691051 | 149.0542 | -0.909235342 | | |
| 2013-11-20 00:54:39 | 5074.787 | 5074.787 | 526.7189 | 8.573057 | 153.0328 | -0.270109587 | | |
| 2013-11-20 00:54:44 | 5075.007 | 5075.007 | 526.6881 | 8.353069 | 151.2603 | -0.554845524 | **5.31866E-15** | **0.00** |
| | | | | **Mean** | **154.71425** | | | |
| | | | | **Std Dev** | **6.225065987** | | | |

# Window-2 Data

| RIGTIME | BITDEPTH | DEPTH | FLWPMPS | HKHT | HKLI | Z-Score | Avg Z-Score | RoC-1W |
|---|---|---|---|---|---|---|---|---|
| 2013-11-20 00:54:49 | 5075.22 | 5075.22 | 526.1302 | 8.139881 | 155.8098 | 0.401074958 | | |
| 2013-11-20 00:54:54 | 5075.345 | 5075.345 | 526.1301 | 8.015089 | 150.2304 | -0.71016118 | | |
| 2013-11-20 00:54:59 | 5075.535 | 5075.535 | 526.1301 | 7.825099 | 147.7147 | -1.211207306 | | |
| 2013-11-20 00:55:04 | 5075.535 | 5075.535 | 526.1299 | 7.825099 | 144.1644 | -1.91831231 | | |
| 2013-11-20 00:55:09 | 5075.745 | 5075.745 | 526.6877 | 7.61471 | 149.5315 | -0.84935947 | | |
| 2013-11-20 00:55:14 | 5075.745 | 5075.745 | 526.6876 | 7.61471 | 153.052 | -0.148189662 | | |
| 2013-11-20 00:55:19 | 5075.948 | 5075.948 | 526.6874 | 7.412321 | 148.4928 | -1.056234936 | | |
| 2013-11-20 00:55:24 | 5075.948 | 5075.948 | 526.6873 | 7.412321 | 152.0693 | -0.343911738 | | |
| 2013-11-20 00:55:29 | 5075.948 | 5075.948 | 525.5435 | 7.412321 | 146.8066 | -1.392071473 | | |
| 2013-11-20 00:55:34 | 5075.948 | 5075.948 | 525.2801 | 7.412321 | 152.818 | -0.194794898 | | |
| 2013-11-20 00:55:39 | 5076.179 | 5076.179 | 525.2801 | 7.181134 | 154.3049 | 0.101347521 | | |
| 2013-11-20 00:55:44 | 5076.179 | 5076.179 | 525.2801 | 7.181134 | 154.773 | 0.194577911 | | |
| 2013-11-20 00:55:49 | 5076.254 | 5076.254 | 525.8358 | 7.092739 | 155.9169 | 0.422405817 | | |
| 2013-11-20 00:55:54 | 5076.359 | 5076.359 | 525.8358 | 7.000344 | 155.3777 | 0.315014605 | | |
| 2013-11-20 00:55:59 | 5076.455 | 5076.455 | 526.6866 | 6.89515 | 149.9416 | -0.767680805 | | |
| 2013-11-20 00:56:04 | 5076.455 | 5076.455 | 525.8067 | 6.89515 | 154.6954 | 0.179122499 | | |
| 2013-11-20 00:56:09 | 5076.569 | 5076.569 | 525.8067 | 6.790356 | 153.4395 | -0.071012187 | | |
| 2013-11-20 00:56:14 | 5076.681 | 5076.681 | 525.8067 | 6.678762 | 149.3485 | -0.885807155 | | |
| 2013-11-20 00:56:19 | 5076.681 | 5076.681 | 525.5718 | 6.678762 | 155.2177 | 0.283147777 | | |
| 2013-11-20 00:56:25 | 5076.865 | 5076.865 | 525.5718 | 6.475973 | 153.2723 | -0.104313023 | | |
| 2013-11-20 00:56:30 | 5076.974 | 5076.974 | 525.5718 | 6.385578 | 152.4866 | -0.260799067 | | |
| 2013-11-20 00:56:35 | 5077.08 | 5077.08 | 525.5718 | 6.279584 | 150.4714 | -0.66216177 | | |
| 2013-11-20 00:56:40 | 5077.176 | 5077.176 | 525.5422 | 6.16759 | 143.7297 | -2.0048905 | | |
| 2013-11-20 00:56:45 | 5077.28 | 5077.28 | 525.3087 | 6.068796 | 151.2075 | -0.515554443 | | |
| 2013-11-20 00:56:50 | 5077.28 | 5077.28 | 525.3087 | 6.068796 | 155.8001 | 0.399143032 | | |
| 2013-11-20 00:56:55 | 5077.383 | 5077.383 | 526.0701 | 5.961601 | 153.1862 | -0.12146136 | | |
| 2013-11-20 00:57:01 | 5077.477 | 5077.477 | 526.0983 | 5.843608 | 145.2667 | -1.69876978 | | |
| 2013-11-20 00:57:07 | 5077.477 | 5077.477 | 526.6855 | 5.843608 | 154.7081 | 0.181651928 | | |
| 2013-11-20 00:57:13 | 5077.687 | 5077.687 | 526.1581 | 5.749213 | 153.4219 | -0.074517538 | | |
| 2013-11-20 00:57:19 | 5077.799 | 5077.799 | 526.1274 | 5.543224 | 151.0411 | -0.548695944 | | |
| 2013-11-20 00:57:24 | 5077.799 | 5077.799 | 526.6851 | 5.543224 | 149.7857 | -0.798731046 | | |
| 2013-11-20 00:57:29 | 5077.893 | 5077.893 | 526.6851 | 5.543224 | 152.675 | -0.223275876 | | |
| 2013-11-20 00:57:34 | 5077.991 | 5077.991 | 526.6849 | 5.336436 | 151.4348 | -0.47028363 | | |
| 2013-11-20 00:57:39 | 5078.089 | 5078.089 | 526.6849 | 5.236042 | 153.6358 | -0.031915572 | | |
| 2013-11-20 00:57:44 | 5078.089 | 5078.089 | 526.1269 | 5.236042 | 153.5964 | -0.039762779 | | |
| 2013-11-20 00:57:49 | 5078.196 | 5078.196 | 526.6847 | 5.124847 | 153.994 | 0.03942629 | | |
| 2013-11-20 00:57:54 | 5078.402 | 5078.402 | 526.1268 | 5.020054 | 151.8531 | -0.38697179 | | |
| 2013-11-20 00:57:59 | 5078.509 | 5078.509 | 525.3073 | 4.932058 | 151.9387 | -0.369923037 | | |
| 2013-11-20 00:58:04 | 5078.608 | 5078.608 | 524.7523 | 4.826864 | 144.4276 | -1.865891378 | | |
| 2013-11-20 00:58:09 | 5078.608 | 5078.608 | 524.1985 | 4.719271 | 151.8271 | -0.39215015 | | |
| 2013-11-20 00:58:14 | 5078.715 | 5078.715 | 524.1985 | 4.619276 | 151.0488 | -0.547162353 | | |
| 2013-11-20 00:58:19 | 5078.819 | 5078.819 | 525.0142 | 4.522081 | 151.8859 | -0.38043909 | | |
| 2013-11-20 00:58:24 | 5078.923 | 5078.923 | 527.8031 | 4.400488 | 155.9891 | 0.436785723 | | |
| 2013-11-20 00:58:29 | 5078.923 | 5078.923 | 526.42 | 4.400488 | 151.0215 | -0.552599631 | | |
| 2013-11-20 00:58:34 | 5079.126 | 5079.126 | 524.198 | 4.302094 | 153.0857 | -0.141477711 | | |
| 2013-11-20 00:58:39 | 5079.229 | 5079.229 | 525.5693 | 4.109304 | 147.3415 | -1.285536683 | | |
| 2013-11-20 00:58:44 | 5079.229 | 5079.229 | 527.8027 | 4.109304 | 146.6974 | -1.413820584 | | |
| 2013-11-20 00:58:49 | 5079.442 | 5079.442 | 527.8027 | 3.898916 | 150.3894 | -0.678493519 | | |
| 2013-11-20 00:58:54 | 5079.557 | 5079.557 | 527.8027 | 3.803321 | 144.7472 | -1.802237388 | | |
| 2013-11-20 00:58:59 | 5079.652 | 5079.652 | 528.0681 | 3.699327 | 151.0017 | -0.556543151 | | |
| 2013-11-20 00:59:04 | 5079.75 | 5079.75 | 528.6603 | 3.699327 | 150.2022 | -0.715777709 | | |
| 2013-11-20 00:59:09 | 5079.853 | 5079.853 | 528.6603 | 3.493738 | 149.7767 | -0.800523555 | | |
| 2013-11-20 00:59:14 | 5079.958 | 5079.958 | 528.6603 | 3.493738 | 149.8662 | -0.782698048 | | |
| 2013-11-20 00:59:19 | 5079.958 | 5079.958 | 528.6603 | 3.384944 | 153.3962 | -0.079636147 | | |
| 2013-11-20 00:59:25 | 5079.958 | 5079.958 | 528.6603 | 3.384944 | 153.1482 | -0.129029731 | | |
| 2013-11-20 00:59:30 | 5079.958 | 5079.958 | 528.6603 | 3.384944 | 156.088 | 0.456483406 | | |
| 2013-11-20 00:59:35 | 5079.958 | 5079.958 | 528.9893 | 3.384944 | 157.2977 | 0.697416545 | | |
| 2013-11-20 00:59:40 | 5079.958 | 5079.958 | 528.9893 | 3.384944 | 156.3085 | 0.500399879 | | |
| 2013-11-20 00:59:45 | 5079.958 | 5079.958 | 527.772 | 3.384944 | 157.1115 | 0.660331524 | | |
| 2013-11-20 00:59:50 | 5079.958 | 5079.958 | 517.1638 | 3.384944 | 160.0203 | 1.239670463 | | |
| 2013-11-20 00:59:55 | 5079.958 | 5079.958 | 513.9845 | 3.384944 | 161.489 | 1.532188031 | | |
| 2013-11-20 01:00:00 | 5079.958 | 5079.958 | 515.8689 | 3.384944 | 162.0695 | 1.647804868 | | |
| 2013-11-20 01:00:05 | 5079.958 | 5079.958 | 512.1454 | 3.384944 | 160.9076 | 1.416391943 | | |
| 2013-11-20 01:00:10 | 5079.958 | 5079.958 | 517.4487 | 3.384944 | 161.0698 | 1.448696941 | | |
| 2013-11-20 01:00:15 | 5079.958 | 5079.958 | 515.0502 | 3.384944 | 159.4234 | 1.120787277 | | |
| 2013-11-20 01:00:20 | 5079.958 | 5079.958 | 517.7023 | 3.384944 | 162.4728 | 1.728129192 | | |
| 2013-11-20 01:00:25 | 5079.958 | 5079.958 | 516.6572 | 3.384944 | 162.2723 | 1.688196072 | | |
| 2013-11-20 01:00:30 | 5079.958 | 5079.958 | 511.5861 | 3.384944 | 159.2246 | 1.081192743 | | |
| 2013-11-20 01:00:35 | 5079.958 | 5079.958 | 520.5508 | 3.384944 | 165.9753 | 2.425713981 | | |
| 2013-11-20 01:00:40 | 5079.958 | 5079.958 | 554.6301 | 3.384944 | 161.2932 | 1.493191 | | |
| 2013-11-20 01:00:45 | 5079.958 | 5079.958 | 537.1087 | 3.384944 | 158.9512 | 1.0267403 | | |
| 2013-11-20 01:00:50 | 5079.958 | 5079.958 | 541.4988 | 3.384944 | 161.4475 | 1.523922572 | | |
| 2013-11-20 01:00:55 | 5079.958 | 5079.958 | 541.4942 | 3.384944 | 158.7494 | 0.986548262 | | |
| 2013-11-20 01:01:00 | 5079.958 | 5079.958 | 544.7885 | 3.384944 | 160.0001 | 1.235647276 | | |
| 2013-11-20 01:16:27 | 5079.932 | 5079.958 | 541.4255 | 3.428142 | 164.7109 | 2.17388637 | | |
| 2013-11-20 01:16:32 | 5080.265 | 5080.283 | 542.2994 | 3.09536 | 158.5546 | 0.947750399 | **5.74248E-15** | **0.079685515** |
| | | | | **mean** | **153.7960447** | | | |
| | | | | **std dev** | **5.020895026** | | | |

# Window-3 Data

| RIGTIME | BITDEPTH | DEPTH | FLWPMPS | HKHT | HKLI | Z-Score | Avg Z-Score | RoC-1W |
|---|---|---|---|---|---|---|---|---|
| 2013-11-20 01:16:37 | 5080.265 | 5080.283 | 542.2994 | 3.09536 | 151.8433 | -0.490149815 | | |
| 2013-11-20 01:16:42 | 5080.265 | 5080.283 | 542.2994 | 3.09536 | 153.3617 | -0.217513505 | | |
| 2013-11-20 01:16:47 | 5080.265 | 5080.283 | 542.2992 | 3.09536 | 161.7435 | 1.287480584 | | |
| 2013-11-20 01:16:52 | 5080.265 | 5080.283 | 542.2992 | 3.09536 | 164.6482 | 1.809033989 | | |
| 2013-11-20 01:16:57 | 5080.362 | 5080.392 | 542.2992 | 2.998165 | 159.3775 | 0.862653457 | | |
| 2013-11-20 01:17:02 | 5080.467 | 5080.492 | 542.2992 | 2.892571 | 151.0328 | -0.635679141 | | |
| 2013-11-20 01:17:07 | 5080.562 | 5080.492 | 542.2992 | 2.797776 | 149.8969 | -0.839635664 | | |
| 2013-11-20 01:17:12 | 5080.562 | 5080.592 | 542.2992 | 2.797776 | 158.6134 | 0.725455482 | | |
| 2013-11-20 01:17:17 | 5080.67 | 5080.692 | 542.2992 | 2.689782 | 163.2242 | 1.553347671 | | |
| 2013-11-20 01:17:22 | 5080.778 | 5080.795 | 542.2992 | 2.582188 | 159.1935 | 0.829615337 | | |
| 2013-11-20 01:17:27 | 5080.878 | 5080.915 | 542.2992 | 2.481794 | 144.7702 | -1.760160277 | | |
| 2013-11-20 01:17:32 | 5080.975 | 5080.915 | 541.7075 | 2.384999 | 156.6482 | 0.372593999 | | |
| 2013-11-20 01:17:38 | 5080.975 | 5081.007 | 541.3772 | 2.384999 | 157.7439 | 0.569332411 | | |
| 2013-11-20 01:17:43 | 5081.079 | 5081.105 | 537.1444 | 2.281405 | 161.9591 | 1.326192642 | | |
| 2013-11-20 01:17:48 | 5081.179 | 5081.105 | 537.1443 | 2.18061 | 144.5042 | -1.807921906 | | |
| 2013-11-20 01:17:53 | 5081.179 | 5081.206 | 537.1443 | 2.18061 | 148.8915 | -1.02016026 | | |
| 2013-11-20 01:17:58 | 5081.286 | 5081.307 | 537.1443 | 2.074217 | 159.4829 | 0.881578554 | | |
| 2013-11-20 01:18:03 | 5081.286 | 5081.307 | 537.1443 | 2.074217 | 155.9175 | 0.241393161 | | |
| 2013-11-20 01:18:08 | 5081.382 | 5081.412 | 537.1443 | 1.977653 | 147.266 | -1.312026911 | | |
| 2013-11-20 01:18:13 | 5081.483 | 5081.508 | 536.8483 | 1.877 | 154.2229 | -0.06288074 | | |
| 2013-11-20 01:18:18 | 5081.59 | 5081.508 | 536.8483 | 1.769712 | 159.8307 | 0.944027782 | | |
| 2013-11-20 01:18:23 | 5081.59 | 5081.615 | 537.4406 | 1.769712 | 140.7151 | -2.488273752 | | |
| 2013-11-20 01:18:28 | 5081.688 | 5081.714 | 536.8481 | 1.672009 | 157.4753 | 0.521103938 | | |
| 2013-11-20 01:18:33 | 5081.79 | 5081.714 | 536.8481 | 1.57025 | 157.7004 | 0.561521768 | | |
| 2013-11-20 01:18:38 | 5081.79 | 5081.816 | 536.8481 | 1.57025 | 161.289 | 1.205872837 | | |
| 2013-11-20 01:18:43 | 5081.894 | 5081.914 | 536.8481 | 1.465911 | 163.2987 | 1.566724518 | | |
| 2013-11-20 01:18:48 | 5081.991 | 5081.914 | 536.8481 | 1.368945 | 150.6005 | -0.713300767 | | |
| 2013-11-20 01:18:53 | 5082.102 | 5082.023 | 536.8481 | 1.258339 | 155.6507 | 0.193487887 | | |
| 2013-11-20 01:18:58 | 5082.196 | 5082.119 | 536.8481 | 1.163585 | 156.6533 | 0.373509729 | | |
| 2013-11-20 01:19:03 | 5082.196 | 5082.22 | 536.8481 | 1.163585 | 151.3362 | -0.581202155 | | |
| 2013-11-20 01:19:08 | 5082.406 | 5082.421 | 536.8481 | 0.9538009 | 155.1479 | 0.103207634 | | |
| 2013-11-20 01:19:13 | 5082.502 | 5082.525 | 536.8481 | 0.8575728 | 147.4225 | -1.283926553 | | |
| 2013-11-20 01:19:18 | 5082.609 | 5082.625 | 536.8481 | 0.750284 | 157.108 | 0.455153387 | | |
| 2013-11-20 01:19:23 | 5082.609 | 5082.625 | 536.8481 | 0.750284 | 154.9712 | 0.071480266 | | |
| 2013-11-20 01:19:28 | 5082.707 | 5082.726 | 536.8481 | 0.6529496 | 158.9774 | 0.790813502 | | |
| 2013-11-20 01:19:33 | 5082.805 | 5082.823 | 536.8481 | 0.5548785 | 159.9836 | 0.971481742 | | |
| 2013-11-20 01:19:38 | 5082.911 | 5082.823 | 536.8481 | 0.4486954 | 154.9075 | 0.060042612 | | |
| 2013-11-20 01:19:43 | 5083.012 | 5082.935 | 536.8481 | 0.3476746 | 157.399 | 0.507403892 | | |
| 2013-11-20 01:19:48 | 5083.111 | 5083.033 | 536.8481 | 0.2488658 | 159.6372 | 0.90928389 | | |
| 2013-11-20 01:19:54 | 5083.111 | 5083.133 | 536.8481 | 0.2488658 | 147.7318 | -1.228390192 | | |
| 2013-11-20 01:20:00 | 5083.215 | 5083.233 | 536.8481 | 0.1452639 | 153.9725 | -0.107841311 | | |
| 2013-11-20 01:20:06 | 5083.317 | 5083.338 | 536.8472 | 0.04239941 | 154.8338 | 0.046809409 | | |
| 2013-11-20 01:20:12 | 5083.422 | 5083.437 | 537.4276 | -0.06267715 | 157.4149 | 0.510258816 | | |
| 2013-11-20 01:20:18 | 5083.526 | 5083.54 | 536.847 | -0.1666477 | 154.1974 | -0.067459392 | | |
| 2013-11-20 01:20:24 | 5083.623 | 5083.644 | 536.847 | -0.2628758 | 148.7564 | -1.044418141 | | |
| 2013-11-20 01:20:30 | 5083.724 | 5083.644 | 536.847 | -0.3638968 | 158.7689 | 0.753376285 | | |
| 2013-11-20 01:20:36 | 5083.724 | 5083.748 | 536.847 | -0.3638968 | 155.3669 | 0.142530179 | | |
| 2013-11-20 01:20:42 | 5083.829 | 5083.846 | 536.847 | -0.4686048 | 156.203 | 0.292656113 | | |
| 2013-11-20 01:20:48 | 5083.929 | 5083.944 | 536.847 | -0.5688884 | 154.5973 | 0.004344652 | | |
| 2013-11-20 01:20:54 | 5084.027 | 5084.052 | 536.847 | -0.6695409 | 153.9041 | -0.120122873 | | |
| 2013-11-20 01:20:59 | 5084.131 | 5084.052 | 536.847 | -0.7712991 | 142.6589 | -2.139254746 | | |
| 2013-11-20 01:21:04 | 5084.131 | 5084.149 | 536.847 | -0.7712991 | 145.5018 | -1.62879784 | | |
| 2013-11-20 01:21:09 | 5084.233 | 5084.258 | 536.847 | -0.8734262 | 155.6372 | 0.191063895 | | |
| 2013-11-20 01:21:14 | 5084.337 | 5084.353 | 536.847 | -0.9770281 | 151.6935 | -0.517047154 | | |
| 2013-11-20 01:21:19 | 5084.441 | 5084.459 | 536.847 | -1.081367 | 150.8974 | -0.659990888 | | |
| 2013-11-20 01:21:24 | 5084.535 | 5084.557 | 536.847 | -1.175015 | 149.8996 | -0.839150866 | | |
| 2013-11-20 01:21:29 | 5084.639 | 5084.664 | 536.847 | -1.278985 | 155.8894 | 0.236347666 | | |
| 2013-11-20 01:21:34 | 5084.741 | 5084.664 | 536.8463 | -1.381481 | 153.9905 | -0.104609321 | | |
| 2013-11-20 01:21:39 | 5084.842 | 5084.767 | 536.8463 | -1.482502 | 152.9508 | -0.291292654 | | |
| 2013-11-20 01:21:44 | 5084.842 | 5084.865 | 536.8463 | -1.482502 | 164.3236 | 1.750750436 | | |
| 2013-11-20 01:21:49 | 5084.943 | 5084.965 | 536.8461 | -1.583154 | 141.9299 | -2.27015034 | | |
| 2013-11-20 01:21:54 | 5085.047 | 5085.068 | 536.8461 | -1.687494 | 157.9672 | 0.609427042 | **5.47412E-15** | **-0.046733573** |
| | | | | **mean** | **154.5731032** | | | |
| | | | | **std dev** | **5.569324201** | | | |

Window-4 Data

| RIGTIME | BITDEPTH | DEPTH | FLWPMPS | HKHT | HKLI | Z-Score | Avg Z-Score | RoC-1W |
|---|---|---|---|---|---|---|---|---|
| 2013-11-20 01:21:59 | 5085.146 | 5085.068 | 536.8461 | -1.786671 | 158.1836 | 1.034896442 | | |
| 2013-11-20 01:22:04 | 5085.146 | 5085.167 | 536.2668 | -1.786671 | 157.6431 | 0.893344316 | | |
| 2013-11-20 01:22:09 | 5085.358 | 5085.268 | 536.2668 | -1.99793 | 156.1321 | 0.497626899 | | |
| 2013-11-20 01:22:14 | 5085.461 | 5085.472 | 536.2668 | -2.101532 | 151.834 | -0.628007136 | | |
| 2013-11-20 01:22:19 | 5085.565 | 5085.576 | 536.8459 | -2.205134 | 155.1755 | 0.247101896 | | |
| 2013-11-20 01:22:24 | 5085.765 | 5085.682 | 536.8459 | -2.404964 | 159.0087 | 1.250982769 | | |
| 2013-11-20 01:22:29 | 5085.875 | 5085.884 | 536.8459 | -2.514834 | 151.1946 | -0.79546029 | | |
| 2013-11-20 01:22:34 | 5085.968 | 5085.884 | 536.8459 | -2.608112 | 150.4579 | -0.988395446 | | |
| 2013-11-20 01:22:39 | 5085.968 | 5085.985 | 536.8459 | -2.608112 | 159.449 | 1.36629341 | | |
| 2013-11-20 01:22:44 | 5086.076 | 5086.09 | 536.8459 | -2.71577 | 153.7447 | -0.127611856 | | |
| 2013-11-20 01:22:49 | 5086.169 | 5086.188 | 536.8459 | -2.809786 | 159.2128 | 1.304434738 | | |
| 2013-11-20 01:22:54 | 5086.277 | 5086.291 | 536.8459 | -2.917074 | 156.4157 | 0.571899208 | | |
| 2013-11-20 01:22:59 | 5086.392 | 5086.392 | 536.8459 | -3.031737 | 156.5517 | 0.607516395 | | |
| 2013-11-20 01:23:04 | 5086.585 | 5086.596 | 536.5615 | -3.224931 | 154.0279 | -0.053444304 | | |
| 2013-11-20 01:23:09 | 5086.688 | 5086.703 | 536.5615 | -3.327795 | 151.6795 | -0.668469307 | | |
| 2013-11-20 01:23:14 | 5086.888 | 5086.9 | 536.8454 | -3.527993 | 149.3253 | -1.285013279 | | |
| 2013-11-20 01:23:19 | 5086.989 | 5087.008 | 536.8454 | -3.629383 | 151.8846 | -0.614755447 | | |
| 2013-11-20 01:23:24 | 5087.096 | 5087.105 | 536.8454 | -3.735934 | 158.0441 | 0.998362637 | | |
| 2013-11-20 01:23:29 | 5087.197 | 5087.213 | 536.2661 | -3.837324 | 155.9187 | 0.441739344 | | |
| 2013-11-20 01:23:34 | 5087.295 | 5087.311 | 536.2661 | -3.935396 | 151.1233 | -0.814133124 | | |
| 2013-11-20 01:23:39 | 5087.517 | 5087.517 | 536.2661 | -4.157347 | 156.3492 | 0.554483452 | | |
| 2013-11-20 01:23:44 | 5087.62 | 5087.62 | 536.2659 | -4.259843 | 155.9195 | 0.441948856 | | |
| 2013-11-20 01:23:49 | 5087.722 | 5087.722 | 536.2659 | -4.36197 | 155.4341 | 0.314826928 | | |
| 2013-11-20 01:23:54 | 5087.938 | 5087.938 | 536.2659 | -4.578759 | 156.1804 | 0.510276238 | | |
| 2013-11-20 01:23:59 | 5088.028 | 5088.028 | 536.2658 | -4.668351 | 150.4911 | -0.979700662 | | |
| 2013-11-20 01:24:04 | 5088.237 | 5088.237 | 536.2658 | -4.877029 | 159.9458 | 1.496400897 | | |
| 2013-11-20 01:24:09 | 5088.334 | 5088.334 | 536.2657 | -4.973995 | 151.8497 | -0.623895446 | | |
| 2013-11-20 01:24:14 | 5088.438 | 5088.438 | 536.2657 | -5.077966 | 154.6621 | 0.112647017 | | |
| 2013-11-20 01:24:19 | 5088.639 | 5088.639 | 536.2657 | -5.298811 | 158.2635 | 1.055821539 | | |
| 2013-11-20 01:24:24 | 5088.75 | 5088.75 | 536.5608 | -5.390615 | 151.1958 | -0.795146021 | | |
| 2013-11-20 01:24:29 | 5088.86 | 5088.86 | 536.5608 | -5.500484 | 154.8247 | 0.155230506 | | |
| 2013-11-20 01:24:34 | 5089.054 | 5089.054 | 535.9821 | -5.705108 | 154.4986 | 0.069827826 | | |
| 2013-11-20 01:24:39 | 5089.158 | 5089.158 | 536.5607 | -5.807603 | 155.8834 | 0.432494589 | | |
| 2013-11-20 01:24:44 | 5089.266 | 5089.266 | 536.5607 | -5.906412 | 155.207 | 0.255351465 | | |
| 2013-11-20 01:24:49 | 5089.367 | 5089.367 | 535.982 | -6.007064 | 156.1526 | 0.502995666 | | |
| 2013-11-20 01:24:54 | 5089.466 | 5089.466 | 536.8445 | -6.116565 | 155.7266 | 0.391430068 | | |
| 2013-11-20 01:24:59 | 5089.57 | 5089.57 | 536.2653 | -6.222748 | 139.0265 | -3.982177096 | | |
| 2013-11-20 01:25:04 | 5089.774 | 5089.774 | 536.2653 | -6.429583 | 150.2224 | -1.050070794 | | |
| 2013-11-20 01:25:09 | 5089.874 | 5089.874 | 536.2653 | -6.537977 | 152.9489 | -0.336024775 | | |
| 2013-11-20 01:25:14 | 5089.985 | 5089.985 | 536.2653 | -6.625726 | 149.9689 | -1.116460182 | | |
| 2013-11-20 01:25:19 | 5090.079 | 5090.079 | 536.2653 | -6.728222 | 151.7532 | -0.649167935 | **-8.7139E-15** | **-2.591836409** |
| | | | | **mean** | **154.2319707** | | | |
| | | | | **std dev** | **3.818381344** | | | |

# APPENDIX-B: WELL-A SPI TOOL REPORT (RUN-1: NO T&D MODEL)

Username: egbepi
Database: EPPR
Date: 16/07/2021 02:43 PM
Saudi Aramco: Confidential

Real-Time Stuck Pipe Index System

أرامكو السعودية saudi aramco

**Summary Report**

| Well | Wellbore | Start Date | End Date | Casing Depth | Cut-off Weight |
|---|---|---|---|---|---|
| HRDH_1476 | HRDH_1476_1 | 04-16-2020 01:00 AM | 04-18-2020 01:00 PM | 9,498 | 100 |

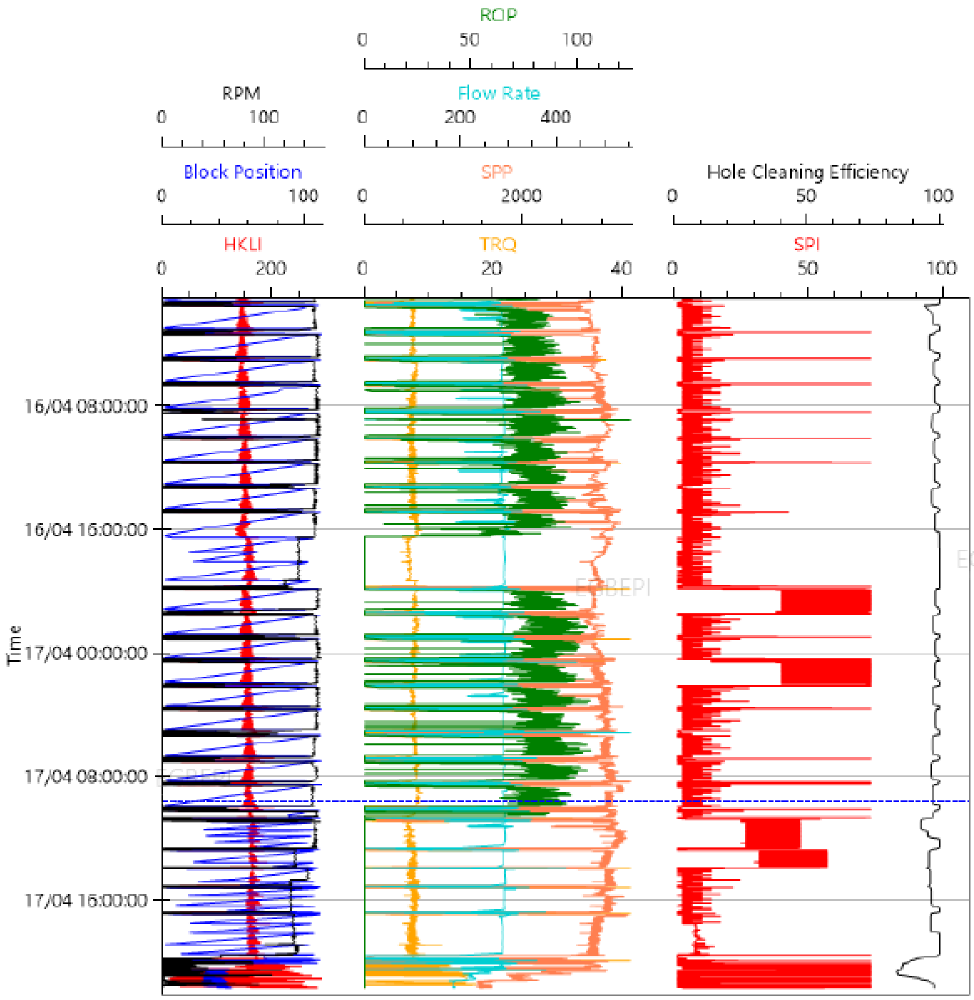

## Summary Report

| Time | Bit Depth | Hole Depth | ROP | RPM | Torque | Flow Rate | SPP | SPI |
|---|---|---|---|---|---|---|---|---|
| 4/16/2020 2:58:05 AM | 12806.10 | 12806.13 | 81.36 | 148.05 | 8.02 | 283.15 | 2884.34 | 21.13 |
| 4/16/2020 3:12:25 AM | 12772.90 | 12806.47 | 0.00 | 0.00 | 0.00 | 289.54 | 2963.94 | 73.63 |
| 4/16/2020 4:55:30 AM | 12868.60 | 12901.09 | 0.00 | 5.72 | 0.00 | 285.04 | 2879.00 | 73.63 |
| 4/16/2020 6:34:10 AM | 12964.20 | 12996.34 | 0.00 | 0.32 | 0.00 | 280.98 | 2875.44 | 73.63 |
| 4/16/2020 8:09:40 AM | 12991.00 | 13089.40 | 0.00 | 150.90 | 6.02 | 294.19 | 3156.93 | 21.13 |
| 4/16/2020 8:23:00 AM | 13056.30 | 13089.40 | 0.00 | 0.00 | 0.00 | 291.85 | 3030.64 | 73.63 |
| 4/16/2020 8:51:00 AM | 13082.10 | 13105.27 | 0.00 | 39.50 | 6.90 | 270.89 | 308.67 | 22.40 |
| 4/16/2020 10:03:55 AM | 13152.00 | 13182.72 | 0.00 | 0.00 | 0.00 | 285.67 | 2924.80 | 73.63 |
| 4/16/2020 10:36:00 AM | 13204.60 | 13204.62 | 77.60 | 149.90 | 7.55 | 286.63 | 2968.38 | 21.13 |
| 4/16/2020 11:03:15 AM | 13240.60 | 13240.58 | 77.00 | 149.88 | 7.71 | 285.36 | 2895.01 | 24.63 |
| 4/16/2020 11:39:05 AM | 13243.90 | 13276.75 | 0.00 | 12.79 | 0.00 | 294.19 | 3122.25 | 73.63 |
| 4/16/2020 12:26:35 PM | 13321.70 | 13321.75 | 79.71 | 149.94 | 7.76 | 283.78 | 2947.93 | 21.13 |
| 4/16/2020 1:21:15 PM | 13368.80 | 13370.51 | 0.00 | 0.00 | 0.00 | 280.06 | 42.75 | 21.13 |
| 4/16/2020 2:28:25 PM | 13449.20 | 13449.23 | 83.22 | 148.24 | 7.69 | 282.84 | 2903.01 | 24.63 |
| 4/16/2020 2:50:55 PM | 13460.50 | 13463.82 | 0.00 | 0.00 | 0.00 | 271.47 | 315.34 | 42.70 |
| 4/16/2020 3:02:40 PM | 13464.70 | 13464.66 | 69.45 | 148.81 | 7.36 | 291.52 | 3055.54 | 21.13 |
| 4/16/2020 7:39:25 PM | 13511.20 | 13558.36 | 0.00 | 21.14 | 0.00 | 292.52 | 2972.83 | 73.63 |

**Summary Report**

| Time | Bit Depth | Hole Depth | ROP | RPM | Torque | Flow Rate | SPP | SPI |
|---|---|---|---|---|---|---|---|---|
| 4/16/2020 7:52:15 PM | 13556.60 | 13558.36 | 0.00 | 148.78 | 7.27 | 292.85 | 2984.39 | 73.63 |
| 4/16/2020 8:02:40 PM | 13562.10 | 13562.08 | 71.69 | 152.98 | 8.18 | 289.22 | 2898.57 | 73.63 |
| 4/16/2020 8:12:40 PM | 13575.00 | 13574.99 | 78.60 | 152.79 | 7.90 | 288.89 | 2913.69 | 73.63 |
| 4/16/2020 8:22:40 PM | 13588.20 | 13588.23 | 80.56 | 152.48 | 8.17 | 288.24 | 2895.45 | 73.63 |
| 4/16/2020 8:32:40 PM | 13601.70 | 13601.67 | 81.55 | 153.02 | 8.36 | 288.57 | 2931.03 | 73.63 |
| 4/16/2020 8:42:40 PM | 13615.70 | 13615.67 | 82.23 | 153.04 | 8.19 | 288.57 | 2901.23 | 73.63 |
| 4/16/2020 8:52:40 PM | 13629.50 | 13629.52 | 83.82 | 153.23 | 8.16 | 288.24 | 2908.35 | 73.63 |
| 4/16/2020 9:02:45 PM | 13643.80 | 13643.80 | 81.31 | 152.86 | 7.62 | 288.57 | 2928.36 | 73.63 |
| 4/16/2020 9:12:45 PM | 13552.90 | 13652.16 | 0.00 | 132.42 | 6.42 | 283.78 | 2756.27 | 73.63 |
| 4/16/2020 9:26:05 PM | 13616.10 | 13652.16 | 0.00 | 14.91 | 0.00 | 292.52 | 2789.17 | 73.63 |
| 4/16/2020 9:50:15 PM | 13665.20 | 13665.24 | 85.04 | 150.84 | 7.96 | 291.52 | 2847.87 | 24.63 |
| 4/16/2020 10:21:00 PM | 13710.40 | 13710.38 | 91.68 | 150.82 | 7.82 | 291.19 | 2931.47 | 21.13 |
| 4/16/2020 10:55:45 PM | 13712.50 | 13747.99 | 0.00 | 96.70 | 7.48 | 287.27 | 2870.55 | 73.63 |
| 4/17/2020 12:23:20 AM | 13808.50 | 13841.64 | 0.00 | 0.00 | 0.00 | 294.87 | 2890.12 | 73.63 |
| 4/17/2020 12:36:00 AM | 13839.20 | 13841.64 | 0.00 | 151.09 | 6.85 | 291.52 | 2950.15 | 73.63 |
| 4/17/2020 12:46:00 AM | 13846.80 | 13846.77 | 0.00 | 152.81 | 7.69 | 293.86 | 2818.97 | 73.63 |
| 4/17/2020 12:56:00 AM | 13855.10 | 13855.07 | 70.33 | 151.81 | 7.77 | 287.27 | 2946.15 | 73.63 |

## Summary Report

| Time | Bit Depth | Hole Depth | ROP | RPM | Torque | Flow Rate | SPP | SPI |
|---|---|---|---|---|---|---|---|---|
| 4/17/2020 1:06:00 AM | 13868.70 | 13868.70 | 84.26 | 152.96 | 7.99 | 287.92 | 2961.71 | 73.63 |
| 4/17/2020 1:16:00 AM | 13882.60 | 13882.61 | 90.96 | 153.09 | 8.19 | 287.27 | 2912.35 | 73.63 |
| 4/17/2020 1:26:00 AM | 13896.90 | 13896.89 | 79.56 | 151.81 | 7.67 | 286.63 | 2914.58 | 73.63 |
| 4/17/2020 1:36:00 AM | 13911.10 | 13911.14 | 82.83 | 152.92 | 7.83 | 286.63 | 2995.51 | 73.63 |
| 4/17/2020 1:46:00 AM | 13925.30 | 13925.33 | 84.74 | 152.90 | 7.55 | 226.42 | 2385.39 | 73.63 |
| 4/17/2020 1:56:00 AM | 13863.40 | 13934.90 | 0.00 | 150.88 | 6.14 | 290.86 | 2929.70 | 73.63 |
| 4/17/2020 2:06:00 AM | 13922.00 | 13934.90 | 0.00 | 58.97 | 8.15 | 285.99 | 2996.84 | 73.63 |
| 4/17/2020 2:28:15 AM | 13948.70 | 13948.67 | 66.32 | 152.08 | 7.63 | 290.53 | 3010.63 | 21.13 |
| 4/17/2020 3:06:10 AM | 14001.20 | 14001.21 | 74.04 | 151.95 | 7.81 | 288.57 | 3030.20 | 28.13 |
| 4/17/2020 3:35:40 AM | 13996.20 | 14029.81 | 0.00 | 7.92 | 0.00 | 289.54 | 2997.29 | 73.63 |
| 4/17/2020 4:23:05 AM | 14078.00 | 14078.03 | 90.72 | 151.74 | 7.80 | 288.57 | 3084.45 | 24.63 |
| 4/17/2020 5:02:15 AM | 14117.90 | 14124.84 | 0.00 | 60.02 | 7.02 | 287.92 | 3008.41 | 21.13 |
| 4/17/2020 5:22:10 AM | 14122.30 | 14124.84 | 0.00 | 0.00 | 0.00 | 0.00 | 44.97 | 21.13 |
| 4/17/2020 6:09:20 AM | 14178.90 | 14178.90 | 82.94 | 148.99 | 7.97 | 288.57 | 3008.85 | 21.13 |
| 4/17/2020 6:50:30 AM | 14187.10 | 14218.33 | 0.00 | 6.87 | 0.00 | 288.89 | 3088.45 | 73.63 |
| 4/17/2020 8:23:15 AM | 14277.40 | 14313.07 | 0.00 | 0.00 | 0.00 | 290.53 | 3059.10 | 73.63 |
| 4/17/2020 8:33:15 AM | 14311.40 | 14313.07 | 0.00 | 0.00 | 0.00 | 268.06 | 216.18 | 21.13 |

## Summary Report

| Time | Bit Depth | Hole Depth | ROP | RPM | Torque | Flow Rate | SPP | SPI |
|---|---|---|---|---|---|---|---|---|
| 4/17/2020 10:07:40 AM | 14377.40 | 14408.57 | 0.00 | 0.00 | 0.00 | 290.20 | 3090.23 | 73.63 |
| 4/17/2020 10:36:35 AM | 14409.30 | 14416.00 | 0.00 | 0.00 | 0.00 | 292.52 | 3074.67 | 73.63 |
| 4/17/2020 10:46:35 AM | 14399.00 | 14416.00 | 0.00 | 0.00 | 0.00 | 163.71 | 138.80 | 54.80 |
| 4/17/2020 10:56:40 AM | 14406.90 | 14416.10 | 0.00 | 149.98 | 7.16 | 290.86 | 3096.01 | 47.16 |
| 4/17/2020 11:06:40 AM | 14357.30 | 14416.10 | 0.00 | 149.83 | 6.95 | 290.86 | 3157.82 | 47.16 |
| 4/17/2020 11:16:40 AM | 14388.70 | 14416.10 | 0.00 | 149.90 | 7.07 | 293.18 | 3132.03 | 47.16 |
| 4/17/2020 11:26:40 AM | 14338.10 | 14416.10 | 0.00 | 149.88 | 7.09 | 294.87 | 3131.59 | 47.16 |
| 4/17/2020 11:36:40 AM | 14368.90 | 14416.10 | 0.00 | 149.90 | 7.10 | 294.19 | 3169.38 | 47.16 |
| 4/17/2020 11:46:40 AM | 14399.80 | 14416.10 | 0.00 | 149.81 | 7.29 | 294.19 | 3183.62 | 47.16 |
| 4/17/2020 11:56:40 AM | 14350.50 | 14416.10 | 0.00 | 148.95 | 7.17 | 294.19 | 3303.68 | 47.16 |
| 4/17/2020 12:06:40 PM | 14381.00 | 14416.10 | 0.00 | 150.80 | 7.07 | 293.86 | 3233.42 | 47.16 |
| 4/17/2020 12:16:40 PM | 14338.00 | 14416.10 | 0.00 | 148.85 | 7.50 | 291.85 | 3218.75 | 47.16 |
| 4/17/2020 12:26:40 PM | 14356.20 | 14416.10 | 0.00 | 149.92 | 7.56 | 291.85 | 3208.52 | 47.16 |
| 4/17/2020 12:45:50 PM | 14332.40 | 14416.10 | 0.00 | 131.41 | 8.01 | 309.08 | 2710.02 | 57.02 |
| 4/17/2020 12:55:50 PM | 14247.50 | 14416.10 | 0.00 | 130.42 | 7.81 | 289.22 | 3090.23 | 57.02 |
| 4/17/2020 1:06:20 PM | 14267.10 | 14416.10 | 0.00 | 129.63 | 7.43 | 288.57 | 3044.43 | 57.02 |
| 4/17/2020 1:16:20 PM | 14286.20 | 14416.10 | 0.00 | 129.58 | 7.42 | 288.89 | 3058.66 | 57.02 |

**Summary Report**

| Time | Bit Depth | Hole Depth | ROP | RPM | Torque | Flow Rate | SPP | SPI |
|---|---|---|---|---|---|---|---|---|
| 4/17/2020 1:26:20 PM | 14305.30 | 14416.10 | 0.00 | 131.41 | 7.77 | 289.22 | 3059.10 | 57.02 |
| 4/17/2020 1:36:20 PM | 14235.70 | 14416.10 | 0.00 | 131.51 | 7.13 | 288.89 | 3010.18 | 57.02 |
| 4/17/2020 1:46:20 PM | 14254.10 | 14416.10 | 0.00 | 129.44 | 7.16 | 289.22 | 3015.08 | 57.02 |
| 4/17/2020 2:38:05 PM | 14188.50 | 14416.10 | 0.00 | 141.73 | 7.52 | 294.19 | 3110.24 | 24.63 |
| 4/17/2020 3:09:50 PM | 14135.10 | 14416.10 | 0.00 | 0.00 | 0.00 | 0.00 | 0.00 | 22.40 |
| 4/17/2020 7:32:25 PM | 13948.10 | 14416.10 | 0.00 | 128.30 | 6.45 | 285.67 | 3039.98 | 73.63 |
| 4/17/2020 7:56:40 PM | 13911.10 | 14416.10 | 0.00 | 0.00 | 0.00 | 293.18 | 3007.07 | 73.63 |
| 4/17/2020 8:07:00 PM | 13828.70 | 14416.10 | 0.00 | 26.76 | 13.15 | 291.19 | 2889.67 | 73.63 |
| 4/17/2020 8:17:05 PM | 13827.50 | 14416.10 | 0.00 | 0.00 | 13.36 | 291.52 | 2914.13 | 73.63 |
| 4/17/2020 8:30:25 PM | 13834.30 | 14416.10 | 0.00 | 29.45 | 5.32 | 291.19 | 2651.32 | 73.63 |
| 4/17/2020 8:40:25 PM | 13827.70 | 14416.10 | 0.00 | 22.19 | 3.22 | 251.26 | 2355.60 | 73.63 |
| 4/17/2020 8:50:55 PM | 13826.90 | 14416.10 | 0.00 | 0.00 | 16.28 | 219.83 | 2020.30 | 73.63 |
| 4/17/2020 9:02:45 PM | 13814.30 | 14416.10 | 0.00 | 0.00 | 15.86 | 224.05 | 1861.54 | 73.63 |
| 4/17/2020 9:14:25 PM | 13811.10 | 14416.10 | 0.00 | 0.00 | 0.00 | 187.12 | 1628.97 | 73.63 |
| 4/17/2020 9:31:10 PM | 13797.70 | 14416.10 | 0.00 | 4.60 | 0.00 | 187.53 | 1447.09 | 73.63 |

## APPENDIX-C: WELL-A SPI TOOL REPORT (RUN-2: WITH T&D MODEL)

**Username: egbepi**
**Database: EPPR**
**Date: 16/07/2021 03:35 PM**
**Saudi Aramco: Confidential**

Real-Time Stuck Pipe Index System

أرامكو السعودية
saudi aramco

**Summary Report**

| Well | Wellbore | Start Date | End Date | Casing Depth | Cut-off Weight |
|---|---|---|---|---|---|
| HRDH_1476 | HRDH_1476_1 | 04-16-2020 01:00 AM | 04-18-2020 01:00 PM | 9,498 | 100 |

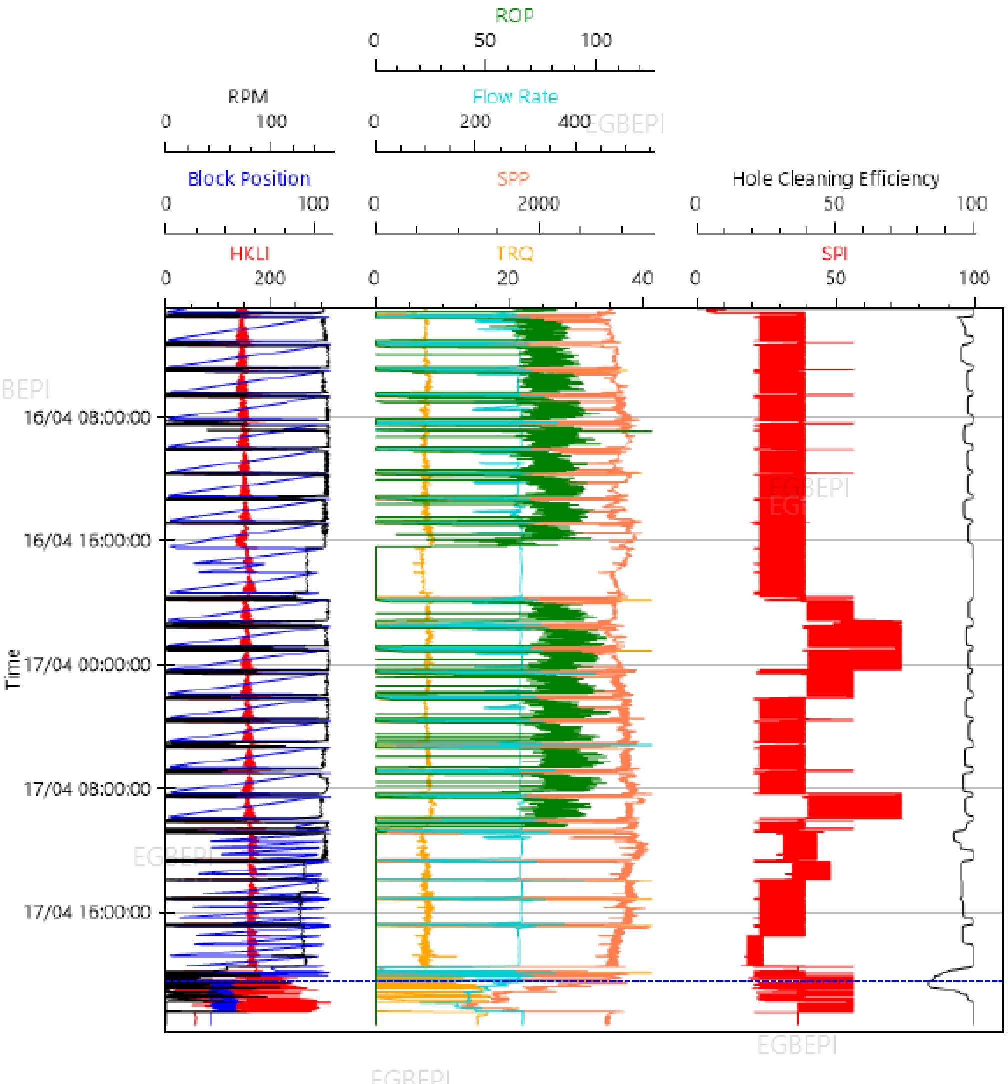

## Summary Report

| Time | Bit Depth | Hole Depth | ROP | RPM | Torque | Flow Rate | SPP | SPI |
|---|---|---|---|---|---|---|---|---|
| 4/16/2020 1:14:50 AM | 12612.70 | 12712.95 | 0.00 | 149.96 | 6.10 | 279.15 | 2820.75 | 38.63 |
| 4/16/2020 1:24:50 AM | 12694.70 | 12712.95 | 0.00 | 66.70 | 5.17 | 275.25 | 2718.47 | 38.63 |
| 4/16/2020 1:36:10 AM | 12710.20 | 12712.95 | 0.00 | 148.76 | 6.55 | 274.37 | 2742.48 | 38.63 |
| 4/16/2020 1:46:10 AM | 12717.40 | 12717.37 | 73.60 | 148.91 | 7.34 | 286.63 | 2888.78 | 38.63 |
| 4/16/2020 1:56:10 AM | 12729.20 | 12729.24 | 71.46 | 147.90 | 7.56 | 284.72 | 2828.75 | 38.63 |
| 4/16/2020 2:06:10 AM | 12740.70 | 12740.71 | 52.03 | 148.83 | 7.27 | 284.41 | 2851.87 | 38.63 |
| 4/16/2020 2:16:10 AM | 12753.30 | 12753.29 | 74.47 | 148.66 | 7.27 | 284.41 | 2848.76 | 38.63 |
| 4/16/2020 2:26:10 AM | 12766.20 | 12766.21 | 82.71 | 149.94 | 7.61 | 283.78 | 2879.45 | 38.63 |
| 4/16/2020 2:36:10 AM | 12778.70 | 12778.68 | 78.35 | 149.85 | 7.38 | 284.09 | 2841.20 | 38.63 |
| 4/16/2020 2:46:15 AM | 12791.20 | 12791.18 | 69.64 | 150.69 | 7.67 | 283.78 | 2879.00 | 38.63 |
| 4/16/2020 2:56:15 AM | 12803.70 | 12803.75 | 79.77 | 148.72 | 7.39 | 283.78 | 2893.23 | 38.63 |
| 4/16/2020 3:12:25 AM | 12772.90 | 12806.47 | 0.00 | 0.00 | 0.00 | 289.54 | 2963.94 | 56.13 |
| 4/16/2020 3:22:30 AM | 12803.50 | 12806.47 | 0.00 | 0.00 | 0.00 | 277.94 | 2015.85 | 38.63 |
| 4/16/2020 3:32:30 AM | 12807.60 | 12807.61 | 74.90 | 153.04 | 7.32 | 287.60 | 2963.49 | 38.63 |
| 4/16/2020 3:42:30 AM | 12820.10 | 12820.14 | 70.50 | 154.03 | 7.42 | 288.24 | 2928.36 | 38.63 |
| 4/16/2020 3:52:30 AM | 12832.80 | 12832.75 | 76.88 | 153.00 | 7.46 | 287.92 | 2925.25 | 38.63 |
| 4/16/2020 4:02:30 AM | 12845.90 | 12845.90 | 74.19 | 152.94 | 7.49 | 287.92 | 2919.02 | 38.63 |

## Summary Report

| Time | Bit Depth | Hole Depth | ROP | RPM | Torque | Flow Rate | SPP | SPI |
|---|---|---|---|---|---|---|---|---|
| 4/16/2020 4:12:30 AM | 12859.20 | 12859.17 | 86.28 | 152.92 | 7.67 | 287.92 | 2912.35 | 38.63 |
| 4/16/2020 4:22:35 AM | 12872.10 | 12872.14 | 88.87 | 152.94 | 7.51 | 287.92 | 2897.23 | 38.63 |
| 4/16/2020 4:32:35 AM | 12885.50 | 12885.51 | 79.57 | 153.00 | 7.47 | 287.60 | 2922.14 | 38.63 |
| 4/16/2020 4:42:35 AM | 12898.30 | 12898.28 | 73.96 | 151.91 | 7.72 | 287.92 | 2924.36 | 38.63 |
| 4/16/2020 4:55:30 AM | 12868.60 | 12901.09 | 0.00 | 5.72 | 0.00 | 285.04 | 2879.00 | 56.13 |
| 4/16/2020 5:05:50 AM | 12898.50 | 12901.09 | 0.00 | 148.95 | 6.72 | 286.31 | 2963.05 | 38.63 |
| 4/16/2020 5:15:50 AM | 12908.10 | 12908.05 | 80.26 | 148.95 | 7.66 | 285.99 | 2926.14 | 38.63 |
| 4/16/2020 5:25:50 AM | 12920.90 | 12920.90 | 79.21 | 148.85 | 7.88 | 285.36 | 2915.91 | 38.63 |
| 4/16/2020 5:35:50 AM | 12933.80 | 12933.82 | 72.38 | 148.81 | 7.75 | 285.36 | 2916.80 | 38.63 |
| 4/16/2020 5:45:50 AM | 12947.00 | 12947.05 | 80.53 | 149.94 | 7.76 | 285.67 | 2869.66 | 38.63 |
| 4/16/2020 5:55:50 AM | 12960.50 | 12960.47 | 80.48 | 149.83 | 7.60 | 285.04 | 2935.03 | 38.63 |
| 4/16/2020 6:05:50 AM | 12973.30 | 12973.33 | 91.58 | 147.71 | 7.57 | 285.04 | 2932.81 | 38.63 |
| 4/16/2020 6:15:55 AM | 12986.60 | 12986.60 | 78.40 | 150.06 | 7.67 | 284.72 | 2947.04 | 38.63 |
| 4/16/2020 6:34:10 AM | 12964.20 | 12996.34 | 0.00 | 0.32 | 0.00 | 280.98 | 2875.44 | 56.13 |
| 4/16/2020 6:44:10 AM | 12992.70 | 12992.68 | 71.09 | 152.88 | 7.14 | 285.36 | 2982.17 | 38.63 |
| 4/16/2020 6:54:10 AM | 13004.80 | 13004.78 | 74.51 | 150.76 | 7.83 | 285.04 | 2979.06 | 38.63 |
| 4/16/2020 7:04:10 AM | 13008.10 | 13008.08 | 0.00 | 151.97 | 6.63 | 289.22 | 2947.04 | 38.63 |

**Summary Report**

| Time | Bit Depth | Hole Depth | ROP | RPM | Torque | Flow Rate | SPP | SPI |
|---|---|---|---|---|---|---|---|---|
| 4/16/2020 7:14:10 AM | 13020.70 | 13020.73 | 74.10 | 151.07 | 7.52 | 288.57 | 2955.04 | 38.63 |
| 4/16/2020 7:24:10 AM | 13034.10 | 13034.10 | 73.97 | 152.96 | 7.27 | 288.89 | 2989.73 | 38.63 |
| 4/16/2020 7:34:10 AM | 13047.70 | 13047.69 | 87.37 | 150.90 | 7.79 | 291.19 | 2980.84 | 38.63 |
| 4/16/2020 7:44:10 AM | 13060.90 | 13060.95 | 75.46 | 151.91 | 7.63 | 291.19 | 2991.51 | 38.63 |
| 4/16/2020 7:54:10 AM | 13074.60 | 13074.57 | 83.14 | 151.95 | 7.53 | 293.52 | 3025.30 | 38.63 |
| 4/16/2020 8:04:35 AM | 13088.30 | 13088.27 | 75.66 | 151.83 | 7.13 | 292.85 | 3104.02 | 38.63 |
| 4/16/2020 8:23:00 AM | 13056.30 | 13089.40 | 0.00 | 0.00 | 0.00 | 291.85 | 3030.64 | 56.13 |
| 4/16/2020 8:33:00 AM | 13089.50 | 13089.55 | 39.45 | 153.99 | 7.03 | 291.52 | 3028.42 | 38.63 |
| 4/16/2020 8:43:00 AM | 13096.60 | 13096.56 | 86.96 | 154.77 | 7.25 | 289.22 | 2998.18 | 38.63 |
| 4/16/2020 8:53:50 AM | 13082.20 | 13105.27 | 0.00 | 152.92 | 6.70 | 292.85 | 3072.00 | 38.63 |
| 4/16/2020 9:03:50 AM | 13118.10 | 13118.15 | 72.68 | 151.81 | 7.47 | 292.85 | 3018.19 | 38.63 |
| 4/16/2020 9:13:50 AM | 13131.30 | 13131.28 | 80.08 | 151.93 | 7.28 | 291.52 | 3191.17 | 38.63 |
| 4/16/2020 9:23:50 AM | 13144.70 | 13144.75 | 87.50 | 154.37 | 6.76 | 292.52 | 3066.22 | 38.63 |
| 4/16/2020 9:33:50 AM | 13158.00 | 13157.98 | 81.37 | 151.87 | 7.05 | 292.52 | 3106.24 | 38.63 |
| 4/16/2020 9:43:50 AM | 13171.40 | 13171.45 | 78.82 | 152.77 | 7.28 | 292.18 | 3078.22 | 38.63 |
| 4/16/2020 9:53:50 AM | 13182.70 | 13182.72 | 4.06 | 152.94 | 6.96 | 292.52 | 3044.87 | 38.63 |
| 4/16/2020 10:03:55 AM | 13152.00 | 13182.72 | 0.00 | 0.00 | 0.00 | 285.67 | 2924.80 | 56.13 |

## Summary Report

| Time | Bit Depth | Hole Depth | ROP | RPM | Torque | Flow Rate | SPP | SPI |
|---|---|---|---|---|---|---|---|---|
| 4/16/2020 10:13:55 AM | 13183.40 | 13183.43 | 44.06 | 151.79 | 8.18 | 289.87 | 3021.75 | 38.63 |
| 4/16/2020 10:24:10 AM | 13189.70 | 13189.66 | 73.80 | 152.02 | 7.33 | 286.63 | 2975.94 | 38.63 |
| 4/16/2020 10:34:10 AM | 13202.20 | 13202.25 | 82.27 | 152.94 | 7.05 | 286.63 | 2949.71 | 38.63 |
| 4/16/2020 10:44:10 AM | 13215.40 | 13215.41 | 84.64 | 151.87 | 7.48 | 286.63 | 2962.16 | 38.63 |
| 4/16/2020 10:54:10 AM | 13228.40 | 13228.39 | 72.94 | 150.11 | 7.54 | 286.31 | 2963.49 | 38.63 |
| 4/16/2020 11:04:10 AM | 13241.80 | 13241.82 | 79.04 | 152.81 | 7.36 | 285.67 | 2871.00 | 38.63 |
| 4/16/2020 11:14:10 AM | 13255.00 | 13255.00 | 81.77 | 151.95 | 7.71 | 285.36 | 2933.70 | 38.63 |
| 4/16/2020 11:24:10 AM | 13268.00 | 13268.00 | 68.22 | 151.28 | 7.31 | 214.67 | 2181.72 | 38.63 |
| 4/16/2020 11:39:05 AM | 13243.90 | 13276.75 | 0.00 | 12.79 | 0.00 | 294.19 | 3122.25 | 56.13 |
| 4/16/2020 11:49:05 AM | 13278.40 | 13278.45 | 57.50 | 152.67 | 7.01 | 291.85 | 3088.90 | 38.63 |
| 4/16/2020 11:59:05 AM | 13285.10 | 13285.09 | 81.40 | 152.10 | 7.48 | 291.85 | 3097.34 | 38.63 |
| 4/16/2020 12:09:05 PM | 13298.10 | 13298.14 | 80.80 | 150.76 | 6.86 | 291.85 | 3041.31 | 38.63 |
| 4/16/2020 12:19:05 PM | 13311.70 | 13311.66 | 87.01 | 151.85 | 7.68 | 284.09 | 2944.81 | 38.63 |
| 4/16/2020 12:29:05 PM | 13325.20 | 13325.17 | 80.34 | 152.10 | 7.27 | 283.78 | 2940.37 | 38.63 |
| 4/16/2020 12:39:05 PM | 13339.00 | 13338.99 | 79.65 | 152.02 | 7.74 | 283.78 | 2897.68 | 38.63 |
| 4/16/2020 12:49:05 PM | 13353.20 | 13353.20 | 84.75 | 153.93 | 7.15 | 284.41 | 2883.00 | 38.63 |
| 4/16/2020 12:59:05 PM | 13366.70 | 13366.72 | 75.89 | 152.88 | 7.34 | 283.47 | 2950.60 | 38.63 |

**Summary Report**

| Time | Bit Depth | Hole Depth | ROP | RPM | Torque | Flow Rate | SPP | SPI |
|---|---|---|---|---|---|---|---|---|
| 4/16/2020 1:09:05 PM | 13339.60 | 13370.51 | 0.00 | 125.30 | 6.43 | 280.98 | 2821.19 | 38.63 |
| 4/16/2020 1:23:45 PM | 13368.60 | 13370.51 | 0.00 | 150.04 | 6.79 | 281.91 | 2951.04 | 38.63 |
| 4/16/2020 1:33:45 PM | 13374.10 | 13374.13 | 75.67 | 148.97 | 7.92 | 280.67 | 2937.26 | 38.63 |
| 4/16/2020 1:43:45 PM | 13387.40 | 13387.39 | 80.25 | 149.27 | 7.72 | 277.94 | 2835.42 | 38.63 |
| 4/16/2020 1:53:45 PM | 13400.70 | 13400.75 | 77.14 | 149.75 | 7.40 | 291.52 | 3026.64 | 38.63 |
| 4/16/2020 2:03:45 PM | 13414.50 | 13414.48 | 78.75 | 149.81 | 7.74 | 289.54 | 3042.65 | 38.63 |
| 4/16/2020 2:13:50 PM | 13428.60 | 13428.61 | 81.39 | 148.95 | 7.60 | 279.15 | 2876.78 | 38.63 |
| 4/16/2020 2:23:50 PM | 13442.60 | 13442.64 | 90.09 | 149.98 | 7.82 | 282.84 | 2920.80 | 38.63 |
| 4/16/2020 2:33:50 PM | 13456.40 | 13456.44 | 92.91 | 148.85 | 7.95 | 294.53 | 3097.34 | 38.63 |
| 4/16/2020 2:50:55 PM | 13460.50 | 13463.82 | 0.00 | 0.00 | 0.00 | 271.47 | 315.34 | 40.66 |
| 4/16/2020 3:00:55 PM | 13462.60 | 13462.58 | 72.64 | 149.73 | 7.42 | 292.52 | 3071.55 | 38.63 |
| 4/16/2020 3:10:55 PM | 13474.80 | 13474.82 | 82.75 | 152.04 | 7.95 | 292.18 | 3081.78 | 38.63 |
| 4/16/2020 3:20:55 PM | 13487.70 | 13487.66 | 74.41 | 150.11 | 7.53 | 292.52 | 3078.67 | 38.63 |
| 4/16/2020 3:30:55 PM | 13501.10 | 13501.06 | 80.47 | 148.87 | 7.79 | 310.58 | 2577.94 | 38.63 |
| 4/16/2020 3:40:55 PM | 13513.60 | 13513.61 | 78.79 | 149.79 | 8.18 | 296.57 | 3179.17 | 38.63 |
| 4/16/2020 3:51:05 PM | 13526.70 | 13526.75 | 71.80 | 149.81 | 8.62 | 296.92 | 3189.84 | 38.63 |
| 4/16/2020 4:01:05 PM | 13535.90 | 13535.87 | 53.27 | 150.00 | 8.59 | 295.55 | 3100.46 | 38.63 |

## Summary Report

| Time | Bit Depth | Hole Depth | ROP | RPM | Torque | Flow Rate | SPP | SPI |
|---|---|---|---|---|---|---|---|---|
| 4/16/2020 4:11:05 PM | 13546.40 | 13546.36 | 73.14 | 149.81 | 7.98 | 292.18 | 3039.09 | 38.63 |
| 4/16/2020 4:21:05 PM | 13556.40 | 13556.41 | 54.48 | 149.92 | 8.38 | 292.18 | 3012.41 | 38.63 |
| 4/16/2020 4:31:05 PM | 13455.30 | 13558.36 | 0.00 | 133.59 | 6.79 | 291.52 | 3146.71 | 38.63 |
| 4/16/2020 4:41:05 PM | 13469.60 | 13558.36 | 0.00 | 133.45 | 6.87 | 291.85 | 3049.76 | 38.63 |
| 4/16/2020 4:51:05 PM | 13484.80 | 13558.36 | 0.00 | 133.57 | 6.84 | 291.85 | 3102.24 | 38.63 |
| 4/16/2020 5:01:05 PM | 13500.40 | 13558.36 | 0.00 | 133.63 | 6.85 | 291.85 | 3064.88 | 38.63 |
| 4/16/2020 5:11:05 PM | 13516.10 | 13558.36 | 0.00 | 133.55 | 6.84 | 292.18 | 3041.31 | 38.63 |
| 4/16/2020 5:21:05 PM | 13531.90 | 13558.36 | 0.00 | 133.40 | 6.87 | 292.52 | 3040.42 | 38.63 |
| 4/16/2020 5:31:05 PM | 13495.30 | 13558.36 | 0.00 | 133.38 | 6.84 | 292.85 | 3037.76 | 38.63 |
| 4/16/2020 5:41:05 PM | 13508.20 | 13558.36 | 0.00 | 134.33 | 6.83 | 292.85 | 3013.30 | 38.63 |
| 4/16/2020 5:51:05 PM | 13521.60 | 13558.36 | 0.00 | 133.38 | 7.00 | 292.85 | 2931.03 | 38.63 |
| 4/16/2020 6:01:05 PM | 13535.50 | 13558.36 | 0.00 | 133.57 | 7.04 | 293.18 | 2914.13 | 38.63 |
| 4/16/2020 6:11:05 PM | 13464.40 | 13558.36 | 0.00 | 133.51 | 7.04 | 292.18 | 2897.23 | 38.63 |
| 4/16/2020 6:21:05 PM | 13477.70 | 13558.36 | 0.00 | 133.47 | 7.15 | 291.85 | 2900.79 | 38.63 |
| 4/16/2020 6:31:05 PM | 13491.60 | 13558.36 | 0.00 | 133.84 | 7.28 | 291.85 | 2894.56 | 38.63 |
| 4/16/2020 6:41:05 PM | 13505.50 | 13558.36 | 0.00 | 133.47 | 7.06 | 291.85 | 2918.58 | 38.63 |
| 4/16/2020 6:51:05 PM | 13520.10 | 13558.36 | 0.00 | 133.61 | 7.19 | 291.19 | 2914.13 | 38.63 |

## Summary Report

| Time | Bit Depth | Hole Depth | ROP | RPM | Torque | Flow Rate | SPP | SPI |
|---|---|---|---|---|---|---|---|---|
| 4/16/2020 7:01:05 PM | 13534.50 | 13558.36 | 0.00 | 133.53 | 7.17 | 291.52 | 2952.82 | 38.63 |
| 4/16/2020 7:11:05 PM | 13548.90 | 13558.36 | 0.00 | 134.49 | 6.84 | 291.19 | 2953.26 | 38.63 |
| 4/16/2020 7:21:05 PM | 13458.10 | 13558.36 | 0.00 | 120.23 | 7.90 | 292.52 | 3001.74 | 38.63 |
| 4/16/2020 7:39:25 PM | 13511.20 | 13558.36 | 0.00 | 21.14 | 0.00 | 292.52 | 2972.83 | 56.13 |
| 4/16/2020 7:52:15 PM | 13556.60 | 13558.36 | 0.00 | 148.78 | 7.27 | 292.85 | 2984.39 | 56.13 |
| 4/16/2020 8:02:40 PM | 13562.10 | 13562.08 | 71.69 | 152.98 | 8.18 | 289.22 | 2898.57 | 56.13 |
| 4/16/2020 8:12:40 PM | 13575.00 | 13574.99 | 78.60 | 152.79 | 7.90 | 288.89 | 2913.69 | 56.13 |
| 4/16/2020 8:22:40 PM | 13588.20 | 13588.23 | 80.56 | 152.48 | 8.17 | 288.24 | 2895.45 | 56.13 |
| 4/16/2020 8:32:40 PM | 13601.70 | 13601.67 | 81.55 | 153.02 | 8.36 | 288.57 | 2931.03 | 56.13 |
| 4/16/2020 8:42:40 PM | 13615.70 | 13615.67 | 82.23 | 153.04 | 8.19 | 288.57 | 2901.23 | 56.13 |
| 4/16/2020 8:52:40 PM | 13629.50 | 13629.52 | 83.82 | 153.23 | 8.16 | 288.24 | 2908.35 | 56.13 |
| 4/16/2020 9:02:45 PM | 13643.80 | 13643.80 | 81.31 | 152.86 | 7.62 | 288.57 | 2928.36 | 56.13 |
| 4/16/2020 9:13:00 PM | 13555.50 | 13652.16 | 0.00 | 131.35 | 6.72 | 283.15 | 2834.09 | 73.63 |
| 4/16/2020 9:26:05 PM | 13616.10 | 13652.16 | 0.00 | 14.91 | 0.00 | 292.52 | 2789.17 | 73.63 |
| 4/16/2020 9:36:05 PM | 13650.80 | 13652.16 | 0.00 | 150.80 | 6.83 | 287.92 | 2903.01 | 73.63 |
| 4/16/2020 9:46:05 PM | 13659.30 | 13659.31 | 90.34 | 149.90 | 7.95 | 291.19 | 2954.15 | 73.63 |
| 4/16/2020 9:56:05 PM | 13673.40 | 13673.44 | 85.40 | 150.88 | 7.80 | 292.18 | 2822.08 | 73.63 |

## Summary Report

| Time | Bit Depth | Hole Depth | ROP | RPM | Torque | Flow Rate | SPP | SPI |
|---|---|---|---|---|---|---|---|---|
| 4/16/2020 10:06:05 PM | 13688.10 | 13688.11 | 99.91 | 151.87 | 8.14 | 292.18 | 2853.65 | 73.63 |
| 4/16/2020 10:16:05 PM | 13702.90 | 13702.87 | 87.05 | 151.09 | 7.86 | 291.52 | 2929.70 | 73.63 |
| 4/16/2020 10:26:10 PM | 13718.10 | 13718.12 | 88.64 | 150.84 | 8.21 | 291.52 | 2938.59 | 73.63 |
| 4/16/2020 10:36:10 PM | 13732.50 | 13732.53 | 88.42 | 150.88 | 7.96 | 290.86 | 2995.07 | 73.63 |
| 4/16/2020 10:46:10 PM | 13747.30 | 13747.29 | 93.03 | 152.10 | 7.97 | 289.54 | 2911.02 | 73.63 |
| 4/16/2020 10:59:55 PM | 13712.80 | 13747.99 | 0.00 | 134.39 | 7.65 | 289.54 | 2842.09 | 73.63 |
| 4/16/2020 11:09:55 PM | 13744.70 | 13744.66 | 70.81 | 151.85 | 7.88 | 291.85 | 2866.10 | 73.63 |
| 4/16/2020 11:19:55 PM | 13758.50 | 13758.53 | 74.87 | 153.74 | 7.69 | 215.58 | 2215.52 | 73.63 |
| 4/16/2020 11:29:55 PM | 13773.00 | 13773.03 | 80.82 | 153.93 | 7.74 | 294.53 | 2888.78 | 73.63 |
| 4/16/2020 11:39:55 PM | 13788.00 | 13788.05 | 82.00 | 153.09 | 7.88 | 294.19 | 2928.81 | 73.63 |
| 4/16/2020 11:50:00 PM | 13802.80 | 13802.80 | 78.16 | 153.97 | 7.67 | 293.86 | 2959.49 | 73.63 |
| 4/17/2020 12:00:00 AM | 13816.40 | 13816.43 | 93.20 | 153.40 | 7.64 | 293.86 | 2978.61 | 73.63 |
| 4/17/2020 12:10:10 AM | 13830.70 | 13830.69 | 87.94 | 152.88 | 7.34 | 214.85 | 2212.41 | 73.63 |
| 4/17/2020 12:20:10 AM | 13769.60 | 13841.64 | 0.00 | 152.94 | 6.05 | 294.87 | 2842.98 | 73.63 |
| 4/17/2020 12:32:15 AM | 13838.90 | 13841.64 | 0.00 | 0.00 | 0.00 | 287.60 | 44.53 | 56.13 |
| 4/17/2020 12:42:15 AM | 13841.90 | 13841.94 | 69.64 | 151.91 | 7.65 | 291.19 | 2989.28 | 56.13 |
| 4/17/2020 12:52:15 AM | 13850.30 | 13850.27 | 83.29 | 152.90 | 7.89 | 287.27 | 2961.27 | 56.13 |

**Summary Report**

| Time | Bit Depth | Hole Depth | ROP | RPM | Torque | Flow Rate | SPP | SPI |
|---|---|---|---|---|---|---|---|---|
| 4/17/2020 1:02:15 AM | 13863.70 | 13863.66 | 81.53 | 151.85 | 8.05 | 287.60 | 2909.24 | 56.13 |
| 4/17/2020 1:12:15 AM | 13877.40 | 13877.39 | 78.50 | 152.90 | 7.76 | 287.60 | 2967.94 | 56.13 |
| 4/17/2020 1:22:15 AM | 13891.70 | 13891.65 | 88.43 | 153.90 | 8.00 | 286.63 | 2956.82 | 56.13 |
| 4/17/2020 1:32:15 AM | 13905.70 | 13905.74 | 85.32 | 150.82 | 7.61 | 286.95 | 2955.49 | 56.13 |
| 4/17/2020 1:42:15 AM | 13920.00 | 13920.02 | 87.23 | 152.14 | 7.46 | 286.63 | 2944.81 | 56.13 |
| 4/17/2020 1:52:15 AM | 13934.00 | 13934.04 | 87.81 | 151.87 | 7.67 | 290.86 | 3049.32 | 56.13 |
| 4/17/2020 2:04:55 AM | 13899.60 | 13934.90 | 0.00 | 8.17 | 0.00 | 287.27 | 3011.07 | 56.13 |
| 4/17/2020 2:15:35 AM | 13932.50 | 13932.50 | 64.79 | 152.94 | 7.38 | 290.86 | 3026.19 | 38.63 |
| 4/17/2020 2:25:35 AM | 13945.20 | 13945.20 | 75.29 | 152.92 | 7.37 | 290.53 | 3067.55 | 38.63 |
| 4/17/2020 2:35:35 AM | 13958.30 | 13958.34 | 75.97 | 154.01 | 7.28 | 290.53 | 3059.10 | 38.63 |
| 4/17/2020 2:45:50 AM | 13972.30 | 13972.34 | 78.23 | 153.02 | 7.23 | 228.03 | 2533.03 | 38.63 |
| 4/17/2020 2:55:50 AM | 13986.60 | 13986.56 | 76.82 | 153.88 | 7.26 | 288.57 | 3032.86 | 38.63 |
| 4/17/2020 3:06:35 AM | 14001.90 | 14001.86 | 91.62 | 152.94 | 7.56 | 288.89 | 3012.85 | 38.63 |
| 4/17/2020 3:16:35 AM | 14016.10 | 14016.07 | 86.07 | 153.04 | 7.91 | 288.24 | 3072.89 | 38.63 |
| 4/17/2020 3:35:40 AM | 13996.20 | 14029.81 | 0.00 | 7.92 | 0.00 | 289.54 | 2997.29 | 56.13 |
| 4/17/2020 3:45:40 AM | 14027.20 | 14027.19 | 63.54 | 151.76 | 7.27 | 288.89 | 3083.11 | 38.63 |
| 4/17/2020 3:55:40 AM | 14040.30 | 14040.26 | 76.93 | 153.04 | 7.44 | 289.22 | 3010.18 | 38.63 |

**Summary Report**

| Time | Bit Depth | Hole Depth | ROP | RPM | Torque | Flow Rate | SPP | SPI |
|---|---|---|---|---|---|---|---|---|
| 4/17/2020 4:05:40 AM | 14053.70 | 14053.74 | 81.01 | 151.70 | 7.47 | 289.87 | 2955.04 | 38.63 |
| 4/17/2020 4:15:40 AM | 14067.50 | 14067.53 | 84.04 | 151.74 | 7.97 | 289.54 | 3002.63 | 38.63 |
| 4/17/2020 4:25:40 AM | 14081.70 | 14081.67 | 92.24 | 150.30 | 8.13 | 288.57 | 3014.19 | 38.63 |
| 4/17/2020 4:35:40 AM | 14095.70 | 14095.69 | 85.33 | 152.44 | 7.75 | 288.57 | 3071.11 | 38.63 |
| 4/17/2020 4:45:40 AM | 14110.00 | 14109.96 | 76.88 | 151.81 | 7.75 | 288.24 | 3108.46 | 38.63 |
| 4/17/2020 4:55:40 AM | 14123.70 | 14123.73 | 80.96 | 151.83 | 7.59 | 288.24 | 3059.99 | 38.63 |
| 4/17/2020 5:13:00 AM | 14088.90 | 14124.84 | 0.00 | 112.76 | 7.90 | 272.04 | 2811.85 | 38.63 |
| 4/17/2020 5:25:15 AM | 14122.10 | 14124.84 | 0.00 | 148.89 | 7.03 | 288.89 | 3099.57 | 38.63 |
| 4/17/2020 5:35:15 AM | 14130.90 | 14130.86 | 92.78 | 150.84 | 7.67 | 289.22 | 3066.22 | 38.63 |
| 4/17/2020 5:45:15 AM | 14144.80 | 14144.75 | 100.50 | 149.83 | 7.98 | 288.89 | 2988.39 | 38.63 |
| 4/17/2020 5:55:15 AM | 14158.80 | 14158.77 | 78.15 | 148.72 | 8.02 | 288.89 | 3066.22 | 38.63 |
| 4/17/2020 6:05:25 AM | 14173.40 | 14173.39 | 84.28 | 149.90 | 8.02 | 288.89 | 3022.19 | 38.63 |
| 4/17/2020 6:15:25 AM | 14187.70 | 14187.74 | 87.59 | 148.91 | 7.87 | 288.57 | 3052.43 | 38.63 |
| 4/17/2020 6:25:30 AM | 14202.10 | 14202.07 | 86.64 | 150.06 | 7.68 | 288.57 | 3026.64 | 38.63 |
| 4/17/2020 6:35:30 AM | 14216.40 | 14216.37 | 76.00 | 148.78 | 7.65 | 288.89 | 3066.66 | 38.63 |
| 4/17/2020 6:50:30 AM | 14187.10 | 14218.33 | 0.00 | 6.87 | 0.00 | 288.89 | 3088.45 | 56.13 |
| 4/17/2020 7:01:05 AM | 14215.60 | 14218.33 | 0.00 | 0.00 | 0.00 | 247.14 | 947.70 | 38.63 |

Real-Time Stuck Pipe Index System

## Summary Report

| Time | Bit Depth | Hole Depth | ROP | RPM | Torque | Flow Rate | SPP | SPI |
|---|---|---|---|---|---|---|---|---|
| 4/17/2020 7:11:05 AM | 14222.90 | 14222.91 | 75.02 | 145.53 | 8.39 | 293.86 | 3125.81 | 38.63 |
| 4/17/2020 7:21:05 AM | 14237.10 | 14237.07 | 76.47 | 145.62 | 8.18 | 291.52 | 3020.86 | 38.63 |
| 4/17/2020 7:31:10 AM | 14251.40 | 14251.45 | 81.03 | 151.89 | 7.96 | 291.19 | 3067.11 | 38.63 |
| 4/17/2020 7:41:10 AM | 14266.30 | 14266.27 | 92.39 | 151.74 | 8.18 | 289.22 | 3149.82 | 38.63 |
| 4/17/2020 7:51:10 AM | 14280.70 | 14280.71 | 84.29 | 151.93 | 7.98 | 290.53 | 3060.88 | 38.63 |
| 4/17/2020 8:01:10 AM | 14294.80 | 14294.76 | 90.05 | 151.83 | 8.17 | 290.53 | 3149.37 | 38.63 |
| 4/17/2020 8:19:50 AM | 14228.70 | 14313.07 | 0.00 | 150.00 | 6.69 | 287.92 | 3293.01 | 73.63 |
| 4/17/2020 8:33:25 AM | 14310.30 | 14313.07 | 0.00 | 0.00 | 0.00 | 323.09 | 1333.69 | 73.63 |
| 4/17/2020 8:43:25 AM | 14317.90 | 14317.86 | 80.77 | 146.64 | 8.07 | 296.23 | 3281.89 | 73.63 |
| 4/17/2020 8:53:25 AM | 14331.20 | 14331.24 | 83.01 | 146.79 | 8.41 | 296.23 | 3274.33 | 73.63 |
| 4/17/2020 9:03:25 AM | 14344.90 | 14344.94 | 81.37 | 146.77 | 8.60 | 288.24 | 3069.77 | 73.63 |
| 4/17/2020 9:13:25 AM | 14358.50 | 14358.53 | 97.48 | 146.79 | 8.43 | 288.24 | 3083.56 | 73.63 |
| 4/17/2020 9:23:25 AM | 14371.70 | 14371.69 | 76.90 | 146.90 | 8.16 | 288.24 | 3087.12 | 73.63 |
| 4/17/2020 9:33:45 AM | 14385.30 | 14385.30 | 84.77 | 147.76 | 8.18 | 287.92 | 3085.34 | 73.63 |
| 4/17/2020 9:43:45 AM | 14398.80 | 14398.84 | 82.31 | 147.76 | 8.02 | 287.92 | 3096.46 | 73.63 |
| 4/17/2020 9:53:45 AM | 14345.40 | 14408.57 | 0.00 | 146.88 | 6.51 | 287.60 | 2992.40 | 73.63 |
| 4/17/2020 10:07:40 AM | 14377.40 | 14408.57 | 0.00 | 0.00 | 0.00 | 290.20 | 3090.23 | 56.13 |

**Summary Report**

| Time | Bit Depth | Hole Depth | ROP | RPM | Torque | Flow Rate | SPP | SPI |
|---|---|---|---|---|---|---|---|---|
| 4/17/2020 10:17:40 AM | 14404.50 | 14404.48 | 71.81 | 152.02 | 7.49 | 292.85 | 3124.47 | 38.63 |
| 4/17/2020 10:36:35 AM | 14409.30 | 14416.00 | 0.00 | 0.00 | 0.00 | 292.52 | 3074.67 | 56.13 |
| 4/17/2020 10:46:35 AM | 14399.00 | 14416.00 | 0.00 | 0.00 | 0.00 | 163.71 | 138.80 | 45.60 |
| 4/17/2020 10:56:40 AM | 14406.90 | 14416.10 | 0.00 | 149.98 | 7.16 | 290.86 | 3096.01 | 42.89 |
| 4/17/2020 11:06:40 AM | 14357.30 | 14416.10 | 0.00 | 149.83 | 6.95 | 290.86 | 3157.82 | 42.89 |
| 4/17/2020 11:16:40 AM | 14388.70 | 14416.10 | 0.00 | 149.90 | 7.07 | 293.18 | 3132.03 | 42.89 |
| 4/17/2020 11:26:40 AM | 14338.10 | 14416.10 | 0.00 | 149.88 | 7.09 | 294.87 | 3131.59 | 42.89 |
| 4/17/2020 11:36:40 AM | 14368.90 | 14416.10 | 0.00 | 149.90 | 7.10 | 294.19 | 3169.38 | 42.89 |
| 4/17/2020 11:46:40 AM | 14399.80 | 14416.10 | 0.00 | 149.81 | 7.29 | 294.19 | 3183.62 | 42.89 |
| 4/17/2020 11:56:40 AM | 14350.50 | 14416.10 | 0.00 | 148.95 | 7.17 | 294.19 | 3303.68 | 42.89 |
| 4/17/2020 12:06:40 PM | 14381.00 | 14416.10 | 0.00 | 150.80 | 7.07 | 293.86 | 3233.42 | 42.89 |
| 4/17/2020 12:16:40 PM | 14338.00 | 14416.10 | 0.00 | 148.85 | 7.50 | 291.85 | 3218.75 | 42.89 |
| 4/17/2020 12:26:40 PM | 14356.20 | 14416.10 | 0.00 | 149.92 | 7.56 | 291.85 | 3208.52 | 42.89 |
| 4/17/2020 12:45:50 PM | 14332.40 | 14416.10 | 0.00 | 131.41 | 8.01 | 309.08 | 2710.02 | 47.82 |
| 4/17/2020 12:55:50 PM | 14247.50 | 14416.10 | 0.00 | 130.42 | 7.81 | 289.22 | 3090.23 | 47.82 |
| 4/17/2020 1:06:20 PM | 14267.10 | 14416.10 | 0.00 | 129.63 | 7.43 | 288.57 | 3044.43 | 47.82 |
| 4/17/2020 1:16:20 PM | 14286.20 | 14416.10 | 0.00 | 129.58 | 7.42 | 288.89 | 3058.66 | 47.82 |

## Summary Report

| Time | Bit Depth | Hole Depth | ROP | RPM | Torque | Flow Rate | SPP | SPI |
|---|---|---|---|---|---|---|---|---|
| 4/17/2020 1:26:20 PM | 14305.30 | 14416.10 | 0.00 | 131.41 | 7.77 | 289.22 | 3059.10 | 47.82 |
| 4/17/2020 1:36:20 PM | 14235.70 | 14416.10 | 0.00 | 131.51 | 7.13 | 288.89 | 3010.18 | 47.82 |
| 4/17/2020 1:46:20 PM | 14254.10 | 14416.10 | 0.00 | 129.44 | 7.16 | 289.22 | 3015.08 | 47.82 |
| 4/17/2020 1:58:10 PM | 14234.80 | 14416.10 | 0.00 | 7.67 | 0.00 | 257.57 | 6.28 | 38.63 |
| 4/17/2020 2:08:10 PM | 14140.60 | 14416.10 | 0.00 | 141.76 | 7.59 | 294.19 | 3087.12 | 38.63 |
| 4/17/2020 2:18:10 PM | 14156.20 | 14416.10 | 0.00 | 143.27 | 7.06 | 293.52 | 3105.79 | 38.63 |
| 4/17/2020 2:28:10 PM | 14171.90 | 14416.10 | 0.00 | 142.74 | 7.85 | 293.86 | 3068.88 | 38.63 |
| 4/17/2020 2:38:10 PM | 14188.80 | 14416.10 | 0.00 | 142.80 | 7.55 | 293.86 | 3144.93 | 38.63 |
| 4/17/2020 2:48:10 PM | 14133.70 | 14416.10 | 0.00 | 126.42 | 7.31 | 294.53 | 3126.25 | 38.63 |
| 4/17/2020 2:58:10 PM | 14167.10 | 14416.10 | 0.00 | 126.98 | 7.50 | 294.53 | 3130.25 | 38.63 |
| 4/17/2020 3:10:15 PM | 14134.60 | 14416.10 | 0.00 | 8.91 | 0.00 | 167.23 | 0.00 | 38.63 |
| 4/17/2020 3:20:15 PM | 14052.60 | 14416.10 | 0.00 | 126.52 | 7.80 | 291.52 | 3083.11 | 38.63 |
| 4/17/2020 3:30:15 PM | 14083.10 | 14416.10 | 0.00 | 127.44 | 7.37 | 293.18 | 3009.74 | 38.63 |
| 4/17/2020 3:40:15 PM | 14114.20 | 14416.10 | 0.00 | 126.69 | 8.13 | 292.18 | 3010.63 | 38.63 |
| 4/17/2020 3:50:15 PM | 14047.30 | 14416.10 | 0.00 | 125.60 | 7.80 | 292.18 | 3119.58 | 38.63 |
| 4/17/2020 4:00:15 PM | 14075.40 | 14416.10 | 0.00 | 126.54 | 7.94 | 292.52 | 3083.11 | 38.63 |
| 4/17/2020 4:10:15 PM | 14103.70 | 14416.10 | 0.00 | 126.37 | 7.51 | 291.52 | 3117.80 | 38.63 |

Real-Time Stuck Pipe Index System

أرامكو السعودية
saudi aramco

**Summary Report**

| Time | Bit Depth | Hole Depth | ROP | RPM | Torque | Flow Rate | SPP | SPI |
|---|---|---|---|---|---|---|---|---|
| 4/17/2020 4:20:15 PM | 14105.70 | 14416.10 | 0.00 | 126.33 | 6.67 | 293.18 | 2933.25 | 38.63 |
| 4/17/2020 4:30:35 PM | 14057.70 | 14416.10 | 0.00 | 126.50 | 7.68 | 292.85 | 3103.57 | 38.63 |
| 4/17/2020 4:40:35 PM | 14086.00 | 14416.10 | 0.00 | 126.29 | 7.56 | 291.85 | 3095.57 | 38.63 |
| 4/17/2020 4:52:10 PM | 14032.10 | 14416.10 | 0.00 | 1.52 | 0.00 | 309.45 | 32.07 | 38.63 |
| 4/17/2020 5:02:15 PM | 13945.90 | 14416.10 | 0.00 | 129.67 | 7.50 | 285.36 | 2975.50 | 38.63 |
| 4/17/2020 5:12:15 PM | 13970.90 | 14416.10 | 0.00 | 128.54 | 7.86 | 285.04 | 2936.81 | 38.63 |
| 4/17/2020 5:22:15 PM | 13996.30 | 14416.10 | 0.00 | 128.49 | 7.65 | 285.04 | 2944.81 | 38.63 |
| 4/17/2020 5:32:25 PM | 13934.00 | 14416.10 | 0.00 | 128.62 | 7.51 | 287.60 | 2923.02 | 23.80 |
| 4/17/2020 5:42:25 PM | 13958.50 | 14416.10 | 0.00 | 128.45 | 7.36 | 286.63 | 2891.90 | 23.80 |
| 4/17/2020 5:52:30 PM | 13983.80 | 14416.10 | 0.00 | 129.50 | 7.02 | 287.27 | 2951.49 | 23.80 |
| 4/17/2020 6:02:30 PM | 14009.00 | 14416.10 | 0.00 | 129.44 | 7.65 | 286.95 | 2978.17 | 23.80 |
| 4/17/2020 6:12:30 PM | 13941.40 | 14416.10 | 0.00 | 129.46 | 7.75 | 286.63 | 2928.36 | 23.80 |
| 4/17/2020 6:22:35 PM | 13966.70 | 14416.10 | 0.00 | 129.52 | 7.22 | 286.95 | 2927.03 | 23.80 |
| 4/17/2020 6:32:45 PM | 13991.90 | 14416.10 | 0.00 | 128.49 | 8.03 | 286.63 | 2851.87 | 23.80 |
| 4/17/2020 6:42:45 PM | 14017.20 | 14416.10 | 0.00 | 128.56 | 7.94 | 286.63 | 2862.55 | 23.80 |
| 4/17/2020 6:52:45 PM | 13934.70 | 14416.10 | 0.00 | 132.63 | 7.30 | 286.31 | 2849.65 | 23.80 |
| 4/17/2020 7:02:45 PM | 13960.10 | 14416.10 | 0.00 | 130.47 | 7.02 | 287.27 | 2940.37 | 23.80 |

**Summary Report**



| Time | Bit Depth | Hole Depth | ROP | RPM | Torque | Flow Rate | SPP | SPI |
|---|---|---|---|---|---|---|---|---|
| 4/17/2020 7:12:45 PM | 13986.20 | 14416.10 | 0.00 | 132.65 | 7.89 | 286.31 | 2913.69 | 23.80 |
| 4/17/2020 7:32:25 PM | 13948.10 | 14416.10 | 0.00 | 128.30 | 6.45 | 285.67 | 3039.98 | 56.13 |
| 4/17/2020 7:56:40 PM | 13911.10 | 14416.10 | 0.00 | 0.00 | 0.00 | 293.18 | 3007.07 | 56.13 |
| 4/17/2020 8:07:00 PM | 13828.70 | 14416.10 | 0.00 | 26.76 | 13.15 | 291.19 | 2889.67 | 56.13 |
| 4/17/2020 8:17:05 PM | 13827.50 | 14416.10 | 0.00 | 0.00 | 13.36 | 291.52 | 2914.13 | 56.13 |
| 4/17/2020 8:30:25 PM | 13834.30 | 14416.10 | 0.00 | 29.45 | 5.32 | 291.19 | 2651.32 | 56.13 |
| 4/17/2020 8:40:25 PM | 13827.70 | 14416.10 | 0.00 | 22.19 | 3.22 | 251.26 | 2355.60 | 56.13 |
| 4/17/2020 8:50:55 PM | 13826.90 | 14416.10 | 0.00 | 0.00 | 16.28 | 219.83 | 2020.30 | 56.13 |
| 4/17/2020 9:02:45 PM | 13814.30 | 14416.10 | 0.00 | 0.00 | 15.86 | 224.05 | 1861.54 | 56.13 |
| 4/17/2020 9:14:25 PM | 13811.10 | 14416.10 | 0.00 | 0.00 | 0.00 | 187.12 | 1628.97 | 56.13 |
| 4/17/2020 9:31:10 PM | 13797.70 | 14416.10 | 0.00 | 4.60 | 0.00 | 187.53 | 1447.09 | 56.13 |
| 4/17/2020 9:42:00 PM | 13795.20 | 14416.10 | 0.00 | 0.00 | 0.00 | 188.21 | 1576.49 | 56.13 |
| 4/17/2020 9:52:00 PM | 13790.60 | 14416.10 | 0.00 | 0.00 | 0.00 | 189.19 | 1444.86 | 56.13 |
| 4/17/2020 10:04:45 PM | 13787.30 | 14416.10 | 0.00 | 0.00 | 0.00 | 163.19 | 1198.50 | 56.13 |
| 4/17/2020 10:18:20 PM | 13861.80 | 14416.10 | 0.00 | 0.00 | 0.00 | 198.25 | 1688.56 | 56.13 |
| 4/17/2020 10:28:20 PM | 13872.30 | 14416.10 | 0.00 | 0.00 | 16.74 | 295.55 | 2874.11 | 36.40 |
| 4/17/2020 10:38:20 PM | 13872.30 | 14416.10 | 0.00 | 0.00 | 16.77 | 295.55 | 2881.67 | 36.40 |

**Summary Report**



| Time | Bit Depth | Hole Depth | ROP | RPM | Torque | Flow Rate | SPP | SPI |
|---|---|---|---|---|---|---|---|---|
| 4/17/2020 10:48:20 PM | 13872.30 | 14416.10 | 0.00 | 0.34 | 15.21 | 295.55 | 2843.87 | 36.40 |
| 4/17/2020 10:58:20 PM | 13872.30 | 14416.10 | 0.00 | 0.00 | 15.24 | 295.21 | 2806.52 | 36.40 |
| 4/17/2020 11:08:20 PM | 13872.30 | 14416.10 | 0.00 | 0.00 | 15.24 | 295.55 | 2822.97 | 36.40 |
| 4/17/2020 11:18:20 PM | 13872.30 | 14416.10 | 0.00 | 0.00 | 15.23 | 294.87 | 2838.98 | 36.40 |

## APPENDIX-D: SAMPLE CALCULATIONS FOR CRV USING RESEARCH MODELS AND DUAN ET AL. (2009) DATA

i. A flow rate of 200 GPM (0.0126 $m^3/s$) is assumed based on Duan et al. (2009) experimental data. The estimated average annular fluid velocity is 0.56 m/s (or 1.71 ft/s)

ii. The hydraulic diameter ($D_{hyd}$) is estimated using equation 4.94 as follows:

$$\frac{4A_f}{S_o + S_i + S_b}$$

a. The fluid open flow area ($A_f$) is calculated from the difference between the previously calculated annulus cross-section area ($A_{ann} = 0.0222\, m^2$) and the cuttings bed area ($A_{bed}$)

b. The cuttings bed area ($A_{bed}$) can be estimated as a function of the flow rate ($Q_{pump} = 0.0126\, m^3/s$), and the critical flow rate ($Q_{crit} = 0.0437\, m^3/s$) required to prevent a cuttings bed build up. The expression from Larsen et al. (1997) is used as follows:

$$A_{bed} = A_{ann}\left(1 - \frac{Q_{pump}}{Q_{crit}}\right) = 0.0158\ m^2 \qquad \text{Eqn. D-1}$$

c. The fluid open flow area ($A_f$) is thus estimated as

$$A_f = 0.0222 - 0.0158 = 0.0064\, m^2$$

d. The wetted perimeters ($S_o, S_i, S_b$) of the wellbore, drill pipe, and cuttings bed are estimated using the expressions by Duan et al. (2009) and using a 50% eccentricity (e = 0.5). Duan et al. (2009) presented a relationship for eccentricity as follows:

$$e = \frac{a}{R-r} \qquad \text{Eqn. D-2}$$

Where a, R, and r are the offset distance between the centre of the wellbore and centre of the drill pipe, wellbore radius, and drill pipe radius, respectively. Based on e = 0.5, the offset distance, “a” is estimated as 0.02225 m.

For the direction of the eccentricity, Duan et al. (2009) proposed the following expression for the vertical offset component ($a_v$) which is used to estimate the minimum and maximum bed height (h)

$a_v = (R - r)eCos\beta = vertical\ offset\ component$ (0≤e≤1, 0≤β≤2π) Eqn. D-3

The minimum ($h_{low}$) and maximum ($h_{high}$) possible bed heights are defined as follows:

$$h_{low} = R - r - a_v \qquad \text{Eqn. D-4}$$

$$h_{high} = R + r - a_v \qquad \text{Eqn. D-5}$$

As Cosβ ≈1 for all cases of β, the expression for $a_v$ simplifies to

$$a_v = (R - r)e \qquad \text{Eqn. D-6}$$

And the minimum and maximum possible bed heights become

$$h_{low} = R - r - e(R - r) \qquad \text{Eqn. D-7}$$

$$h_{high} = R + r - e(R - r) \qquad \text{Eqn. D-8}$$

Substituting for values yields.

$$h_{low} = 0.0225m\ and\ h_{high} = 0.1363m\ respectively$$

Recall that the bed area ($A_{bed}$) was calculated as 0.0158 $m^2$. Hence the height of the cuttings bed can be estimated by iteratively solving the below transcendental equation

$$A_{bed} = R^2 \cos^{-1}\left(\frac{R-h}{R}\right) - (R-h)\sqrt{2Rh - h^2} \qquad \text{Eqn. D-9}$$

And the cuttings bed height, h, is estimated as 0.112m by iteration. Thus, implying that $h_{low} < h = 0.112m < h_{high}$

Depending on the bed height, Duan et al. (2009) proposed different sets of equations for estimating the wetted perimeters. For the case under review, the wetted perimeters are estimated using the below sets of equation. For other cases ($h \leq h_{low}\ and\ h \geq h_{high}$), refer to Duan et al. (2009).

$$S_o = 2R\cos^{-1}\left(\frac{h-R}{R}\right) = 17.065 \qquad \text{Eqn. D-10}$$

$$S_i = 2R\cos^{-1}\left(\frac{h-R+a_v}{r}\right) = 11.151 \qquad \text{Eqn. D-11}$$

$$S_b = 2\sqrt{R^2 - (R-h)^2} - 2\sqrt{r^2 - (R-h-a_v)^2} = 0.1001 \qquad \text{Eqn. D-12}$$

e. Based on (a) – (e) above, the hydraulic diameter ($D_{hyd}$) is estimated as 0.00055

iii. Estimate the generalized Reynold's number and the Taylor's number to determine the flow regime (laminar or turbulent) at 200 GPM

f. The generalized Reynold's number is estimated using equation 4.95 as follows:

$$R_e^g = \frac{D_{hyd}^n \rho_h U^{2-n}}{8^{n-1}K} = 782$$

$$n = 0.72; K = 0.0254; U = 1.97\, m/s\,;\ \rho_h = 1022.27\ \ kg/m^3$$

The Taylor's number is estimated using equation 3.1 as follows (Taylor, 1923):

$$T_a = \frac{\omega^2 r_i (r_o - r_i)^3}{\gamma^2} = 1.014$$

$$\gamma = \frac{\mu}{\rho} = 0.000027\ m^2/s\,;\ \omega = 2.33\,rev/s\ (i.e.\,140\ RPM)$$

Based on the Reynold's and Taylor's number, flow is laminar

iv. The bed friction factor ($f_b$) is estimated using equation 4.92

$$f_b = \frac{16}{R_e^g} = 0.0205$$

v. The bed shear stress, $\tau_{wb}$, is estimated using equation 4.90

$$\tau_{wb} = \frac{f_b \rho_b U_b^2}{2} = 30.96$$

$U_b$ and $\rho_b$ are estimated using equations 4.5 and 4.6 respectively

vi. The particle Reynold's number is estimated using equation 4.52. The local particle velocity ($V_r$) is obtained using equation 4.97, and the local particle velocity gradient ($\frac{dV_r}{dy}$) is estimated using equation 4.84.

$$R_{ep} = 1.42;\ V_r = 0.0258\,m/s;\ y = 3.4 \times 10^{-7}m;\ \frac{dV_r}{dy} = 75884\ s^{-1}$$

vii. Dimensionless shear rate (η) is estimated as = 1

viii. The drag coefficient is estimated using equations 4.53 and 4.56, respectively. As $R_{ep} > 1$, the lift coefficient is estimated using equation 4.69. The redefined drag and lift coefficients are estimated using equation 4.60 and 4.61, respectively.

$$C_D = 20.14;\ C_D' = 982.43;\ C_L = 3.65;\ C_L' = 178.06$$

ix. The gravity, drag, lift, buoyancy, and resultant Van Der Waal forces are estimated using equations 4.57, 4.58, 4.59, 4.71, and 4.78, respectively

$$F_g = 7.63 \times 10^{-7}N;\ F_D = 1.04 \times 10^{-4}N;\ F_L = 1.89 \times 10^{-5}N;$$

$$F_b = 4.78 \times 10^{-7}N;\ F_{vanR} = -6.63 \times 10^{-26}N$$

x. The equilibrium of moments around the contact point of a cutting that is just about to move is estimated using equation 4.70. When the solution converges to zero, the flow rate and the average annular fluid velocity calculated at that point correspond to the CRV. In this case, as follows

$$CRV = 0.57\, m/s\,;\; Q_{pump} = 0.0126\ m^3/s$$

**PUBLICATIONS**

EGBE, P. I., AL-MOUSA, F., and GADALLA, A., 2020. A Novel Application of Filter Cake Remover to Free Differential Stuck Pipe, SPE Paper No. 202416 (copyright)

EGBE, P. I. and ITURRIOS, C., 2020. Mitigating Drilling Hazards in a High Differential Pressure Well Using Managed Pressure Drilling and Cementing Techniques, SPE / IPTC Paper No. 20180 (copyright)

Patent Application: A Method For Real-Time Stuck Pipe Risk Prediction Assessment During Drilling Operations (October 2020)